Injectable hydrogels for innovative clinical applications

Giuseppe Alonci

UNIVERSITÉ DE STRASBOURG

ÉCOLE DOCTORALE DES SCIENCES CHIMIQUES

Institut de Science et d'Ingénierie Supramoléculaires

THÈSE présentée par :

Giuseppe ALONCI

soutenue le : **12 décembre 2018**

pour obtenir le grade de : **Docteur de l'université de Strasbourg**

Discipline/ Spécialité : Chimie

Injectable hydrogels for innovative clinical applications

THÈSE dirigée par :

Mme DE COLA Luisa	Professeur, Université de Strasbourg

RAPPORTEURS :

Mme PELLEGRINI Graziella	Professeur, University of Modena and Reggio Emilia
M. LAHANN Joerg	Professeur, University of Michigan, United States

---

AUTRES MEMBRES DU JURY :

M. BALL Vincent	Professeur, Université de Strasbourg
M. BIGINI Paolo	Nanobiology Unit Head, Mario Negri Institute

There are also extraordinary problems, and it may well be their resolution

that makes the scientific enterprise as a whole so particularly worthwhile.

But extraordinary problems are not to be had for the asking.

They emerge only on special occasions,

prepared by the advance of normal research.

Thomas Kuhn

The structure of scientific revolutions

Acknowledgement

Science is not a personal quest, but a collective effort. This thesis would not exist without the contributions of several researchers and colleagues, that helped me not only with equipment and measures, but overall with their personal support, their experience and their knowledge.

I would like to start by thanking Prof. Luisa De Cola, my supervisor during these three years in Strasbourg, for her continuous support and encouragement, all the ideas, the brain storming and for challenging me with ambitious projects and collaborations.

Most of this thesis has been conducted in collaboration with the Institut Hospitalo-Universitaire (IHU) and the Research Institut against Digestive Cancer (IRCAD) of Strasbourg. Not all the chemists have the opportunity to collaborate on almost a daily basis with surgeons and doctors, and for this I would like to thank Prof. Silvana Perretta, that has been my reference at IRCAD and our main collaborator for the projects of injectable hydrogels for ESD and fistula sealing. This collaboration gave me the special occasion to take a glance into the complex work of our medical partners, and I cannot properly express how grateful I am for this opportunity. I want to express my gratitude also to Prof. Mariano Gimenez, responsible for the percutaneous hernia project, for the opportunity he gave me but also for his optimism and energy!
I would like to really say «Thank you!» also to Dr. Pietro Riva, Dr. Ludovica Guerrero, Dr. Alain Garcia, Dr. Sun Gyo Lim and Dr. Pietro Mascagni, not only for being talented scientists and for their fundamental contribution to this thesis, but also for being good friends, their patience with me in explaining all the details of their job and for always making me feel at home even in an operating room.

I would like to reserve also a special thanks to Prof. Olof Ramström and his group in Stockholm, where I spent one month learning to work with bacteria culture, and to Solvay Laboratory of the Future, in particular to Dr. Pascal Hervé and to Dr. Steven Meeker, for hosting me three months in Bordeaux and teaching me all the basis of rheology (and for… the wine!).

Now, this should be the moment for the family… But I have three different families to thank!

First, I would like to thank my “real” family: my father, my mother and my brother, for all their support and for always being my safety net in each occasion.

Then, I would like to thank my ResMoSys family: Albano, Ligia, Camilla, Antanas, John, Qiang, Marion, Vanessa, Guille, Zhang and Suzanne. ResMoSys has been much more than just “a network”, it has been a fundamental part of my doctoral experience. We had an amazing time together, both in the official and unofficial meetings: thank you guys!

Third, I want to thank my “ISIS family”: all the De Cola group, including all the Erasmus and Master students. To write down all the names would require a second thesis, so I will just thank you all. Doing a PhD is hard, stressful, discouraging and exhausting: I would not have arrived until here without you and without the friendship, the laughter, the food, the climbing, the games and the double rainbows.

The last but not the least: Thank you Martina.
Not only because, if it was not for you, I would have never arrived in Strasbourg,
but because you are the most important part of my life.

Table of contents

Résumé de thèse

Depuis leur introduction au début des années 1960[1], les hydrogels ont suscité un intérêt considérable dans le domaine biomédical, grâce à leur biocompatibilité, leurs propriétés élastiques, leur forte teneur en eau, et leur structure 3D poreuse - permettant la perméation de l'oxygène et des nutriments et donc la croissance et la prolifération cellulaires – en imitant la matrice extra-cellulaire [2–4]

Comparés aux hydrogels naturels, tels que la cellulose ou le chitosane, les hydrogels synthétiques covalents offrent de nouvelles opportunités pour l'incorporation de fragments chimiques réactifs aux stimuli, pour permettre une meilleure reproductibilité et un contrôle plus large de la structure chimique et de la fonctionnalisation, et par conséquences des propriétés rhéologique et une meilleure stabilité.

Cependant, les hydrogels synthétiques peuvent être moins biocompatibles que leurs équivalents naturels et leur synthèse peut nécessiter des initiateurs de radicaux toxiques et plusieurs étapes de purification.

Les polyamidoamines (PAAm)[5] sont une classe d'hydrogels covalents bien connus dans la littérature pour leur biocompatibilité, leur facilité de réglage chimique et les conditions de réaction modérées requises pour leur synthèse. Leur préparation est basée sur l'addition d'amines nucléophiles à des doubles liaisons conjuguées par aza-Michael et ne nécessite pas d'initiateur radicalaire ni d'étape de purification. La réaction est conduite dans l'eau et le temps de gélification peut être contrôlé avec précision en contrôlant la température, qui peut aller de la température ambiante jusqu'à 80 °C (***Figure 1***).

Notre group a déjà montré la synthèse d'un hydrogel hybride composé d'un réseau polyamidoamine, réticulé avec des nanoparticules de silice mésoporeuses, et nous avons démontré que ce système permet la croissance et la prolifération des cellules souches mésenchymateuses et que nous pouvons contrôler la libération de molécules bioactives, telles que les chimiokines, à partir des nanoparticules. [6]

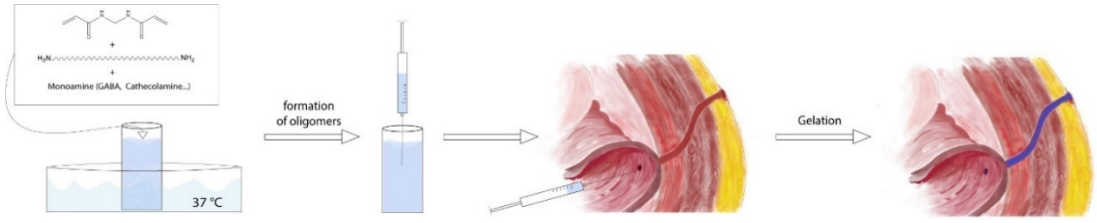

Figure 1 Schéma de synthèse de l'hydrogel et son application en tant que colle injectable pour le traitement des fistules.

Les poly(amidoamines) sont donc des candidats prometteurs pour des applications en chirurgie et en biomédecine, car elles combinent l'utilisation de conditions synthétiques douces - telles que la température ambiante, l'utilisation d'eau comme solvant et l'absence d'initiateurs de radicaux - avec une excellente biocompatibilité et injectabilité, un prix bas des matières premières et une grande flexibilité dans le squelette moléculaire qui permet une fonctionnalisation facile.

La chimie de l'acide hyaluronique a également été explorée.

Une des procédures cosmétiques les plus demandées est l'utilisation d'un agent de comblement, comme l'acide hyaluronique,[7,8] pour donner une apparence plus jeune en remplaçant la perte de volume dû au vieillissement normal.

L'acide hyaluronique est un polysaccharide naturellement présent dans le corps humain et impliqué dans différents processus physiologiques, tels que la cicatrisation.

L'acide hyaluronique pur est rapidement métabolisé et dégradé dans la peau et des injections fréquentes sont donc nécessaires. En effet, la formulation commerciale moderne contient de l'acide hyaluronique réticulé - l'agent de réticulation le plus couramment utilisé étant l'éther diglycidylique de 1,4-butanediol (BDDE) - pour assurer un effet durable.[9]

Nous présentons ici une stratégie de réticulation différente basée sur la lysine, afin d'éviter l'utilisation de molécules hautement réactives telles que le BDDE. La logique de notre idée est d'utiliser l'activation de l'hyaluronane pour favoriser le couplage avec la L-lysine, en suivant différentes stratégies basées sur la modification chimique de l'acide hyaluronique ou sur l'activation des groupes -COOH.

Discussion

Dans la ***Figure 2***, la viscosité de cisaillement et la rhéologie oscillatoire à 37 ° C d'une solution de pré-gel PAAm sont représentées. On peut voir que pour les 140 premières minutes à partir du début de la synthèse, la viscosité est presque constante, à une valeur fixe η ($\dot{\gamma} = 10\ s^{-1}$) ≈ 0.01 Pa · s. Entre 140 et 150 minutes, la viscosité augmente de 0.015 Pa.s à 0.04 Pa·s, puis commence à augmenter asymptotiquement. La rhéologie des oscillations montre que dans cette condition, le matériau reste un fluide très visqueux et que la gélification se produit à environ 155 minutes lorsque G'= G''. La gélification s'est produite en environ cinq minutes sur plus de deux heures et demie de synthèse!

Ce comportement est en effet d'un grand intérêt et nous avons émis l'hypothèse que nous pouvions utiliser cette cinétique particulière pour développer un matériau injectable.

Les matériaux mous biocompatibles ont récemment trouvé des applications en endoscopie interventionnelle pour faciliter la résection des tumeurs muqueuses. Lorsque des lésions néoplasiques se trouvent dans des organes pouvant être facilement endommagés par la perforation, tels que l'estomac, l'intestin et l'œsophage, la formation d'un coussin de liquide sous-muqueux (SFC) est nécessaire pour soulever la tumeur du muscle sous-jacent pendant la procédure utilisée pour la résection des néoplasies, la dissection sous-muqueuse endoscopique (ESD).[10,11]

Nous avons développé un hydrogel hybride biodégradable injectable (dPAA), capable de former une SFC et de faciliter les ESD. L'hydrogel, à base de polyamidoamines, contient des nanocapsules de silice sécable liées de façon covalente à son réseau. Ces particules

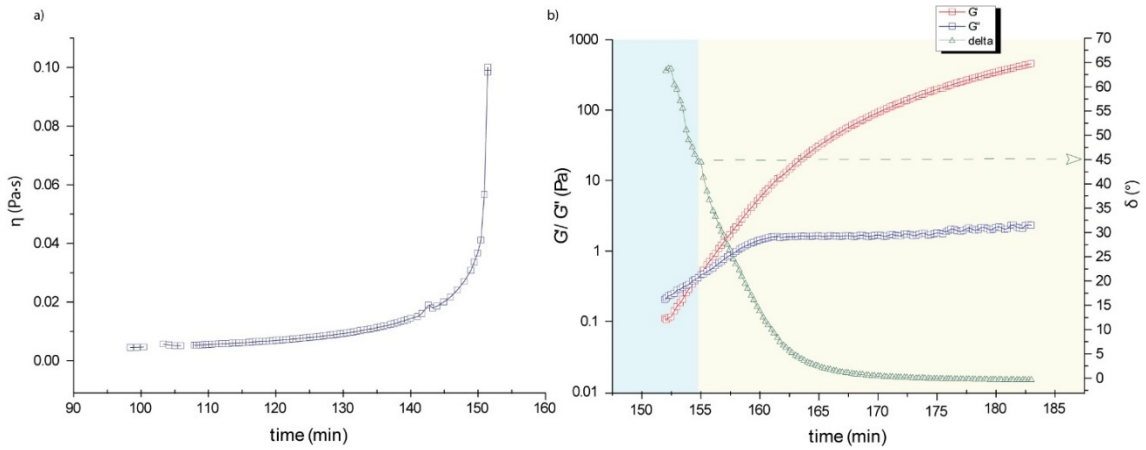

Figure 2 Cinétique de gélification d'un hydrogel PAAm composé de [MBA] = 0,864 M, [GABA] = 0,323 M et [PEHA] = 0,215 M. Viscosité en cisaillement ($\dot{\gamma}$ = 10 s-1) (a) et rhéologie des oscillations (f = 0,5 Hz), γ = 1%) (b) en fonction du temps depuis le début de la synthèse.

procurent une élasticité à l'hydrogel et permettent la libération de molécules lors d'un stimulus externe qui détruit les nanocapsules.

Pour favoriser la dégradation, l'hydrogel est composé de fragments disulfure clivables qui sont réduits par les cellules lors de la sécrétion de glutathion (GSH). Le même stimulus déclenche la rupture des nanocapsules de silice; par conséquent, tout le matériel hybride peut être complètement dégradé et sa décomposition dépend entièrement de la présence de cellules.

La solution de précurseur d'hydrogel a montré une gélification rapide lorsqu'elle a été injectée *in vivo* et a permis une élévation élevée de la muqueuse de longue durée, en maintenant le volume de coussin constant pendant la dissection. L'adhérence optimale de l'hydrogel à la couche de muscolaris assure une protection optimale, réduisant ainsi le risque de perforation. Ce nouveau matériau peut apporter une solution aux limitations de l'ESD et favoriser la guérison des tissus après une intervention chirurgicale.

La cinétique de dégradation du dPAA a été examinée en mesurant les variations du rapport de gonflement en fonction du temps en présence d'une solution de GSH faiblement concentrée (c'est-à-dire une solution de GSH 10 μM), imitant l'environnement extracellulaire.

L'investigation de l'injectabilité et du temps de gélification a ensuite été réalisée *in vivo*. La dPAA présentait un temps de gélification d'environ 3 minutes lorsqu'elle était injectée dans la couche sous-muqueuse chez un porc vivant.

Les conditions physiologiques de température (37 °C) contribuent à accélérer la gélification. La formation d'enchevêtrements mécaniques entre les fibres de collagène et le squelette de dPAA pourrait également contribuer à la formation d'un réseau d'hydrogel interpénétré, favorisant la formation et l'adhésion plus rapides d'un hydrogel stable et élastique *in situ*. Ce changement morphologique a été observé par Microscopie Electronique à Balayage (MEB) des tissus explantés, ce qui a effectivement montré des interactions entre l'échafaudage hydrogel et les fibres de collagène.

Nous avons examiné la formation et la durée d'une SFC *ex-vivo* en comparant la dPAA à une solution saline isotonique. La meilleure performance du nanocomposite dPAA dans *ex-vivo* a donc été confirmé *in vivo* chez un porc vivant (***Figure 3***). Nous établissons d'abord des tailles de lésions appropriées d'env. 3 cm de diamètre dans l'estomac porcin puis 8 ml de la solution d'hydrogel ont été injectés dans la sous-muqueuse.

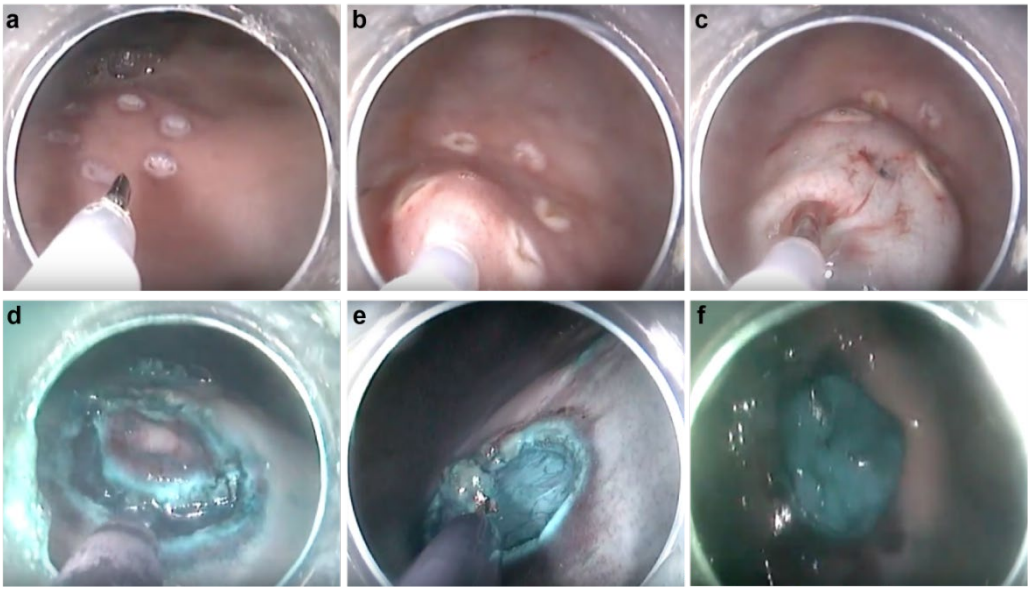

Figure 3 Vues endoscopiques des différentes étapes de la procédure ESD effectuées en utilisant le dPAA coloré au bleu de méthylène. Mise en place de la lésion, env. 3 cm de diamètre (a); injection de la solution de dPAA (b); formation du SFC après gélification du dPAA (c); coupe circonférentielle (d); résection complète avec couche protectrice de dPAA restée collée au muscolaris (e); blessure qui est laissée après ESD avec une couche de dPAA (f)

Une comparaison avec la solution saline normale (NS) généralement utilisée n'a montré initialement aucune différence significative par rapport à la SFC formée par la dPAA. Cependant, l'élévation de la SFC formée par le NS avait manifestement diminué après 15 min, en raison de la diffusion rapide du NS au site cible et de l'absorption du liquide par le tissu. Il était donc nécessaire de répéter les injections pour maintenir la sous-muqueuse soulevée et être capable de terminer la chirurgie.

Une autre application possible c'est le traitement percutané de la hernie inguinale.

Pour être adapté à l'application souhaitée, le matériau doit être facile à préparer pour une application immédiate en salle d'opération, facile à injecter mais capable de se gélifier avant de s'étendre de la zone souhaitée, il doit adhérer fortement aux tissus environnants, être non dégradable, suffisamment élastique et mécaniquement résistant pour supporter un stress élevé. Il devrait également être non cytotoxique et ne pas favoriser les réactions inflammatoires.

Sur la ***Figure 4a***, il est indiqué le schéma réactionnel pour la synthèse des matériaux. La synthèse est basée sur la polyaddition aza-Michael entre des doubles liaisons conjuguées et des amines basiques, dans notre cas entre le *N*, *N*'-méthylènebisacryalmide (MBA), l'acide γ-aminobutyrique (GABA) et un réticulant diamine, en particulier la pentaéthylène-hexamine (PEHA) et la 2,2'-(éthylènedioxy)bis(éthylamine) (EDBE).

Dans ces conditions, la solution de pré-gel est limpide et homogène après 5 minutes et l'hydrogel est formé en 24 ± 2 minutes. L'injection est effectuée après exactement 20 minutes à partir du début de la synthèse.

L'agent de réticulation et le degré de réticulation ont une grande influence sur les propriétés du réseau, la porosité, le temps de gélification, le module élastique et la biocompatibilité d'un hydrogel. La pentaéthylène-hexamine (PEHA) a été choisie en raison de la grande hydrophilie, de la souplesse imposée par une chaîne plus longue et de la possibilité de réticuler le réseau en plusieurs points, chaque groupe NH pouvant potentiellement réagir avec une double liaison. Les PEHA-hydrogels peuvent avoir un module de stockage très élevé (G') lorsque la quantité de réticulant est élevée, mais ils manquent alors d'élasticité.

Dans ce travail, nous avons décidé d'utiliser un système mixte réticulant contenant une partie de PEHA et une partie de 2,2-Ethylènedioxybis(éthylamine) (EDBE). L'EDBE ne peut réticuler qu'avec les deux groupes amines primaires situés aux extrémités de la chaîne, mais l'hydrophilie est garantie par la présence des fractions éthylènedioxy. Selon notre hypothèse, cela devrait augmenter l'élasticité et la porosité de l'hydrogel.

La faible viscosité de la solution de pré-gel peut toutefois avoir une influence négative sur la dispersion du fluide après l'injection. Pour ces raisons, nous avons décidé d'utiliser un réseau d'alginate de sodium et d'hydrogel PAAm. L'alginate de sodium est un hydrogel naturel non biodégradable bien connu, déjà approuvé en Europe et aux États-Unis pour les applications alimentaires et cliniques. Les solutions d'alginate sont visqueuses et

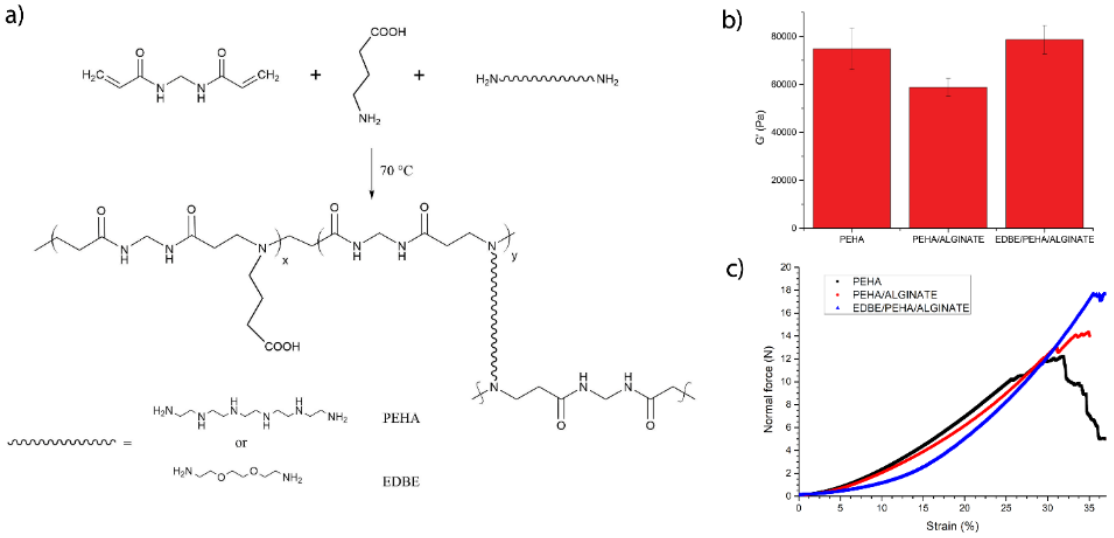

Figure 4 Schéma réactionnel pour la synthèse de l'hydrogel (a). Module élastique (b) et courbes contrainte-déformation (c) pour les trois échantillons d'hydrogel.

peuvent se gélifier en quelques secondes lorsqu'elles sont en contact avec une solution d'ions calcium, formant un hydrogel souple biocompatible, et n'ont aucune influence sur la formation du réseau PAAm. Nous avons émis l'hypothèse que l'utilisation d'une solution d'eau visqueuse à 2% d'alginate de sodium au lieu de l'eau pure pour la synthèse de l'hydrogel permettrait une moindre dispersion après les injections.

La ***Figure 4b*** indique le module de stockage (G') des trois hydrogels. Comme prévu, l'hydrogel PEHA/EDBE/ALG a le meilleur comportement. Ces valeurs sont comparables à celles rapportées dans la littérature pour les muscles et les tendons.

Pour évaluer la cytocompatibilité des matériaux, nous avons mesuré la viabilité des cellules HeLa pendant une semaine avec le test alamarBlue® et les résultats sont présentés sur la ***Figure 5***.

Pour tous les trois hydrogels, il est possible d'observer une augmentation significative de l'activité métabolique au fil du temps. La ***Figure 5b*** montre les cellules HeLa se développant sur l'hydrogel PEHA/EDBE/ALG après sept jours, colorées avec du DAPI pour le noyau et avec de l'AlexaFluor Phalloidin 647 pour l'actine.

Nous avons également jugé utile d'examiner s'il était possible d'utiliser le même matériau pour obtenir des microparticules d'hydrogel, qui pourraient à l'avenir être utilisés à différentes fins, de l'administration du médicament à l'encapsulation cellulaire.[12,13]

Des essais préliminaires, réalisés avec la méthode de l'émulsion inversée, ont montré qu'il était possible de synthétiser des microparticules de PAAm et qu'elles pouvaient être utilisées pour libérer des antibiotiques.

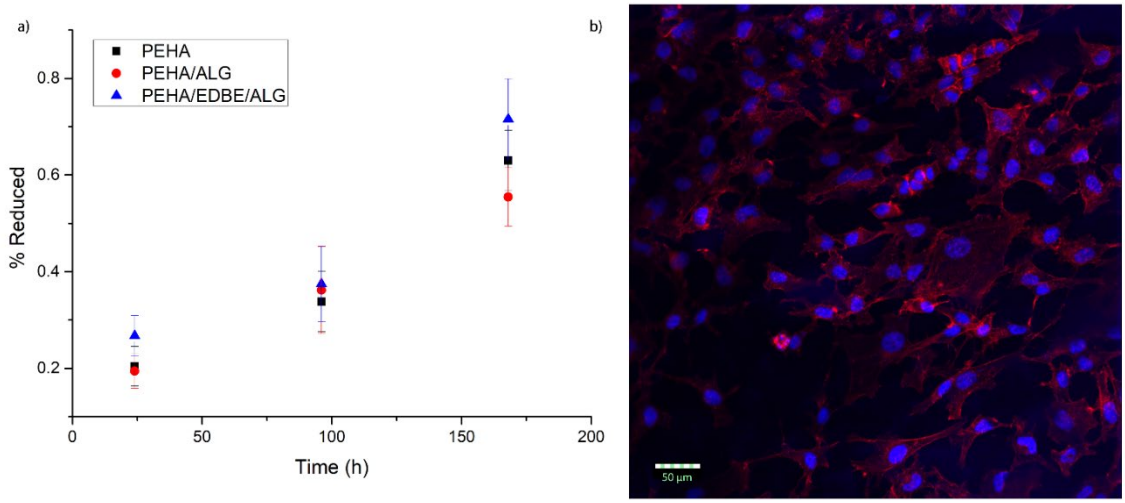

Figure 5 Test AlamarBlue (a) sur cellules HeLa en croissance sur les hydrogels PEHA/eau (noir), PEHA/ALG (rouge) et PEHA/EDBE/ALG (bleu) après 1, 4 et 7 jours; b) L'image confocale des cellules HeLa se développant au-dessus de l'hydrogel PEHA/EDBE/ALG après sept jours. L'actine est colorée avec AlexaFluor Phalloidin 647 et la région nucléaire avec DAPI.

Nous étudions également les possibilités d'encapsulation de cellules bactériennes vivantes, mais une optimisation supplémentaire du matériel est nécessaire.

Une formulation différente de matériaux PAAm peut être utilisée comme adhésif pour la fermeture des fistules.

Les fistules sont des connexions pathologiques entre deux organes creux ou avec la peau, pouvant résulter de plusieurs raisons, telles que des complications postopératoires ou comme un effet secondaire de la maladie de Chron. Ce sont des pathologies très graves pouvant entraîner une mauvaise qualité de vie, des douleurs chroniques, des infections et même la mort.[14,15]

Malheureusement, la thérapie n'est pas simple et même la chirurgie n'est pas toujours résolutive. Certains matériaux adhésifs, tels que les cyanoacrylates, ont été proposés pour fermer le tractus fistulaire, mais ils ont des effets secondaires neurologiques importants.

Nous avons imaginé que les hydrogels de PAAm injectables peuvent également s'appliquer à cette pathologie, en fermant la communication pathologique et permettant la prolifération cellulaire et la cicatrisation. Cependant, les hydrogels standard PAAm ne sont pas directement applicables dans ce cas, car ils percoleraient en dehors de la fistule avant la gélification.

Pour résoudre ce problème, nous avons développé une crème à base d'un solution pré-gel de PAAm préparé dans l'alginate de sodium 2% - comme phase aqueuse - et une phase organique composée d'huiles végétales comestibles, de tensioactifs approuvés par la FDA et d'autres molécules généralement reconnues comme sûres dans les formulations

Figure 6 Crème à base d'un solution pré-gel de PAAm

cosmétiques. La crème (***Figure 6***) possède un comportement d'amincissement par cisaillement et une contrainte importante, ce qui lui permet d'être injectée puis de rester en place jusqu'à la gélification du réticule de PAAm.

Dans un troisième projet, nous avons décidé d'explorer la chimie de **l'acide hyaluronique**.[9,16]

Le but de ce travail est de développer une stratégie pour la réticulation de l'acide hyaluronique avec un acide aminé naturel, la L-lysine, pour obtenir un produit final complètement naturel et biocompatible. Une stratégie peut être l'activation du groupe carboxylique de la partie acide glucuronique de l'acide hyaluronique pour favoriser une

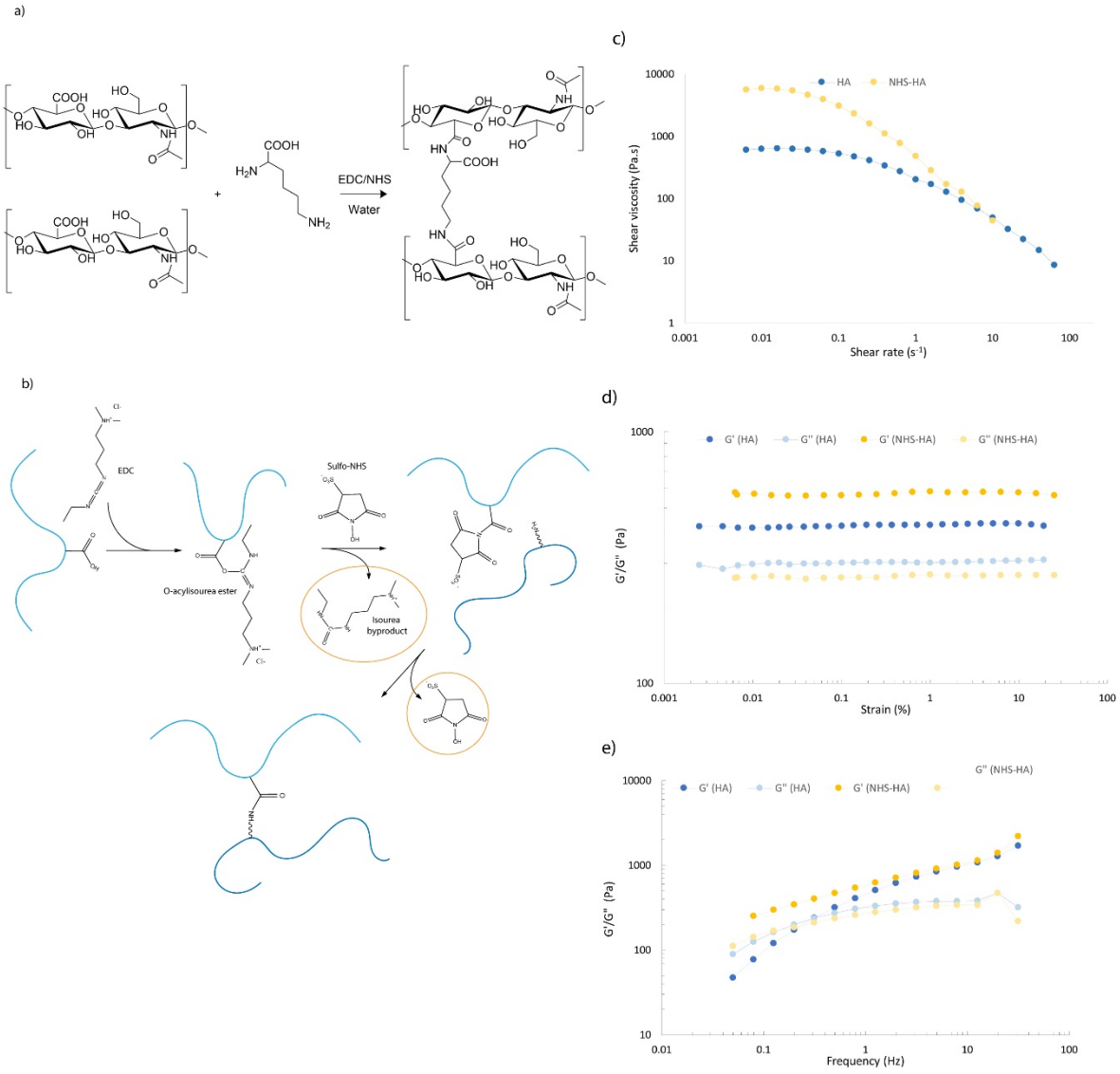

Figure 6 Acide hyaluronique réticulé avec L-lysine et EDC / sulfo-NHS et mécanisme réactionnel (a-b). Viscosité de cisaillement de l'acide hyaluronique pur (bleu) et de l'acide hyaluronique réticulé (jaune) (c). Balayage de stress (f = 1 Hz) et balayage de fréquence (σ = 1%) de l'acide hyaluronique pur et réticulé (d-e).

réaction avec les groupes amine de l'agent de réticulation à base de lysine pour former une liaison amide (***Figure 7***).

Une approche prometteuse consiste à utiliser le chlorhydrate de 1-éthyl-3-(-3-diméthylaminopropyl)carbodiimide (EDC) comme agent d'activation du groupe carboxylique, conjointement avec le *N*-hydroxysulfosuccinimide (sulfo-NHS) ou le 1-hydroxybenzotriazole (HOBt) pour faciliter davantage la réaction.

L'examen rhéologique du produit brut confirme l'efficacité de la réaction de réticulation. La ***Figure 7c*** montre la viscosité de cisaillement de l'acide hyaluronique pur (HA) par rapport à l'acide hyaluronique réticulé (NHS-HA). La viscosité à faible cisaillement est supérieure d'un ordre de grandeur pour le NHS-HA (5600 Pa.s à 0,0063 s-1) par rapport à l'acide hyaluronique vierge (600 Pa.s au même taux de cisaillement). L'analyse oscillatoire confirme encore la réticulation. Les balayages d'amplitude révèlent une large gamme viscoélastique linéaire, le NHS-HA ayant un G 'supérieur et un G inférieur par rapport à l'acide hyaluronique pur, confirmant que le matériau se comporte plus comme un solide élastique par rapport à l'acide hyaluronique pur.

Conclusion

Nous avons étudié les propriétés des gels de poly (amido amine) et nous avons démontré qui il est possible d'obtenir des microparticules de PAAm qui en future peut être utilisé pour l'encapsulation de bactérie ou pour encapsuler de molécules bioactives, tel quel les antibiotiques.

Un hydrogel hybride dégradable a été développé avec succès en incorporant des nanocapsules sécables dans un hydrogel à base de polyamidoamines contenant des ponts disulfure.

Nous avons démontré que les liaisons disulfure des nanoparticules incorporées et du réseau peuvent être complètement clivées en 3 jours lorsque l'hydrogel est incubé dans une solution de GSH imitant la concentration extracellulaire (10 μM). Plus important encore, la dPAA obtenue a soutenu la prolifération de cellules et a subi une dégradation complète en réponse aux molécules sécrétées, sans stimulus externe.

La solution aqueuse d'hydrogel a été injectée dans la sous-muqueuse d'un estomac de porc *in vivo*. Il a formé un hydrogel élastique en 3 minutes et un résultat aussi important nous

a incités à utiliser l'hydrogel dPAA comme nouvel agent d'injection sous-muqueuse en cas d'ESD.

Nous avons également développé des matériaux élastiques non dégradables à base de PAAm à utiliser pour la réparation de la hernie percutanée peu invasive. Le matériau obtenu est élastique, adhésif sur les tissus environnants et cytocompatibles.

Nous avons montré qu'il est possible de réticuler l'acide hyaluronique avec un acide aminé naturel, la L-Lysine, et que le matériau final est prometteur pour des applications en chirurgie esthétique du visage.

References

(1) Wichterle, O.; Lím, D. Hydrophilic Gels for Biological Use. *Nature* **1960**, *185* (4706), 117–118.

(2) Caló, E.; Khutoryanskiy, V. V. Biomedical Applications of Hydrogels: A Review of Patents and Commercial Products. *Eur. Polym. J.* **2015**, *65*, 252–267.

(3) Buwalda, S. J.; Boere, K. W. M.; Dijkstra, P. J.; Feijen, J.; Vermonden, T.; Hennink, W. E. Hydrogels in a Historical Perspective: From Simple Networks to Smart Materials. *J. Control. Release* **2014**, *190*, 254–273.

(4) Xu, Q.; Zhang, Z.; Xiao, C.; He, C.; Chen, X. Injectable Polypeptide Hydrogel as Biomimetic Scaffolds with Tunable Bioactivity and Controllable Cell Adhesion. *Biomacromolecules* **2017**, *18* (4), 1411–1418.

(5) Ferruti, P. Poly(Amidoamine)s: Past, Present, and Perspectives. *J. Polym. Sci. Part A Polym. Chem.* **2013**, *51* (11), 2319–2353.

(6) Fiorini, F.; Prasetyanto, E. A.; Taraballi, F.; Pandolfi, L.; Monroy, F.; López-Montero, I.; Tasciotti, E.; De Cola, L. Nanocomposite Hydrogels as Platform for Cells Growth, Proliferation, and Chemotaxis. *Small* **2016**, *12* (35), 4881–4893.

(7) Papakonstantinou, E.; Roth, M.; Karakiulakis, G. Hyaluronic Acid, a Key Molecule in Skin Aging. *Dermatoendocrinol.* **2012**, No. December, 253–258.

(8) Attenello, N. H.; Maas, C. S. Injectable Fillers: Review of Material and Properties. *Facial Plast. Surg.* **2015**, *31* (1), 29–34.

(9) Tezel, A.; Fredrickson, G. H. The Science of Hyaluronic Acid Dermal Fillers. *J. Cosmet. Laser Ther.* **2008**, *10* (1), 35–42.

(10) Kumano, I.; Ishihara, M.; Nakamura, S.; Kishimoto, S.; Fujita, M.; Hattori, H.; Horio, T.; Tanaka, Y.; Hase, K.; Maehara, T. Endoscopic Submucosal Dissection for Pig Esophagus by Using Photocrosslinkable Chitosan Hydrogel as Submucosal Fluid Cushion. *Gastrointest. Endosc.* **2012**, *75* (4), 841–848.

(11) Maple, J. T.; Abu Dayyeh, B. K.; Chauhan, S. S.; Hwang, J. H.; Komanduri, S.; Manfredi, M.; Konda, V.; Murad, F. M.; Siddiqui, U. D.; Banerjee, S. Endoscopic Submucosal Dissection. *Gastrointest. Endosc.* **2015**, *81* (6), 1311–1325.

(12) McClements, D. J. Designing Biopolymer Microgels to Encapsulate, Protect and Deliver Bioactive Components: Physicochemical Aspects. *Adv. Colloid Interface Sci.* **2017**, *240*, 31–59.

(13) Plamper, F. A.; Richtering, W. Functional Microgels and Microgel Systems. *Acc. Chem. Res.* **2017**, *50* (2), 131–140.

(14) Pfeifer, J.; Tomasch, G.; Uranues, S. The Surgical Anatomy and Etiology of Gastrointestinal Fistulas. *Eur. J. Trauma Emerg. Surg.* **2011**, *37* (3), 209–213.

(15) Evenson, A. R.; Fischer, J. E. Current Management of Enterocutaneous Fistula. *J. Gastrointest. Surg.* **2006**, *10* (3), 455–464.

(16) Highley, C. B.; Prestwich, G. D.; Burdick, J. A. Recent Advances in Hyaluronic Acid Hydrogels for Biomedical Applications. *Curr. Opin. Biotechnol.* **2016**, *40*, 35–40.

1. Biomedical applications of hydrogel-based materials

In this chapter, we will introduce some general concepts about hydrogel chemistry and their application in medicine, in particular in minimally-invasive surgery.

In the first part, we will introduce some general concepts about hydrogels. We will focus on the different type of hydrogels and their characteristics, and we will also give an overview on the different bonds that keeps together their 3D-structure and that determine their mechanical properties.
The main differences between synthetic and natural hydrogels, covalent and non-covalent hydrogels, will be analyzed in order to better understand how to design the optimal material for a specific application.
In the second part, we will show how hydrogels can be conveniently employed for different applications in biomedicine, such as in tissue engineering or regenerative medicine.
In the last part, we will present some relevant topics connected to the new advances in minimally-invasive surgery and we will outline some unmet needs to which material scientists can contribute.

1.1 What is a biomaterial?

A biomaterial is a substance that is engineered with the specific aim of being employed for a medical purpose, therapeutic or diagnostic. Several uses of biomaterials exist, such as prothesis, implants, artificial valves, drug release and drug delivery or even tissue engineering, i.e. the design of 3D scaffolds that promote the controlled and organized cell growth for the artificial production of living tissues.[1] This topic is so broad that it requires transversal competencies and the coordination of different expertise, such as chemists, material scientists, biologists, biomedical engineers and doctors.

Biocompatibility is the most important requirement that any biomaterials must meet. Different definitions of biocompatibility are reported in literature, but in general it is possible to say that a biocompatible material should be non-toxic, should integrate well with the surrounding tissues and should not give place to dangerous inflammatory reactions.[2]

Depending on the specific application, biomaterials can be degradable with time or in response to very specific stimuli, or they can be non-degradable and thus able to resist to corrosion and to the action of all the molecules naturally present in the host organism. If the material is degradable, it is of the utmost importance to verify that also its degradation products are not dangerous and easily expelled from the body. It is also fundamental to check whether the degradation happens in a controlled way and give enough time to the material to exercise its action.[3]

In any case, it should have appropriate mechanical and rheological properties, such as hardness, elasticity or stress compliance.[4] As we will see in the final chapters, injectable hydrogels for skin filling should be soft and elastic, in order not to be noticed after injection, while materials used for hernioplasty should still be very elastic, but also harder in order to sustain the high stress connected to normal human activities.

Considering all these factors, the number of different possible applications and the specific needs of each particular use, it is important to underline that a biomaterial can be perfectly suitable and biocompatible for a certain application in a selected area of the body but can become dangerous if used in a different way or in a different position.

1.2 What is a hydrogel?

Hydrogels are three-dimensional, hydrophilic, polymeric networks able to imbibe large amount of water or biological fluids without dissolution.[5] Thus, hydrogel are formed by polymeric chains containing hydrophilic groups, such as -OH or -COOH, that do not dissolve in water because they are held together by some kind of crosslinking, either covalent or non-covalent.

From a rheologic point of view, a gel should not flow in zero-shear conditions, meaning that it should behave like a solid and its elastic modulus (G') should be higher than the viscous modulus (G'').[4,6] However, it may show shear-thinning properties and start to flow when a stress is applied.[7]

Despite being known since long time, they started to be seriously investigated only after the pioneering work of Lim and Wichterle in 1960.[8] Since then, their use in the medical and biological field have been widely explored, leading to a variety of materials with different properties and functions.[1,9,10]

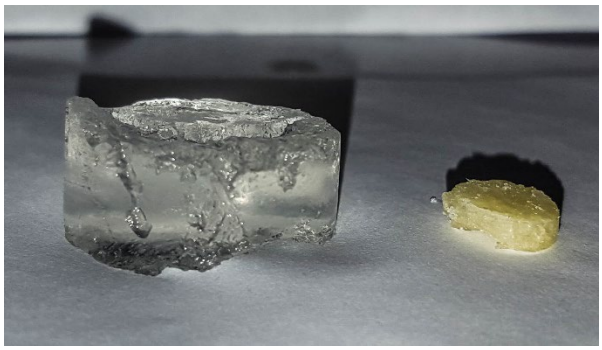

Figure 1.1 Example of hydrogel in the swollen (left) and dry (right) state.

A hydrogel can be constituted from up to 99% of water (***Figure 1.1***), and this typical high hydrophilicity – together with the tissue-like elasticity and the porous structure - makes them similar to the living tissues and allows the permeation of oxygen and nutrients.

In their ground-breaking paper published in Nature in 1960,[8] Lim and Wichterle showed how hydrogels can be used for the preparation of soft contact lenses. Their elasticity and biocompatibility, together with the hydrophilicity, high water retention and oxygen permeability, are perfect matches for ocular applications. The cornea – the transparent membrane present in the outermost anterior part of the eye – is indeed not vascularized, and thus must rely on the interaction with the surrounding environment for oxygenation. The

contact lenses proposed by Wichterle and Lim, based on poly-2-hydroxyethylmethacrylate (PHEMA), started to be distributed already in 1962, but they become a commercial success in 1971 with the FDA approval. The material remained substantially unchanged for almost twenty years, when the first contact lenses based on silicone hydrogels were introduced.

This application shows a classic example of how many parameters need to be considered for each application and demonstrate that hydrogels are promising materials for a variety of applications in the biomedical sector.

In general, we can distinguish the hydrogels in different classes, depending on their origin and on the different type of bonds that hold together their structure.[11]

Looking at their origin, we can distinguish between synthetic and natural hydrogels. Examples of natural hydrogels are collagen,[12] fibrin, pectin, starch, hyaluronic acid or alginic acid derivatives,[13] but many other materials exist. Natural hydrogels are widely spread in the living kingdom; indeed, they are characterized by high biocompatibility and tolerability, that make them very interesting for several applications. As we will see in the final chapter of this thesis, hyaluronic acid is the most commonly used material in cosmetic surgery as a dermal filler and possesses a fundamental role in physiological homeostasis of the skin.[14,15]

Polysaccharides-based hydrogels have been used for several other applications. For example, they have been used for cartilage and osteochondral tissue engineering,[16,17] for wound healing,[18,19] or as injectable materials in medicine.[20–24]

However, natural hydrogels have also some important drawbacks that sometimes hinder their applications. In particular, the control on their molecular backbone is limited and their chemical modification can be difficult, meaning that it can be complicated to obtain material with special properties.

Synthetic hydrogels[25,26] offer a higher degree of control on the chemical structure and they can be carefully designed to have very specific properties. However, they can be less biocompatible than their natural counterpart, an important constraint in biomedical applications. Also, the synthetic procedure can be long and complex, increasing the price of the final material and so reducing their applicability in real-world situation.

We have already seen an example before with the use of poly (hydroxyethyl methacrylate) by Wichterle and Lim for the preparation of soft contact lenses. Other examples of synthetic hydrogels are poly (vinyl alcohol) (PVA), poly (ethylene glicole) (PEG), poly (N-isopropylacrylamide) (PNIPAam), poly (amidoamine)s (PAAm, see Chapter 2 for a deep discussion) and many others. Synthetic hydrogels can be designed in order to have special properties, such as degradability in response to a specific stimulus. It is also possible to design

smart materials whose properties change depending on the surrounding environment, like in temperature- or pH-responsive hydrogels.[27,28]

It should be remarked that these distinctions are only indicative, and a blurred border exists. For examples, natural hydrogels can be chemically-modified and functionalized to gain stimuli-responsive properties or other characteristic, while some synthetic hydrogels (such as. PAAm) demonstrated high cyto- and biocompatibility, while others are synthetized starting from natural monosaccharaides or amino acids.

1.3 Covalent and non-covalent hydrogels

A fundamental aspect that dictate most of the properties of a hydrogel is the covalent or non-covalent nature of its polymeric network. Albeit being possibly very dilute, the three-dimensional network is responsible for the rheological properties of the hydrogel, it cohesivity and for its ability to interact with the surrounding environment. Indeed, to be defined a gel, a material must also have a solid-like behavior due to a crosslinked network.[6] From a quantitative point of view, this corresponds to having an elastic modulus higher than the viscous modulus.

The bonds that keep together the components of the network can be different in nature but can be approximately divided in covalent bonds and non-covalent interactions (***Figure 1.2***).

In covalent hydrogels, the polymeric chains are crosslinked through the formation of covalent bonds between the monomers or through the use of polyfunctional cross-linker that may link together two or more chains. Generally speaking, covalent hydrogels have higher elastic modulus compared to non-covalent ones and they do not dissolve in water.

Covalent crosslinking may be defined as “irreversible” - because of the usual stability of covalent bonds – and does not show a clear reversible sol-gel transition, in contrast to non-covalent hydrogels where gelation is reversible and strongly condition-dependent.

Different mechanism may be responsible for covalent crosslinking, such as ionic polymerization or radical polymerization. For example, aza-Michael polyaddition between amines and N,N’-methylenbisacrylamide is responsible for the formation of PAAm network.[29] This reaction may be carried aqueous media at room temperature – in contrast to many other type of additions – and can thus be widely exploited for biomedical application,[30]

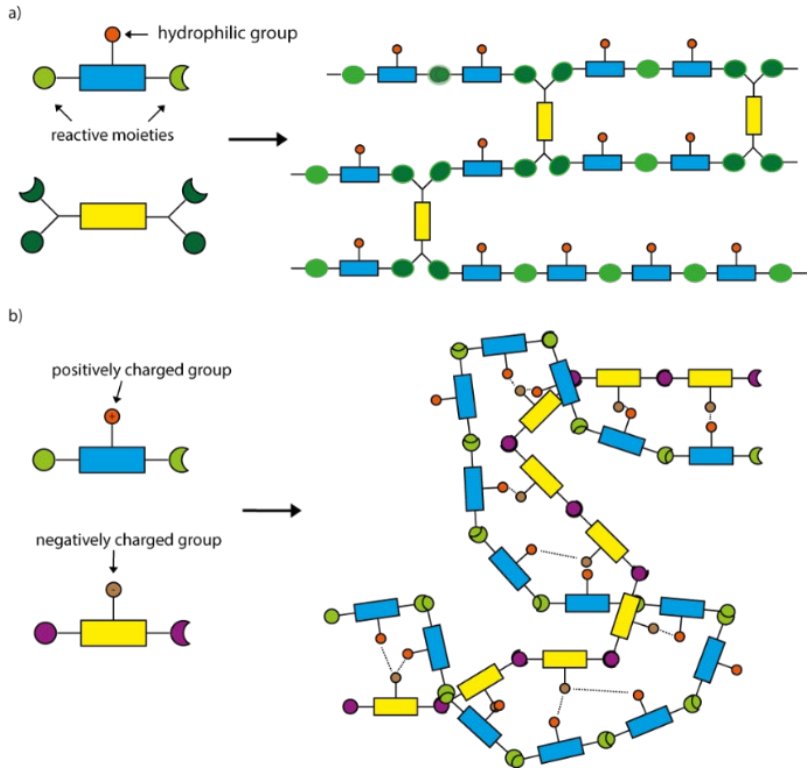

Figure 1.2 Schematic structure of a covalent cross-linked hydrogel (a); Schematic structure of a coacervate non-covalent hydrogel (b).

as we will investigate in detail in Chapter 2. Another variant of the Michael polyaddition, the thiol-ene reaction, can also be conveniently employed to obtain biocompatible hydrogels for drug delivery.[31] Acrylates-containing molecules can also be activated with UV-light and react to form completely crosslinked covalent hydrogels.[21] By changing the amount of crosslinker, its length and valency, it is possible to tune the mechanical properties of the hydrogels.[32]

It should be underlined that, despite generally regarded as "strong", also covalent bonds may be broken. Indeed, several stimuli-responsive covalent systems exist and exploit the special reactivity of functional groups such as esters, thioketals, acetals, imines, hydrazones et cetera, that may break or form in particular conditions. For example, Konieczynska, Grinstaff *et al* showed how the thiol-thioester exchange reaction can be used to engineer a hydrogel that may dissolve on demand and that can be used as a dressing in burn wounds to reduce pain and discomfort for the patient.

In Chapter 3 we will present a redox-responsive hydrogel crosslinked with a disulfide-containing molecule, and thus able to break selectively in a reducing environment.

In non-covalent hydrogels, small molecules or polymeric chains are held together by weak interactions, such as electrostatic forces, dispersion forces (mostly for organogel) or hydrogen bonds. The process of gelation, in this case, does not depend on the reaction with another

molecule, but instead on changes in pH, temperature or concentration that trigger the start of the self-assembly of the chains in high-ordered structures.[26,33]

For example, the hydroxyl groups of poly (vinyl alcohol) may interact with hydrogen bonds and lead to a self-assembly of the polymer backbone in crystalline domains, a process normally triggered with freeze-thaw cycling.

In ***Figure 1.2b*** it is reported a generic scheme of a non-covalent hydrogel in which the crosslinking is exerted by ionic interactions between a positively charged chain and a negative charged chain (coacervate hydrogels). Another very famous example of ionic crosslinked hydrogel is calcium alginate.[13] Alginate-based hydrogels are widely used in biomedicine for different applications, from dressings and wound healing to drug delivery and tissue engineering.[34] Alginate is a natural polysaccharide originally extracted from brown algae and normally sold as the sodium salt. Sodium alginate slowly dissolve in water forming a viscous solution, but it immediately gels in presence of calcium ions,[35] that may interact with the negative charges of the carboxylic groups, as shown in ***Figure 1.3***.

Hydrogen bonds are also widely employed for the formation of hydrogels, and they are especially important for the formation of hydrogel based on oligopeptides. Countless examples exist, with peptide-based hydrogels probably being the most studied. Peptides can self-assemble into fibrillar structures, that after can interact and entangle to form a hydrogel under specific pH, solvent and temperature conditions. Peptide-based hydrogels have been used in drug delivery,[36,37] as mucoadhesive systems,[38] in several tissue engineering applications - such as spinal cord repair [39] - or in medicine and surgery.[40]

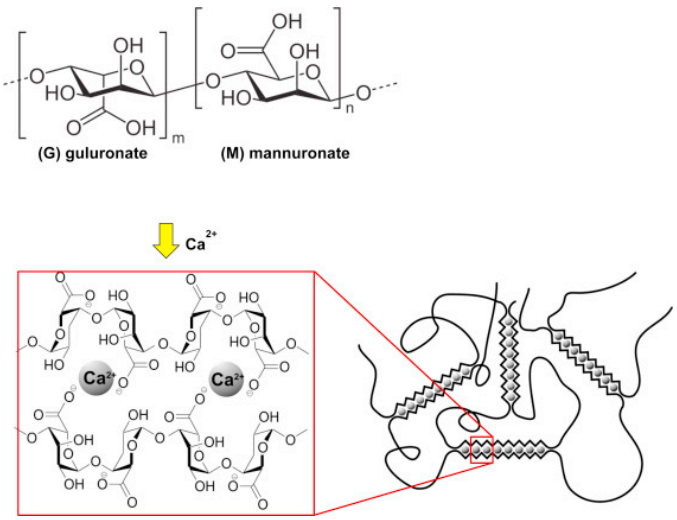

Figure 1.3 Alginate hydrogel proposed mechanism of gelation. Reproduced with permission from 10.1016/j.carbpol.2015.05.021

A famous example of a thermo-responsive non-covalent hydrogel is Poly(N-isopropylacrylamide), or PNIPAm, that since its discovery in 1956 has been employed in a countless number of possible applications,[41] including drug delivery[42–44] and injectable materials.[45–48]

PNIPAm is soluble in water at room temperature but undergoes a coil-to-globule transition when heating, decreasing its solubility as the temperature of the solution rises.[49] An entropically-driven dehydration of polymer components happens at the lowest critical solution temperature (LCST), leading to a transition between hydrophilic and hydrophobic behavior (**Figure *1.4***).

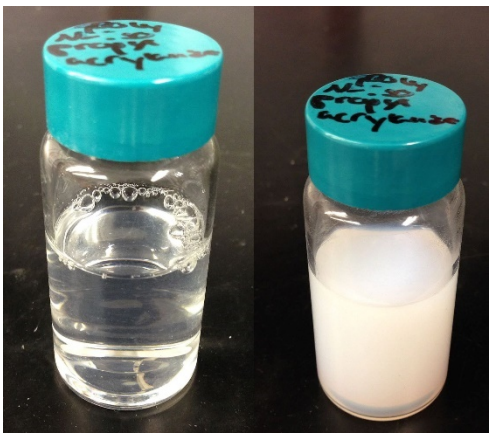

Figure 1.4 Behavior of a thermo-responsive polymer below the LCST (left) ad above the LCST (right). Source: wikimedia

Thus, at temperature below the LCST the material behave as an injectable solution, that solidifies at temperature above the LCST. This temperature can be tailored by appropriately designing the material and preparing suitable copolymers of PNIPAm, in order to engineer materials with a LCST≈ 37 °C. However, PNIPAm is non-degradable, and even its degradable copolymers may release toxic components.[48]

1.4 Mucoadhesive properties of materials

Wound closure is a topic of the utmost importance in surgery. Different techniques are available today, such as adhesive tape, suturing, staples and surgical glues,[50] each one with specific advantages and drawbacks. The decision on which kind of closuring techniques is better suitable for a specific patient relies on the responsibilities of the

surgeon, that must consider different factors such as the extension and location of the wound, the possibility of the infections, the resistance needed and, possibly, the aesthetic outcomes. Suturing is still the gold standard[51] and it is widely employed in a broad range of contexts, as it offers the opportunity to use threads of different shapes, dimensions and materials.

However, suturing can cause scarring of the skin and its outcomes are strictly dependant on the skills of the surgeon. In all cases, it is a technique that requires time, patience and is not always straightforward to apply in minimally invasive surgery, especially in endoscopic surgery. Even though some devices for endoscopic suturing are already in the market, such as Apollo OverStitch,[52] they are expensive and not always easy to use.

In these cases, the possibility of using a surgical glue would be highly beneficial for an easy, effective, cheap and fast closure. Today, the two most common options are fibrin glue and cyanoacrylates.[53,54]

Fibrin glue is obtained with the combination of platelet-rich blood derivatives (both autogenous or allogenous) mixed with thrombin. Despite having several advantages,[55,56] especially in term of biocompatibility, it is not suitable for any applications where mechanical stress is expected, because of its poor adhesive and mechanical properties.[57]

Cyanoacrylates are synthetic polymer sealants whose mechanism of action is based on the reaction between the water/blood contained into the tissues with highly reactive monomers. They have several advantages compared to fibrin glue, such as the superior adhesive strength and the fast formation, that lead to their extensive use in suture-less surgery.[58,59] However, cyanoacrylates don not have the same level of cyto- and biocompatibility of fibrin glue and they are associated with increased health risks and neutotoxicity.[60,61] Other materials require irradiation with UV-light to trigger the adhesion,[62,63] a problematic approach in hard-to-reach areas.

The development of the optimal suturing material is still an unmet need for the surgical community. Tissue-adhesive hydrogels could present a valid response to such need, because of their inherent ability to firmly adhere to tissues, even in areas where mechanical stress is expected. Moreover, they can be synthetized to have a passive role in haemostasis and sealing,[63] or they can be functionalized in order to exert a specific activity, such as promoting healing of complex and chronic wounds.[64]

With *bioadhesion* we refer to the state in which two materials, of which at least one has biological origins, adhere together through interfacial forces. If this adhesion is mediated

by a layer of mucous, then the term mucoadhesion is employed.[65] Mucoadhesion is of an important concept not only in surgery, but also for applications in pharmaceutics and drug delivery. The development of special materials to guarantee the adhesion of tablet and pills in the intended location is indeed of great importance.[12,66,67]

The mechanism of mucoadhesion is extremely complex and a number of factors need to be considered. Some of the interactions that can be exploited to engineer a material with optimal adhesion properties are ionic interactions, hydrogen bonds, covalent bonds and hydrophobic forces. A complete review on this topic was published by John D. Smart in 2005[65] and by Vitaliy V. Khutoryanskiy in 2011.[68]

The microscopic nature of the material has also a great influence on the adhesion strength and microengineered hydrogels are becoming more and more common in the tissue engineering field.[69] One classic examples of the importance of the nanostructure in bioadhesion is the ability of geckos to stick to almost any surface, thanks to the strong non-covalent interactions mediated by the microscopic fibrillar structures that cover their footpads maximising Van der Waals interactions.[70] After its discovery in 2002, this phenomenon inspired several researchers on their quest for the perfect adhesive material.[71–74]

As we will see in the beginning of Chapter 3, a common approach for the synthesis of mucoadhesive hydrogel is also the functionalization with catechol-containing moieties. This approach is inspired by the observation that mussels adhere to rocks and other submarine surfaces thanks to the use of special filaments, known as byssus (***Figure 1.5***), composed by

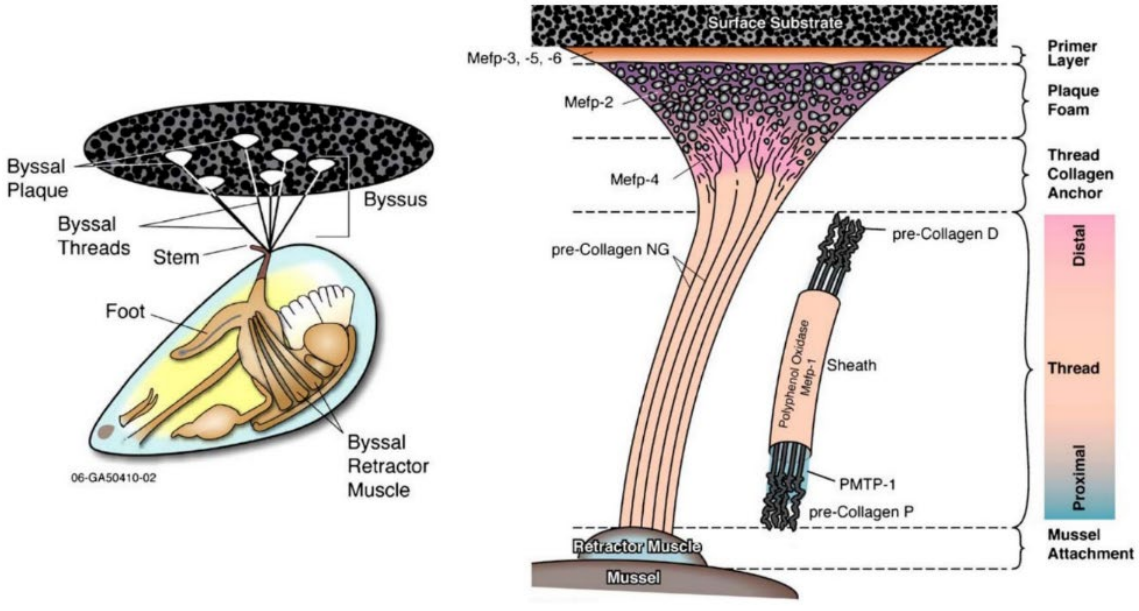

Figure 1.5 Mechanism of mussel adhesion. Reproduced with permission from 10.1007/s10126-007-9053-x

several mussel foot proteins that are rich in catechol-based amino acids, such as L-3,4-dihydroxyphenylalanine (L-DOPA).

However, even though non-covalent interactions are widely employed in designing of bioadhesive and mucoadhesive formulations, covalent interactions and mechanical interlocks are the most relevant mechanism we are interested in this work, because of their superior retention ability and adhesion strength.

1.5 Minimally-invasive surgery

In the last century, surgery has undergone several deep transformations, that greatly improved the chance of survival for the patients and reduced intra- and post-operative pain and dangerous complications. One of the biggest revolutions in surgery, after the introduction of anesthesia and antiseptic procedure, is the introduction of laparoscopic and minimally-invasive surgery.[75]

In contrast to laparotomy, where a large incision is made to allow direct access to the abdominal cavity or to any relevant anatomical structure, in laparoscopy only small incisions are made to allow the introduction of a camera and of the surgical tools.

The first reported laparoscopic procedure in humans was performed by the Swedish surgeon Hans Christian Jacobaeus,[76,77] who employed the procedure for diagnostic purpose. In the following years, new advances were made possible – especially in gynecology - by new surgical tools and by the introduction of digital cameras. However, in the 70-80s laparoscopic procedures in general surgery were still considered taboo and in gynecology too laparoscopy was considered almost only as a diagnostic method. Kurt Semm is today recognized as one of the top innovators in the field, and in the 70s he was the first to perform several gynecologic procedures by interventional laparoscopy[78] and he performed the first laparoscopic appendectomy[79] in 1983. Inspired from the work of Kurt Semm, the German Surgeon Eric Mühe was the first to perform a laparoscopic cholecystectomy in 1985. Both Kurt Semm and Eric Mühe faced indifference or even a strong resistance by the scientific community, that was not ready to accept these innovations.[80]

Today, a minimally-invasive approach is routine for several procedures and the appearance of surgical robot - such as the *da Vinci® surgical system* from Intuitive - allows for an increased precision and a wider horizon of possibilities.

Minimally-invasive surgery today is applied for several different pathologies. To cite only a few examples - apart from the classic laparoscopic appendectomy and cholecystectomy – we can remember laparoscopic colectomy, sleeve gastrectomy, hysterectomy, hernioplasty[81] and even spinal surgery for the correction of scoliosis.[82] In traditional procedures, two or three accesses to the abdominal cavity are required, to obtain a good triangulation between the camera and the surgical tools. Trocars are the most commonly used ports for this purpose, and they are available in different models and dimensions. However, also single-port laparoscopy is possible, generally using the patient umbilicus as the only access point, in order to reduce scarring and pain.

In any case, despite leading to less complications, decreasing post-operative pain and decreasing hospitalization time, laparoscopic procedures still require the introduction of trocars and surgical tool in the abdomen and to make (small) external incisions. In recent years, the surgical community started to evaluate the opportunity to perform surgery using only the natural orifices of the body (Natural Orifice Transluminal Endoscopic Surgery, NOTES).[83,84]

In this approach, an endoscope is introduced trough a natural orifice - such as the mouth, the anus or the vagina - and the abdominal cavity is reached through an internal incision performed with surgical tools introduced through the operating ports of the endoscope.

Endoscopy is a technique employed to visualize the internal portion of the body using a flexible instrument connected to a camera and a light source. Interventional endoscopy allows the operator to perform surgical procedures without the need of any external or internal incision to reach is target area.

Endoscopic submucosal dissection (ESD) is a minimally-invasive endoscopic procedure that can be used to remove early-stage gastric cancer. It consists in the endoscopic injection of a fluid in the submucosal space of the stomach - where it acts as a submucosal fluid cushion which reduce the risk to damage the deeper layers of the stomach wall – followed by the resection of the mucosal lesion.

We will discuss this topic in more detail in Chapter 3, where we will report the development of new degradable and injectable material for ESD.

In Chapter 4, we will show the development of a novel hydrogel formulation, a PAAm-based cream, that can be used for the endoscopic treatment of fistulas, i.e. abnormal connections between two hollow organs or between one hollow organ and the outside of the body.[85]

In Chapter 4, we will also show the development of a material to be used for the percutaneous treatment of inguinal hernia. In contrast to laparoscopic surgery, where incision of the skin and the other deeper layers is required, in percutaneous surgery the operator uses needle or catheters under image guidance provided by ultrasound, CT scan or fluoroscopy.[86–88]

References

(1) Peppas, N. A.; Hilt, J. Z.; Khademhosseini, A.; Langer, R. Hydrogels in Biology and Medicine: From Molecular Principles to Bionanotechnology. *Adv. Mater.* **2006**, *18* (11), 1345–1360.

(2) Yu, L.; Ding, J. Injectable Hydrogels as Unique Biomedical Materials. *Chem. Soc. Rev.* **2008**, *37* (8), 1473–1481.

(3) Ebbesen, M. F.; Gerke, C.; Hartwig, P.; Hartmann, L. Biodegradable Poly(Amidoamine)s with Uniform Degradation Fragments via Sequence-Controlled Macromonomers. *Polym. Chem.* **2016**, *7* (46), 7086–7093.

(4) Murata, H. Rheology - Theory and Application to Biomaterials. *Polymerization* **2012**, 403–426.

(5) Caló, E.; Khutoryanskiy, V. V. Biomedical Applications of Hydrogels: A Review of Patents and Commercial Products. *Eur. Polym. J.* **2015**, *65*, 252–267.

(6) Picout, D. R.; Ross-Murphy, S. B. Rheology of Biopolymer Solutions and Gels. *Sci. World J.* **2003**, *3*, 105–121.

(7) Avery, R. K.; Albadawi, H.; Akbari, M.; Zhang, Y. S.; Duggan, M. J.; Sahani, D. V.; Olsen, B. D.; Khademhosseini, A.; Oklu, R. An Injectable Shear-Thinning Biomaterial for Endovascular Embolization. *Sci. Transl. Med.* **2016**, *8* (365).

(8) Wichterle, O.; Lím, D. Hydrophilic Gels for Biological Use. *Nature* **1960**, *185* (4706), 117–118.

(9) Buwalda, S. J.; Boere, K. W. M.; Dijkstra, P. J.; Feijen, J.; Vermonden, T.; Hennink, W. E. Hydrogels in a Historical Perspective: From Simple Networks to Smart Materials. *J. Control. Release* **2014**, *190*, 254–273.

(10) Saul, J. M.; Williams, D. F. Hydrogels in Regenerative Medicine. *Handb. Polym. Appl. Med. Med. Devices* **2013**, 279–302.

(11) Okay, O. General Properties of Hydrogels. In *Hydrogel Sensors and Actuators*; Gerlach, G., Arndt, K. F., Eds.; Elsevier, 2010; Vol. 6, pp 1–15.

(12) Lee, Y. A. L.; Zhang, S.; Lin, J.; Langer, R.; Traverso, G. A Janus Mucoadhesive and Omniphobic Device for Gastrointestinal Retention. *Adv. Healthc. Mater.* **2016**, *5* (10), 1141–1146.

(13) K. Y. Lee, D. J. M. Alginate : Properties and Biomedical Applications. *Prog. Polym. Sci.* **2012**, *37* (1), 106–126.

(14) Tezel, A.; Fredrickson, G. H. The Science of Hyaluronic Acid Dermal Fillers. *J. Cosmet. Laser Ther.* **2008**, *10* (1), 35–42.

(15) Beasley, K. L.; Weiss, M. A.; Weiss, R. A. Hyaluronic Acid Fillers: A Comprehensive Review. *Facial Plast. Surg.* **2009**, *25* (2), 86–94.

(16) Radhakrishnan, J.; Subramanian, A.; Krishnan, U. M.; Sethuraman, S. Injectable and 3D Bioprinted Polysaccharide Hydrogels: From Cartilage to Osteochondral Tissue Engineering. *Biomacromolecules* **2017**, *18* (1), 1–26.

(17) Suchaoin, W.; Bonengel, S.; Grießinger, J. A.; Pereira De Sousa, I.; Hussain, S.; Huck, C. W.; Bernkop-Schnürch, A. Novel Bioadhesive Polymers as Intra-Articular Agents: Chondroitin Sulfate-Cysteine Conjugates. *Eur. J. Pharm. Biopharm.* **2016**, *101*, 25–32.

(18) Hoque, J.; Prakash, R. G.; Paramanandham, K.; Shome, B. R.; Haldar, J. Biocompatible Injectable Hydrogel with Potent Wound Healing and Antibacterial Properties. *Mol. Pharm.* **2017**, *14* (4), 1218–1230.

(19) Wijekoon, A.; Fountas-Davis, N.; Leipzig, N. D. Fluorinated Methacrylamide Chitosan Hydrogel Systems as Adaptable Oxygen Carriers for Wound Healing. *Acta Biomater.* **2013**, *9* (3), 5653–5664.
(20) Kang, K. J.; Min, B. H.; Lee, J. H.; Kim, E. R.; Sung, C. O.; Cho, J. Y.; Seo, S. W.; Kim, J. J. Alginate Hydrogel as a Potential Alternative to Hyaluronic Acid as Submucosal Injection Material. *Dig. Dis. Sci.* **2013**, *58* (6), 1491–1496.
(21) Yuan, L.; Wu, Y.; Gu, Q. sheng; El-Hamshary, H.; El-Newehy, M.; Mo, X. Injectable Photo Crosslinked Enhanced Double-Network Hydrogels from Modified Sodium Alginate and Gelatin. *Int. J. Biol. Macromol.* **2017**, *96*, 569–577.
(22) Hou, J.; Li, C.; Guan, Y.; Zhang, Y.; Zhu, X. X. Enzymatically Crosslinked Alginate Hydrogels with Improved Adhesion Properties. *Polym. Chem.* **2015**, *6* (12), 2204–2213.
(23) Rabbani, S.; Rabbani, A.; Mohagheghi, M. A.; Mirzadeh, H.; Amanpour, S.; Alibakhshi, A.; Anvari, M. S.; Ghazizadeh, Y. A Novel Approach for Repairing of Intestinal Fistula Using Chitosan Hydrogel. *J. Biomater. Appl.* **2010**, *24* (6), 545–553.
(24) Bernkop-Schnürch, A.; Kast, C. E.; Richter, M. F. Improvement in the Mucoadhesive Properties of Alginate by the Covalent Attachment of Cysteine. *J. Control. Release* **2001**, *71* (3), 277–285.
(25) Ahmed, E. M. Hydrogel: Preparation, Characterization, and Applications: A Review. *J. Adv. Res.* **2015**, *6* (2), 105–121.
(26) Garner, J.; Park, K. Types and Chemistry of Synthetic Hydrogels. In *Gels Handbook*; Demirci, U., Khademhosseini, A., Eds.; World Scientific, 2016; pp 17–44.
(27) Willner, I. Stimuli-Controlled Hydrogels and Their Applications. *Acc. Chem. Res.* **2017**, *50* (4), 657–658.
(28) Tamayol, A.; Akbari, M.; Zilberman, Y.; Comotto, M.; Lesha, E.; Serex, L.; Bagherifard, S.; Chen, Y.; Fu, G.; Ameri, S. K.; et al. Flexible PH-Sensing Hydrogel Fibers for Epidermal Applications. *Adv. Healthc. Mater.* **2016**, *5* (6), 711–719.
(29) Ferruti, P.; Marchisio, M. A.; Duncan, R. Poly(Amido-Amine)s: Biomedical Applications. *Macromol. Rapid Commun.* **2002**, *23* (5–6), 332–355.
(30) Ferruti, P. Poly(Amidoamine)s: Past, Present, and Perspectives. *J. Polym. Sci. Part A Polym. Chem.* **2013**, *51* (11), 2319–2353.
(31) Kharkar, P. M.; Rehmann, M. S.; Skeens, K. M.; Maverakis, E.; Kloxin, A. M. Thiol-Ene Click Hydrogels for Therapeutic Delivery. *ACS Biomater. Sci. Eng.* **2016**, *2* (2), 165–179.
(32) Peppas, N. A.; Huang, Y.; Torres-Lugo, M.; Ward, J. H.; Zhang, J. Physicochemical Foundations and Structural Design of Hydrogels in Medicine and Biology. *Annu. Rev. Biomed. Eng.* **2000**, *2* (1), 9–29.
(33) Carraher, C. E.; Jr. Introduction to Polymer Chemistry,. **2006**, *58* (11), 528.
(34) Augst, A. D.; Kong, H. J.; Mooney, D. J. Alginate Hydrogels as Biomaterials. *Macromol. Biosci.* **2006**, *6* (8), 623–633.
(35) Bruchet, M.; Melman, A. Fabrication of Patterned Calcium Cross-Linked Alginate Hydrogel Films and Coatings through Reductive Cation Exchange. *Carbohydr. Polym.* **2015**, *131*, 57–64.
(36) Shi, Y.; Wang, Z.; Zhang, X.; Xu, T.; Ji, S.; Ding, D.; Yang, Z.; Wang, L. Multi-Responsive Supramolecular Hydrogels for Drug Delivery. *Chem. Commun.* **2015**, *51* (83), 15265–15267.

(37) Xu, X. D.; Liang, L.; Chen, C. S.; Lu, B.; Wang, N. L.; Jiang, F. G.; Zhang, X. Z.; Zhuo, R. X. Peptide Hydrogel as an Intraocular Drug Delivery System for Inhibition of Postoperative Scarring Formation. *ACS Appl. Mater. Interfaces* **2010**, *2* (9), 2663–2671.
(38) Tang, C.; Miller, A. F.; Saiani, A. Peptide Hydrogels as Mucoadhesives for Local Drug Delivery. *Int. J. Pharm.* **2014**, *465* (1–2), 427–435.
(39) Li, L.-M.; Han, M.; Jiang, X.-C.; Yin, X.-Z.; Chen, F.; Zhang, T.-Y.; Ren, H.; Zhang, J.-W.; Hou, T.-J.; Chen, Z.; et al. Peptide-Tethered Hydrogel Scaffold Promotes Recovery from Spinal Cord Transection via Synergism with Mesenchymal Stem Cells. *ACS Appl. Mater. Interfaces* **2017**, *9* (4), 3330–3342.
(40) Smith, D. J.; Brat, G. A.; Medina, S. H.; Tong, D.; Huang, Y.; Grahammer, J.; Furtmüller, G. J.; Oh, B. C.; Nagy-Smith, K. J.; Walczak, P.; et al. A Multiphase Transitioning Peptide Hydrogel for Suturing Ultrasmall Vessels. *Nat. Nanotechnol.* **2016**, *11* (1), 95–102.
(41) Schild, H. G. Poly (N-Isopropylacrylamide): Experiment , Theory and Application. *Prog. Polym. Sci.* **1992**, *17*, 163–249.
(42) Zhang, J.; Cui, Z.; Field, R.; Moloney, M. G.; Rimmer, S.; Ye, H. Thermo-Responsive Microcarriers Based on Poly(N-Isopropylacrylamide). *Eur. Polym. J.* **2015**, *67*, 346–364.
(43) Okano, T.; Bae, Y. H.; Jacobs, H.; Kim, S. W. Thermally On-off Switching Polymers for Drug Permeation and Release. *J. Control. Release* **1990**, *11* (1–3), 255–265.
(44) Schmaljohann, D. Thermo- and PH-Responsive Polymers in Drug Delivery. *Adv. Drug Deliv. Rev.* **2006**, *58* (15), 1655–1670.
(45) Patenaude, M.; Hoare, T. Injectable, Degradable Thermoresponsive Poly(Nisopropylacrylamide) Hydrogels. *ACS Macro Lett.* **2012**, *1* (3), 409–413.
(46) Teodorescu, M.; Andrei, M.; Turturicə, G.; Stənescu, P. O.; Zaharia, A.; Sârbu, A. Novel Thermoreversible Injectable Hydrogel Formulations Based on Sodium Alginate and Poly(N-Isopropylacrylamide). *Int. J. Polym. Mater. Polym. Biomater.* **2015**, *64* (15), 763–771.
(47) Chou, P. Y.; Chen, S. H.; Chen, C. H.; Chen, S. H.; Fong, Y. T.; Chen, J. P. Thermo-Responsive in-Situ Forming Hydrogels as Barriers to Prevent Post-Operative Peritendinous Adhesion. *Acta Biomater.* **2017**, *63*, 85–95.
(48) Ma, Z.; Nelson, D. M.; Hong, Y.; Wagner, W. R. A Thermally Responsive Injectable Hydrogel Incorporating Methacrylate-Polylactide for Hydrolytic Lability. *Biomacromolecules* **2011**, *11* (7), 1873–1881.
(49) Wu, C.; Wang, X. Globule-to-Coil Transition of a Single Homopolymer Chain in Solution. *Phys. Rev. Lett.* **1998**, *80* (18), 4092–4094.
(50) Yag-Howard, C. Sutures, Needles, and Tissue Adhesives: A Review for Dermatologic Surgery. *Dermatologic Surg.* **2014**, *40* (SUPPL. 9), 3–15.
(51) Deolekar, S.; Thakur, B. A.; Bairolia, K.; Deolekar, S.; Jan, S. J. Comparison of Conventional Suturing and Tissue Adhesive (2-Octyl Cyanoacrylate) for Port Site Skin Closure in Laparoscopic Surgeries. **2017**, *4* (1), 204–208.
(52) Stavropoulos, S. N.; Modayil, R.; Friedel, D. Current Applications of Endoscopic Suturing. *World J. Gastrointest. Endosc.* **2015**, *7* (8), 777.
(53) Bhat, Y. M.; Banerjee, S.; Barth, B. A.; Chauhan, S. S.; Gottlieb, K. T.; Konda, V.; Maple, J. T.; Murad, F. M.; Pfau, P. R.; Pleskow, D. K.; et al. Tissue Adhesives: Cyanoacrylate Glue and Fibrin Sealant. *Gastrointest. Endosc.* **2013**, *78* (2), 209–215.

(54) Scognamiglio, F.; Travan, A.; Rustighi, I.; Tarchi, P.; Palmisano, S.; Marsich, E.; Borgogna, M.; Donati, I.; De Manzini, N.; Paoletti, S. Adhesive and Sealant Interfaces for General Surgery Applications. *J. Biomed. Mater. Res. - Part B Appl. Biomater.* **2016**, *104* (3), 626–639.
(55) Spotnitz, W. D. Fibrin Sealant: The Only Approved Hemostat, Sealant, and Adhesive—a Laboratory and Clinical Perspective. *ISRN Surg.* **2014**, *2014*, 1–28.
(56) Abel, M. E.; Chiu, Y. S. Y.; Russell, T. R.; Volpe, P. A. Autologous Fibrin Glue in the Treatment of Rectovaginal and Complex Fistulas. *Dis. Colon Rectum* **1993**, *36* (5), 447–449.
(57) Silver, F. H.; Wang, M. C.; Pins, G. D. Preparation and Use of Fibrin Glue in Surgery. *Biomaterials* **1995**, *16* (12), 891–903.
(58) Losi, P.; Burchielli, S.; Spiller, D.; Finotti, V.; Kull, S.; Briganti, E.; Soldani, G. Cyanoacrylate Surgical Glue as an Alternative to Suture Threads for Connective Tissue Graft in Gingival Recession: A Case Report. *J. Surg. Res.* **2010**, *163*, 53–58.
(59) Bot, G.; Bot, K.; Ogunrantu, J.; Onah, J.; Sule, A.; Hassan, I.; Dung, E. The Use of Cyanoacrylates in Surgical Anastomosis: An Alternative to Microsurgery. *J. Surg. Tech. Case Rep.* **2010**, *2* (1), 44–48.
(60) Leggat, P. A.; Kedjarune, U.; Smith, D. R. Toxicity of Cyanoacrylate Adhesives and Their Occupational Impacts for Dental Staff. *Ind Heal.* **2004**, *42* (2), 207–211.
(61) Leggat, P. A.; Smith, D. R.; Kedjarune, U. Surgical Applications of Cyanoacrylate Adhesives: A Review of Toxicity. *ANZ J. Surg.* **2007**, *77* (4), 209–213.
(62) Annabi, N.; Zhang, Y. N.; Assmann, A.; Sani, E. S.; Cheng, G.; Lassaletta, A. D.; Vegh, A.; Dehghani, B.; Ruiz-Esparza, G. U.; Wang, X.; et al. Engineering a Highly Elastic Human Protein-Based Sealant for Surgical Applications. *Sci. Transl. Med.* **2017**, *9* (410).
(63) Lang, N.; Pereira, M. J.; Lee, Y.; Friehs, I.; Vasilyev, N. V.; Feins, E. N.; Ablasser, K.; O'Cearbhaill, E. D.; Xu, C.; Fabozzo, A.; et al. A Blood-Resistant Surgical Glue for Minimally Invasive Repair of Vessels and Heart Defects. *Sci. Transl. Med.* **2014**, *6* (218).
(64) Bouten, P. J. M.; Zonjee, M.; Bender, J.; Yauw, S. T. K.; Van Goor, H.; Van Hest, J. C. M.; Hoogenboom, R. The Chemistry of Tissue Adhesive Materials. *Prog. Polym. Sci.* **2014**, *39* (7), 1375–1405.
(65) Smart, J. D. The Basics and Underlying Mechanisms of Mucoadhesion. *Adv. Drug Deliv. Rev.* **2005**, *57* (11), 1556–1568.
(66) Bhalekar, M. R.; Bargaje, R. V.; Upadhaya, P. G.; Madgulkar, A. R.; Kshirsagar, S. J. Formulation of Mucoadhesive Gastric Retentive Drug Delivery Using Thiolated Xyloglucan. *Carbohydr. Polym.* **2016**, *136*, 537–542.
(67) Mansuri, S.; Kesharwani, P.; Jain, K.; Tekade, R. K.; Jain, N. K. Mucoadhesion: A Promising Approach in Drug Delivery System. *React. Funct. Polym.* **2016**, *100*, 151–172.
(68) Khutoryanskiy, V. V. Advances in Mucoadhesion and Mucoadhesive Polymers. *Macromol. Biosci.* **2011**, *11* (6), 748–764.
(69) Khademhosseini, A.; Langer, R. Microengineered Hydrogels for Tissue Engineering. *Biomaterials* **2007**, *28* (34), 5087–5092.
(70) Autumn, K.; Sitti, M.; Liang, Y. A.; Peattie, A. M.; Hansen, W. R.; Sponberg, S.; Kenny, T. W.; Fearing, R.; Israelachvil, J. N.; Full, R. J. Evidence for van Der Waals Adhesion in Gecko Setae. *PNAS* **2002**, *99* (19), 12252–12256.
(71) Mahdavi, A.; Ferreira, L.; Sundback, C.; Nichol, J. W.; Chan, E. P.; Carter, D. J.

D.; Bettinger, C. J.; Patanavanich, S.; Chignozha, L.; Ben-Joseph, E.; et al. A Biodegradable and Biocompatible Gecko-Inspired Tissue Adhesive. *Proc. Natl. Acad. Sci.* **2008**, *105* (7), 2307–2312.

(72) Lee, H.; Lee, B. P.; Messersmith, P. B. A Reversible Wet/Dry Adhesive Inspired by Mussels and Geckos. *Nature* **2007**, *448* (7151), 338–341.

(73) Autumn, K.; Gravish, N. Gecko Adhesion: Evolutionary Nanotechnology. *Philos. Trans. R. Soc. A Math. Phys. Eng. Sci.* **2008**, *366* (1870), 1575–1590.

(74) Kim, J. K.; Varenberg, M. Biomimetic Wall-Shaped Adhesive Microstructure for Shear-Induced Attachment: The Effects of Pulling Angle and Preliminary Displacement. *J. R. Soc. Interface* **2017**, *14* (137).

(75) Lee-Kong, S.; Feingold, D. L. The History of Minimally Invasive Surgery. *Semin. Colon Rectal Surg.* **2013**, *24* (1), 3–6.

(76) Hatzinger, M.; Kwon, S. T.; Langbein, S.; Kamp, S. Hans Christian Jacobaeus: Inventor of Human Laparoscopy and Thoracoscopy. *J. Endourol.* **2006**, *20* (11), 848–850.

(77) Lee, P.; Mathur, P. N.; Colt, H. G. Advances in Thoracoscopy: 100 Years since Jacobaeus. *Respiration* **2010**, *79* (3), 177–186.

(78) Semm, K.; Mettler, L. Technical Progress in Pelvic Surgery via Operative Laparoscopy. *Am. J. Obstet. Gynecol.* **1980**, *138* (2), 121–127.

(79) Semm, K. Endoscopic Appendectomy. *Endoscopy* **1983**, *15*, 59–64.

(80) Litynski, G. S. Erich Mühe and the Rejection of Laparoscopic Cholecystectomy (1985): A Surgeon Ahead of His Time. *JSLS* **1998**, *2* (4), 341–346.

(81) Esposito, C.; St. Peter, S. D.; Escolino, M.; Juang, D.; Settimi, A.; Holcomb, G. W. Laparoscopic Versus Open Inguinal Hernia Repair in Pediatric Patients: A Systematic Review. *J. Laparoendosc. Adv. Surg. Tech.* **2014**, *24* (11), 811–818.

(82) Cloney, M. B.; Goergen, J. A.; Bohnen, A. M.; Smith, Z. A.; Koski, T.; Dahdaleh, N. The Role of Minimally Invasive Techniques in Scoliosis Correction Surgery. *Minim. Invasive Surg.* **2018**, *2018*.

(83) Arulampalam, T.; Patterson-Brown, S.; Morris, A. J.; Parker, M. C. Natural Orifice Transluminal Endoscopic Surgery. *Ann. R. Coll. Surg. Engl.* **2009**, *91* (6), 456–459.

(84) Sheu, E. G.; Rattner, D. W. Natural Orifice Transluminal Endoscopic Surgery (NOTES^{TM}). In *The SAGES Manual: Operating Through the Endoscope*; Kroh, M., Reavis, K. M., Eds.; SAGES, **2016**; p 463.

(85) Falconi, M.; Pederzoli, P. The Relevance of Gastrointestinal Fistulae in Clinical Practice: A Review. *Gut* **2001**, *49 Suppl 4*, iv2-10.

(86) Botezatu, I.; Marinescu, R.; Laptoiu, D. Minimally Invasive – Percutaneous Surgery – Recent Developments of the Foot Surgery Techniques. **2015**, *8*, 87–93.

(87) Guarracino, F.; Cabrini, L.; Baldassarri, R.; Petronio, S.; De Carlo, M.; Covello, R. D.; Landoni, G.; Gabbrielli, L.; Ambrosino, N. Noninvasive Ventilation for Awake Percutaneous Aortic Valve Implantation in High-Risk Respiratory Patients: A Case Series. *Journal of cardiothoracic and vascular anesthesia*. **2010**, pp 3124–3130.

(88) Pendyala, L.; Jabara, R.; Robinson, K.; Chronos, N. Passive and Active Polymer Coatings for Intracoronary Stents: Novel Devices to Promote Arterial Healing. *J. Interv. Cardiol.* **2009**, *22* (1), 37–48.

2. Poly(amidoamine)s: a rational study

In the previous chapter, we have introduced hydrogels, which are a class of materials that includes a broad spectrum of substances, with a wide range of different chemical, physical and biological properties. Among all the possible alternatives, we have focused on a specific class of synthetic hydrogels: poly(amidoamine)s.

The use of hydrogels for medical applications has some important constraints that need to be addressed carefully. Primarily, the final material must be non-cytotoxic, biocompatible and it needs to have tailored mechanical properties for the intended applications. It should also be cheap, simple to prepare, easy to use for doctors or surgeons and, preferably, it should not require any new device to be applied - thus fitting well within existing technologies and protocols.

Poly(amidoamine)s are promising candidates for applications in surgery and biomedicine, because they combine the use of mild synthetic conditions - such as room temperature, use of water as a solvent and absence of radical initiators – with excellent biocompatibility, injectability, low price of the starting reagents and a great flexibility in the molecular backbone that allows for an easy functionalization.

In the first part of this chapter, we analyze the structure and general properties of these materials and we describe how we tuned their rheological properties and kinetic of gelation.

In the second part, we show that it is to synthesize microgels based on PAAm hydrogels and, as a proof of concept, we investigate their use for drug delivery and cell encapsulation.

2.1 Poly(amidoamine)s - chemistry and state of the art

Poly(amidoamine)s (PAAm) are a class of covalent, synthetic hydrogels first introduced by Paolo Ferruti in 1967 and since then extensively studied.[1] Today, more than 32.000 patents have been reported on PAAm (Source: Google patents), with possible applications in many different field, from drug delivery to resins.[2–4] In general, there are two very different systems that have been employed under the name "poly(amidoamine)s": these are dendrimer-like poly(amidoamine)s particles (so called "PAMAM") and linear or crosslinked polymers ("PAAm"). These last ones are the main topic of this thesis.

The general synthetic scheme for a PAAm hydrogel is shown in ***Figure 2.1a***. From a chemical point of view, PAAm hydrogels are formed by an aza-Michael polyaddition of

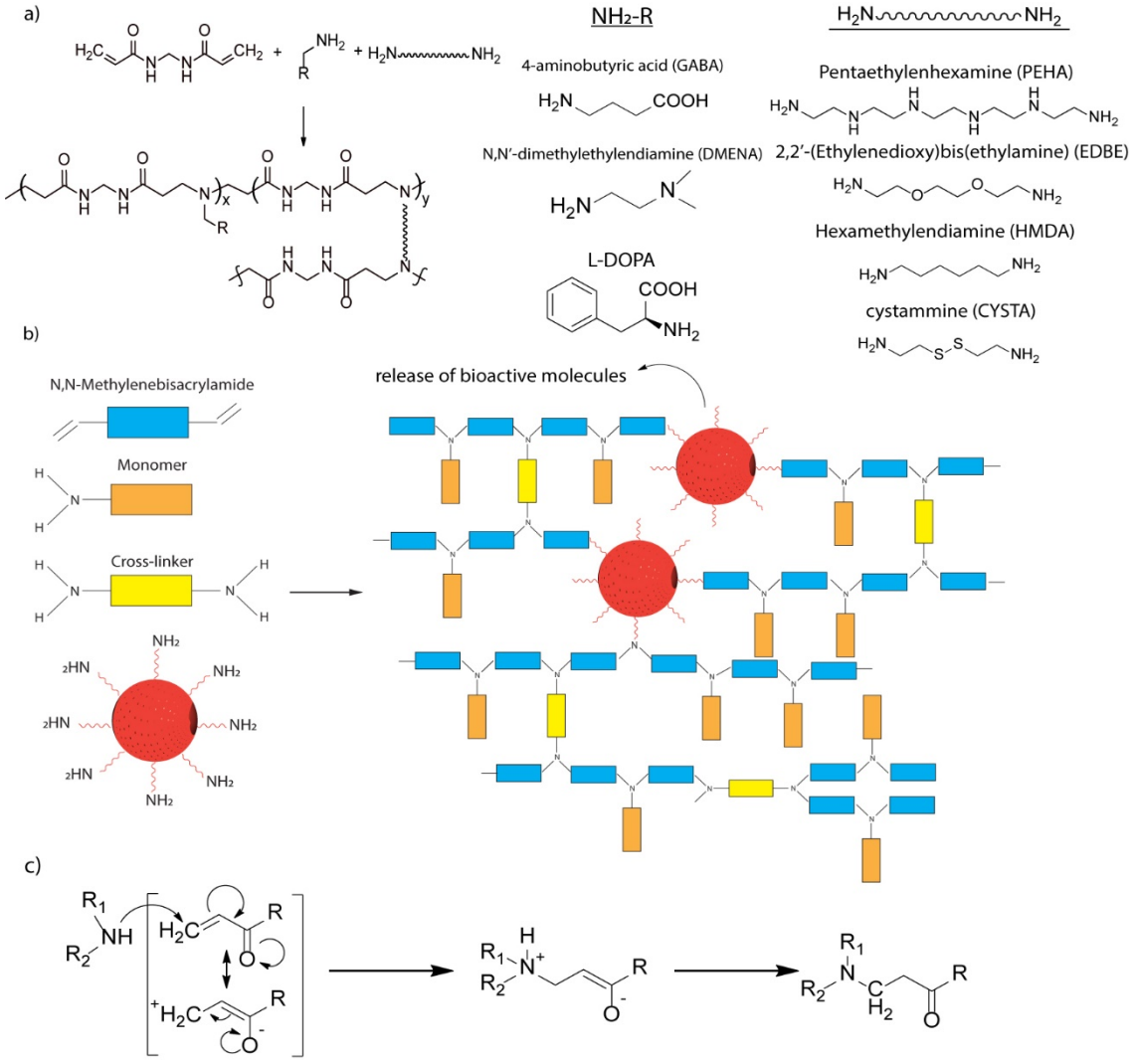

Figure 2.1 Reaction scheme for the synthesis of a PAAm hydrogel (a). The good reactivity of amino groups allows the functionalization of the material with nanoparticles, to obtain hybrid materials (b). Reaction mechanism of an aza-Michael reaction (c).

a nucleophilic primary or secondary amine (Michael donor) to a conjugated double bond (Michael acceptor).[5] At first, the monomers react to form soluble oligomers, and a clear homogeneous pre-gel solution is obtained. The viscosity of the pre-gel solution remains almost constant for a certain period, from ten minutes to several hours, until complete gelation (i.e. the elastic modulus become higher than the viscous modulus) occurs in approximately five minutes. The polymerization proceeds in water, at room temperature, and no radical initiator or catalyst are required. The most common approach consists in using N,N'-methylenebisacrylamide (MBA) as a Michael acceptor, a monoamine to extend the chain and to add specific pending groups to the molecular backbone, and a secondary diamine as crosslinker. This allows a great degree of freedom in the functionalization of the material, because any amino-containing structure can be employed as co-reactant. For example, it is possible to obtain hybrid materials by adding mesoporous silica nanoparticles with the surface functionalized with amino groups. These nanoparticles can give to the material special properties, such as the ability to release enzymes or any bioactive molecules (***Figure 2.1b***). Any protic solvent can be used for the synthesis, such as methanol or ethanol. However, the best results are obtained in water, with significant higher yields than other solvents, and reaction rates more than 10 times faster compared to organic solvents.[6] As shown in ***Figure 2.1c***, the reaction mechanism involves a stepwise addition of the lonely pair of the amine nitrogen on the terminal carbon of the conjugated double bond. A protic solvent is mandatory to stabilize the partial negative charge on the carbonyl oxygen in the first step of the reaction and, overall, to neutralize the zwitterionic intermediate.

Various considerations need to be made on the reactivity of the amino group. As expected, secondary amines react faster than primary amines because of the higher nucleophilicity due to the hyperconjugative effect of the alkyl groups. Steric hindrance also plays an important role and may negatively influence the reaction outcome. A complete review on this topic was published in 2017 by François Ganachaud.[5]

In ***Figure 2.1a*** are reported some of the crosslinkers and monoamines that have been employed in this work.

The reaction occurs only in basic conditions. Normally, the amines used for the reaction are basic enough to act not only as nucleophiles but also as bases. However, in certain cases it may be necessary to add an external base to promote the reaction, such as a non-

reactive amine (as triethylamine) or an inorganic hydroxide, such as LiOH. Alkaline metals salts have also been suggested as possible catalyst for the reaction.[7]

Laura Hartmann and coworkers[8,9] have reported the use of an innovative method to synthetize PAAm with highly controllable structures using a solid-phase synthesis that allows a very precise control of the chemical structure of the final product. This method was employed to add breakable crosslinkers to the structure, looking for possible future applications in drug delivery.

PAAm have been widely employed in biomedicine for several purposes,[10] such as drug and gene delivery[11–15], 3D-cell cultures,[16,17] DNA complexation[18] and regenerative medicine.[19] Recently, in our group we have shown that PAAm hydrogels can be covalently-linked to mesoporous silica nanoparticles and that this nanocomposite material is able to release bioactive molecules - such as SDF-1α - and support the growth of bone-marrow mesenchymal stem cells.[20]

2.2 Properties of poly (amido amine)s hydrogels

2.2.1 Rational design of the material

The great versatility of PAAm, in terms of chemical and mechanical characteristics, offers a broad window of opportunity in the biomedical area. Each specific application requires a careful study in order to propose the best material for the intended use, which then translates into a process of development and characterization of the material and a complete analysis of its properties.

The following chapters describe the design and optimization of several hydrogels to be used for some specific applications in gastrointestinal and general surgery - such as fistula closure, tumor resection or hernia repair. Several parameters were considered throughout the investigation, together with the biocompatibility. These include the price of the starting reagents, the easiness of the synthesis and of the injection, the gelation time *in-vivo*, the ability to adhere to the surrounding tissues, the elasticity of the material and its degradation in presence of body fluids or cells.

In this chapter, we evaluate in general terms how factors such as the crosslinking degree, synthetic conditions and chemical composition influence some of the properties of the material, such as the equilibrium degree of swelling, the gelation time and the mechanical characteristics.

As first step, we should reflect on how to design the basic skeleton of the material, that can be modified in order to tackle each specific usage. As discussed in the introduction to this chapter, PAAm are formed through an aza-Michael polyaddition of a nucleophile - the Michael donor - to the activated double bond of a Michael acceptor, like α,β-unsaturated carbonyl compounds. Different Michael acceptors have been reported in literature, for example 2,2-bis(acrylamido)acetic acid[16] or polyethylene glycol diacrylate[21] or other derivatives containing breakable functional groups.[22] For the work reported in this thesis, we decided to use N,N'-methylenebisacrylamide (MBA) as a Michael-acceptor because of the low toxicity, low price and wide availability.

A secondary diamine (i.e. a tetra-functional Michael donor) was employed as a crosslinker, in order to achieve the formation of a complete 3D network, instead of a linear polymer. Several molecules can be used for this purpose, and some are reported in ***Figure***

2.1a. The choice of the crosslinker is of primary importance, because it will influence not only the mechanical properties, but also the gelation time. Moreover, some diamines are toxic and volatile and thus their use in injectable materials should be avoided when possible. We decided to use pentaethylenhexamine (PEHA) as a standard reference polyamine for our materials because of the low volatility and the possibility of reaction also of the secondary amines of the chain, that allow for a greater flexibility in the material design. Other diamines have also been tested, such as ethylendiamine or hexamethylendiamine, but gelation times were usually longer, and the useful concentration range was narrower.

An interesting opportunity is to use amino acid or other natural products as crosslinkers, such as L-Lysine. However, in these cases it may be necessary to add a base to promote the reaction and the gelation time may become extremely long.[23]

The material obtained by the reaction of MBA alone with a crosslinker is normally very rigid and fragile[1] and the lack of elasticity is detrimental for most applications in surgery. The use of a monoamine as a monomer in the polymerization reaction thus can be beneficial to increase the elasticity of the material. We decided to use γ-aminobutyric acid (GABA) as a monoamine in the formulation of the hydrogel, because of its biocompatibility, low cost and because it can form non-covalent links - in particular hydrogen bonds - between the entangled chains of the hydrogel, thus favoring elasticity and cohesivity.

What described before is the composition of the basic skeleton of the hydrogel synthetized during this thesis; such composition and monomers choice was then differently tuned for each specific application, as described in the next chapters.

2.2.2 Influence of the polyamine crosslinker on mechanical properties

Factors such as the degree of crosslinking and the length of the crosslinker are crucial for the kinetic of formation, the swelling and the mechanical properties of hydrogels.[24] In the next paragraph, we describe how crosslinking influences swelling and gelation kinetic.

It is generally accepted that increasing the degree of crosslinking in a hydrogel will lead to an increase of the elastic modulus. For example, it has been reported from Nermin

Orakdogen and Oguz Okay[25] that in poly(acrylamide) hydrogels obtained by free-radical crosslinking copolymerization of acrylamide and N,N'-methylenebisacrylamide (MBA) the elastic modulus G' was getting higher at increasing concentrations of MBA. However, also other factors need to be considered, such as how well the chains are solvated, their rigidity and the presence of charges.[26]

To investigate how elasticity and rigidity of PAAm hydrogels are influenced by the nature and concentration of the crosslinker, we have performed uniaxial compression tests on hydrogels obtained with different crosslinkers at different concentrations.

Hydrogel cylinders were obtained by pouring the pre-gel solutions in aluminum molds and waiting at least 48 hours after the beginning of gelation, to ensure that the reaction was completed. Each hydrogel was then cut in slices of approximately 6-10 mm of height and 12 mm of diameter, the dimensions of each sample was accurately measured to calculate the surface area *A,* and a compression ramp was executed with a 35 mm plate-plate geometry at a speed of 0.01 mm/s.

In ***Figure 2.2*** we report the behavior of a typical PAAm hydrogel under compression stress. A small layer of low-viscosity silicon oil was applied on the two plates of the instruments and on the top of the hydrogel to allow free slippage and reduce friction stress.[27] Normal force F_n is recorded as a function of gap *l* and the experiment is continued until complete failure of the material or until the maximum normal force allowed by the instrument is reached.

For a perfect elastic solid, it is possible to write that the stress $\sigma = \frac{F_n}{A}$ is directly proportional to the strain $\varepsilon = \frac{\Delta l}{l_0}$, with l_0 being the initial height of the sample. However, as it is possible to observe from Figure 2.2 *Compression test on hydrogel cylinders*, the compression of the material in the z-axis leads to a deformation in the perpendicular x-

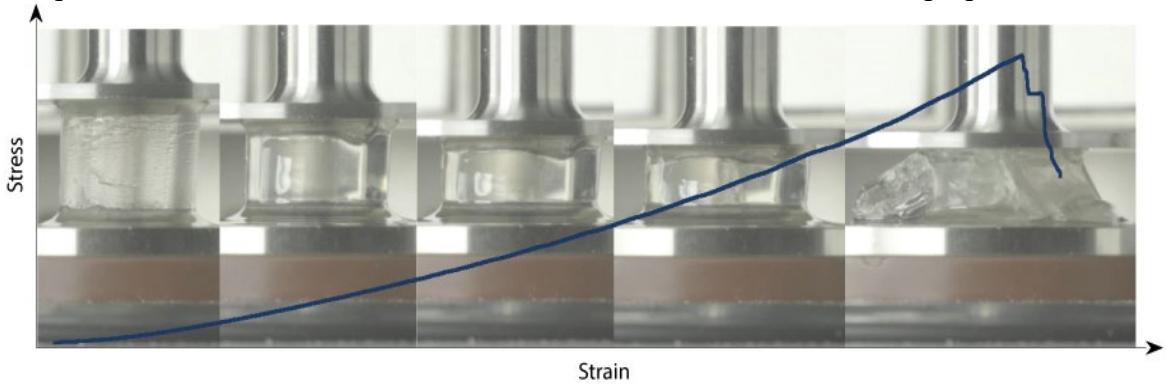

Figure 2.2 Compression test on hydrogel cylinders

and y-axis. If for small deformation this phenomenon - known as barreling effect - is negligible, it becomes important at higher deformation. To compensate for this,[28,29] in the case of soft hydrogel it is possible to write:

$$\sigma = -E(\lambda - \lambda^{-2}) \quad (1)$$

with $\lambda = \frac{l}{l_0}$.

It is possible to demonstrate[30] that in general the compressive elastic modulus E is linked to the shear modulus G through the relationship $E = 2G\,(1 + v)$, with v being the Poisson's ratio of the material. For ideal rubber-like materials,[31] $v=0.5$ and thus $E = 3G$. Hydrogels are normally considered to have $0.4<v<0.5$, even if some exceptions exist. [32,33]

In ***Figure 2.3a*** are reported the stress-strain curves of four different PAAm hydrogels prepared with increasing concentration of PEHA as a polyamine crosslinker. The hydrogels behave as an elastic brittle solid with an extended linear range and a sharp, total

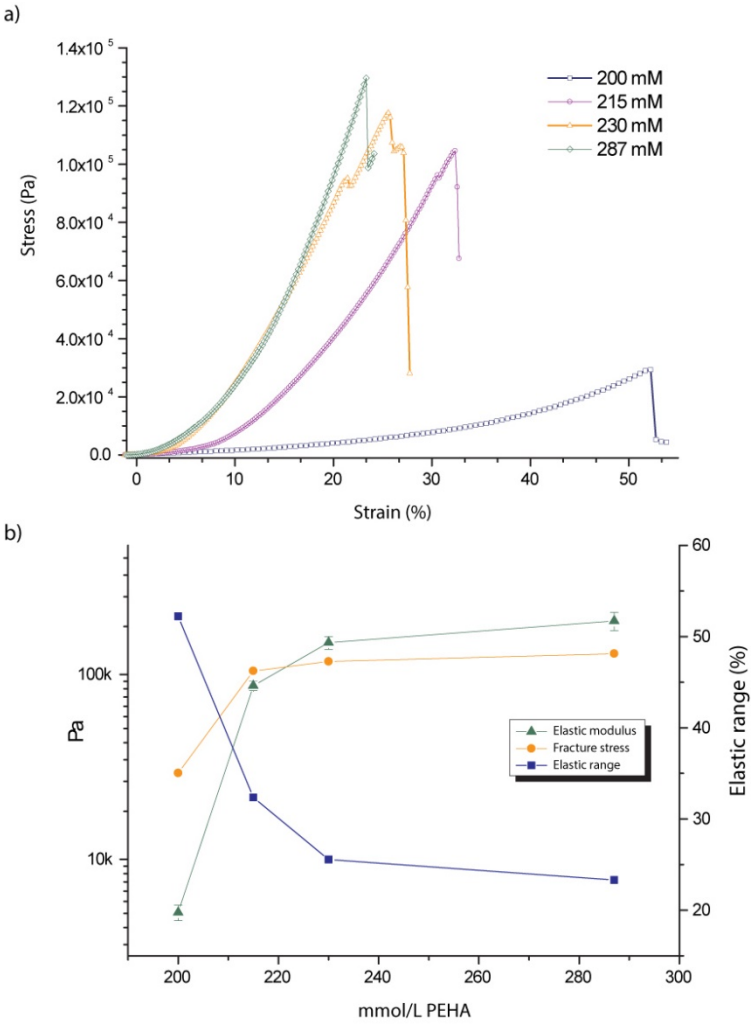

Figure 2.3 Stress-strain curves for PAAm hydrogels with [MBA]=0.864 M, [GABA]=0.323 M and [PEHA]= 0.200 M (blue), 0.215 M (violet), 0.230 M (orange) and 0.287 M (green).

failure at the fracture stress. As the concentration of crosslinker increases, the linear elastic range decreases while the fracture stress increases. This is more evident in ***Figure 2.3b***, where it is possible to observe how the elastic modulus E and the fracture stress σ_{max} increases with the concentration of PEHA. The elastic modulus was calculated by interpolation of the stress-strain curves with Equation (1) between 10 and 15% strain for each sample. For each composition, three samples were measured, and the final error expressed taking into account also the error in the measure of the diameter of the samples (+/- 0.05 mm).

2.2.3 Kinetic of gel formation

The synthesis and gelation of the PAAm hydrogel can be mainly divided in three phases. First, all the reagents - MBA, monoamine and crosslinker - are mixed together with water in a vial and warmed at 37 °C. The solubility of MBA in water at room temperature is low (20 g/L at 20 °C), and an initial suspension is thus obtained. After some minutes, when the reaction starts, the mixture turns to a homogeneous and injectable low-viscosity fluid. The material keeps this behavior for a certain time, from 30 min to several hours - or even days depending on the reaction conditions - and then it suddenly turns into an elastic hydrogel. The possible injection window of the material corresponds to the time between the homogenization of the initial suspension and the final gelation and it is critical to control it accurately.
For biomedical applications of such hydrogels, there are three different needs to be considered:

a) The injectable solution must be obtained in a simple and fast way by the medical personnel in the operating room;
b) The injection window must be as broad as possible to accommodate for complications during the surgery or the preparation of the patient;
c) After injection, the hydrogel should solidify in a reasonable short time, in order to avoid diffusion outside the interested area.

To have a complete understanding of the synthesis and formation process, we have analyzed gelation kinetic in different conditions, for example by changing the concentration of the reactants or the temperature.

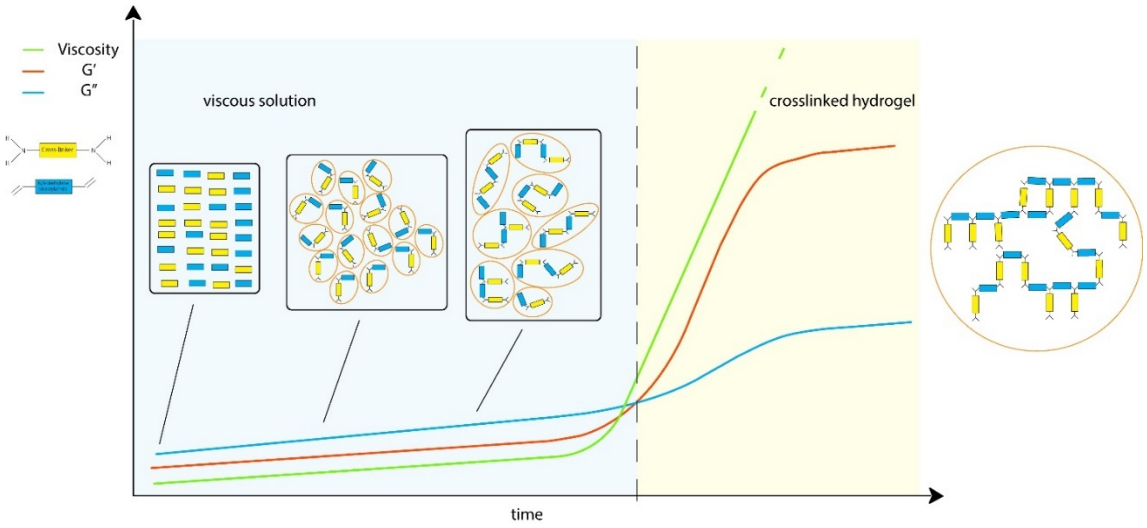

Figure 2.4 Mechanism of step-growth polymerization.

As we have reported in the introduction, the polymerization of PAAm hydrogels follow a step-growth mechanism, as depicted in ***Figure 2.4***.

At the beginning of the reaction, the monomers react to form low-molecular weight oligomers. This first step corresponds to the initial dissolution phase of the monomer mixture. After all the monomers have reacted to form dimers, these react to form trimers and tetramers, and so on. In general, a complex mixture of oligomers with different molecular weight is obtained, with the average molecular weight slowly increasing with time.

An interesting result of this mechanism is that the molecular weight of the oligomers - and thus the viscosity of the solution (green line) - grows very slowly for a long period of time, before starting to increase steadily at a critical time point. For crosslinked networks formed by multifunctional monomers, this point corresponds to the start of gelation. Rheological measures can be employed to unequivocally measure the gelation time by analyzing how the elastic modulus G' and the loss modulus G'' changes with time. When the reaction starts, the solution behaves like a low-viscosity semi-ideal fluid. The loss module (blue line) is higher than the elastic modulus (red line), and both have very low values. During the growth phase - as the viscosity of the solution increases - both G' and G'' slowly increase, but the phase-shift angle (δ) remains constant near 80-90°. After a

condition-dependent critical time, viscosity starts to increase abruptly and G' increases faster than G''.

Gelation occurs when G'= G'' and δ= 45°, thus indicating the transition between a viscous solution (blue zone of the graphic) and an elastic gel (yellow zone). After some minutes, G' becomes several orders of magnitude higher than G'' and δ≈ 0°, indicating the formation of a quasi-ideal elastic solid.

We have investigated this process for our hydrogel using a Thermofischer HAAKE Mars 40 rheometer equipped with a cylindrical coaxial 25 mm geometry and a solvent trap to avoid solvent loss due to evaporation. This geometry was chosen to avoid solvent evaporation during gelation, a process extremely difficult to avoid using plate-plate or cone-plate geometries, even when equipped with a solvent trap.

The mixture of monomers, water and crosslinker was stirred in a closed vial placed on a thermostatically-controlled water bath. When the solution became homogeneous, it was transferred in the cup of the coaxial geometry, pre-warmed together with the upper rotor at the proper temperature. The hydrogel was covered with a thin layer of low-viscosity silicon oil to prevent solvent evaporation, and the viscosity of the solution was recorded over time at a shear rate of 10 s^{-1}. The instrument was set to automatically switch to the oscillation mode (f= 0.5 Hz, γ=1%) when η ($\dot{\gamma}$=10 s^{-1})> 0,1 Pa·s.

In ***Figure 2.5*** are reported the shear viscosity and the oscillatory rheology at 37 °C of a pre-gel solution composed by [MBA]=0.864 M, [GABA]=0.323 M and [PEHA]= 0.215 M. It is possible to see that for the first 140 minutes from the start of the synthesis the viscosity is almost constant, near a fixed value η ($\dot{\gamma}$=10 s^{-1}) ≈ 0.01 Pa·s. For comparison, in the same conditions η_{water} ($\dot{\gamma}$=10 s^{-1}) ≈ 0.001 Pa·s. Between 140 and 150 minutes the viscosity increases from 0.015 Pa·s to 0.04 Pa·s, then it starts to increase asymptotically. Oscillation rheology shows that in these conditions the material is still a very viscous fluid, and gelation occurs at about 155 minutes when G'=G''. Gelation occurred in about five minutes over more than two hours and a half of synthesis!

This behavior is indeed of great interest and we hypothesized that we can use this peculiar kinetic to develop an injectable material.

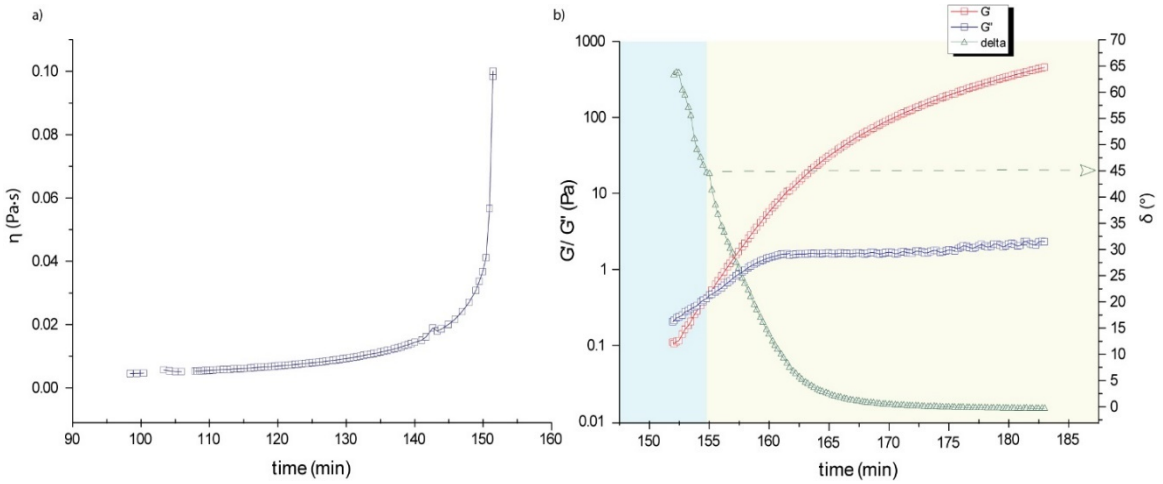

Figure 2.5 Gelation kinetic at 37 °C of a PAAm hydrogel composed by [MBA]=0.864 M, [GABA]=0.323 M and [PEHA]= 0.215 M. Shear viscosity (γ=10 s^{-1}) (a) and oscillation rheology (f= 0.5 Hz, γ= 1%) (b) as a function of time from the start of the synthesis.

In ***Figure 2.6*** is reported the gelation time at 25 °C for some hydrogels containing increasing amount of crosslinker, in particular ethylendiamine (ENA) and pentaethylehexamine. Hydrogels synthesized using PEHA as a crosslinker form generally faster and the useful molar ratio of crosslinker is broader in comparison to ENA, ranging from 12% to more than 45%. With ethylendiamine the useful range is between 24 and 38%, with higher amount hindering gelation.

In ***Figure 2.7*** the gelation time is reported at fixed concentration of MBA and variable concentration of GABA and PEHA at 37°C. From Figure 2.a it is possible to observe that gelation time is directly proportional to the concentration of γ-aminobutyric acid, while increasing the concentration of pentaethylenhexamine in the range between 180 and 400 mM produces an exponential decrease in gelation time.

Gelation times were measured by keeping approximately constant the concentration of GABA while varying the concentration of PEHA and vice versa, while the concentration of MBA was kept fixed at 0.864 M. At an approximately fixed concentration of [GABA]= 300 mM, the useful range of concentration for PEHA to obtain gelation goes from 180 to 400 mM. By considering that each double bond reacts with one amino group and by hypothesizing that only the terminal amino groups of PEHA reacts, we would obtain that gelation happens with a ratio double bond/amino groups from 1.30 to 0.78, with an ideal ratio being 1 (i.e. [PEHA]= 280 mM for [GABA]=300 mM).

This great variability can be explained by considering the possibility of more than two amino groups reacting for each molecule of PEHA at lower concentration, and less than

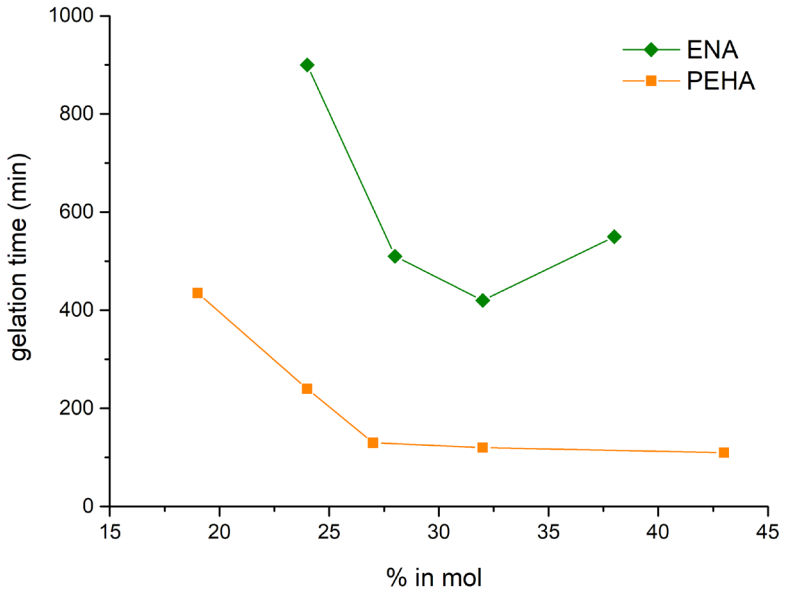

Figure 2.6 Gelation time for hydrogels containing increasing amount of diamine crosslinker at fixed concentrations of [GABA]=0.323 M and [MBA]= 0.864 M

two at higher concentration. This can be confirmed by gelation time - that decrease only of 10-20 minutes at [PEHA] >> 300 mM - and by the elastic modulus, that at higher concentration of PEHA stops increasing, indicating that the maximum degree of crosslinking has been reached.

We have attempted to mathematically fit the gelation kinetic curves in order to obtain an expression of gelation time as a function of the concentration of starting materials, keeping the concentration of MBA as a fixed reference. The fit was done with the software Origin by hypothesizing an exponential decrease of gelation time as a function of [PEHA] and a linear increase as a function of [GABA], thus considering appropriate an equation such as:

$$t = k_{PEHA} e^{-\frac{[PEHA]}{t_0}} + k_{GABA}[GABA] \qquad (2)$$

where k_{PEHA} and k_{GABA} are the kinetic constants of PEHA and GABA. ***Figure 2.7b*** shows that the calculated and theoretical value are in good accordance, considering that the experimental error in gelation time is on average of 5 minutes. However, this expression is purely experimental-based, and it is valid only in the range of concentrations normally used. No attempts to give a theoretical description or a general kinetic equation will be made.

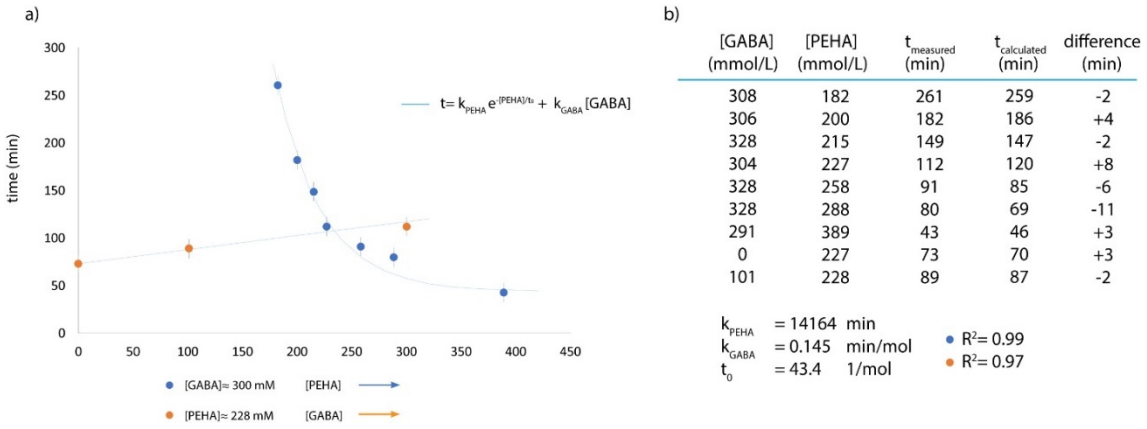

[GABA] (mmol/L)	[PEHA] (mmol/L)	$t_{measured}$ (min)	$t_{calculated}$ (min)	difference (min)
308	182	261	259	-2
306	200	182	186	+4
328	215	149	147	-2
304	227	112	120	+8
328	258	91	85	-6
328	288	80	69	-11
291	389	43	46	+3
0	227	73	70	+3
101	228	89	87	-2

Figure 2.7 Gelation time at 37 °C and fixed concentration [MBA]= 0.864 M and [GABA]= 0.3 M (blue dots) and at fixed concentration [MBA]= 0.864 M and [PEHA]= 0.228 M (orange dots). Blue line, fitting curve $t=k_{PEHA}e^{-[PEHA]/t} + k_{GABA}[GABA]$ (a). Measured and calculated value of gelation time for different samples (b).

2.2.4 Swelling and porosity

Swelling is an important parameter in hydrogel characterization, because the passage from the dry collapsed state to the swollen state is linked to an increase in biocompatibility, porosity, and a faster nutrients and oxygen diffusion. (***Figure 2.8***).

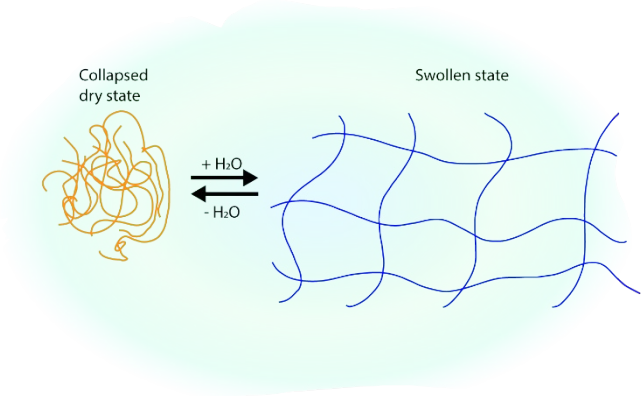

Figure 2.8 Schematic structure of a hydrogel in his collapsed (left) and swollen state (right).

In general, the swelling ability of a certain hydrogel is function of different parameters,[34–38] such as the degree of crosslinking, the presence of charges, the nature of the solvent, the ionic strength or the pH. In simple systems, the increase in crosslinking and elastic modulus leads to a reduced swelling, while the presence of charges can increase the swelling. For amphoteric materials, such as PAAm hydrogels, the situation is more complicated, because an increase in crosslinking leads also to an increase in charge

concentration: moreover, the relationship between the pH and the amount of charged group becomes more complex in such systems.

In ***Figure 2.9*** is reported the equilibrium water content of hydrogels synthesized with different crosslinkers in different concentrations at pH=2, 5, 7.4 and 9. Three different crosslinkers were employed: ethylendiamine (23 and 37% molar ratio), hexamethylendiamine (HMDA, 13 and 23%) and pentaethylenhexamine (12-22%). For hexamethylendiamine and ethylendiamine the concentration range of crosslinker is limited and it was not possible to match the two concentrations. We have thus selected a range of concentrations for PEHA that is comparable to that of HMDA, in order to compare the two longer crosslinkers.

As shown in ***Figure 2.9c-f***, the kinetic of swelling seems to be independent of pH and in any case a stable equilibrium degree of swelling was observed between 2 and 5 h. The equilibrium water content (EWC) can be defined as $EWC = \frac{W_{wet} - W_{dry}}{W_{wet}}$ where W_{wet} and W_{dry} represent the mass of the hydrogel sample after and before swelling.

For all the materials analyzed, the experiment was performed by freeze-drying the hydrogels, recording the weight of the dry hydrogel, soaking it in a buffer solution and weighting the swollen hydrogel at defined time points. At least three samples were employed for each hydrogel at each pH. After the end of the measurement, each sample was lyophilized, covered with a 10 nm layer of gold and its morphology was observed at SEM. The hydrogels, as expected, showed a porous structure with polydisperse pore in the range of 50-200 μm, thus allowing cell penetration and colonization. No significative difference was observed between the different samples, except for an apparent higher porosity for hydrogels containing 12% PEHA **(*Figure 2.9b*)**.

Porosity is the first requirement to allow cells to penetrate and populate the gel. The mean diameter and the shape of the pores determine the diffusion rate of oxygen and nutrients, therefore the extent to which cells can proliferate inside the hydrogel scaffold. In addition, cells must be able to move in the gel and to proliferate and/or differentiate. These last processes are strongly influenced by the morphology of the scaffold.[38b] For example, pores of 5-15 μm are reported to be suitable for fibroblast proliferation, while bigger pores, in the range of 20-125 μm, are required for mature mammalian cells.[38c]

The EWC of the hydrogels shows a strong dependence on the amount of crosslinker and on the pH. Except for the ENA 37%, all the hydrogels show a maximum swelling at pH=5.

Interestingly, a higher amount of crosslinker seem to be positively linked with an increase in swelling at lower pH, while at higher pH the behavior is reversed for ENA and HDMA hydrogels.

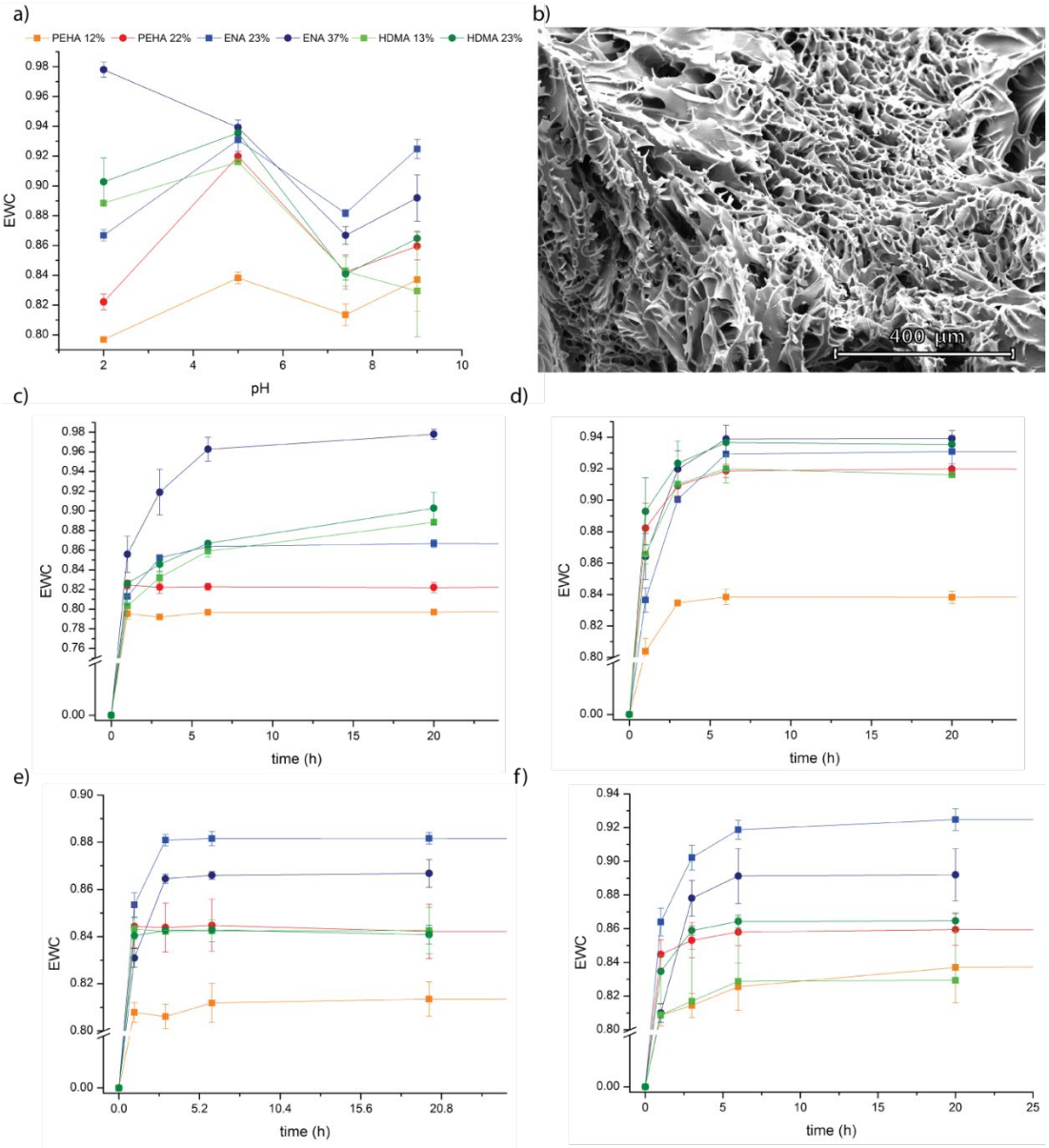

Figure 2.9 Equilibrium water content of hydrogels synthesized with different crosslinkers in function of the pH (a). SEM of a lyophilized hydrogel after swelling (b). Swelling kinetic at pH=2 (c), pH= 5 (d), pH=7.4 (e) and pH=9 (f).

2.3 PAAm-based microgel particles

Once we have analyzed how different factors, such as the concentration of crosslinking, influence the properties of the bulk hydrogel. We also investigated the possibility to use the same material for obtaining hydrogel microparticles, envisaging their use for different purposes: from drug delivery to cell encapsulation.

Usually, the term "nanogel" is used when referring to hydrogel particles of less than 100 nm in diameter, while the terms "microgel" or "microbeads" are preferred when considering particles between 100 nm and 100 μm.[39] Also, the term "nanosphere" will be used to specify that the internal structure of the particles is composed by a 3D hydrogel network, while with "nanocapsules" or "core-shell" nanoparticles we will refer to particles composed by an outer polymeric layer and an inner aqueous core (***Figure 2.10***). In contrast to hard particles, such as inorganic ones, hydrogel particles may contain important amount of solvent even in their collapsed state. Also, their swelling properties can be easily controlled, and it is possible to design systems that swell in different ways depending on the pH, ionic strength, redox potential, temperature or composition of the solvent.[40]

By taking advantage of these properties, it is possible to variate hydrogel particles volume, pore size, mesh size or surface potential by changing the conditions of their chemical

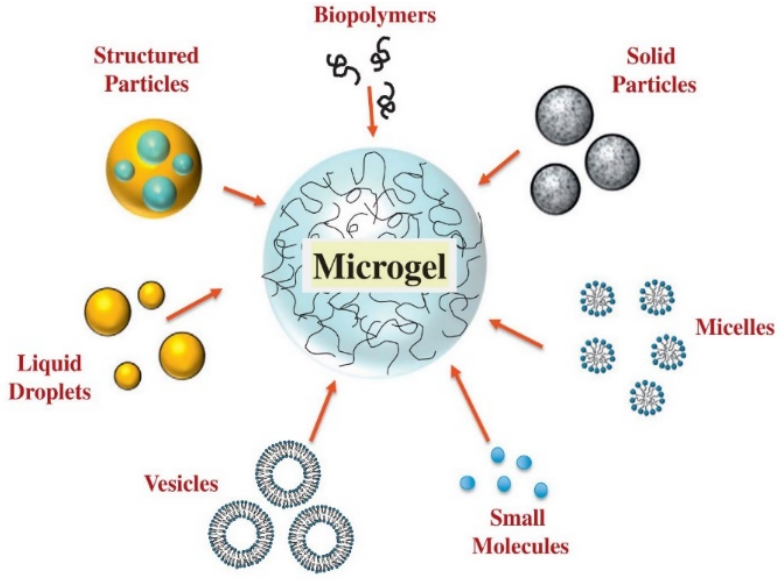

Figure 2.10 Different cargos can be loaded onto microgel systems. Reproduced with permission from: 10.1016/j.cis.2016.12.005

surrounding. This allow the design of particles for drug delivery with variable pore size, that can release their cargo very gradually or only under very specific conditions.[41]

Several applications for microgels and nanogels are reported in literature.[42,43] For example, R. J. Composto *et al.* used a dextran/lysozyme-based core-shell nanogel system to cover silver nanoparticles that could be used for antibacterial applications.[44] In this case, the hydrogel coating was used limit cellular uptake, and thus toxicity, while increasing the antibacterial efficacy.

J. Zach Hilt and coworkers used pH-responsive hydrogel nanoparticles - composed by methacrylic acid and poly (ethylene glycol) diacrylate - for pulmonary drug delivery, while thermo-responsive multi-shell hollow nanogels based on PNIPAm have been reported in 2016 by Potemkin and Richtering.[45] In a similar way, many other systems have been reported exploiting bigger microgel particles for drug delivery.[46,47]

Another challenge involves the development of novel biomaterials in which living eukaryotic or bacterial cells can be encapsulated, leading to potential applications in agriculture, medicine, vaccines, food industry, biocatalysis *et cetera*. For example, microgel particles can be used to protect living cells from the immune system for transplant in diabetic patients.[48–50] Also, the gastrointestinal microbiota plays different important roles in human physiology and some pathologies have been linked to imbalance in the amount, typology and location of the symbiont bacteria of the human body.[51]

An important step in this direction was first example of encapsulation reported by Chang in 1964,[52] who used polymer microcapsule to encapsulate erythrocytes hemosylate. After this study, most scientists focused their research on natural polymers, alginate in the first place,[51,53] but also hyaluronic acid, collagen or chitosan have been used.[54]

Different techniques exist for the preparation of hydrogel particles, such as droplet microfluidic,[55] surfactant-free precipitation,[56] micro- and nano-emulsions, reverse-phase emulsification, polymerization in template and many others.[40]

The most common methods employed for cell encapsulation are schematized in ***Figure 2.11***. In the simple extrusion method, drop of the cell-containing pre-gel solution reacts with a second solution that triggers an immediate gelation. This method is widely used with alginate-based systems, that immediately gel in contact with solutions containing calcium ions.

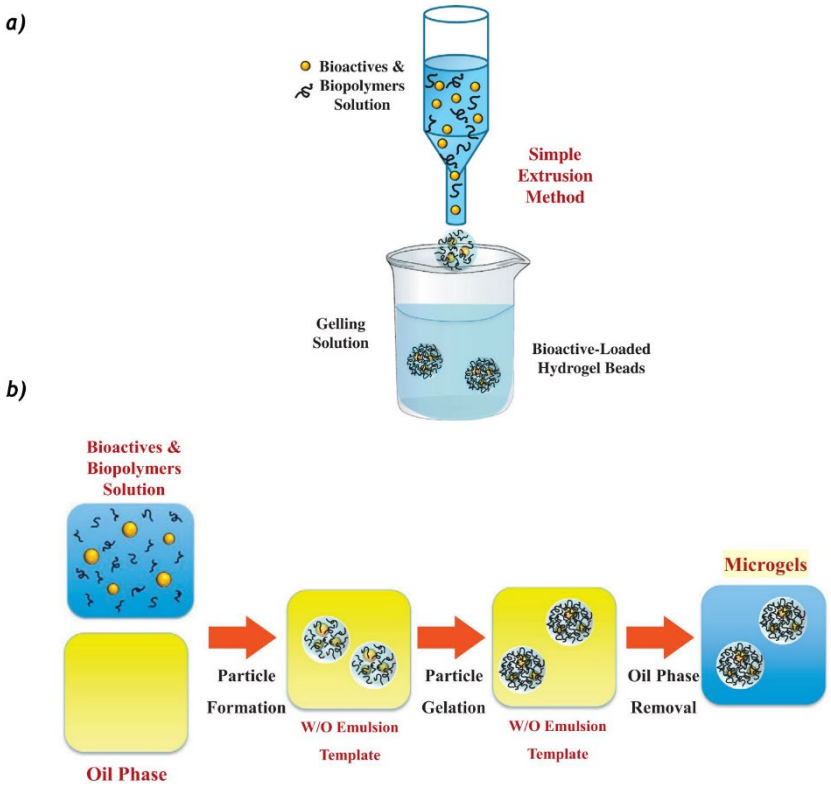

Figure 2.11 Scheme of the two most common methods for the preparation of microgel and tliving-cell encapsulation: simple extrusion method (a) and emulsification method (b). Reproduced with permission from 10.1016/j.cis.2016.12.005

Another method consists in preparing a microemulsion of the pre-gel solution, normally a water-in-oil (W/O) emulsion, and then let the crosslinking reaction to start leading to a microgel dispersion, that need to be purified from the oil and the surfactants.[57]

2.3.1 Hydrogel microparticles for antibiotic delivery

Considering the kinetic of gelation of PAAm hydrogel, we decided to employ the microemulsion method for the synthesis of the microgel (MGs). In particular, we planned to inject the pre-gel PAAm solution into a mixture of apolar organic solvent and surfactant – under strong stirring or under sonication – until gelation was completed, to wash then the particles with ethanol and water to remove all the unreacted surfactant.

In a typical procedure, a pre-gel solution composed by [MBA]= 864 mM, [PEHA]= 280 mM for [GABA]=300 mM is flash-injected in a mixture of cyclohexane and surfactant under vigorous stirring. The mixture is left under stirring overnight.

In the first set of trials, this procedure was performed with different surfactants in different concentrations, such as sodium dodecyl sulphate (SDS), Bis(2-ethylhexyl) sulfosuccinate sodium salt (AOT) or Triton^{TM} X-100 (Triton-x). However, an amorphous jelly material was obtained in all the cases.

The procedure was then modified by using sonication instead of stirring to form the emulsion.

200 μL of the pre-gel solution, prepared as before, were injected in 35 mL of a mixture of cyclohexane and surfactant and left under sonication overnight. The day after, water was added to the mixture to extract the particles, and the aqueous phase was collected, centrifuged and washed with 50% EtOH, pure ethanol, then 50% ethanol again, and finally three times with water. After freeze-drying, a fine powder was obtained.

In ***Figure 2.12*** we show the SEM pictures obtained after the synthesis and purification of microgel particles in different conditions. Different surfactants at diverse concentrations were used. With SDS, only amorphous material was obtained in all the cases.

In ***Figure 2.12a*** we report the best result obtained using AOT as a surfactant. The particles obtained were aggregated and polydisperse, with diameters ranging from 0.1 to 10 μm. Better results were obtained with Triton-X. In ***Figure 2.12b*** we report the material obtained using 16% of Triton-X as a surfactant together with 16% n-hexanol as a stabilizer. We hypothesized that n-hexanol could help to stabilize the emulsion, but unfortunately the result achieved was not as good as expected.

We then investigate the effect of the stage of formation of the pre-gel at the moment of injection on the morphology of the final material. ***Figure 2.12c-d*** show the results of the injection of the hydrogel in 7.5% Triton-X in cyclohexane at 70% of the gelation time (c) and at 90% of the gelation time (d). Late-injection start to show the formation of particles embedded in amorphous material. Changing the concentration of Triton-X to 20% (e) or 15% (f) allowed the formation of a more regular material, with polydisperse particles of average diameter 1± 0.5 μm, and yield of 75% in respect to the mass of the injected hydrogel.

Despite the polydispersity of the particles, we proceeded to test if they could be useful for the delivery of antibiotics as a model cargo.

First, we tested if the MG particles showed any sign of toxicity toward bacteria. Two different microorganisms were used, the gram-negative *E. coli* and the gram-positive *S. aureus*.

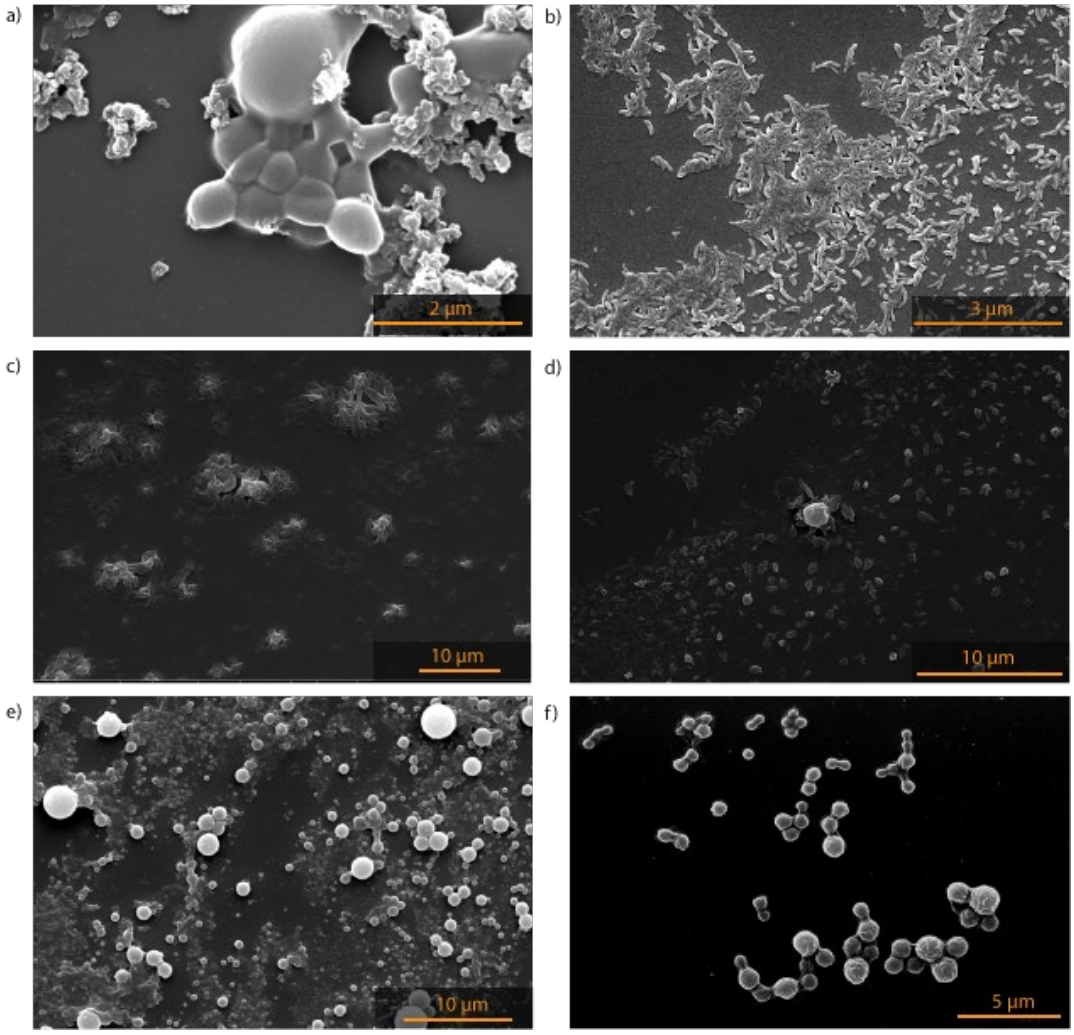

Figure 2.12 SEM images of microgel synthesized with the microemulsion method. Microgel prepared in cyclohexane with 3% AOT (a); 16% Triton-x and 16% n-hexanol (b); 7.5% Triton-x (c); 7.5% Triton-x and late injection (d); 20% Triton-x and late injection (e); 15% Triton-x and late injection (f).

The following experiments were performed by the author in the laboratory of Prof. Olof Ramstrom at KTH, Stockholm, in the framework of the European project that supported my PhD.

The growth curve for each bacterium was obtained, in triplicate, by measuring over time the optical density (OD) of a suspension obtained diluting 500 µL of bacteria in the log phase at OD= 0.5 in 6.5 mL of LB II broth at 37 °C. Each point was measured in triplicate and each experiment was performed first in pure LB II broth and after in a 1 mg/mL suspension of MGs in LB II broth. As shown in ***Figure 2.13a,*** no effect of the MG was observed on the growth of bacteria, confirming that the microgels are non-toxic for the bacteria.

In a second experiment, we studied the effect of an antibiotic loaded into the MG.

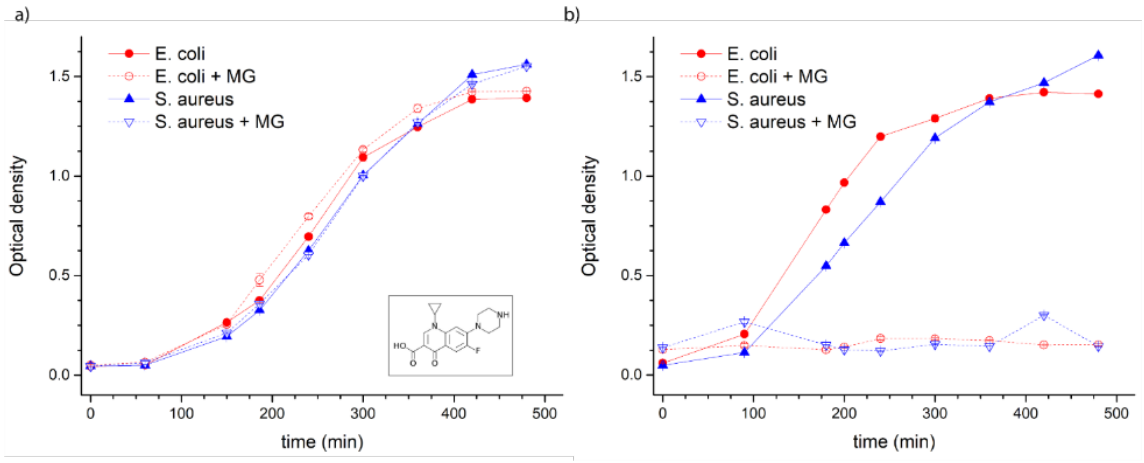

Figure 2.13 Growth curve for *E. Coli* and *S. Aureus* at 37 °C in LB II broth with and without 1 mg/mL pristine MG particle (a) or with and without ciprofloxacin-loaded 0.1 mg/mL MG particles. Inset: Structure of Ciprofloxacin

We selected ciprofloxacin as a model cargo, because of its low solubility in water at physiological pH and higher solubility in pH=2 HCl buffer. This property makes ciprofloxacin suitable for a simple loading at low pH and a slow release at neutral pH. Also, similar hydrogel systems have already been proposed for the delivery of ciprofloxacin,[58,59] confirming the validity of our model.

The particles were loaded by preparing a dispersion of 47.2 mg/mL MGs in a 375 µg/mL solution of ciprofloxacin in a pH=2 HCl buffer. After one night under stirring, the particles were centrifuged, washed with five portions of distilled water and freeze-dried. The loading efficiency and the exact kinetic of release were not determined, but they will be evaluated in future experiments.

To confirm that the loading was effective, the previous experiment was repeated, and the growth curves of *E. coli* and *S. aureus* were obtained in pure culture media and in 0.1 mg/mL dispersion of MGs loaded with ciprofloxacin (***Figure 2.13b***). Considering a theoretical loading of 100%, this would lead to a final concentration of ciprofloxacin of 8 µg per mg of microgel, or 0.8 µg/mL in the final bacteria solution considering also a 100% release. This concentrations were chosen by taking into accounts that the minimum inhibitor concentration of ciprofloxacin to inhibit 50% of the bacterial cells (MIC 50) for *E.Coli* K12 is 8 ng/mL,[60] while the MIC 50 for *S. Aureus* is 250 ng/mL.[61] We expect to see a stop in the growth of *E. Coli* if the efficiency of the combined loading/release process is higher than 1%, and we expect to see an influence also on *S. Aureus* if the efficiency is higher than 25%. As reported in ***Figure 2.13b,*** a 0.1 mg/mL of loaded MG

solution was able to completely stop the growth of both *E.Coli* K12 and *S. Aureus* ATCC® 29213.

2.3.4 Hydrogel microparticles for bacteria encapsulation

The previous experiment showed that pristine MG particles are not-toxic for bacterial cells. Thus, we decided to investigate whether PAAm-based MG could be used for bacteria encapsulation. Indeed, the most commonly used material for this purpose, calcium alginate, is difficult to functionalize, it is not breakable, and it is not resistant to the acidic pH of the stomach.

PAAm microgels, on the other side, can be appropriately designed to be stimuli-responsive or to break only in very specific situations, such as in the intestine but not in the stomach.

The microgel were synthesized by emulsion polymerization as before, however the pre-gel solution was prepared at 37 °C using culture media, instead of distilled water, as a solvent. We planned to add the bacteria to the pre-gel solution immediately before the preparation of the emulsion.

The synthetic strategy that we have chosen before is not directly applicable to systems containing living cells, because of the use of toxic organic solvents and surfactants. To solve these issues, we decided to investigate the formation of microgel particles employing vegetable oils and food-grade surfactants for the preparation of the emulsion. First, we investigated if the bacteria would survive in the pre-gel solution, that possesses a higher-than-normal pH that can be detrimental for bacteria viability even if prepared using culture media as a solvent. A quick assessment was done by using *S. salivarious* bacteria as a model organism. $1x10^6$ cells were mixed with the pre-gel solution prepared with [MBA]= 864 mM, [PEHA]= 280 mM for [GABA]=300 mM. The bacteria were previously stained with the Hoechst staining for the nucleus, added to the pre-gel solution in the moment it became homogeneous and immediately after observed using a confocal microscope equipped with a 63x oil-immersion objective. In ***Figure 2.14***, we report confocal images of *S. salivarious* stained with Hoechst 33342 after 1 hour at 37 °C in their usual culture medium (Brain and hearth infusion broth, BHI) and after 1 hours in the

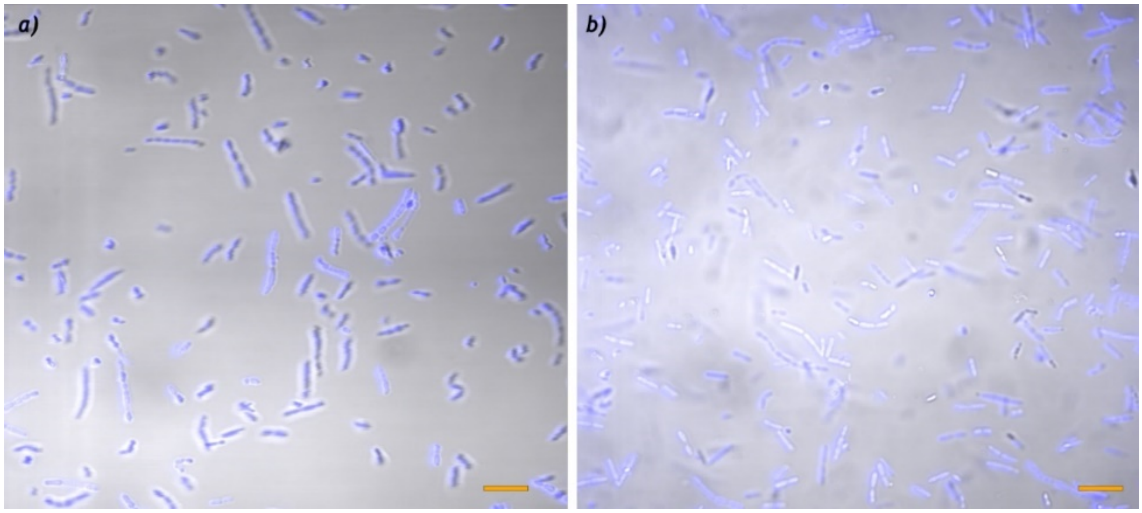

Figure 2.14 *S. Salivarious* stained with Hoechst 33342, exc. 355 nm, observed with a 63x oil-immersion objective in BHI culture medium (a) or in the pre-gel solution, after hydrogel formation (b). Scale bar is 10 µm.

pre-gel solution prepared in BHI, when the hydrogel was formed. In the pre-gel solution the bacteria kept their shape and no release of DNA was observed. The bacteria maintained their usual motility in the pre-gel solution, but stopped moving after the hydrogel was formed, probably because of being entrapped in the hydrogel network. Even if we plan to execute a live/dead assay to confirm the viability of the bacteria, this first experiment strongly suggests that the bacteria should not be harmed by the pre-gel solution.

The synthesis of the microgel was performed using sunflower oil as a non-polar phase for the preparation of the emulsion, while Span 40 was employed as a surfactant because of its biocompatibility.[62]

The use of sonication should be avoided when working with living cells, so we investigated the best conditions to obtain uniform and not-aggregated particles without sonicating. Also, Span 80 was used as a surfactant instead of Span 40 because of its higher solubility in oil at room temperature.

In ***Figure 2.15*** we report the confocal images of MGs obtained by flash-injecting 4% of pre-gel solution – prepared as previously state in this chapter - at 75% or 90% of gelation time (second row), with 0.4% (***Figure 2.15*****a** and **d**) or 3% of Span 80 (***Figure 2.15*****b, c, e** and **f**). Samples **b** and **e** were prepared in static conditions, after preparing the emulsion by energetic manual mixing, while samples **a, c, d** and **f** were prepared under magnetic stirring. A small amount of fluorescein sodium salt was added to the pre-gel solution to better visualize the particles. The results show that static conditions give the best results

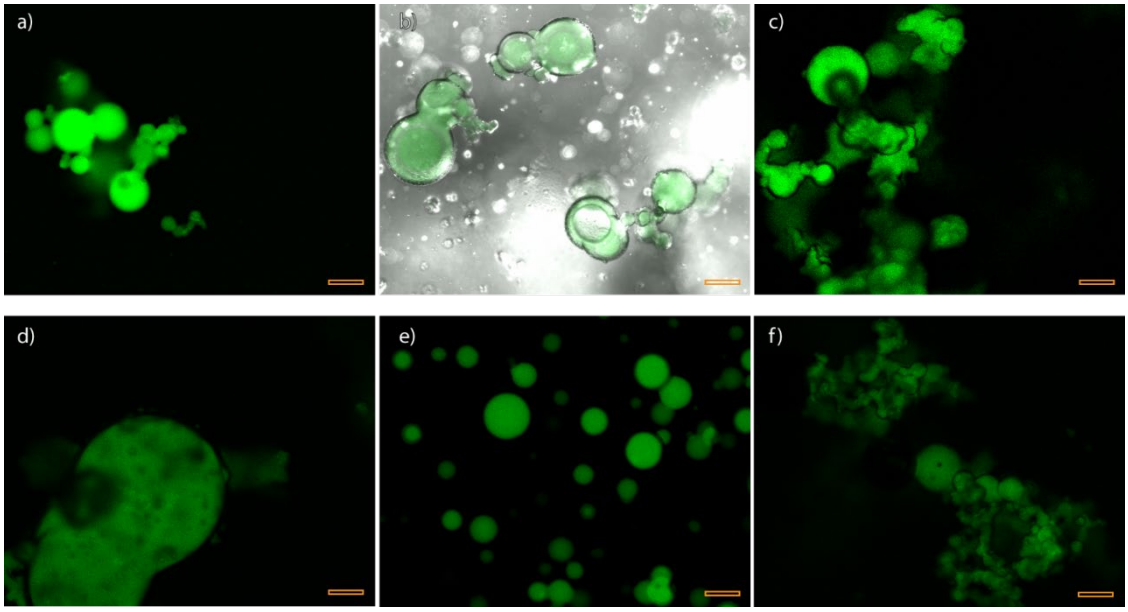

Figure 2.15 Confocal images of PAAm-microgel, stained with fluorescein sodium salt, synthesized in different conditions and with different concentrations of Span 80. 4% pre-gel solution at 75% (first row) or 90% of gelation time (second row), with 0.4% (a and d) or 3% Span 80 (b, c, e and f). Samples b and e were prepared in static conditions, after preparing the emulsion by energetic manual mixing, while samples a, c, d and f were prepared under magnetic stirring.

in terms of homogeneity of the particles and aggregation, while stirring produced large aggregates of particles. The best results were obtained with a 3% concentration of Span 80, with lower concentrations leading to more a disperse system or to particle aggregation.

The experiment was repeated using a degradable hydrogel (dPAAm) synthetized using a redox-responsive disulphide-containing crosslinker – cystamine (CYSTA) – instead of pentaethylenhexamine. We also substituted GABA with N,N-dimethylethylendiamine (DMENA), in order to maintain a basic environment suitable for the aza-Michael addition. The structure of the precursors is reported in ***Figure 2.1*** and a full characterization of this material will be presented in Chapter 3.

The dPAAm pre-gel solution was prepared using [MBA]= 0.864 mM, [DMENA]= 427 mM and [CYSTA]=192 mM and flash injected at 90% of the gelation time in a mixture of sunflower oil with 3% Span 80 at 40 °C, for a final hydrogel concentration of 0.75%. After five minutes of hand-shaking, the emulsion was left to rest overnight in static conditions.

The day after, the particles were washed with saline solution six times and deposited on a SEM sample holder. SEM imaging (***Figure 2.16a***) shows non-aggregated but polydisperse particles in the diameter range 1-10 μm.

The same experiment was repeated in presence of *S. salivarius.* The pre-gel solution was prepared using BHI as a solvent, and 100.000 bacterial cells/mL were added just before flash-injecting the pre-gel in the oil and surfactant mixture. The day after, the particles were washed with three portions of BHI, three portions of saline solutions. A SEM image of the sample is reported in ***Figure 2.16b*** and show bigger particles, with diameter ranging from 5 to 15 µm. Smaller bacteria-like structures were also observed, but it was not possible to univocally identify them.

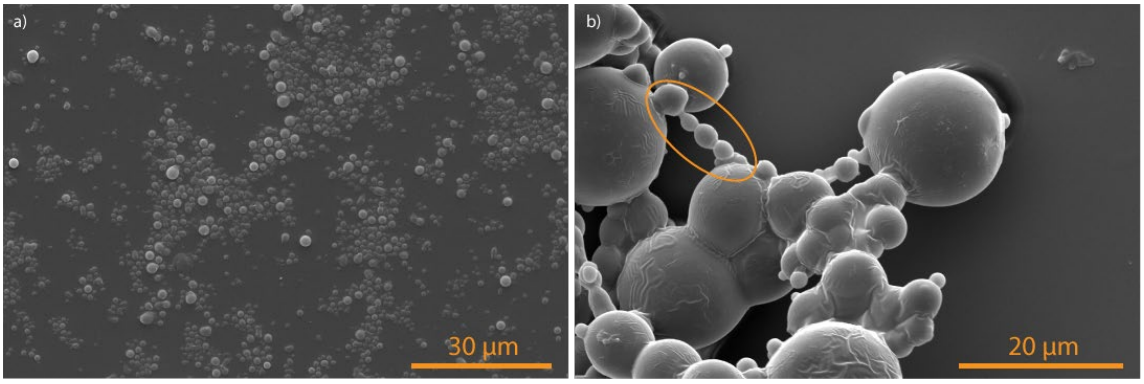

Figure 2.16 dPAAm microgels synthesized in sunflower oil. SEM picture of the pristine material (a) and of the dPAAm prepared in culture media in presence of bacteria (b). In figure (b), the orange circle highlights bacteria-like structures.

2.4 Conclusions

Poly (amido amine)s are a class of synthetic, covalent hydrogels that can be synthetized in water, at room temperature and without any toxic radical initiator.

We have shown that they offer great flexibility in their synthesis and that their molecular backbone can be easily modified to meet the required needs. For example, by appropriately changing the concentration and chemical nature of the crosslinker it is possible to change the reaction kinetic, the swelling and the rheological properties of the material.

The preparation of PAAm-based microparticles has been accomplished and preliminary data show that they are promising materials for drug delivery and cell encapsulation. However, the work conducted was only a preliminary investigation and further experiments are still required. In particular, the synthesis of the microgel need to be optimized to obtain a more monodisperse system and a complete statistical analysis is still missing. Also, the exact kinetic of drug release need to be evaluated and different hydrophilic or hydrophobic drugs could be tested.

We have evidences indicating that the PAAm hydrogels are not toxic for bacteria and we have shown that it is possible to synthetize microgel particles in reacting conditions that are compatible with bacteria cells. However, for the moment we lack conclusive evidences demonstrating that bacteria encapsulation with the proposed method is actually happening. Further experiments will be conducted, such as live/dead staining of bacteria on the bulk hydrogel, cryo-FIB to confirm that the bacteria are encapsulated in the microgel particles, and release of the bacteria from the dPAAm-microgels in order to verify the viability of the bacteria after the process of encapsulation.

2.5 Experimental part

2.5.1 Synthesis of the PAAm hydrogels

In a standard synthesis, 200 mg (1.3 mmol) of MBA and 50 mg (0.48 mmol) of GABA were weighted in a glass vial. 1.5 mL of water were added, together with 75 mg (0.32 mmol) of PEHA. The material was left under magnetic stirring in a water bath at 37 °C, and a homogenous clear solution was formed after 45 minutes. An elastic hydrogel was obtained after 145 minutes.
The synthesis can be modified by changing the temperature, amount of water, concentration and nature of crosslinker and concentration and nature of the monoamine monomer.

2.5.2 Shear rheology

Kinetic measures were performed on a Thermofischer HAAKE Mars 40 rheometer equipped with a Peltier temperature module TM-PE-C for cylinders. A coaxial cylinder geometry composed of the rotor CC25 DIN Ti and the cup CCB25 DIN was used. A pre-gel solution was prepared as reported in the previous paragraph. After equilibration of the geometry at the requested temperature, 17 mL of the pre-gel solution were inserted in the system. The measure was started after five minutes of equilibration and all the data are reported as function of the time from the start of the synthesis of the hydrogel. The shear viscosity of the pre-gel solution was measured at $\dot{\gamma}$=10 s-1. When η> 0.1 Pa·s, oscillation was started at f= 0.5 Hz and γ=1%.

2.5.3 Compression tests and data analysis

Hydrogel cylinders were prepared by pouring the pre-gel solution into an aluminum mold of approximately 2 cm diameter. 24 h after hydrogel formation, the cylinders were carefully removed from the mold and cut in smaller cylinders of approximately 2-5 cm height. The cylinders were covered with a small layer of silicon oil and compression was performed using a 35 mm plate-plate geometry at a 0.02 mm/s speed.

Three samples were measured for each hydrogel. The elastic modulus was determined by fitting the stress-strain curve using the equation:

$$\sigma = -E(\lambda - \lambda^{-2})$$

The interpolation was made in a 10% strain interval comprised between 10 and 30% strain, depending on the sample, because of the small irregularity on their surfaces. The initial height was also considered a free parameter to be optimized, in the range h_0-2%< $h_{optimized}$<h_0.

2.5.4 Microgel particles for drug delivery

200 mg (1.3 mmol) of MBA and 50 mg (0.48 mmol) of GABA were weighted in a glass vial. 1.5 mL of water were added, together with 90 mg (0.39 mmol) of PEHA. The material was left under magnetic stirring in a water bath at 37 °C.

In the meantime, 5 mL of Triton X-100 and 30 mL of cyclohexane were mixed in a 100 mL round-bottom flask and left under sonication. At 90% of the gelation time, 200 µL of the pre-gel solution were quickly injected in the organic phase and the system was left under sonication overnight.

The day after, 20 mL of water were added, and the suspension was centrifuged at 4000 rpm for 20 minutes. The organic phase was removed, and the particles were washed with 50% EtOH, then pure ethanol, 50% ethanol again, and finally three times with water.

After freeze-drying, a white powder was obtained.

Yield: 150 mg (75% compared to an approximate mass of 200 mg of pre-gel solution).

2.5.5 Ciprofloxacin encapsulation

The particles were loaded by preparing a dispersion of 47.2 mg/mL MGs in a 375 µg/mL solution of ciprofloxacin in 0.01 M HCl solution. After one night under stirring, the particles were centrifuged, washed with five portions of cold distilled water and freeze-dried.

2.5.6 Microgel particles for bacteria encapsulation

200 mg of MBA (1.3 mmol) and 65 mg of cystamine dihydrochloride (0.29 mmol) were weighted in a glass vial. 1.5 mL of BHI broth were added, together with 110 mg of N,N-dimethylethylendiamine (1.25 mmol). The material was left under magnetic stirring in a water bath at 40 °C.

In the meantime, a 3% solution of Span 80 mL in 200 mL of sunflower oil was prepared in a 500 mL round-bottom flask, and left under stirring at 40 °C.

At 90% of the gelation time, 150 µL of 1.000.000 CFU/mL *S. salivarius* dispersion was added to the pre-gel solution. The pre-gel/bacteria mixture was quickly injected in the apolar phase, vigorously mixed by hand for 5 minutes and left to rest at 40°C overnight.

The day after, 100 mL of BHI medium were added, and the suspension was centrifuged at 4000 rpm for 10 minutes. The organic phase was removed, and the particles were washed with BHI medium for five times, then one time with saline solution.

References

(1) Ferruti, P. Poly(Amidoamine)s: Past, Present, and Perspectives. *J. Polym. Sci. Part A Polym. Chem.* **2013**, *51* (11), 2319–2353.

(2) Favors, K. D.; Ringold, C. E.; Luo, Y.; Hagiopol, C. Polyamidoamine-Epihalohydrin resins, method of manufacture, and uses thereof. US 8,785,593 B2, **2014**.

(3) Ranucci, E.; Ferruti, P.; Fenili, F.; Manfredi, A.; Mauro, N.; Fernandez-Busquets, X.; Urban, P. Amphoteric Polyamidoamines in the Treatment of Malaria. EP 2 732 821 A1, **2014**.

(4) Allen, A. J.; Sau, A. C. Silyl-linked Polyamidoamine and their preparation. US 6,315,865 B1, **2001**.

(5) Genest, A.; Portinha, D.; Fleury, E.; Ganachaud, F. The Aza-Michael Reaction as an Alternative Strategy to Generate Advanced Silicon-Based (Macro)Molecules and Materials. *Prog. Polym. Sci.* **2017**, *72*, 61–110.

(6) Ranu, B. C.; Banerjee, S. Significant Rate Acceleration of the Aza-Michael Reaction in Water. *Tetrahedron Lett.* **2007**, *48* (1), 141–143.

(7) Zintchenko, A.; Van Der Aa, L. J.; Engbersen, J. F. J. Improved Synthesis Strategy of Poly(Amidoamine)s for Biomedical Applications: Catalysis by "Green" Biocompatible Earth Alkaline Metal Salts. *Macromol. Rapid Commun.* **2011**, *32* (3), 321–325.

(8) Ebbesen, M. F.; Gerke, C.; Hartwig, P.; Hartmann, L. Biodegradable Poly(Amidoamine)s with Uniform Degradation Fragments via Sequence-Controlled Macromonomers. *Polym. Chem.* **2016**, *7* (46), 7086–7093.

(9) Hartmann, L.; Krause, E.; Antonietti, M.; Börner, H. G. Solid-Phase Supported Polymer Synthesis of Sequence-Defined, Multifunctional Poly(Amidoamines). *Biomacromolecules* **2006**, *7* (4), 1239–1244.

(10) Ferruti, P.; Marchisio, M. A.; Duncan, R. Poly(Amido-Amine)s: Biomedical Applications. *Macromol. Rapid Commun.* **2002**, *23* (5–6), 332–355.

(11) Cohen, S.; Coué, G.; Beno, D.; Korenstein, R.; Engbersen, J. F. J. Bioreducible Poly(Amidoamine)s as Carriers for Intracellular Protein Delivery to Intestinal Cells. *Biomaterials* **2012**, *33* (2), 614–623.

(12) Coué, G.; Freese, C.; Unger, R. E.; James Kirkpatrick, C.; Engbersen, J. F. J. Bioresponsive Poly(Amidoamine)s Designed for Intracellular Protein Delivery. *Acta Biomater.* **2013**, *9* (4), 6062–6074.

(13) Van Der Aa, L. J.; Vader, P.; Storm, G.; Schiffelers, R. M.; Engbersen, J. F. J. Intercalating Quaternary Nicotinamide-Based Poly(Amido Amine)s for Gene Delivery. *J. Control. Release* **2014**, *195*, 11–20.

(14) Yu, Z. Q.; Yan, J. J.; You, Y. Z.; Zhou, Q. H. Bioreducible and Acid-Labile Poly(Amido Amine)s for Efficient Gene Delivery. *Int. J. Nanomedicine* **2012**, *7*, 5819–5832.

(15) Pettit, M. W.; Griffiths, P.; Ferruti, P.; Richardson, S. C. Poly(Amidoamine) Polymers: Soluble Linear Amphiphilic Drug-Delivery Systems for Genes , Proteins and Oligonucleotides. *Ther. Deliv.* **2011**, *2* (7), 907–917.

(16) Tocchio, A.; Martello, F.; Tamplenizza, M.; Rossi, E.; Gerges, I.; Milani, P.; Lenardi, C. RGD-Mimetic Poly(Amidoamine) Hydrogel for the Fabrication of Complex Cell-Laden Micro Constructs. *Acta Biomater.* **2015**, *18*, 144–154.

(17) Jacchetti, E.; Emilitri, E.; Rodighiero, S.; Indrieri, M.; Gianfelice, A.; Lenardi, C.; Podestà, A.; Ranucci, E.; Ferruti, P.; Milani, P. Biomimetic Poly(Amidoamine) Hydrogels as Synthetic Materials for Cell Culture. *J. Nanobiotechnology* **2008**, *6*, 1–15.
(18) Hartmann, L.; Häfele, S.; Peschka-Süss, R.; Antonietti, M.; Börner, H. G. Tailor-Made Poly(Amidoamine)s for Controlled Complexation and Condensation of DNA. *Chem. - A Eur. J.* **2008**, *14* (7), 2025–2033.
(19) Magnaghi, V.; Conte, V.; Procacci, P.; Pivato, G.; Cortese, P.; Cavalli, E.; Pajardi, G.; Ranucci, E.; Fenili, F.; Manfredi, A.; et al. Biological Performance of a Novel Biodegradable Polyamidoamine Hydrogel as Guide for Peripheral Nerve Regeneration. *J. Biomed. Mater. Res. - Part A* **2011**, *98 A* (1), 19–30.
(20) Fiorini, F.; Prasetyanto, E. A.; Taraballi, F.; Pandolfi, L.; Monroy, F.; López-Montero, I.; Tasciotti, E.; De Cola, L. Nanocomposite Hydrogels as Platform for Cells Growth, Proliferation, and Chemotaxis. *Small* **2016**, *12* (35), 4881–4893.
(21) Wang, J.; He, H.; Cooper, R. C.; Yang, H. In Situ-Forming Polyamidoamine Dendrimer Hydrogels with Tunable Properties Prepared via Aza-Michael Addition Reaction. *ACS Appl. Mater. Interfaces* **2017**, *9* (12), 10494–10503.
(22) Tenório-Neto, E. T.; Guilherme, M. R.; Lima-Tenório, M. K.; Scariot, D. B.; Nakamura, C. V.; Rubira, A. F.; Kunita, M. H. Synthesis and Characterization of a PH-Responsive Poly(Ethylene Glycol)-Based Hydrogel: Acid Degradation, Equilibrium Swelling, and Absorption Kinetic Characteristics. *Colloid Polym. Sci.* **2015**, *293* (12), 3611–3622.
(23) Manfredi, A.; Ranucci, E.; Morandi, S.; Mussini, P. R.; Ferruti, P. Fast and Quantitative Manganese Sorption by Polyamidoamine Resins. *J. Polym. Sci. Part A Polym. Chem.* **2013**, *51* (4), 769–773.
(24) Okay, O. General Properties of Hydrogels. In *Hydrogel Sensors and Actuators*; Gerlach, G., Arndt, K. F., Eds.; Elsevier, 2010; Vol. 6, pp 1–15.
(25) Orakdogen, N.; Okay, O. Correlation between Crosslinking Efficiency and Spatial Inhomogeneity in Poly(Acrylamide) Hydrogels. *Polym. Bull.* **2006**, *57* (5), 631–641.
(26) Oosten, A. S. Van; Galie, P. A.; Janmey, P. A. Mechanical Properties of Hydrogels. In *Gels Handbook*; Demirci, U., Khademhosseini, A., Eds.; World Scientific, **2016**; pp 67–79.
(27) Steffe, J. F. *Rheological Methods in Food Process Engineering*; Freeman Press, **1996**.
(28) Muniz, E. C.; Geuskens, G. Compressive Elastic Modulus of Polyacrylamide Hydrogels and Semi-IPNs with Poly(N-Isopropylacrylamide). *Macromolecules* **2001**, *34* (13), 4480–4484.
(29) Collins, M. N.; Birkinshaw, C. Physical Properties of Crosslinked Hyaluronic Acid Hydrogels. *J. Mater. Sci. Mater. Med.* **2008**, *19* (11), 3335–3343.
(30) Chippada, U.; Yurke, B.; Langrana, N. A. Simultaneous Determination of Young's Modulus, Shear Modulus, and Poisson's Ratio of Soft Hydrogels. *J. Mater. Res.* **2010**, *25* (3), 545–555.
(31) Mott, P. H.; Roland, C. M. Limits to Poisson's Ratio in Isotropic Materials. *Phys. Rev. B - Condens. Matter Mater. Phys.* **2009**, *80* (13), 1–4.
(32) Takigawa, T.; Morino, Y.; Urayama, K.; Masuda, T. Poisson's Ratio of Polyacrylamide (PAAm) Gels. *Polym. Gels Networks* **1996**, *4* (1), 1–5.
(33) Urayama, K.; Takigawa, T.; Masuda, T. Poisson's Ratio of Poly(Vinyl Alcohol) Gels. *Macromolecules* **1993**, *26* (12), 3092–3096.

(34) Ganji, F.; Vasheghani-Farahani, S.; Vasheghani-Farahani, E. Theoretical Description of Hydrogel Swelling: A Review. *Iran. Polym. J.* **2010**, *19* (5), 375–398.
(35) De, K. S.; Aluru, N. R.; Johnson, B.; Crone, W. C.; Beebe, D. J.; Moore, J. Equilibrium Swelling and Kinetics of PH-Responsive Hydrogels: Models, Experiments, and Simulations. *J. Microelectromechanical Syst.* **2002**, *11* (5), 544–555.
(36) Brannon-Peppas, L.; Peppas, N. A. Equilibrium Swelling Behavior of PH-Sensitive Hydrogels. *Chem. Eng. Sci.* **1991**, *46* (3), 715–722.
(37) Yang, T. *Mechanical and Swelling Properties of Hydrogels*. Doctoral thesis, KTH Stockholm, **2012**.
(38) a) Peppas, N. A.; Huang, Y.; Torres-Lugo, M.; Ward, J. H.; Zhang, J. Physico-chemical Foundations and Structural Design of Hydrogels in Medicine and Biology. *Annu. Rev. Biomed. Eng.* **2000**, *2* (1), 9–29.
b) Loh, Q. L.; Choong, C. Three-Dimensional Scaffolds for Tissue Engineering Applications: Role of Porosity and Pore Size. *Tissue Eng. Part B Rev.* **2013**, 19 (6), 485–502.
c) Staruch, R. M. T.; Glass, G. E.; Rickard, R.; Hettiaratchy, S. P.; Butler, P. E. M. Injectable Pore-Forming Hydrogel Scaffolds for Complex Wound Tissue Engineering: Designing and Controlling Their Porosity and Mechanical Properties. *Tissue Eng. Part B Rev.* **2017**, 23 (2), 183–198.
(39) Hamidi, M.; Azadi, A.; Rafiei, P. Hydrogel Nanoparticles in Drug Delivery. *Adv. Drug Deliv. Rev.* **2008**, *60* (15), 1638–1649.
(40) McClements, D. J. Designing Biopolymer Microgels to Encapsulate, Protect and Deliver Bioactive Components: Physicochemical Aspects. *Adv. Colloid Interface Sci.* **2017**, *240*, 31–59.
(41) Plamper, F. A.; Richtering, W. Functional Microgels and Microgel Systems. *Acc. Chem. Res.* **2017**, *50* (2), 131–140.
(42) Wu, H. Q.; Wang, C. C. Biodegradable Smart Nanogels: A New Platform for Targeting Drug Delivery and Biomedical Diagnostics. *Langmuir* **2016**, *32* (25), 6211–6225.
(43) Cuggino, J. C.; Molina, M.; Wedepohl, S.; Igarzabal, C. I. A.; Calderón, M.; Gugliotta, L. M. Responsive Nanogels for Application as Smart Carriers in Endocytic PH-Triggered Drug Delivery Systems. *Eur. Polym. J.* **2016**, *78*, 14–24.
(44) Coll Ferrer, M. C.; Dastgheyb, S.; Hickok, N. J.; Eckmann, D. M.; Composto, R. J. Designing Nanogel Carriers for Antibacterial Applications. *Acta Biomater.* **2014**, *10* (5), 2105–2111.
(45) Schmid, A. J.; Dubbert, J.; Rudov, A. A.; Pedersen, J. S.; Lindner, P.; Karg, M.; Potemkin, I. I.; Richtering, W. Multi-Shell Hollow Nanogels with Responsive Shell Permeability. *Sci. Rep.* **2016**, *6* (December 2015), 1–13.
(46) Xue, B.; Kozlovskaya, V.; Liu, F.; Chen, J.; Williams, J. F.; Campos-Gomez, J.; Saeed, M.; Kharlampieva, E. Intracellular Degradable Hydrogel Cubes and Spheres for Anti-Cancer Drug Delivery. *ACS Appl. Mater. Interfaces* **2015**, *7* (24), 13633–13644.
(47) Chen, M. H.; Chung, J. J.; Mealy, J. E.; Zaman, S.; Li, E. C.; Arisi, M. F.; Atluri, P.; Burdick, J. A. Injectable Supramolecular Hydrogel/Microgel Composites for Therapeutic Delivery. *Macromol. Biosci.* **2018**, *1800248*, 1–12.
(48) Santos, E.; Pedraz, J. L.; Hernández, R. M.; Orive, G. Therapeutic Cell Encapsulation: Ten Steps towards Clinical Translation. *J. Control. Release* **2013**,

170 (1), 1–14.
(49) Nafea, E. H.; Poole-Warren, A. M. L. A.; Martens, P. J. Immunoisolating Semi-Permeable Membranes for Cell Encapsulation: Focus on Hydrogels. *J. Control. Release* **2011**, *154* (2), 110–122.
(50) De Vos, P.; Lazarjani, H. A.; Poncelet, D.; Faas, M. M. Polymers in Cell Encapsulation from an Enveloped Cell Perspective. *Adv. Drug Deliv. Rev.* **2014**, *67–68*, 15–34.
(51) Burgain, J.; Gaiani, C.; Linder, M.; Scher, J. Encapsulation of Probiotic Living Cells: From Laboratory Scale to Industrial Applications. *J. Food Eng.* **2011**, *104* (4), 467–483.
(52) Chang, T. M. S. Semipermeable Microcapsules. *Science (80-.).* **1964**, *146*, 524–525.
(53) Orive, G.; Tam, S. K.; Pedraz, J. L.; Hallé, J. P. Biocompatibility of Alginate-Poly-l-Lysine Microcapsules for Cell Therapy. *Biomaterials* **2006**, *27* (20), 3691–3700.
(54) Nicodemus, G. D.; Bryant, S. J. Cell Encapsulation in Biodegradable Hydrogels for Tissue Engineering Applications. *Tissue Eng. Part B Rev.* **2008**, *14* (2), 149–165.
(55) Rossow, T.; Lienemann, P. S.; Mooney, D. J. Cell Microencapsulation by Droplet Microfluidic Templating. *Macromol. Chem. Phys.* **2017**, *218* (2), 1–14.
(56) Ekkelenkamp, A. E.; Jansman, M. M. T.; Roelofs, K.; Engbersen, J. F. J.; Paulusse, J. M. J. Surfactant-Free Preparation of Highly Stable Zwitterionic Poly(Amido Amine) Nanogels with Minimal Cytotoxicity. *Acta Biomater.* **2016**, *30*, 126–134.
(57) Amamoto, Y.; Otsuka, H.; Takahara, A. Synthesis and Characterization of Polymeric Nanogels. In *Nanomaterials for the Life Sciences*; Kumar, C. S. S. R., Ed.; WILEY-VCH Verlag GmbH, 2011; Vol. 10, pp 27–57.
(58) Ma, X.; Xiao, Y.; Xu, H.; Lei, K.; Lang, M. Preparation, Degradation and in Vitro Release of Ciprofloxacin-Eluting Ureteral Stents for Potential Antibacterial Application. *Mater. Sci. Eng. C* **2016**, *66*, 92–99.
(59) Singh, B.; Varshney, L.; Sharma, V. Design of Sterile Mucoadhesive Hydrogels for Use in Drug Delivery: Effect of Radiation on Network Structure. *Colloids Surfaces B Biointerfaces* **2014**, *121*, 230–237.
(60) Aagaard, J.; Madsen, P. O.; Rhodes, P.; Gasser, T. MICs of Ciprofloxacin and Trimethoprim for Escherichia Coli: Influence of PH, Inoculum Size and Various Body Fluids. *Infection* **1991**, *19* (S3), S167–S169.
(61) Fernández-Hidalgo, N.; Gavaldà, J.; Almirante, B.; Martín, M. T.; Onrubia, P. L.; Gomis, X.; Pahissa, A. Evaluation of Linezolid, Vancomycin, Gentamicin and Ciprofloxacin in a Rabbit Model of Antibiotic-Lock Technique for Staphylococcus Aureus Catheter-Related Infection. *J. Antimicrob. Chemother.* **2010**, *65* (3), 525–530.
(62) Behera, B.; Sagiri, S. S.; Pal, K.; Srivastava, A. Modulating the Physical Properties of Sunflower Oil and Sorbitan Monopalmitate-Based Organogels. *J. Appl. Polym. Sci.* **2013**, *127* (6), 4910–4917.

3. Hydrogels for endoscopic submucosal dissection

In the previous chapter, we have shown that poly(amidoamine)s hydrogels have peculiar characteristics that can be exploited to obtain injectable, biocompatible materials. They can be synthetized in water, at room temperature, they do not require any purification step, the synthesis is effective even without the use of radical initiators, they have a porous structure that allows cell penetration and they can be easily functionalized with special chemical moieties and with silica-based materials. Also, the peculiar gelation kinetic make the pre-gel solution easy to inject and thus make them promising candidates as injectable materials in clinical applications.

Herein, we show that these materials have excellent perspective for the use as a suitable submucosal fluid cushion for Endoscopic Submucosal Dissection (ESD). ESD is a minimally-invasive technique employed for the removal of early-stage tumors of the gastrointestinal tract. The material that we have developed of this application is a nanocomposite, breakable, non-toxic, injectable PAAm hydrogel that solidifies in less than five minutes in the submucosal layer of the stomach, esophagus or colon. The material is redox-responsive, and its degradation can be triggered by the release of glutathione from cells, such as fibroblast, and can be functionalized with mesoporous silica nanoparticles or with breakable nanoshells, in order to achieve the release of bioactive molecules from these nanocontainers.

The strong adhesion to the surrounding tissues of the developed material allows the reduction of the risk of complications, bleeding and perforations during the surgery. Also, a thin layer of hydrogel remains in place - adherent to the tissues - even after the surgery, allowing the protection of the lesion and the deliver any required drug.

This work was conducted in collaboration with Dr. Federica Fiorini and Etienne Piantanida (Laboratoire de Chimie et des Biomatériaux Supramoléculaires, Strasbourg), and with Prof. Silvana Perretta, Dr. Pietro Riva, Dr. Ludovica Guerrero and Dr. Lim Sun Gyo (IRCAD-Institut de Recherche contre les Cancers de l'Appareil Digestif, Strasbourg and IHU-Institut de chirurgie guidée par l'image, Strasbourg).

Part of this chapter and some figures have already been published in a paper (Injectable Hybrid Hydrogels, with Cell-Responsive Degradation, for Tumor Resection, DOI: 10.1021/acsabm.8b00189), in the PhD thesis of Dr. Federica Fiorini and an international patent application has been filed (L. De Cola, G. Alonci, S. Perretta, P. Riva, F. Fiorini, WO 2018/134268 Al).

3.1 Endoscopic Submucosal Dissection

According to the 2014 World Cancer Report[1] by the International Agency for Research on Cancer (IARC), stomach cancer is the fifth most common cancer in the world and it affect mainly patients in Asia, that accounts for three quarter of all the cases. In 2012, 952'000 new cases and 732'000 deaths were estimated worldwide. Risk factors include infection by *H. Pylori*, smoke, high consumption of processed red meat, salt-preserved and smoked foods, pickled vegetables and low intakes of fresh fruit and vegetables.

Interestingly, despite increased incidence, Asian patients often have better outcomes in comparison to Western ones. This discrepancy can be readily justified by considering that the more aggressive screening programs in the East allow for an early detection of tumoral lesions. The prognosis for late gastric tumors is often nefarious and even radical gastrectomy is not effective.[2]

For early-stage gastric tumors there are good chances of a complete healing an minimally-invasive or even endoscopic approaches can be used to remove the lesions with minimal stress for the patient.[3,4]

Endoscopic Submucosal Dissection (ESD) was first introduced in Japan 1988 and today is a well-established technique indicated for the treatment of small carcinoma lesion (<3 cm) where no risk of lymph node metastasis exists.[5,6]

A schematic view of this procedure is reported in ***Figure 3.1***. After marking of the lesion, a fluid is injected to obtain a submucosal fluid cushion (SFC) that can separate the submucosal from the mucosal layer below it, allowing protection of the stomach wall. An incision is made, and the lesion is dissected using a T-knife, reducing the risk of perforation. Histopathologic analysis is then performed on the collected specimen.

The quality of the SFC plays a critical role in reducing the risk of perforation and damage to the muscularis layer underneath the submucosa.

The ideal SFC fluid should be cost-effective, non-toxic, easy to inject and should maintain the mucosal elevation for all the time required by the surgery.[7] Normal saline solution (NS) is the most used one: it is easy to inject, cheap and widely-available. However, the obtained mucosal elevation is low and short-lasting. Multiple injections are thus required, increasing the risk for complications and the length of the procedure.

Other fluids have been under investigation, such as hydroxypropyl methylcellulose, fibrinogen mixture, chitosan, glycerol, sodium hyaluronate, sodium alginate or dextrose solution.[7–9] However, these solutions are often difficult to inject due to their high viscosity, they are cumbersome to prepare or highly expensive[10]. Sodium Hyaluronate is often used, but it is expensive, hard to inject and can stimulate tumor proliferation.

In general, these materials do not change physical state upon injection, and thus a compromise between injectability, mechanical properties and spreading speed in the surrounding tissues is necessary. On the contrary, a material with a sharp sol-gel transition would be beneficial to solve these problems.

In this regard, thermo-responsive hydrogels, such as a poly(lactic acid-co-glycolic acid)-poly(ethylene glycol)-poly(lactic acid-co-glycolic acid) triblock copolymer, have also been described in literature.[11,12] These materials are fully synthetic hydrogels with temperature-induced sol-gel transition at about 37 °C. Unfortunately, they still require

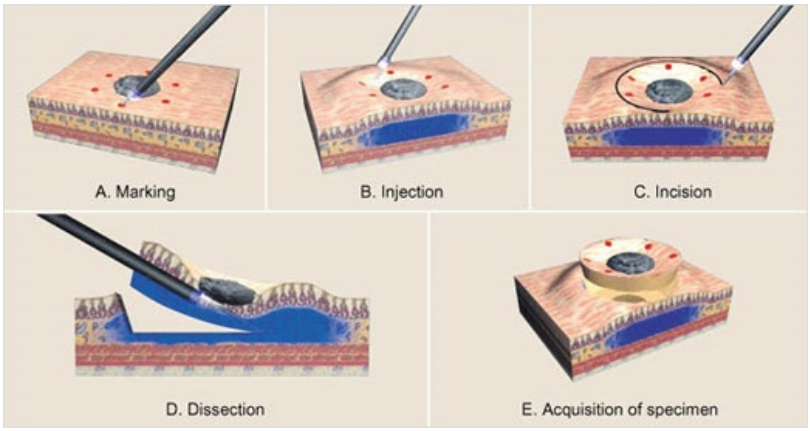

Figure 3.1 Scheme of Endoscopic Submucosal Dissection procedure. After marking of the lesion (a), a fluid is injected to separate the mucosal from the submucosal layer (b). Using a specialized endoscopic knife an incision is made (c) and the mucosal flap is dissected (d). The specimen is then collected for histopathologic analysis. (reproduced from www.ec21.com)

high injection pressure and may lead to clotting inside the endoscopic sheet used for the injection.[13–15]

UV-curable materials have also been reported, for example photo-crosslinkable chitosan hydrogel,[16,17] but their use requires specialized instruments, can be extremely difficult in hard-to-reach areas and UV light can promote inflammation in the nearby tissues.

Thus, the development of new materials that can selectively solidify inside the body, using alternative factors to trigger gelation, may be of great interest for the medical community.

3.2 Discussion

The main concept behind the use of PAAm hydrogels for ESD is that, after injection, they can not only form non-covalent interactions and hydrogen bonds, but they may also react with the amino group of the surrounding tissues and mechanically interlock with the surrounding tissues by entrapping them in the PAAm 3D-network. This would allow the formation of a layer of material that can protect the gastric wall until complete healing of the wound and release any bioactive molecule the surgeons would consider beneficial.

All these properties require a complex design of the material. To be efficacious, the final material needs to be injectable, to quickly solidify after injection, to be adhesive to the tissue, to be degradable and to be able to release bioactive molecules if required.

As we will show in the next paragraphs, we have carefully designed a material that meets all these requirements.

The hydrogel was then tested *in-vitro* for cell-mediated degradation and cytocompatibility, followed by *in-vivo* experiments on porcine models to evaluate the feasibility of the material ad a submucosal fluid cushion for gastric, esophageal and colon ESD.

3.2.1 Functionalization of the PAAm hydrogels to improve adhesion

We evaluated the opportunity to prepare a hydrogel functionalized with specific functional groups, in particular with catecholamines, in order to make them mucoadhesive, so that they can remain in place after submucosal injection and adhere strongly to the surrounding tissues,

It is well-known that catechol-containing moieties are correlated with improved adhesion even in difficult situations, such as underwater.[18] The use of catechols to improve adhesion is bioinspired, in particular is derived by the observation that Mussels (*Mytilus Bissal*) are able to adhere strongly to their environment even underwater. Mussels adhere to the surfaces through some collagen-rich appendices known as "byssus", that contains a broad range of *mussel foot proteins* (MFP). The initial discovery by J.H. Waite[19,20] that MFP are rich in catechol-containing groups and (L)-3,4-dihydroxyphenilalanine (L-DOPA) opened a new field in adhesive materials development and inspired several works.[21–28] This approach has been followed also to prepare cytocompatible materials,[29,30] such as the one reported by H. J. Cha *et al* in 2015 for urinary fistula sealing.[18] However, the preparation of these adhesives is very complicated and requires the purification of recombinant proteins[31] and/or extensive synthetic procedures.

We hypothesized that adding catecholamines to the PAAm hydrogel backbone could improve their adhesive properties, as already reported for other hydrogels.[26,32]

We identified two possible alternatives: L-DOPA and Dopamine. Both are natural molecules present in the human body, with L-DOPA being an amino acid used in the therapy of Parkinson disease and an intermediate in the biosynthesis of Dopamine, a neurotransmitter produced in the brain and involved in several major roles in animal physiology.

The reaction scheme for the synthesis of catechol-modified PAAm hydrogel is reported in ***Figure 3.2***. Shortly, MBA, catecholamine, crosslinker and water are mixed together in a glass vial at 37 °C. A dark brown, fragile hydrogel is obtained. After 24 h, the hydrogel is dark and rigid, with no obvious difference between the hydrogel synthetized with Dopamine and the one synthetized with L-DOPA.

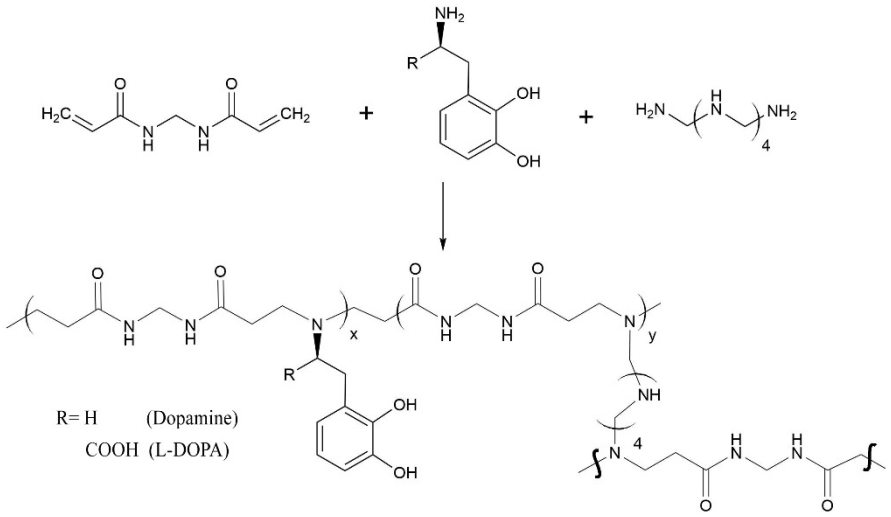

Figure 3.2 Synthesis of PAAm hydrogels functionalized with L-DOPA (R= -COOH) or Dopamine (R= -H).

We hypothesized that the dark color can be linked to the well-known process of oxidation of catecholamine and we conducted the same reaction, in a round bottom flask, under inert atmosphere (N_2) using standard Schlenck techniques. The liquid pre-gel solution was transferred under N_2 in a glass vial and left to rest until complete gelation. The hydrogel obtained was only slightly yellow, but it was quickly oxidized when exposed to air. To verify if some non-crosslinked reactant was still present, fresh prepared hydrogel were washed with degassed water under N_2 and then both the hydrogel and the solution were exposed to the air overnight. Both the hydrogel turned dark, and the same happened with the washing water from the L-DOPA hydrogel, while the washing solutions from the Dopamine hydrogel were still clear. This behavior shows that a large amount of L-DOPA does not react to form the hydrogel and remains as a free unreacted molecule. This is compatible with what we observed for other amino acids. However, also the dopamine-functionalized hydrogel (dopaPAAm) showed oxidation even if no release was observed, confirming that also the covalently-linked molecules can still be oxidized.

The effect of pH on the oxidation of adhesive catecholamine-functionalized materials is well-known,[33,34] and it is established that oxidation is linked with a reduced adhesion. We elaborated two different strategies to avoid oxidation: working at lower pH and adding a reducing agent to the reactant mixture, as shown in ***Figure 3.3***.

In ***Figure 3.3a*** we compare the oxidation of a standard dopamine-functionalized PAAm hydrogel (left) with a hydrogel prepared with the 5% of ascorbic acid as an anti-oxidant,

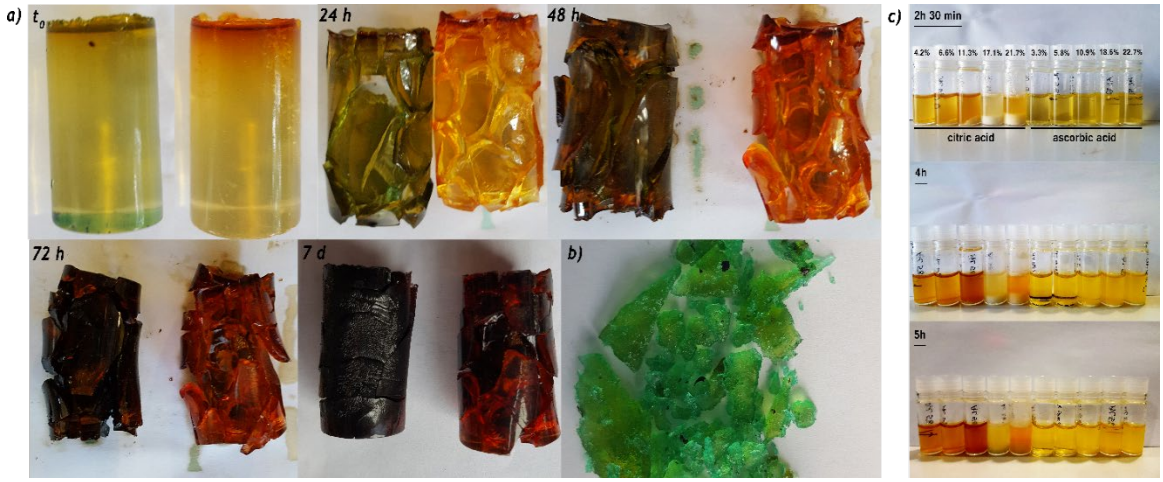

Figure 3.3 Oxidation of dopamine-functionalized PAAm hydrogels with (right) or without (left) 5% ascorbic acid, when left in open contact with air in a controlled moisture environment (a). Oxidation of a dopamine-functionalized hydrogel after 21 days in a closed vial (b). Oxidation of dopamine-functionalized hydrogel over time with increasing concentrations of citric acid or ascorbic acid (c).

both synthesized and stored under inert atmosphere previous to being exposed to air. The hydrogels were kept with 100% humidity to avoid shrinking due to water evaporation.

Oxidation starts in both cases immediately after the gel are removed from the inert atmosphere. However, the hydrogel containing ascorbic acid seems to oxidize at lower speed and with a different mechanism, confirmed by the difference in colour between the two samples. However, after 24 h in both case the hydrogels started to crack and after 7 days they were completely oxidized.

Figure 3.3b shows a dopaPAAm hydrogel prepared under inert atmosphere and then left in a closed vial not hermetically sealed for 21 days, to simulate the conditions of a low-oxygen environment.

Figure 3.3c shows dopaPAAm hydrogels prepared in normal atmosphere, at 37 °C, with increasing concentrations of citric acid (4.2, 6.8, 11.2, 17.1 and 21.7%, the last two supersaturated) and ascorbic acid (3.3%, 5.9%, 10.9%, 18.6 and 22.7%, the last one supersaturated). After 90 minutes, all the hydrogels prepared with ascorbic acid show an intense yellow colour, while the pre-gel solutions prepared in citric acid show a darker hue indicating the beginning of oxidation. After 150 minutes, the hydrogel prepared with ascorbic acid were formed and they all show a stable intense yellow colour, but a concentration of ascorbic acid greater than 10% was associated with less transparency. In the case of citric acid, after 5 hours only the hydrogel with 4% of acid was formed, while the others were still not formed and did not form in the following days. Also, no protection

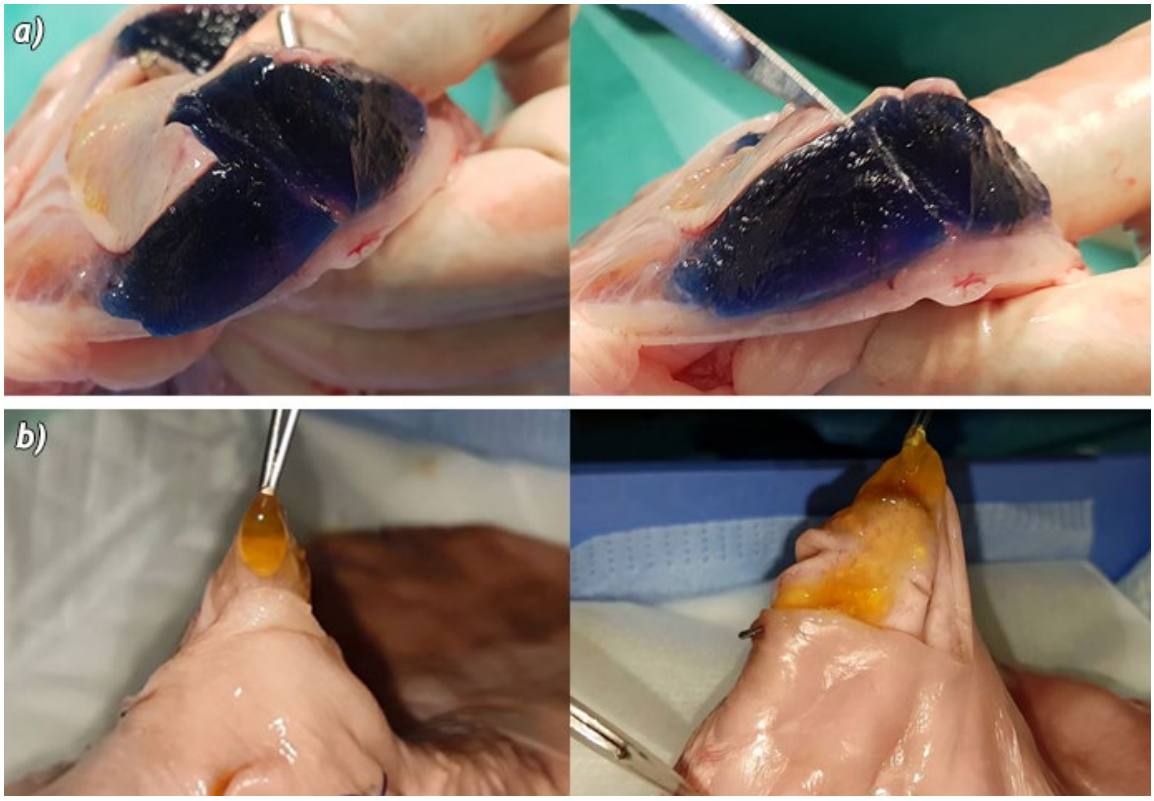

Figure 3.4 PAAm hydrogel 30 minutes after injection shows optimal adhesion to the surrounding tissues (a). dopaPAAm hydrogel + 5% ascorbic acid 30 minutes after adhesion shows optimal adhesion but it is less integrated with the surrounding tissues (b).

from oxidation was observed in any case. However, we observed that while oxidation may reduce adhesion through non-covalent forces, it may lead to crosslinking with the proteins of the living tissues, and we decided to verify adhesion on animal tissues.[35]

Preliminary adhesion tests (***Figure 3.4***) were performed *ex-vivo* on a porcine stomach by injecting the dopaPAAm hydrogel with 5% ascorbic acid - 10 minutes before the expected gelation time - and comparing the adhesion with a regular PAAm hydrogel. Both the hydrogels were prepared with the same concentration of [MBA]= 0.864 M, [PEHA]= 0.215 M and [monoamine]= 0.323 M (GABA or dopamine).

In both cases, the hydrogels were injected in the submucosa of the stomach wall, using a 23-gauge standard needle, after 135 minutes from the start of the synthesis at 37 °C. The materials were easy to inject, and no significative spreading was observed. After 30 minutes, the stomach wall was opened with a scalpel and adhesion was evaluated. Both hydrogels shown optimal adhesion to the surrounding tissues, they were hard to remove and able to sustain the full weight of the stomach. The dopaPAAm hydrogel however was

less integrated with the surrounding tissues in comparison to the standard GABA-containing PAAm hydrogel.

Considering these results, we decided to focus our attention to the properties of the standard PAAm hydrogels and three sample with different concentrations of crosslinker were prepared and tested for endoscopic injection (***Figure 3.5***). Three hydrogels were prepared at 60 °C, directly in the operating room, with increasing concentration of crosslinker, [PEHA]= 215, 260 and 287 mM. Each sample was injected *ex-vivo* in a porcine stomach wall through an endoscopic needle, 5 minutes after the pre-gel solution was ready and after cooling down to an acceptable temperature. We observed that all the three hydrogels were injectable, but the hydrogel prepared with the lowest concentration of PEHA was the easiest to inject, as expected. After 30 minutes from injection, the stomachs were opened and the material exposed.

As expected, the materials prepared with lower concentration of crosslinker were softer and better integrated with the surrounding tissues, while more crosslinked hydrogels formed a harder cushion, which still showed a very good adhesion.

We noticed that some of the hydrogels that were perfectly formed after injection, were still liquid in the vial and we thought that it was worth to investigate this unusual behavior.

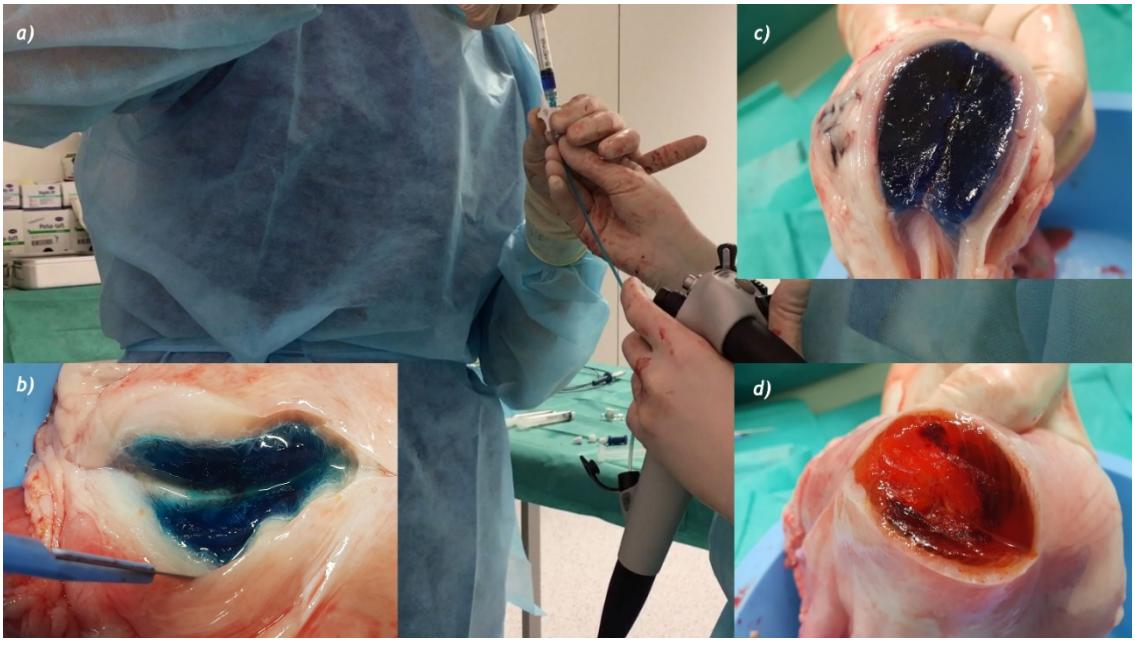

Figure 3.5 Endoscopic injection of PAAm hydrogels (a) at different concentration of PEHA. [PEHA]= 215 mM, light blue hydrogel (b). [PEHA]= 260 mM dark blue hydrogel (c). [PEHA]= 287 mM red hydrogel (d).

We decided to repeat the experiment, performing the injections immediately after the homogenous pre-gel solutions were obtained and exposing the hydrogels at different times. With our great surprise, we observed that already after five minutes from injection all the hydrogels were formed and adhesive, even if – at the same temperature – the pre-gel solution required hours to solidify in the vial.

This behavior even increased our interest for this material, because the unexpected immediate formation of the hydrogel in the tissue would allow a broad injection time-window and would allow to perform ESD without the need to wait for the hydrogel to be formed.

We investigated this behavior in other organs, in order to find an explanation for this relevant difference in gelation kinetic. Hydrogel injections were performed in the intestinal lumen, colon submucosa, esophagus submucosa, kidney, liver, pancreas and lymph nodes. The same behavior was observed in the submucosa layer of the colon and esophagus and in the lymph nodes, while in the kidney, liver and pancreas no gelation was observed and the hydrogel was spread in the surrounding tissues after injection. In the intestinal lumen, no decrease of gelation time was observed and, even by waiting for the appropriate gelation time, hydrogel adhesion was acceptable but not comparable in strength to the one observed in the submucosal space.

We tried to investigate the effect of different factors that could influence gelation time, such as pH or temperature. Regarding the pH, as we have seen for the hydrogel prepared with citric acid, a lower pH hinders the reaction. This is compatible with the aza-Michael addition mechanism: at lower pH an increased percentage of amino groups is protonated, and thus not nucleophilic enough to react. Also, the pH of submucosa is reported to be approximately 7, and thus should not influence gelation.[36]

Temperature as a major influence on gelation time, however the hydrogels were synthesized *in-vial* at 37 °C while the ex-vivo injection in the stomach was performed at room temperature. As before, we should then expect a longer (*ex-vivo*) or equal (*in-vivo*) gelation time.

To rule out the effect of enzymes or unknown catalyst present in the tissues, we performed the synthesis of the pre-gel solution and then we added a 1x1 cm specimen extracted from

the submucosa layer to 3 mL of pre-gel solution. No difference in gelation time was observed.

Further experiments on this regard will be presented in the next sections.

The material we presented in this section is, however, not useful in real-life ESD application, because of the lack of degradability.

In the next section we will present a novel redox-responsive degradable nanocomposite PAAm hydrogel that should facilitate the work of the surgeon and reduce side-effects and discomfort for the patients.

3.2.2 Synthesis of a nanocomposite GSH-responsive degradable PAAm hydrogel

PAAm hydrogels are known for their biocompatibility, and in the previous paragraphs we have shown that they are also injectable endoscopically and that they solidify *in-situ* after just some minutes.

However, in order to be applicable as injectable materials for ESD in real-life situations, they also need to be degraded in the human body after the end of the surgery.

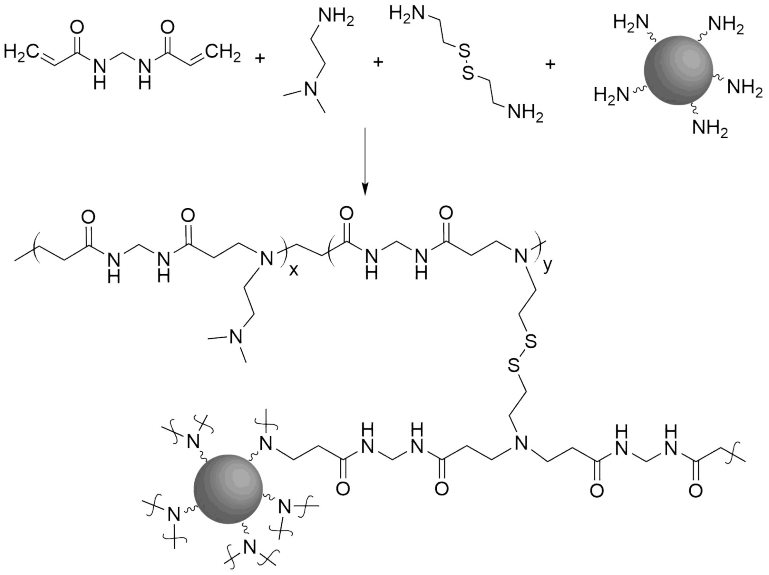

Figure 3.6 Scheme of the synthesis of the nanocomposite breakable dPAAm hydrogel

On this regard, we decided to prepare a nanocomposite degradable hydrogel (dPAAm) based on a disulphide-containing crosslinker – to trigger degradation in response to the change in redox potential due to cell growth and proliferation – and degradable silica nanocapsules able to release on demand a bioactive molecule. The general synthetic scheme is reported in ***Figure 3.6***.

We have selected a redox-mediated degradation mechanism because of the abundance of glutathione in the extracellular matrix. Glutathione (GSH) is a short oligopeptide (γ-l-glutamyl-l-cysteinyl-glycine) synthetized in the body from the amino acids L-cysteine, L-glutamic acid, and glycine and it is responsible for maintaining the redox homeostasis in the body and it prevents oxidative stress to cells acting as anti-oxidant. Its concentration is in the millimolar range inside the cell, while in the extracellular matrix it is in the micromolar range.[37] Thus, it is possible to exploit the release of glutathione from the cells colonizing the hydrogel to trigger the degradation of the scaffold.[38–41]

Cystamine dihydrochloride has been employed as a redox-responsive crosslinker, while N,N-dimethylethylendiamine (DMEDA) has been employed as a monoamine co-reactant. Breakable organosilica nanocapsules (BNCs) functionalized with amino groups were covalently grafted to the network to allow the release of bioactive molecules. These particles have already been described in the past by our group[42] and it has already been demonstrated that they are able to entrap and release proteins in their active conformation.

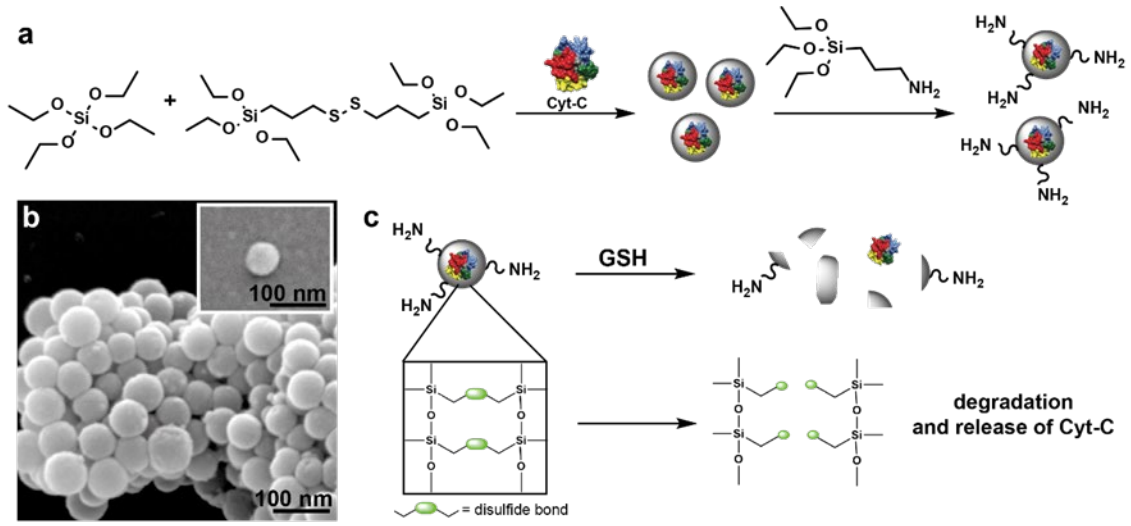

Figure 3.7 Scheme of the synthesis and functionalization of BNCs containing disulfide moieties in the framework and loaded with Cyt-C inside the silica capsule (a). SEM image of the BNCs after functionalization, in the insert SEM picture of a naked nanoparticle (b); degradation of the BNCs (c).

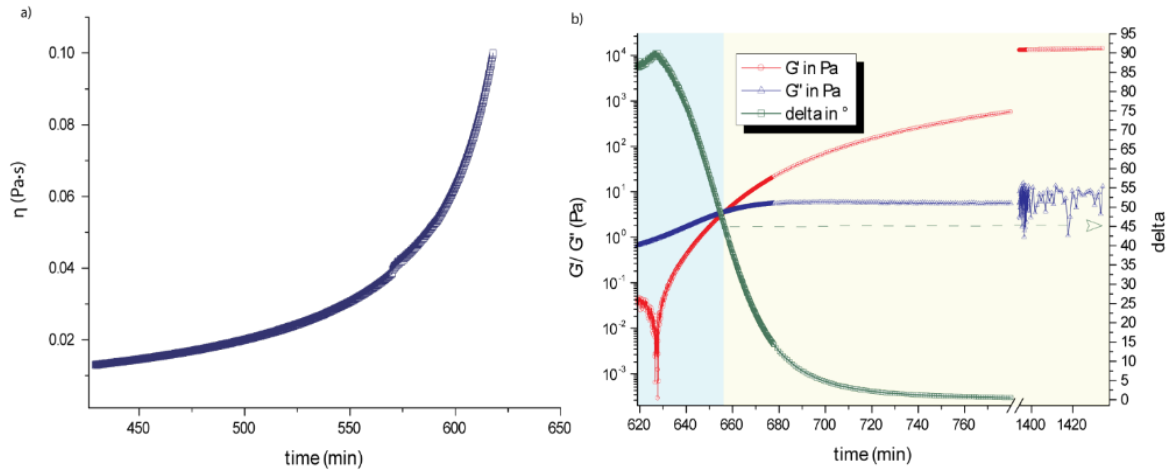

Figure 3.8 Gelation kinetic for a dPAAm synthetized without BCNs at double of the usual concentrations of reagents. [MBA]= 1.728 M, [DMENA]= 0.854 M and [CYSTA]= 0.384 M.

The BNCs also contain disulphide bridges in their structure, to be renally-excreted and completely cleaved from the body.

A scheme of the synthesis and functionalization of the breakable nanocapsules, as well as the SEM of the pristine and functionalized BNCs and of the degradation via GSH, is displayed in ***Figure 3.7.***

In order to exploit these BNCs to obtain a nanocomposite hydrogel, it was necessary to functionalize their surface with amino groups so that they can act as a polyamine crosslinker. This result was accomplished by simple stirring of a BNCs suspension in ethanol in presence of 3-aminopropyltriethoxysilane.

The functionalization was confirmed with a qualitative ninhydrin test and by the shift of ζ-potential, from -10.5 mV for the the pristine nanocapsules to + 2.2 mV for the amino-functionalized ones.

Different hydrogels with different concentrations of nanoparticles were prepared, and we found that the optimal concentration of nanoparticles was approximatively 1 mg/mL. At higher concentrations, particles start to aggregate, leading to phase separation and inhomogeneity of the material.

The synthesis of the hydrogel was conducted as usual. We have decided to use DMEDA as a monoamine co-reactant because of the higher basicity in comparison to GABA, that can help to activate the cystamine salt (CYSTA).

In a standard synthesis, the following concentrations of reagents were used: [MBA]= 0.864 mM, [DMENA]= 427 mM and [CYSTA]=192 mM. At 37 °C, approximatively 48 hours are required to start gelation and obtain a clear, soft hydrogel. The same synthesis has been repeated by changing the concentration of crosslinker from 20% dry weight to 10 and 40% or by decreasing the amount of water – and thus increasing the concentration of all the reagents (***Figure 3.8***). This last material shows a shorter gelation time - approximately 11 hours at 37 °C compared to more than 48 h for the regular dPAAm hydrogel – and after formation has a high rigidity with G'≈ 15 kPa.

For comparison, the dPAAm hydrogel prepared with the standard synthesis have G'≈ 6 kPa, as reported in ***Figure 3.9a***. These measures were performed by Prof. Francisco Monroy and Dr. Ivan López-Montero, Universidad Complutense de Madrid.

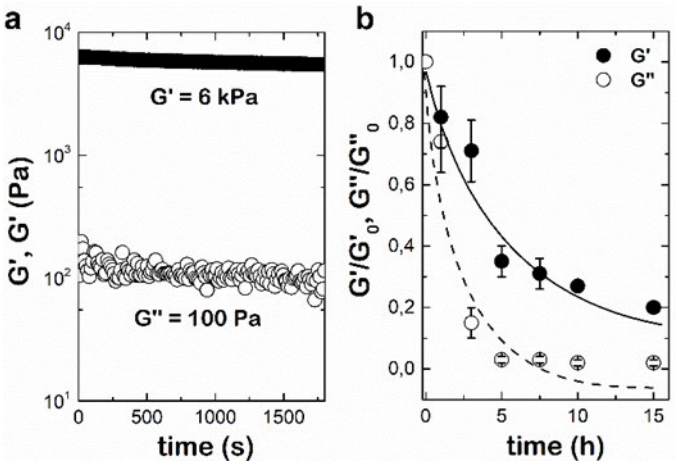

Figure 3.9 Oscillatory shear rheology of the standard dPAAm hydrogel (a). Degradation of the dPAAm hydrogel with GSH 10 μM.

Interestingly, the loss modulus G'' is two order of magnitude higher in the less concentrated hydrogel (100 Pa *vs* 5 Pa), showing that the standard dPAAm has also a more viscous behavior compared to the most concentrated one. This different rheological behavior can be exploited to tailor different materials with the optimal mechanical characteristics for the intended applications.

After discussing with our partner surgeons, we decided to focus our attention on the standard dPAAm hydrogel, because we imagined that a softer material would be easier to cut during the ESD.

3.2.3 In-vial and in-vitro dPAAm degradation

To prove the degradability of the system, we performed a preliminary test by analyzing the change in rheological behavior of the nanocomposite dPAAm upon incubation with a 10 mM GSH solution. From **Figure b** it is possible to observe that after five hours of incubation the elastic modulus G' decreased to approximately 35% of its initial value, while the loss modulus decreased to 1%. After 15 hours G'' was unchanged and G' decreased to 20% of the initial value. This shows that, under the influence of a reducing environment simulated by the presence of GSH, the hydrogel keep is structural integrity during the first part of the degradation process, thus allowing the slow release of the bioactive molecules contained in the BCNs *in-situ.* To confirm these results, we repeated the test with 10 μM GSH by following the degradation of the material by measuring the equilibrium degree of swelling (EDS), defined as:

$$EDS = \frac{W_{wet} - W_{dry}}{W_{dry}}$$

In ***Figure 3.10a,*** we report the result of the swelling test for a freeze-dried dPAAm hydrogel incubated with a 10 μM GSH solution or with a phosphate buffer solution at pH= 7.4 (PBS). In the first hours, the EDS increases for both samples, until reaching a maximum after approximately 24 h. In this first phase, the increase in weight due to water absorbed overcome the weight loss due to degradation by GSH. After 48 h, there is clear decrease in weight for the sample in glutathione, compared to the one in PBS. After 72 hours, the hydrogel in GSH is completely degraded, while in PBS even after 6 days the weight loss is negligible. To confirm that also the BCNs can break in these conditions, we report in ***Figure 3.10b*** STEM pictures showing the degradation of the BCNs in a 10 μM solution of GSH after 24h. This further confirms that the particles can release their content before the complete degradation of the scaffold.

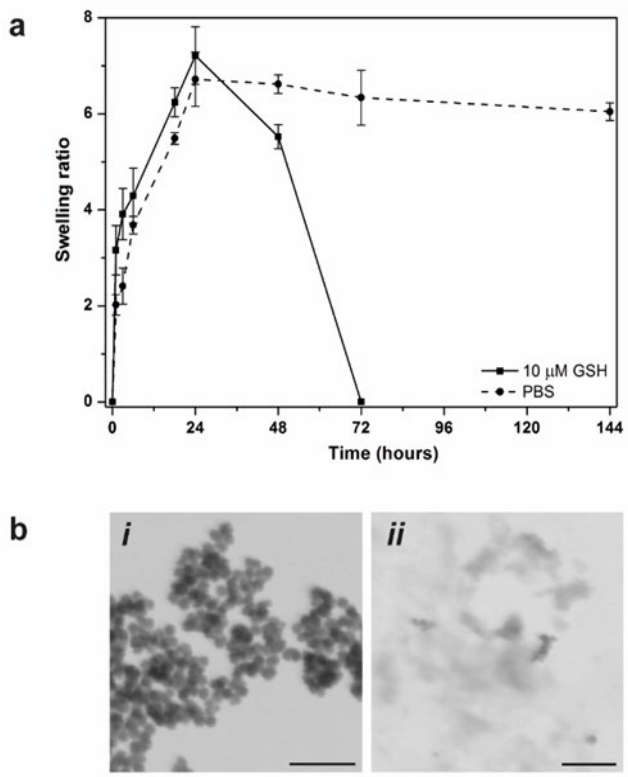

Figure 3.10 dPAA hydrogel degradation in 10 μM GSH solution (solid line) and in PBS (dashed line) (a). STEM images of the BNCs before (i) and after exposure to 10 μM GSH for 24 h (ii) (b).

Also, the low concentration of glutathione needed to trigger degradation is compatible with the GSH concentration in the extracellular matrix. To prove that the material is degradable also through the action of cells, we seeded Human Dermal Fibroblast (HDFa) on top of the hydrogels and looked at the degradation profile (*in-vitro* assays performed by Dr. Federica Fiorini). For these experiments, we have selected HDFa among other cell lines because they are between the most common cells in connective tissues, they physiologically reside in the extracellular matrix and they play a fundamental role in all phases of wound healing.[43]

First, we investigated the cytocompatibility of the material by measuring cell viability through the alamarBlue® assay each day for four days. 2.5 x 105 HDFa cells were seeded on top of dPAAm hydrogel cylinders (diameter: 8 mm; height: 1 mm; cell density: 5000 cells/mm^2), that were previously sterilized with 95% ethanol and rinsed with PBS and high-glucose DMEM. The alamarBlue® test allows to quantify cells metabolic activity by measuring their ability to reduce Resazurin, the non-fluorescent active ingredient of alamarBlue® reagent, into Resorufin, a compound that is red in color and highly fluorescent. By measuring the percentage of reduced reagent in a fixed time slot it is

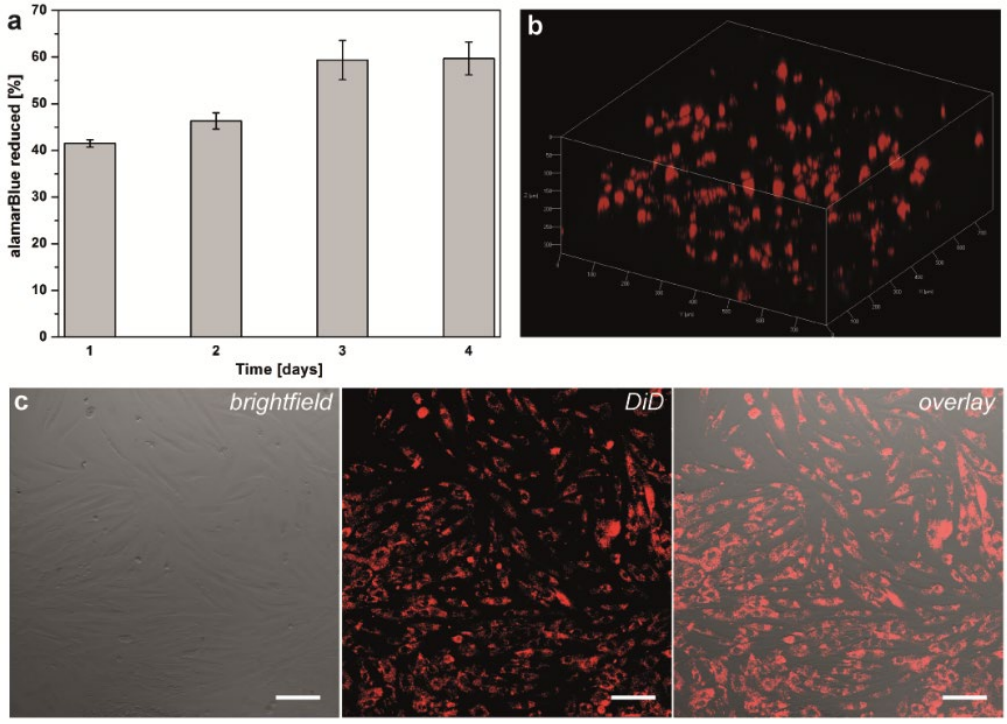

Figure 3.11 alamarBlue® assay on HDFa cells growing on dPAAm hydrogel (a). Z-stack picture showing that HDFa cells completely colonized the material (b); Confocal images of HDFa cells, scale bar= 100 µm. Cells were stained in red with Vybrant DiD.

possible to have an indication of cell viability. As reported in ***Figure a***, a steady increase in the concentration of the reduced form was observed during four days of incubation.

Confocal images (***Figure 3.11b*** and ***c)*** confirms that cells are completely colonizing the material and are viable and adherent to the gel surface. The 3D Z-stack picture confirms that the cells are actively growing in the bulk of the hydrogel, and not only at the top surface.

As we were expecting, we observed a degradation of the scaffold upon cells proliferation. In ***Figure 3.12***, we show that already after 12 hours from seeding, it was already possible to observe clear sign of degradation for the cell-containing dPAAm hydrogel in comparison to the acellular control. Complete degradation was observed after 96 hours, a result in line with what we reported in the *in-vial* GSH degradation test. Some degradation (17% in 96 hours) was observed also in the acellular control dPAAm hydrogel and can be attributed to the slightly reducing culture media and the presence of thiol-containing proteins in the foetal bovine serum contained in the culture medium. During the degradation, the cells moved to the bottom of the well, but no decrease in cells viability

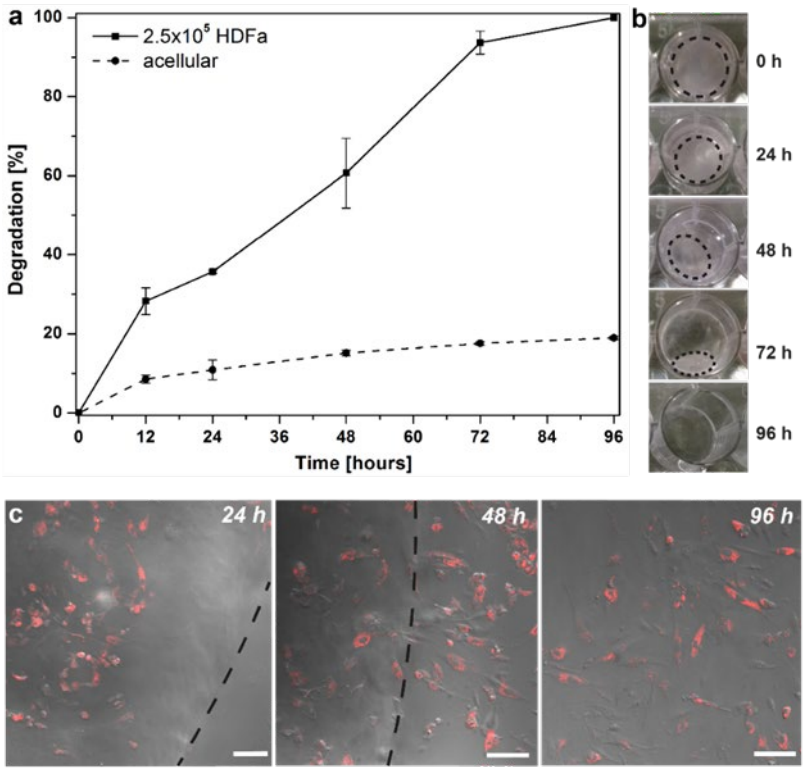

Figure 3.12 HDFa-mediated degradation of the dPAAm hydrogel, measured by weight loss in comparison to the initial weight of the acellular hydrogel equilibrated in DMEM culture media (a). Cell-mediated degradation of the dPAA. The dashed line only as an eye-guide (b). Overlay of brightfield and fluorescence images of the HDFa colonizing the dPAAm hydrogel and gradually moving to the bottom of the well plate as the scaffold get degraded. Scale bar= 100 μm (c).

was observed. These results demonstrate that the dPAAm hydrogel can be degraded by the secretion of GSH from growing cells and that also the degradation products of the hydrogel are non-toxic, confirming what was already reported by other authors.[44]

3.2.4 Release of the model protein Cytochrome C

The fragmentation of the BNCs in presence of a reducing 10 μM solution of GSH for 24 h was already shown in Figure 3.10 b.

In **Figure 3.13**, we report the kinetic of release of Cytochrome-C encapsulated in nanocapsules. Cytochrome C was used as a model protein to study the release kinetics thanks to its strong absorption in the visible region, due to the presence of the eme group. The BNCs were thus embedded into the dPAA and the Cyt-C released from the nanocomposite was investigated, by incubating the scaffold in the 10 μM solution of GSH in PBS.

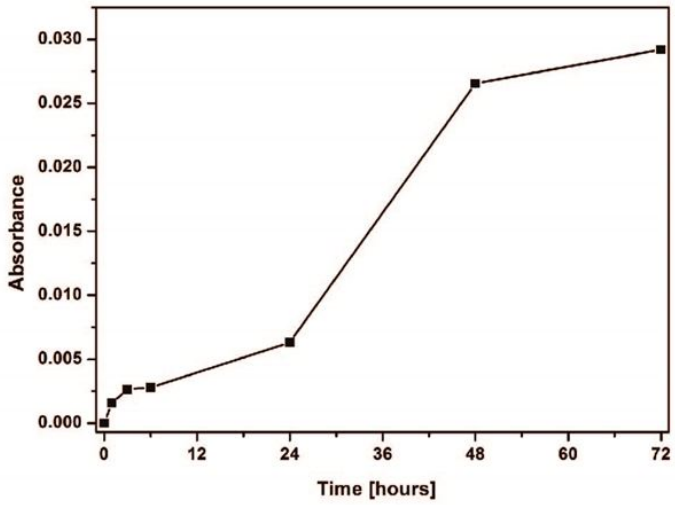

Figure 3.13 Kinetic of release of Cytochrome C from the nanocomposite PAAm. Absorbance measured at λ= 410 nm

The cumulative release of Cyt-C from the dPAAm shows a slow release in the first 6 hours, followed by an increase of detected Cyt-C. The release of Cyt-C from the scaffold is highly augmented by the degradation of the hydrogel structure, which can be seen from the shape of the curve between 24 and 72 hours, showing a steep growth in absorption. By comparing the detected absorbance with a calibration curve obtained my measuring the absorbance of Cytochrome C at different concentration, the overall amount of protein release from the scaffold was estimated to be 67% of the initial loading.

3.2.5 dPAAm as Submucosal Fluid Cushion for ESD

In paragraph 2.1 of this chapter, we have shown that PAAm are injectable through a 23-gauge needle and through an endoscopic needle, and that after injection they rapidly form a stable SFC.

Herein, we will demonstrate that dPAAm hydrogels have the same behavior, that they act in a significantly better way in comparison to normal saline solution (NS) and that they are suitable candidate for ESD.

The pre-gel solution can be easily prepared in about 30 minutes, directly in the operating room, by simple mixing of pre-dosed amount of precursor. Depending on the stability of the encapsulated drug, the pre-gel solution can also be frozen and defrost just before use. The long gelation time *in-vial* ensures a broad injection window, while the extremely

short gelation time *in-vivo* allow a rapid surgery and a reduced risk of perforation or bleeding.

The reason for the faster gelation *in-vivo* is still unclear. As we have written before, we have already ruled out the effect of temperature and pH. Indeed, a less basic pH should hinder gelation, while higher temperature in the living tissues cannot justify such as big change. Also, we noticed that fast gelation happens also in cold *ex-vivo* tissues. We hypothesize that the observed gelation is due to a complex mixture of covalent crosslinking and intermolecular forces. In particular - considering the collagen-rich nature of the submucosal space - we imagine that, on one hand, pendant-amino groups in the collagen molecules can enhance the covalent crosslinking between the gel and the tissues, while on the other hand H-bonds and other non-covalent interactions between the amino and hydroxyl groups of collagen and the amino or carbonyl groups of the dPAAm may lead to the formation of a interpenetrating hydrogel network that promote the formation of an elastic gel. On this regard, we noticed that a harder SFC is obtained when the material is injected on a late stage of the synthesis. In ***Figure 3.14a*** we show the SEM picture of a dPAAm sample extracted after an *in-vivo* ESD procedure on a porcine model. The image shows the presence of long fibers, normally absent in the hydrogel. Similar structures can be endoscopically observed *in-vivo* in the submucosa space, as shown in ***Figure 3.14b***, after hydrogel injection and mucosa dissection. We propose that this may

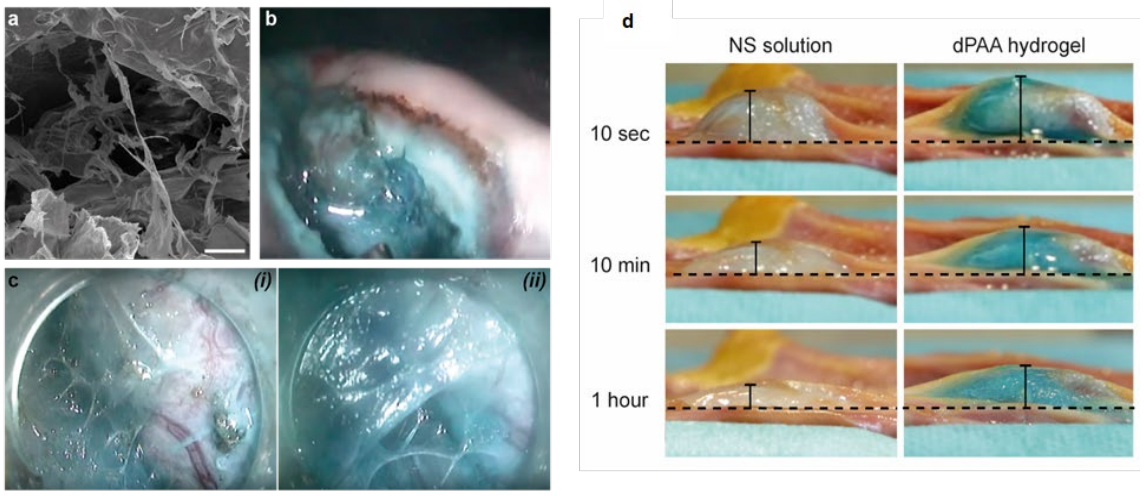

Figure 3.14 SEM image of a hydrogel sample after being injected for ESD, showing the presence of collagen fibers in the hydrogel matrix (a), scale bar is 100 µm. Endoscopic view of the dPAAm hydrogel (stained with Methylene Blue) formed *in-vivo* (b) and close up (c) that shows fibrous formation in the adherent material, similar to the ones observed at the SEM. *Ex-vivo* injection of NS or blue-stained dPAAm into a porcine stomach (d). Height values (black bar) obtained for NS were 6.7 mm, 4.2 mm and 2.9 mm after 10 sec, 10 min and 1 h respectively; for dPAAm were 8.3 mm, 6.4 mm, 5.8 mm after 10 sec, 10 min and 1 h respectively.

confirm the role of collagen in SFC formation, although no definitive data are yet available.

To confirm that dPAAm can sustain mucosal elevation for prolonged time, we compared the SFC obtained by injection of dPAAm hydrogel with the one from normal saline solution. In ***Figure 3.14d*** we show the time evolution of the SFC obtained by the injection of 2 mL of normal saline solution or dPAAm hydrogel (stained in blue for better visualization) in an explanted porcine stomach. The camera was placed perfectly perpendicular to the supporting plane to avoid any artefact or perspective error, and a length reference (not shown) was used to compare the height of the SFC. We observed that immediately after injection a protrusion is formed, as expected. The height after 10 seconds was taken as a reference and other measures were performed after 10 minutes and 1 hour, that approximately corresponds to the length of an ESD procedure.

Immediately after injection, we can observe a small difference in the height of the two fluid cushions, 8.3 mm for the dPAAm hydrogel and 6.7 mm for the NS solution. After 10 minutes, the height of the SFC was reduced to 4.2 mm for the NS (62%) and 6.4 for the dPAAm (77%). After one hour, only a negligible elevation can be observed for the NS (2.9 mm, 43%), while for the dPAAm hydrogel the elevation remained almost unchanged (5.8 mm, 70%). The difference in initial height already shows that a portion of the NS immediately spread on the surrounding tissues, even after just 10 seconds, while the dPAAm spreading was significantly slower. After the test, exposure of the dPAAm cushion confirmed the formation of soft hydrogel.

Considering these *ex-vivo* promising results, we decided to evaluate dPAAm nanocomposite hydrogel performance *in-vivo*. All the procedures were performed in triplicate on living pigs in Strasbourg, at IRCAD-Institut de Recherche contre les Cancers de l'Appareil Digestif and at IHU-Institut de chirurgie guidée par l'image. Saline solution was employed as a reference material.

All the steps of the procedure are reported in ***Figure 3.15***. After marking the site of the injection, simulating a lesion of approximately 3 cm in diameter, 8 mL of dPAAm

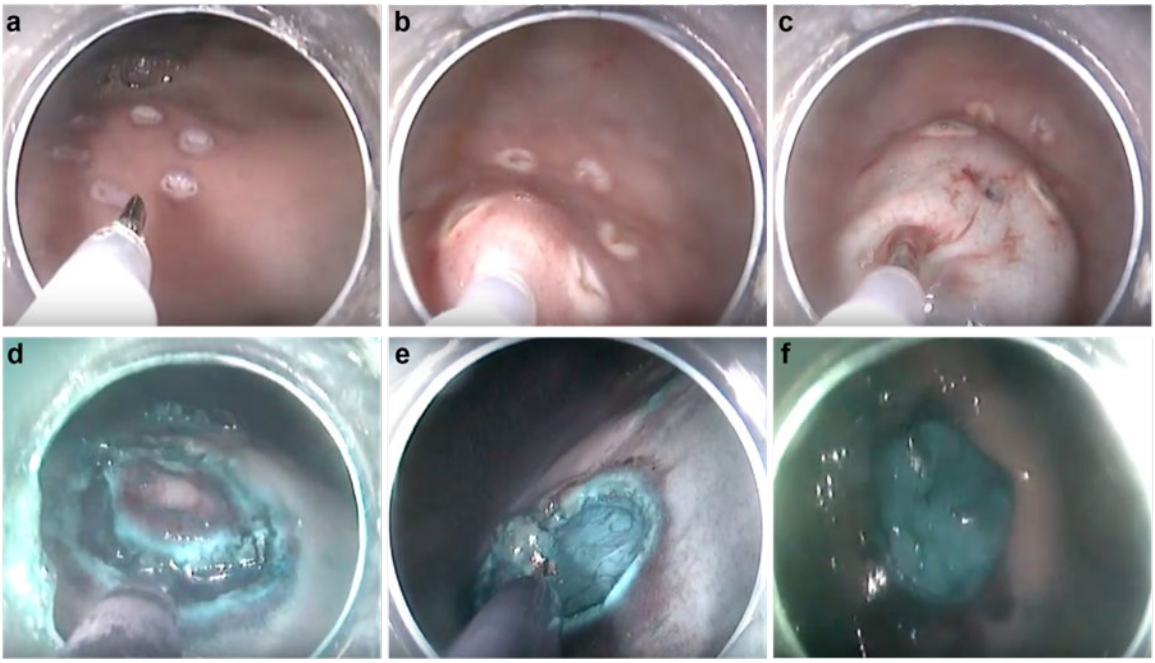

Figure 3.15 Endoscopic views of the different steps of the ESD procedure performed using the dPAA stained with Methylene Blue. Setting of the lesion, approx. 3 cm in diameter (a); injection of the dPAA solution (b); formation of the SFC after gelation of the dPAA (c); circumferential cutting (d); complete resection with protective layer of dPAA that remained adhered to the muscolaris (e); wound left after ESD with layer of the dPAA (f).

hydrogel or saline solution were injected in the submucosal space. Good elevation was immediately obtained both with the dPAAm hydrogel and with saline solution, however after approximately ten minutes a second injection of NS was required to account for the sharp decrease in mucosa elevation, while in the case of the dPAAm hydrogel the elevation remained stable during all the procedure. No bleeding or perforations were observed, the lesions were resected *en bloc* without significant damage to the underneath tissues and the resected specimen was easily collected at the end of the procedure, an essential step in real cases to get accurate histopathologic analysis and to ensure clear resection margin. At the end of the procedure, a thin layer of hydrogel remained adherent to the wound, ensuring protection to the stomach wall and allowing the release of bioactive molecules, such as antibiotics, chemokines, corticoids or adrenaline. Interestingly, we observed that the presence of the BCNs only marginally alters the adhesion or injectability properties of the dPAAm. Thus, it is possible to tailor the hydrogel to the need of the biomedical industry finding the best compromise between costs, regulatory problems and bioactivity.

To prove that the hydrogel is not toxic in an animal model, ESD procedures were performed of six pigs; in each pig, two ESD were performed in the stomach using the dPAAm hydrogel and two were performed using NS solution. We employed the

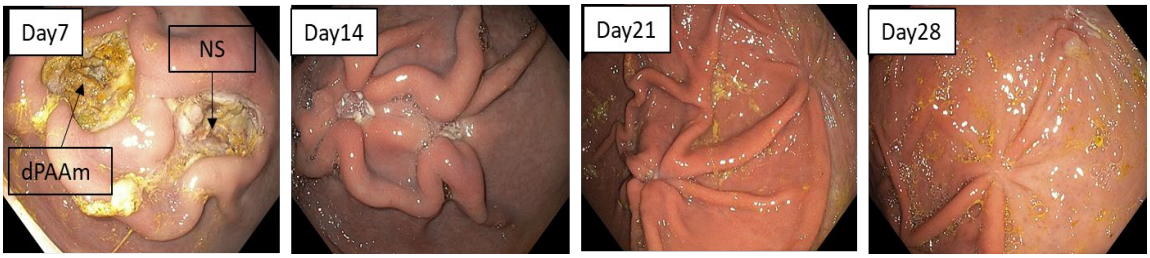

Figure 3.16 Comparison of wound healing after stomach ESD with dPAAm hydrogel (left lesion) and NS (right lesion) in a porcine model.

nanocomposite dPAAm hydrogel without any drug loading, in order to investigate the property of the pristine material. In all cases, the procedure with the dPAAm hydrogel was superior to the NS, with reduced operating time and higher comfort for the surgeon.

After surgery, the pigs were controlled at regular intervals to check the healing of the wound over time and endoscopic images taken after 1, 2, 3 and 4 weeks are reported in ***Figure 3.16***.

The pigs did not show any sign of discomfort apart from what can be expected after a similar surgery. An endoscopic check after one week showed that all the hydrogels were already completely degraded, while the lesions were starting to heal. In the following days, the difference in healing rate between the dPAAm hydrogel and the NS were observed: no major differences were found.

After 28 days, the animals were sacrificed, the specimens from the lesions were collected and a histopathologic analysis was conducted. The results however showed minor ulcers and inflammation in the sites where the dPAAm hydrogel was used.

This can be explained by the presence of traces of unreacted DMDA, whose high pH can promote minor damages and inflammation damage the surrounding tissues.

Further studies are in progress to solve the issue, such as substituting DMDA with less toxic amines or changing the reaction conditions to improve the conversion of the monomers into oligomers before injection.

3.4 Conclusions

We successfully designed an injectable, nanocomposite, degradable poly (amido amine)s-based hydrogel for applications as a submucosal fluid cushion in endoscopic submucosal dissection. The material is composed of breakable nanocapsules embedded in a PAAm network crosslinked with a redox-responsive crosslinker: cystamine. The material can undergo a process of degradation in response to the presence of living cells, thanks to the presence of a disulfide bridge in the diamine crosslinker, that may be cleaved by the glutathione released from the cells colonizing the material. The embedded BNCs can release proteins or other bioactive molecules in response to cell proliferation, that also trigger the breakage of the BNCs allowing the easy expulsion of the nanosized, non-toxic degradation fragments.

We have shown that the proposed material is not cytotoxic, that degrade in response to the growth of human dermal fibroblast and that it is easily injectable through a regular 23 G endoscopic needle. Upon injection, the dPAAm hydrogel forms a stable SFC with a clear longer elevation compared to normal saline solution. Also, preliminary *in-vivo* studies showed that the material is effective in preventing bleeding and perforation.

It is still unclear the exact mechanism that leads to an immediate gelation of the material after injection, but we hypothesized that it can be linked through non-covalent interactions between the oligomers chains and the collagen fibers present in the submucosal space.

Further experiments are in progress to finely tune the basicity of the material and the synthetic conditions in order to reduce the basicity of the pre-gel solution and avoid any possible complications after surgery.

3.5 Experimental part

3.5.1 Materials

Triton X-100, Ammonium hydroxide solution (28% NH_3), 3-chloropropyltriethoxysilane, Cytochrome C from equine heart, L-Glutathione reduced, n-hexanol, N,N'-Methylenbisacrylamide, Pentaethylenehexamine (technical grade), Tetraethyl Orthosilicate, Triethylamine were purchased from Sigma-Aldrich. Bis[3-(triethoxysilyl)propyl]disulfide was purchased by ABCR. 4-aminobutyric acid was purchased from Fluka.

3.5.2 Synthesis and functionalization of BNCs

Triton X-100 (7.08 ml) and n-hexanol (7.20 ml) were dissolved in cyclohexane (30 ml). Separately, a 5 mg/mL aqueous solution (1.20 ml) of cytochrome C from equine heart, Cyt-C, was mixed with tetraethyl orthosilicate (0.16 µl) and bis[3-(triethoxysilyl)propyl]disulfide (0.24 ml). After stirring, this mixture was added to the former organic medium. Eventually, 200 µl of 30% ammonia aqueous solution were added and the water-oil emulsion was stirred overnight at room temperature.

After that, pure acetone (80 ml) was added to the reaction mixture in order to precipitate the material and the BNCs (40 mg) were recovered by means of centrifugation, washing several times with water and ethanol.

Then, the surface of the obtained BNCs was functionalized to afford amino-functionalized breakable nanocapsules. The surface functionalization was performed as follows. 40 mg of nanocapsules were suspended in ethanol (5 ml). 3-aminopropyltriethoxysilane (0,094 mmol, 22 µl) and triethylamine (TEA, 10 µl) were added to the suspension, which was stirred at room temperature for 18 hours.

The precipitate was then washed five times with distilled water, to afford 30 mg of BNCs.

3.5.3 Degradation kinetic in presence of GSH

Degradation of dPAA hydrogels was examined in the presence of reduced glutathione (GSH), a disulfide reducing agents.

Briefly, the lyophilized hydrogels samples were incubated at 37 °C in 2 mL of a PBS solution with a GSH concentration of 10 μM. dPAA hydrogels were incubated in PBS alone as a control.

The degradation kinetics were then evaluated via swelling ratio (SR) measurements in time. SR were measured by a gravimetric method. In brief, lyophilized hydrogel samples were immersed in PBS at 37 °C. Then, the samples were removed from PBS at set time points (after 1 h, 6 h, 12 h, 24 h, 48 h, 72 h, 144 h), blotted free of surface water using filter paper and their swollen weights were measured on an analytical balance. The SR were then calculated as a ratio of weights of swollen hydrogel (Ws) to dried hydrogel (Wd), using the following equation:

$$SR = \frac{W_s - W_d}{W_d}$$

Degradation time was defined as the time where there were no longer sufficient crosslinks to maintain the 3D network and the material was completely disintegrated. Experimentally, complete degradation was determined when we could observe a limpid solution, without solid residues.

3.5.4 Mechanical characterization of dPAA by shear rheology

We determined the viscoelastic response of dPAA gels under oscillatory shear stress in a broad range of strain amplitudes and deformation rates. In this work, only rheological data in the linear regime are shown (at γ = 1%, f = 1 Hz and T = 37ºC). The mechanical degradation experiments were performed at similar conditions (γ = 1%, ω = 1 Hz and T = 37ºC) and the time evolution of the shear moduli were monitored upon GSH addition. Prior to starting any rheological measurement at the working temperature, the sample is subjected to pre-shearing at constant strain in the linear regime and constant frequency (1 Hz).

3.5.5 Release of model protein Cyt-C

Cytochrome-C, Cyt-C, was used as a model protein to study the release kinetics thanks to its strong absorption in the visible region, due to the presence of the eme group.
The BNCs were thus embedded into the dPAA and the Cyt-C released from the nanocomposite was investigated, by incubating the scaffold in the 10 μM solution of GSH in PBS.
The release of CytC was followed recording monitoring the UV absorption of the supernatant, at λ= 410 nm, at set time points, after centrifugation to remove debris of the degraded material.

3.5.6 In vitro cell culturing

Cryopreserved human dermal fibroblast, adult (HDFa) were purchased from Thermo Fisher and the culture was initiated as suggested on the protocol. HDFa were grown in Medium 106 supplemented with Low Serum Growth Supplement (LSGS, Thermo Fisher). Cells were kept in 75 cm2 culture flasks (Corning Inc., NY, USA) at 37 °C with a controlled atmosphere of 5% CO2 and were grown until reaching 80 to 85% of confluence. Then, they were washed twice with PBS and treated with trypsin/EDTA solution to detach them from the flask surface. Cells were split every 2-3 days; the medium was changed every other day.

3.5.7 In vitro cell culturing onto the nanocomposite hydrogels

The hydrogel scaffolds equilibrated by adding culture media at 37°C. HDFa were detached from the culture flask by trypsination and approximately 2.5x105 cells were seeded onto the hydrogel scaffolds. Then, the samples were placed in the incubator (37°C, 5% CO2) for about 30 minutes and fresh media was cautiously added on the top of the hydrogels to supply cells with nutrients. This was done to allow anchorage of the cells onto the scaffolds.

3.5.8 Cell staining and viability studies

Cell viability was assessed using alamarBlue assay. Briefly, the alamarBlue solution was added to the culture medium (1:10 dilution) of unstained cells growing onto hydrogel scaffolds. After 3h incubation, 200 µL of the media were transferred to a 96-well plate and absorbance signals generated from the dye resazurin (dark blue) being reduced to resorufin (pink) by metabolically active cells were recorded using a VICTOR X5 Multilabel Plate Reader (Perkin Elmer).

Each sample was tested in three replicates and the results were expressed as percentage of reduced alamarBlue.

The viability of cells after complete degradation of the dPAA was measured by with a TC20™ Automated Cell Counter (Bio-Rad).

Where required (confocal fluorescence microscopy images), HDFa were stained with Vybrant DiD (Life Technologies, Thermo Fisher Scientific, Waltham, MA, USA), following the reported protocol, prior to seeding them onto the scaffolds.

3.5.9 Synthesis of the dPAA hydrogel

In a typical synthesis, 200 mg of MBA (1.3 mmol) and 65 mg of cystamine dihydrochloride (0.29 mmol) are weighted in a glass vial. 1.5 mL of water are added, together with 110 mg of N,N-dimethylethylendiamine (1.25 mmol). The material is left under magnetic stirring and a homogenous clear solution is formed after 1 h.

An elastic hydrogel is formed approximately 18 h after the start of the synthesis. The synthesis can be adjusted controlling the amount of water (1 mL or 0.75 mL) in order to obtain a harder hydrogel or a faster gelation time.

3.5.10 Evaluation of the gelation and formation of SFC ex vivo

Fresh porcine stomachs were used for the ex vivo tests. The hydrogel solution was injected into the submucosal layers of the pig stomach using a 23-gauge needle. The dose was 2 ml for each sample and the stomach was kept to a temperature of about 37 °C with a lamp to ensure simulation of in vivo conditions. Gelation of the dPAA samples was

assessed by cutting open the tissue after the desired time. The experiment was repeated three times.

References

(1) Wild, B. W. S. and C. P. World Cancer Report 2014. **2014**, 630.

(2) McLatchie, G.; Borley, N.; Chikwe, J. *Oxford Handbook of Clinical Surgery*; **2013**.

(3) Orditura, M.; Galizia, G.; Sforza, V.; Gambardella, V.; Fabozzi, A.; Laterza, M. M.; Andreozzi, F.; Ventriglia, J.; Savastano, B.; Mabilia, A.; et al. Treatment of Gastric Cancer. *World J. Gastroenterol.* **2014**, *20* (7), 1635–1649.

(4) De Manzoni, G.; Marrelli, D.; Baiocchi, G. L.; Morgagni, P.; Saragoni, L.; Degiuli, M.; Donini, A.; Fumagalli, U.; Mazzei, M. A.; Pacelli, F.; et al. The Italian Research Group for Gastric Cancer (GIRCG) Guidelines for Gastric Cancer Staging and Treatment: 2015. *Gastric Cancer* **2017**, *20* (1), 20–30.

(5) Ono, H.; Yao, K.; Fujishiro, M.; Oda, I.; Nimura, S.; Yahagi, N.; Iishi, H.; Oka, M.; Ajioka, Y.; Ichinose, M.; et al. Guidelines for Endoscopic Submucosal Dissection and Endoscopic Mucosal Resection for Early Gastric Cancer. *Dig. Endosc.* **2016**, *28* (1), 3–15.

(6) Maple, J. T.; Abu Dayyeh, B. K.; Chauhan, S. S.; Hwang, J. H.; Komanduri, S.; Manfredi, M.; Konda, V.; Murad, F. M.; Siddiqui, U. D.; Banerjee, S. Endoscopic Submucosal Dissection. *Gastrointest. Endosc.* **2015**, *81* (6), 1311–1325.

(7) Ferreira, A.; Moleiro, J.; Torres, J.; Dinis-Ribeiro, M. Solutions for Submucosal Injection in Endoscopic Resection: A Systematic Review and Meta-Analysis. *Endosc. Int. Open* **2015**, *04* (01), E1–E16.

(8) Kang, K. J.; Min, B. H.; Lee, J. H.; Kim, E. R.; Sung, C. O.; Cho, J. Y.; Seo, S. W.; Kim, J. J. Alginate Hydrogel as a Potential Alternative to Hyaluronic Acid as Submucosal Injection Material. *Dig. Dis. Sci.* **2013**, *58* (6), 1491–1496.

(9) Kusano, T.; Etoh, T.; Akagi, T.; Ueda, Y.; Shiroshita, H.; Yasuda, K.; Satoh, M.; Inomata, M.; Shiraishi, N.; Kitano, S. Evaluation of 0.6% Sodium Alginate as a Submucosal Injection Material in Endoscopic Submucosal Dissection for Early Gastric Cancer. *Dig. Endosc.* **2014**, *26* (5), 638–645.

(10) Hwang, J. H.; Konda, V.; Abu Dayyeh, B. K.; Chauhan, S. S.; Enestvedt, B. K.; Fujii-Lau, L. L.; Komanduri, S.; Maple, J. T.; Murad, F. M.; Pannala, R.; et al. Endoscopic Mucosal Resection. *Gastrointest. Endosc.* **2015**, *82* (2), 215–226.

(11) Cao, L.; Li, Q.; Zhang, C.; Wu, H.; Yao, L.; Xu, M.; Yu, L.; Ding, J. Safe and Efficient Colonic Endoscopic Submucosal Dissection Using an Injectable Hydrogel. *ACS Biomater. Sci. Eng.* **2016**, *2* (3), 393–402.

(12) Yu, L.; Xu, W.; Shen, W.; Cao, L.; Liu, Y.; Li, Z.; Ding, J. Poly(Lactic Acid-Co-Glycolic Acid)-Poly(Ethylene Glycol)-Poly(Lactic Acid-Co-Glycolic Acid) Thermogel as a Novel Submucosal Cushion for Endoscopic Submucosal Dissection. *Acta Biomater.* **2014**, *10* (3), 1251–1258.

(13) Tran, R. T.; Palmer, M.; Tang, S. J.; Abell, T. L.; Yang, J. Injectable Drug-Eluting

Elastomeric Polymer: A Novel Submucosal Injection Material. *Gastrointest. Endosc.* **2012**, *75* (5), 1092–1097.

(14) Fernández-Esparrach, G.; Shaikh, S. N.; Cohen, A.; Ryan, M. B.; Thompson, C. C. Efficacy of a Reverse-Phase Polymer as a Submucosal Injection Solution for EMR: A Comparative Study (with Video). *Gastrointest. Endosc.* **2009**, *69* (6), 1135–1139.

(15) Ifkovits, J. L.; Burdick, J. A. Review: Photopolymerizable and Degradable Biomaterials for Tissue Engineering Applications. *Tissue Eng.* **2007**, *13* (10), 2369–2385.

(16) Kumano, I.; Ishihara, M.; Nakamura, S.; Kishimoto, S.; Fujita, M.; Hattori, H.; Horio, T.; Tanaka, Y.; Hase, K.; Maehara, T. Endoscopic Submucosal Dissection for Pig Esophagus by Using Photocrosslinkable Chitosan Hydrogel as Submucosal Fluid Cushion. *Gastrointest. Endosc.* **2012**, *75* (4), 841–848.

(17) Ishihara, M.; Kumano, I.; Hattori, H.; Nakamura, S. Application of Hydrogels as Submucosal Fluid Cushions for Endoscopic Mucosal Resection and Submucosal Dissection. *J. Artif. Organs* **2015**, *18* (3), 191–198.

(18) Kim, H. J.; Hwang, B. H.; Lim, S.; Choi, B. H.; Kang, S. H.; Cha, H. J. Mussel Adhesion-Employed Water-Immiscible Fluid Bioadhesive for Urinary Fistula Sealing. *Biomaterials* **2015**, *72*, 104–111.

(19) Waite, J. H.; Tanzer, M. L. The Bioadhesive of Byssus: A Protein Containing L-DOPA. *Biochem. Biophys. Res. Commun.* **1980**, *96* (4), 1554–1561.

(20) Waite, J. H. Nature's Underwater Adhesive Specialist. *Int. J. Adhes. Adhes.* **1987**, *7* (1), 9–14.

(21) Wei, Q.; Achazi, K.; Liebe, H.; Schulz, A.; Noeske, P. L. M.; Grunwald, I.; Haag, R. Mussel-Inspired Dendritic Polymers as Universal Multifunctional Coatings. *Angew. Chemie - Int. Ed.* **2014**, *53* (43), 11650–11655.

(22) Kim, B. J.; Oh, D. X.; Kim, S.; Seo, J. H.; Hwang, D. S.; Masic, A.; Han, D. K.; Cha, H. J. Mussel-Mimetic Protein-Based Adhesive Hydrogel. *Biomacromolecules* **2014**, *15* (5), 1579–1585.

(23) Lee, B. P.; Konst, S. Novel Hydrogel Actuator Inspired by Reversible Mussel Adhesive Protein Chemistry. *Adv. Mater.* **2014**, *26* (21), 3415–3419.

(24) Li, L.; Smitthipong, W.; Zeng, H. Mussel-Inspired Hydrogels for Biomedical and Environmental Applications. *Polym. Chem.* **2015**, *6* (3), 353–358.

(25) Ji, Y.; Ji, T.; Liang, K.; Zhu, L. Mussel-Inspired Soft-Tissue Adhesive Based on Poly(Diol Citrate) with Catechol Functionality. *J. Mater. Sci. Mater. Med.* **2016**, *27* (2), 1–9.

(26) Yavvari, P. S.; Srivastava, A. Robust, Self-Healing Hydrogels Synthesised from Catechol Rich Polymers. *J. Mater. Chem. B* **2015**, *3* (5), 899–910.

(27) Guo, Z.; Ni, K.; Wei, D.; Ren, Y. Fe^{3+} -Induced Oxidation and Coordination Cross-Linking in Catechol–chitosan Hydrogels under Acidic PH Conditions. *RSC Adv.* **2015**, *5* (47), 37377–37384.

(28) Hou, S.; Ma, P. X. Stimuli-Responsive Supramolecular Hydrogels with High

Extensibility and Fast Self-Healing via Precoordinated Mussel-Inspired Chemistry. *Chem. Mater.* **2015**, *27* (22), 7627–7635.

(29) Brennan, M. J.; Kilbride, B. F.; Wilker, J. J.; Liu, J. C. A Bioinspired Elastin-Based Protein for a Cytocompatible Underwater Adhesive. *Biomaterials* **2017**, *124*, 116–125.

(30) Fan, C.; Fu, J.; Zhu, W.; Wang, D. A. A Mussel-Inspired Double-Crosslinked Tissue Adhesive Intended for Internal Medical Use. *Acta Biomater.* **2016**, *33*, 51–63.

(31) Jeon, E. Y.; Hwang, B. H.; Yang, Y. J.; Kim, B. J.; Choi, B. H.; Jung, G. Y.; Cha, H. J. Rapidly Light-Activated Surgical Protein Glue Inspired by Mussel Adhesion and Insect Structural Crosslinking. *Biomaterials* **2015**, *67*, 11–19.

(32) Lee, B. P.; Dalsin, J. L.; Messersmith, P. B. Synthesis and Gelation of DOPA-Modified Poly(Ethylene Glycol) Hydrogels. *Biomacromolecules* **2002**, *3* (5), 1038–1047.

(33) Cencer, M.; Liu, Y.; Winter, A.; Murley, M.; Meng, H.; Lee, B. P. Effect of PH on the Rate of Curing and Bioadhesive Properties of Dopamine Functionalized Poly(Ethylene Glycol) Hydrogels. *Biomacromolecules* **2014**, *15* (8), 2861–2869.

(34) Maier, G. P.; Bernt, C. M.; Butler, A. Catechol Oxidation: Considerations in the Design of Wet Adhesive Materials †. *Biomater. Sci.* **2018**, No. 2.

(35) Yang, J.; Stuart, M. A. C.; Kamperman, M. Jack of All Trades : Versatile Catechol Crosslinking Mechanisms. *Chem. Soc. Rev.* **2014**, *43* (24), 8271–8298.

(36) *Oxygen Transport to Tissue XXXIV*; Welch, W. J., Palm, F., Bruley, D. F., Harrison, D. K., Eds.; Springer, 2013; Vol. 765.

(37) Forman, H. J.; Zhang, H.; Rinna, A. Glutathione: Overview of Its Protective Roles, Measurement, and Biosynthesis. *Mol Asp. Med* **2009**, *30* (1–2), 1–12.

(38) Kharkar, P. M.; Kiick, K. L.; Kloxin, A. M. Design of Thiol- and Light-Sensitive Degradable Hydrogels Using Michael-Type Addition Reactions. *Polym. Chem.* **2015**, *6* (31), 5565–5574.

(39) Hartmann, L.; Häfele, S.; Peschka-Süss, R.; Antonietti, M.; Börner, H. G. Sequence Positioning of Disulfide Linkages to Program the Degradation of Monodisperse Poly(Amidoamines). *Macromolecules* **2007**, *40* (22), 7771–7776.

(40) Wu, H. Q.; Wang, C. C. Biodegradable Smart Nanogels: A New Platform for Targeting Drug Delivery and Biomedical Diagnostics. *Langmuir* **2016**, *32* (25), 6211–6225.

(41) Kar, M.; Vernon Shih, Y. R.; Velez, D. O.; Cabrales, P.; Varghese, S. Poly(Ethylene Glycol) Hydrogels with Cell Cleavable Groups for Autonomous Cell Delivery. *Biomaterials* **2016**, *77*, 186–197.

(42) Prasetyanto, E. A.; Bertucci, A.; Septiadi, D.; Corradini, R.; Castro-Hartmann, P.; De Cola, L. Breakable Hybrid Organosilica Nanocapsules for Protein Delivery. *Angew. Chemie - Int. Ed.* **2016**, *55* (10), 3323–3327.

(43) P., B. Wound Healing and the Role of Fibroblasts. *J. Wound Care* **2013**, *22* (8), 407–412.

(44) Emilitri, E.; Guizzardi, F.; Lenardi, C.; Suardi, M.; Ranucci, E.; Ferruti, P. Novel Poly(Amidoamine)-Based Hydrogels as Scaffolds for Tissue Engineering. *Macromol. Symp.* **2008**, *266* (1), 41–47.

4. Special hydrogel formulations for clinical applications

In the previous chapters, we have shown that poly(amidoamine)s hydrogels are promising materials for biomedical applications because of their peculiar properties and biocompatibility.

PAAm-based hydrogels can be prepared with non-expensive commercially-available starting products, the covalent backbone can be easily modified to add special functionalities and their mechanical properties can be tuned to match the one requested by the specific application. Also, their kinetic of gelation allows easy injectability, making them suitable materials for applications in minimally-invasive surgery.

In Chapter 3, we have demonstrated that nanocomposite degradable PAAm hydrogels are a promising alternative to saline solution for Endoscopic Submucosal Dissection.

In this chapter we will analyze how different hydrogel formulations, such as hybrid alginate-containing PAAm hydrogels or hydrogel-based creams can be used in minimally-invasive surgery for the treatment of fistulas or for the percutaneous treatment of direct inguinal hernia.

The work on hernia was conducted in collaboration with Prof. Mariano Gimenez, Dr. Federico Davrieux and Dr. Alain Garcia.

For the work on fistula treatment, we thank Prof. Silvana Perretta and Dr. Ludovica Guerrero.

Part of the rheological measures were performed at Solvay Laboratory of the Future under the supervision of Dr. Pascal Hervé.

4.1 Surgical approaches to inguinal hernia

Today, inguinal hernia represents a significant health and social problem, and is one of the most common disease in developed country, with more than 20 million hernia repair procedures performed annually worldwide.[1]

Inguinal hernias accounts for approximately 75% of all the cases of abdominal wall hernias.[2] Not only it may cause pain and discomfort to the patients, but un untreated inguinal hernia may lead to more sever and potentially life-threatening consequences - such as obstruction or intestinal ischemia - that need urgent surgical therapy to be resolved.[3]

Since the introduction in 1984 of "tension-free" hernia repair, the Lichtenstein tecnique[4] has been accepted as a gold standard both unilateral and bilateral inguinal hernias. In comparison to the standard tissue repair technique that - despite being introduced by Bassini as early as in 1887 and being refined in the following year - has still a 10-15% overall recurrence rates, the tension-free method significantly decreases the risk of recurrence[2] and the costs of the surgery while improving reliability and safety. In the standard approach, the external and internal oblique muscles are pulled together under tension, while in the tension-free method a synthetic or biological mesh is placed in the correct position. Despite the introduction of laparoscopic techniques, post-operative chronic pain is still an issue, and it is main caused by damage to the nerve fibers, by inflammation or by the contact between the mesh and the nerves.

Research on inguinal hernia treatments focuses mainly on improving the surgical techniques or on developing new materials for prosthetic meshes. Today, a wide choice of materials is available to the surgeons for hernioplasty procedures, from standard non-degradable polypropylene meshes, to degradable ones in polylactic acid. In the last years, biological meshes have also been introduced,[5] but their use is limited only to very selected situations.

Different laparoscopic, endoscopic and even robotic techniques have also been developed for hernia treatment, such as Transabdominal Preperitoneal (TAPP), Extraperitoneal (TEP) or Flexible Endoscopic Preperitoneoscopy (FLEPP). The use of these techniques reduces pain and discomfort for the patients and reduces hospitalization time in

comparison to open surgery, but unfortunately requires extensive training and has a steep learning curve.[6]

In this section, we will present a new totally percutaneous approach to the problem, in which an injectable, non-degradable PAAm hydrogel is injected in the inguinal region, solidifying *in-situ* and thus removing the need for the placement of a prosthetic mesh. This new technique would allow for a simpler and more patient-friendly treatment of inguinal hernia, without all the side-effects of open or laparoscopic procedures.

Percutaneous surgery (i.e. "surgery through the skin") is a recent development in minimally-invasive surgery. Percutaneous approaches, in a similar way to interventional radiology, do not use large incisions, scalpels or trocars, but rely on the use of needles, wires, catheters or stents employed under image guidance. Indeed, the surgeon relies on ultrasound (US), computed tomography scan (CT), fluoroscopy or other techniques to identify the target point and navigate through the human body to reach it. In recent years, the introduction of new techniques of image fusion gave to the surgeons the opportunity to combine together - in real time - the information obtained from different imaging modalities, such as US and CT, having a clearer picture of the anatomical landmark they need and improving the precision of image guidance.[7–10]

Some of the advantages of this approach are the use of local anesthesia - instead of general anesthesia - the reduced intervention time and the reduced chances of infections and complications. To cite a few examples, percutaneous techniques have been used in foot surgery[11,12] or in tumor ablation.[13–16]

In our idea, a percutaneous image-assisted injection of an especially-designed hydrogel for inguinal hernia treatment would allow to reduce hospitalization time, post-operative chronic pain, reduce the costs of the surgery, the possibility of damaging healthy tissues and thus lead to a better comfort for the patient.

4.2 Hybrid hydrogels for percutaneous treatment of inguinal hernia

4.2.1 Design and synthesis of the material

Since their introduction in the early '60,[17] hydrogels have attracted considerable interest in the biomedical field to mimic the extra-cellular matrix, thanks to their biocompatibility, elastic properties, high water content and the porous 3D structure that allows permeation of oxygen and nutrients and thus cell growth and proliferation[18–21]. Compared to natural hydrogels, such as cellulose or chitosan, synthetic covalent hydrogels offer new opportunities for the incorporation of stimuli-reactive chemical moieties and allow a broader control on chemical structure and functionalization, on mechanical properties and a better reproducibility. However, synthetic hydrogels can be less biocompatible than their natural counterpart and their synthesis may require toxic radical initiators and several purification steps.

Polyamidoamines (PAAm) are a class of covalent hydrogels well-known in literature for their biocompatibility, the easy chemical tunability and the mild reaction conditions required.[22,23] Their synthesis is based on a aza-Michael addition of nucleophilic amines to conjugated double bonds and it doesn't require any radical initiator or purification step. The reaction is conducted in water and gelation time can be precisely controlled by controlling the temperature, that can range from room temperature to up to 80 °C.

In a previous paper,[21] we have shown the synthesis of a hybrid hydrogel composed by a PAAm network crosslinked with mesoporous silica nanoparticles and we have demonstrated that this system allows mesenchymal stem cells growth and proliferation and that we can control the release of bioactive molecules, such as chemokines, from the nanoparticles.

In previous chapter, we have shown how a degradable PAAm-based hydrogel can be injected and used for endoscopic submucosal dissection.

Herein, we present an injectable hydrogel composed of an interpenetrating network of sodium alginate/PAAm for percutaneous hernia treatment.

The material we report is not cytotoxic, straightforward to prepare, strongly adhesive to the living tissues, stable over time and with optimal mechanical strength and elasticity.

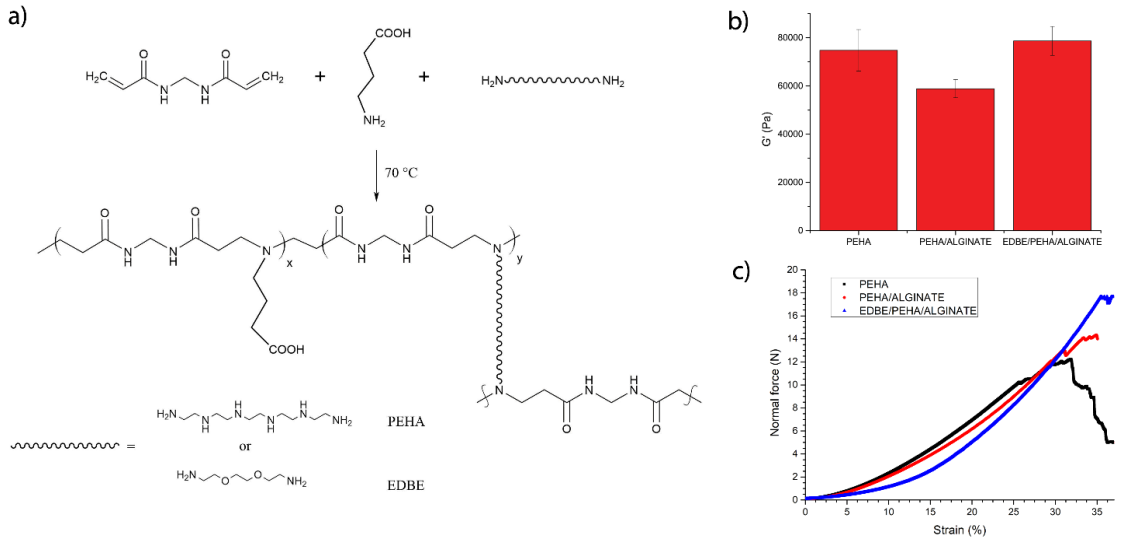

Figure 4.1 Reaction scheme for the synthesis of a PAAm hydrogel. Crosslinker can be either PEHA, EDBE or a combination of both (a); Elastic modulus the PEHA hydrogel in water, PEHA in alginate and EDBE/PEHA in alginate (b); Stress-strain curve for PEHA hydrogel in water (black), PEHA in alginate (red) and EDBE/PEHA in alginate (blue) (c)

In order to be suitable for the desired application, the material should be easy to prepare for immediate application in the operating room, easy to inject but able to gelify before spreading away from the desired area, it should adhere strongly to the surrounding tissue, be non-degradable, elastic and mechanically resistant enough to sustain high stress. It should also be non-cytotoxic and should not promote inflamatory reactions.

In ***Figure 4.1*** we report the reaction scheme for the synthesis of the material. The synthesis is based on aza-Michael reaction between conjugated double bonds and basic amines, in our case between N,N'-methylenebisacryalmide (MBA), γ-aminobutiric acid (GABA) and a diamine crosslinker, in particular pentaethylenhexamine (PEHA) and 2,2'-(Ethylenedioxy)bis(ethylamine) (EDBE). All the hydrogels were prepared keeping the same concentration of MBA and GABA. The reaction can be conducted at any temperature between room temperature and 80 °C and gelation time change accordingly. After the starting materials are mixed together, in water or in 2% sodium alginate, a suspension of the only slightly water-soluble MBA is obtained. The reaction starts immediately and after a certain amount of time, normally between 30 minutes and 1 hour at room temperature depending on the amount of amino-crosslinker, MBA is completely dissolved, and a clear non-viscous solution is obtained. The polymerization follows a step-growth mechanism, so the viscosity of the solution remains very low until some minutes before gelation happens. This allows for easy injection of the material even moments before gelation. We decided to work at 70 °C to reduce the time needed to obtain

the injectable pre-gel solution. In these conditions, the pre-gel solution is clear and homogeneous after 5 minutes and the hydrogel is formed in 24 ± 2 minutes. The injection is performed after exactly 20 minutes from the start of the synthesis.

The crosslinker and degree of crosslinking has great influence on network properties, porosity, gelation time, elastic modulus and biocompatibility of an hydrogel.[24–26] Pentaethylenhexamine (PEHA) was chosen because of the high hydrophilicity, the flexibility imposed by a longer chain and the possibility to crosslink the network in more points, considering that each NH group is potentially able to react with a double bond. PEHA-hydrogels can have very high storage modulus (G') when the amount of crosslinker is high, but then they lack elasticity and cytotoxicity increase. In this work we decided to use a mixed amino-crosslinker system containing a part of PEHA and a part of 2,2'-(Ethylenedioxy)bis(ethylamine) (EDBE). EDBE can react only with the two primary amino group on the end of the chain, but hydrophilicity is guaranteed by the presence of the oxygen atoms of the ethylendioxy moieties. In contrast to PEHA, that can react in more point of the chain and thus can reduce the mesh-size, this allow to have greater flexibility. The use of crosslinkers containing longer carbon chains (such as hexamethylendiamine) would lead to a reduce hydrophilicity and to the formation of hydrophobic domains. In our intentions, we expect that the use of EDBE as a crosslinker should increase the elasticity and the porosity of the hydrogel.

In ***Figure 4.2***, we report the SEM image of a hydrogel obtained by the reaction of MBA and GABA with EDBE, that shows a regular porous structure compatible with cell colonization and nutrients exchange.

We decided to add γ-aminobutiric acid (GABA) as a monoamine monomer, as explained in Chapter 2, to improve the rheological properties and biocompatibility of the material. GABA is a natural neurotransmitter, it is safe, clinically approved and it is commercially available as a dietary supplement. We decided to use GABA to partially decrease the overall positive charge on the hydrogel backbone and to increase the mesh size of the hydrogel.

The low viscosity of the pre-gel solution can however have negative influence on fluid dispersion after injection. For these reasons, we decided to employ an IPN network of sodium alginate and PAAm hydrogel.

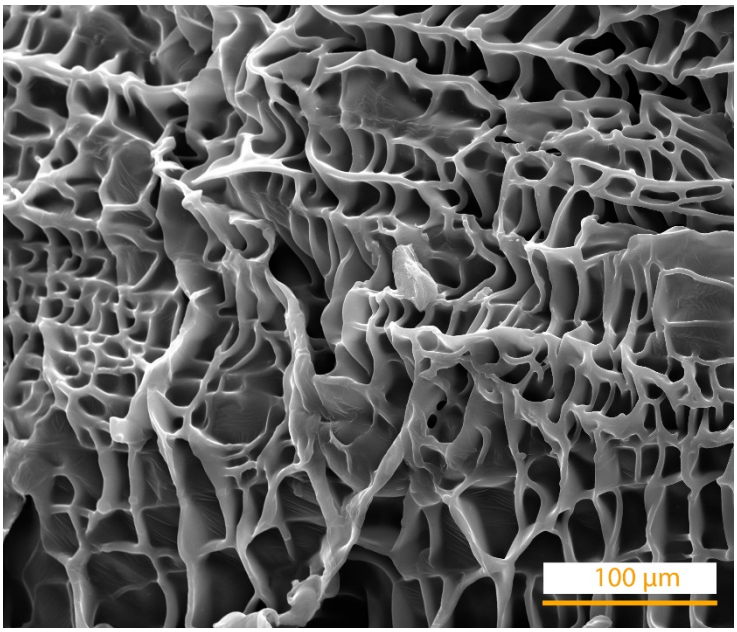

Figure 4.2 SEM picture of a hybrid hydrogel containing [EDBE]= 400 mM and [GABA]= 300 mM and [MBA]= 0.864 mM

Sodium alginate is a well-known natural, non-biodegradable hydrogel that is already approved in Europe and USA for food and clinical applications[19]. Alginate solutions are viscous and can solidify in seconds when in contact with a solution of calcium ions, forming a soft biocompatible hydrogel, and have no influence on PAAm network formation. We hypothesized that employing a viscous 2% sodium alginate water solution instead of pure water for hydrogel synthesis would allow less material dispersion after injections.

4.2.2 Rheological characterization and *in-vitro* toxicity

We decided to investigate the rheological and biological properties of three promising materials, in order to prove that they are suitable candidates for percutaneous hernia repair. In all cases, we kept constant the concentration of [MBA]= 864 mM and [GABA]= 300 mM. The first hydrogel was prepared as a reference with [PEHA]= 215 mM in water. Then, we prepared the same hydrogel in 2% sodium alginate and a third hydrogel was prepared using [PEHA]=129 mM and [EDBE]=220 mM in 2% sodium alginate.

In ***Figure 4.1b*** we report the storage modulus (G') of the three hydrogels. In all the cases the modulus is similar for all the three hydrogels, in the range of 70 kPa, even if it is slightly lower when we compare PEHA/WATER hydrogel with PEHA/ALG. A

compression test (***Figure 4.1c***) was performed on hydrogel cylinders of 1.90 cm diameter and approximately 8 mm height. It shows that adding alginate has a small positive influence on the maximum loading, 10 N at 25.6% strain for the PEHA/water and 13 N at 30,8% for the PEHA/ALG. As expected, PEHA/EDBE/ALG hydrogel had the best behavior and was able to sustain a load of 17.5 N (maximum normal force allowed by the instrument) at 35.5% strain. These values are comparable to the ones reported in literature for muscles and tendons.[27]

Both MBA, PEHA and EDBE, as pure compounds, have a significant toxicity as reported in their SDS. The hydrogel formation follows however a step-growth mechanism and in the moment of injection we expect that the concentration of the pure starting materials is negligible. To assess the cytocompatibility of the materials, we have measured the viability of HeLa cells for one week with the alamarBlue® test and the results are shown in ***Figure 4.3***.

The alamarBlue® test is employed to assess cell viability, and it measures the difference in absorbance between the dye resazurin (dark blue) and its reduced form resorufin (pink), produced by the reducing environment of metabolically active cells.

After synthesis, each hydrogel was cut in small cylinders, of approximatively 0.5 mm height and 1 cm diameter. The cylinders were sterilized with 95% ethanol and then washed with PBS and culture media. 20.000 HeLa cells were seeded on top of each hydrogel and cell viability was assessed after 1d, 4d and 7d. For each time point four to six replicated were considered, in order to minimize the error expected taking into account

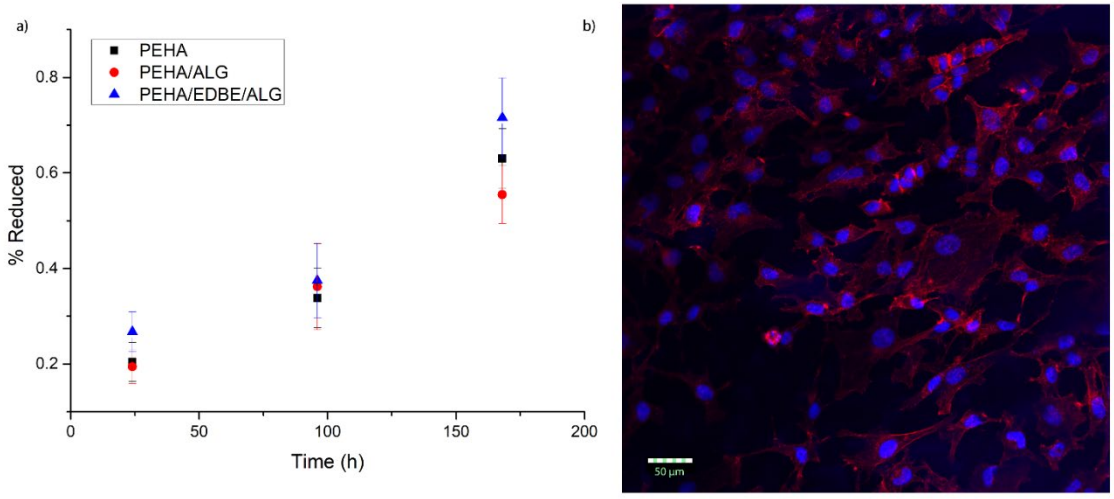

Figure 4.3 AlamarBlue test on HeLa cells growing on the PEHA/water (black), PEHA/ALG (red) and PEHA/EDBE/ALG (blue) hydrogels after 1, 4 and 7 days (a); Confocal image of HeLa cells growing on top of PEHA/EDBE/ALG hydrogel after seven days. Actin is stained with AlexaFluor Phalloidin 647 and the nuclear region with DAPI (b).

that a certain number of cells can slip out of the hydrogel surface before being able to adhere.

As reported in ***Figure 4.3a***, for all the three hydrogel it is possible to observe a significant increment of metabolic activity over time, although it is not possible to observe a statistically significant difference between the samples. The experiment was interrupted after seven days because all the hydrogels were completely colonized by HeLa cells. ***Figure 4.3b*** shows HeLa cells growing on the PEHA/EDBE/ALG hydrogel after seven days, stained with DAPI for the nucleus and with AlexaFluor Phalloidin 647 for Actin. Cells are well adherent to the hydrogel and colonized all the 3D structure.

4.2.3 Preliminary in-vivo assays

To evaluate the feasibility of the procedure and the toxicity of the materials, we designed a prospective comparative study in a porcine animal model with a 4 days survival period. This study was carried out at IHU-Strasbourg (France), in collaboration with the DAICIM Foundation (Argentina). The surgical procedures were performed by Prof. Mariano Gimenez and Dr. Federico Davrieux.

Five pigs (Sus scrofa domesticus), of both sexes, with weights ranging from 27 to 39 kg, were used. All the procedures were performed under general anesthesia.

The target area forms a triangle comprised between the bladder (internal), the major oblique muscle (posterior and external) and the epigastric artery (anterior and external) and was identified with CT scan with intravenous contrast. The epigastric artery was used as an anatomical landmark point when placing the needle. After having properly identified the area, using aseptic technique and with the support of ultrasonography (US) and fusion of images (Software Fusion VD10A Siemens - Germany) a 18G needle was introduced. The correct positioning of the needle was checked by performing a new CT-scan. Then, a hydro-dissection of the broad planes of the inguinal region was performed, using 5 mL of normal saline solution and the effect were verified with a new CT scan.

In the meantime, the pre-gel solution was prepared - at 70 °C - by mixing 15 mL of a 2% alginate solution of [PEHA]=129 mM and [EDBE]=220 mM with a pre-weighted mixture of MBA and GABA, so that their final concentration would be [MBA]= 864 mM and [GABA]= 300 mM.

After having verified the correct positioning of the needle and the quality of the hydro-dissection, 10 mL of hydrogel were injected exactly 22 minutes from the start of the synthesis at 70 °C, including two minutes at room temperature to cool down the material. Once completed the injection of the material, the needle was removed, controlling for a few minutes the existence of hematoma or hemorrhages. The position of the material was confirmed by CT and US and the same procedure was repeated on the left inguinal region. After surgery, the animals were returned to the animal facility and received water and food freely, analgesics, antibiotics (Cefalexine 15mg/kg) and gastric protectors (Proton Pump Inhibitors - PPI). All the pigs survived the surgery and no sign of distress more than expected were observed. No hemorrhagic complications were observed.

After the survival period (4 days), the animals were sacrificed, and a bilateral dissection of the inguinal region was performed to check for material position, consistency and adhesion to the surrounding tissues. The result is shown in ***Figure 4.4***. The material was perfectly adherent, well-integrated with the nearby anatomical structures, it was elastic and with optimal consistency. No sign of spreading outside the desired area was observed and in 8 out of 10 cases no signs of inflammation were observed,

Blood samples were collected before the surgery and before the euthanasia and showing no significative difference in the value of C-reactive protein.

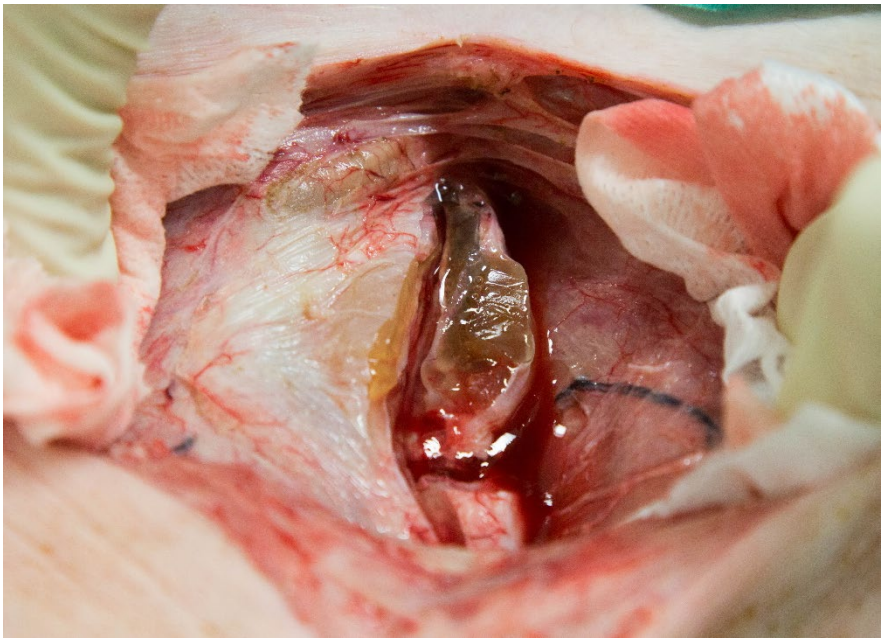

Figure 4.4 Position of the hybrid PAAm/alginate hydrogel four days after injection. The material remained in the intended position and is adherent to the surrounding tissues.

In two cases, local inflammatory reactions occurred. One corresponded to mastitis related to the incorrect position of the material (around the mammary gland). In the second one, the local inflammatory reaction was lymphadenitis of unknown cause.

4.3 Hydrogel-based creams for fistula closure

Fistulas are abnormal pathological connections between two hollow organs or with the skin, that can result from several reasons, such as complications after surgery, radiotherapy or as a side-effect of Chron's Disease.[28] Fistulas are very serious pathologies,[28] that may lead to a poor quality of life, chronic pain, infection and even death.

Unfortunately, the therapy for fistulas is not straightforward and even the surgical approach it is not always resolutive.[29–33] Some surgical adhesives, such as cyanoacrylates,[20,34–36] have been proposed to close the fistulous tract, but they have important neurological side effects.[37,38] For example, n-butyl cyanoacrylate has been used for the early treatment of fistula after hypospadias surgery in children, but failed in three cases over ten.[39]

Fibrin glue also has been used, but with alternating results depending on the location and complexity of the fistula.[40–42] Other materials have been also proposed such as collagen, chitosan[43] and PEG-based or catechol-based sealants,[44,45] but they suffer of disadvantages such as poor adhesion, low mechanical resistance or difficult injectability.

We imagined that injectable PAAm hydrogels can be applicable also for this condition, by closing the pathological communication and allowing cell proliferation and thus permanent fistula closure and cicatrization. However, standard PAAm hydrogels are not directly applicable in this case, because they would percolate outside the fistula before gelation. To solve this problem, we developed a cream based on a pre-gel PAAm solution in alginate as the water phase, and an organic phase composed by edible vegetable oils, FDA-approved surfactants and other molecules generally recognized as safe in cosmetic formulations. In our intentions, the creams should possess a shear-thinning behavior and yeld-stress, allowing them to be injected and then stay in position until gelation of the PAAm backbone occur.

4.3.1 PAAm-based cream formulation and preliminary *ex-vivo* results

In contrast to applications as in ESD or hernia, where the material is confined into a specific anatomical structure, in the case of fistulas the material needs to solidify

Figure 4.5 Ex-vivo test of a hybrid alginate/PAAm hydrogel for fistula closure on a fistula model prepared by anastomosis of a section of small bowel on the stomach wall.

immediately after injection, in order not to percolate out from the intended location. Thus, normal PAAm kinetic of gelation is not adequate for this purpose. As a first trial, we attempted to use a solution of PAAm hydrogel in alginate, in a similar way to what was done for hernia treatment, by triggering the gelation using a solution of calcium chloride. However, this would lead to an immediate blockage of the endoscopic needle, because of the instantaneous gelation of alginate when in contact with calcium chloride.

The idea was to inject a solution of sodium alginate, followed by the immediate injection of a concentrated hydrogel solution and then by the injection of calcium chloride. In this way, we hoped to avoid the blockage of the endoscopic needle because the alginate and calcium chloride solutions would have been in contact only outside of the injection system. After triggering gelation of the alginate network, in our intention the hydrogel would have stayed in position for the time needed to obtain gelation also the PAAm backbone. In ***Figure 4.5*** we show a preliminary ex-vivo test in which the three-component alginate-PAAm-$CaCl_2$ was tested on a fistula model obtained by suturing a section of the small bowel – closed at one extremity – on a porcine stomach wall. The three components were injected in the previously described order using an endoscope, and after finishing the injections the endoscopic needle was immediately flushed with saline solution.

Unfortunately, we observed that working with open system still lead to percolation of the precursors before gelation was obtained. In a closed system, gelation was immediate after all the three injections were performed and the material obtained was solid and homogenous. However, it was not adhesive to the surrounding tissues and we were able to remove it just by gentle squeezing. Also, this method was too complex to be realistically used in real-life situations.

Thus, we decided to change strategy and we investigated the possibility of using a self-standing PAAm-based cream that would then solidify some minutes after the surgery. In contrast to percutaneous hernia treatment or to ESD, where the material needed to have a

very low viscosity to pass through a 18 G or 21 G needle, in this case the material can also be thicker because it is possible to use 1.8 mm endoscopic sheath for the injection.

Creams are emulsions composed of an oil phase dispersed in a water phase. The main components of a cream, together with water and oil, are surfactants and thickeners,[46] together with small amounts of stabilizer and preservatives.

In our first attempt, the PAAm cream was prepared by employing the pre-gel solution as the main component of the water phase, while for the oil phase we employed a mixture of vegetable oils - in particular a mixture of coconut oil and sunflower oil. Coconut oil was chosen because of the high amount of saturated fatty acid, such as lauric acid, that lead to an increase in the melting point and thus make the cream thicker at body temperature.[47] We added 1-hexadecanol to the oil phase, that together with glycerol acts as a thickener and stabilizer. A 0.1% of commercial ZnO nanoparticles (20-100 nm) were added for their antibacterial properties.

The choice of the surfactant or surfactants mixture is of the utmost importance to obtain a stable emulsion.[48,49] An important parameter to consider on this regard is the hydrophilic-lipophilic balance ratio (HLB),[50] a parameter used to empirically state how hydrophobic or hydrophilic is a certain molecule. The two most common used surfactants are the ones of the Span (more hydrophobic) and Tween (more hydrophilic) families, and we decided to employ a mixture of 66% Span 40 (Sorbitan monopalmitate, HLB= 6.7) and 33% Tween 80 (HLB=15, PEG-20 Sorbitan monooleate), for a total 10% of surfactants in respect to the mass of the oil phase, as commonly reported in literature for similar systems.[51–53]

The simplest system we investigated was composed by 8% sunflower oil, 3% coconut oil, 3.3% glycerol, 0.5% Tween 80, 1% Span 40, 1.6% 1-hexadecanol, 0.1% ZnO nanoparticles and 82% of water. The oil-phase, composed of vegetable oils, surfactants and 1-hexadecanol, was warmed at 70 °C and hand-stirred until homogeneity.

The emulsion was prepared by mixing at 70 °C the oil phase with the water phase - containing water, glycerol and ZnO - with a hand-held blender and continuing to blend until the temperature of the cream dropped to approximately 35 °C. The cream was then left to rest overnight.

The material obtained was a white cream, but rheological analysis (red curve in ***Figure 4.6***) showed that the material had a low viscosity and very soft yield stress, approximately 2 mPa with a viscosity of 0.11 Pa·s.

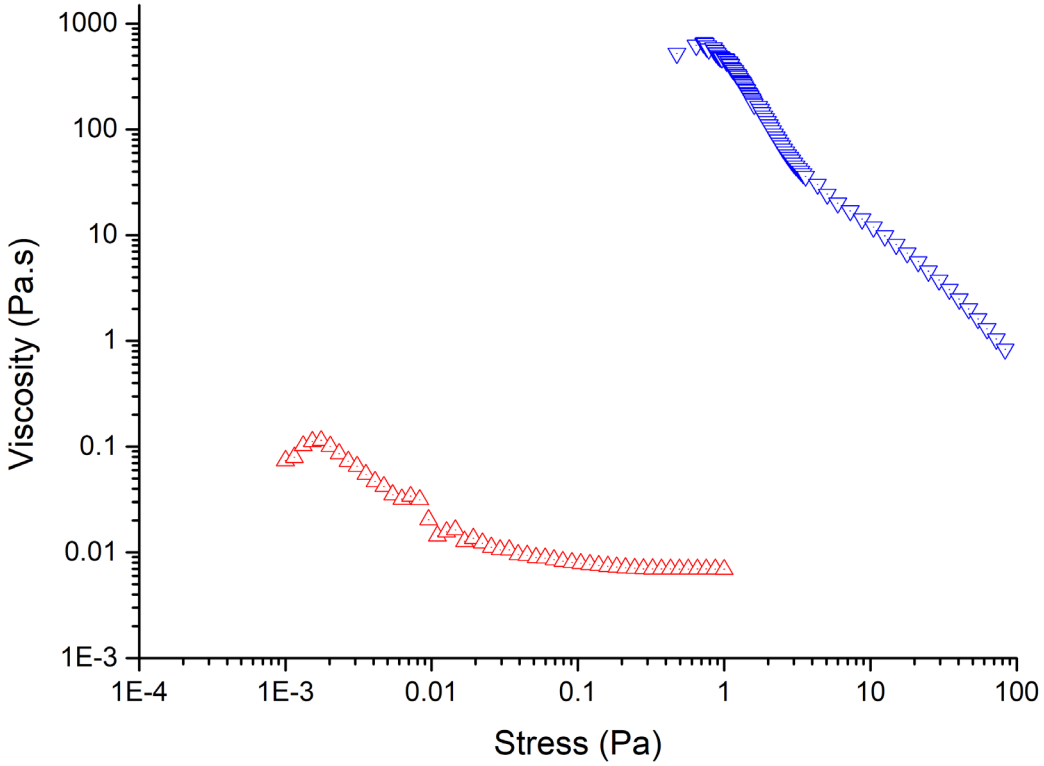

Figure 4.6 Flow curve at 37 °C of a cream composed by a W/O emulsion of 11% oil phase in water (red curve) and in 0.4% sodium alginate/ 3% sodium hyaluronate (blue).

Unfortunately, these data reveal that the obtained cream was easy to inject but not able to sustain is own weight, and thus not applicable in our procedure.

To improve the rheological properties, we added a 0.4% sodium alginate and 3% hyaluronic acid to the formulation in order to increase steady-viscosity and add a more definite yield stress. The blue curve in ***Figure 4.6*** show the flow curve of a cream prepared as stated before but adding alginate and hyaluronic acid to the water phase. The result is a clear increment of viscosity (645 Pa·s at the maximum of the flow curve) and a soft yield stress at 0.75 Pa.

The same material was prepared again, using a pre-gel solution [MBA]= 864 mM, [GABA]= 300 mM and [PEHA]= 215 mM in 0.4% NaAlg and 3% hyaluronic acid. The cream was prepared as stated before at 70 °C, as soon as the pre-gel solution was homogeneous, approximately after five minutes from the start of the synthesis. After cooling down to an acceptable temperature, part of the cream was frozen, in order to be preserved for *ex-vivo* assays.

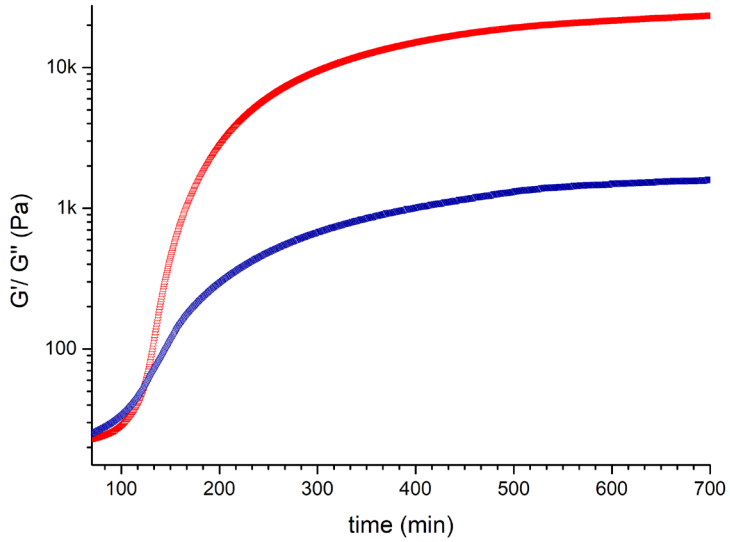

Figure 4.7 Kinetic of gelation at 37 °C for the PAAm-cream prepared with [MBA]= 864 mM, [GABA]= 300 mM and [PEHA]= 215 mM in 0.4% NaAlg and 3% hyaluronic acid at γ= 1% and f= 1 Hz.

The kinetic of gelation of the cream was investigate at 37 °C and is reported in ***Figure 4.7***. In the first part of the synthesis, G' and G'' have very similar values, in the range of 5-15 Pa, and gelation happens after approximately 120 minutes from the start of the synthesis. The material is completely formed after 12 hours and has G'≈ 15 kPa while G''≈ 1 kPa, showing that the material is a strong elastic solid.

Figure 4. 8a show the consistency of the material at 37 °C, that flows slowly and is able to sustain is weight for a limited time. Interestingly, the material can be frozen, and it is undefinedly stable. It can defrost just before use in the operating room, making its use simple and straightforward. Preliminary *ex-vivo* endoscopic assays on porcine fistula

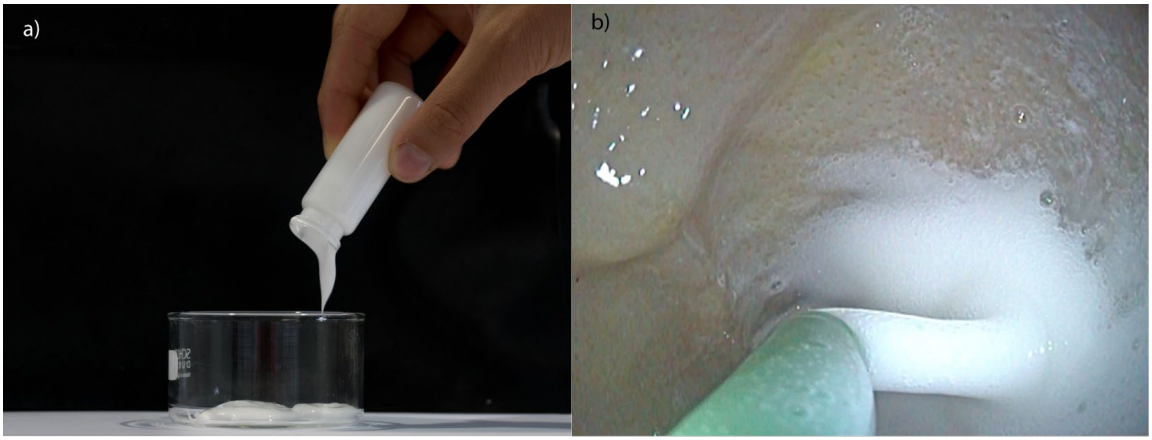

Figure 4. 8 Cream obtained with a PAAm pre-gel solution in 0.4% sodium alginate and 3.3% hyaluronic (a). The same cream endoscopically injected in a fistula model after being frozen immediately after preparation and defrost just before injection (b).

model showed, however, that the material was still easy to inject but not solid enough after injection to stay in place.

This is probably due to the fact that the material presents only a very soft yield stress and behave as a viscous fluid after injection.

We then investigated a new strategy, in which the cream was prepared in a 2% sodium alginate solution, partially crosslinked through the addition of a small amount of Ca^{2+} ions. Two different samples were prepared, keeping the same composition of the oil phase but increasing the concentration of glycerol to 20% and of sodium alginate to 2% in the water phase, for which in ***Figure 4.9*** we present the flow curves and the amplitude sweeps.

The first sample was prepared with 80% water phase and 20% oil phase, while the second had only 10% oil phase. In both cases, the crosslinking was performed using 8% of $CaCl_2$ in respect to the volume of the water phase. Higher concentrations of calcium lead to a non-injectable elastic material, while lower concentrations lead to a reduced viscosity and yield stress.

As confirmed by the flow curves, the samples prepared with higher amount of water phase as a higher yield stress, at 1.4 Pa stress and 2300 Pa·s compared to the one prepared with a lower percentage of water phase, that present a less-defined, soft yield stress near 1 Pa with a plateau in viscosity at approximately 750 Pa·s. The amplitude sweeps presented in ***Figure 4.9b*** show that the material synthetized with a higher amount of oil phase have a solid-to-liquid transition at 27% strain and G'= G''= 35 Pa, while the cream prepared with a higher percentage of oil phase behave as a solid for almost all the shear stress range, with G'=G''= 23 Pa at γ= 74%.

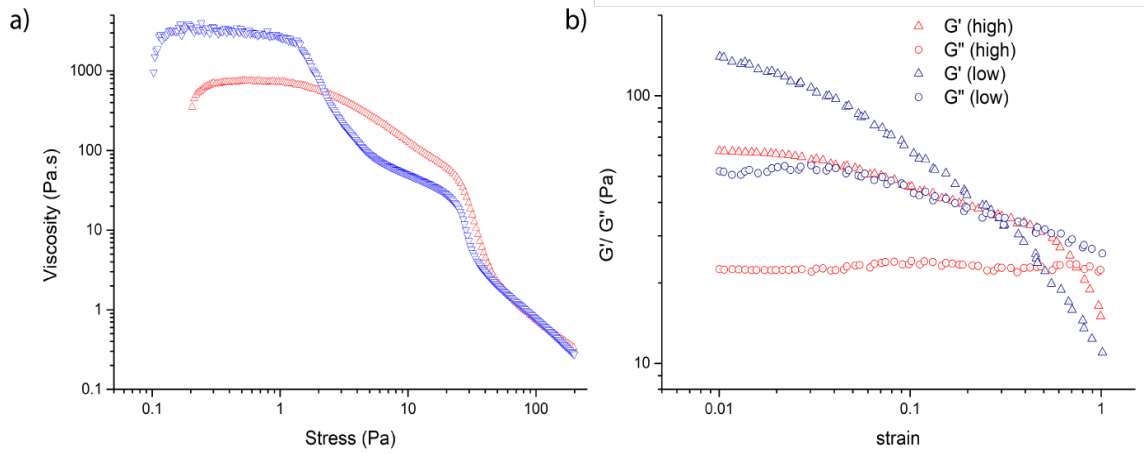

Figure 4.9 Rheology of creams prepared with 2% sodium alginate crosslinked with $CaCl_2$. Flow curves of samples prepared with 20% oil phase (red curve) and 10% oil phase (blue curve) (a). Amplitude sweeps at f= 1 Hz (b).

We can conclude that the alginate-crosslinked PAAm creams have good rheological that prospects a future employment in fistula closure.
However, further experiments are required in order to determine how cells behave in presence of the material and to investigate the applicability of this new cream formulation in *ex-vivo* and *in-vivo* fistulas.

4.4 Conclusions

PAAm-based hydrogels have peculiar properties that make them suitable as injectable, biocompatible materials for different applications in minimally-invasive surgery. Interestingly, different formulations of these hydrogels are possible, such as microgel (chapter 2) and creams, as we have discussed in this chapter. Hybrid alginate/PAAm hydrogels can, for example, be used for the percutaneous treatment of direct inguinal hernia. By carefully designing the material, it is possible to obtain a material with high elasticity and similar rheological properties to natural tissues, that can be injected with a regular 18 G needle and placed in the proper position through the combined use of CT and ultrasound techniques. We have shown that this material, when properly injected, solidifies *in situ* without spreading away to the nearby tissues. Short-term preliminary survival studies on pigs demonstrated that the material does not produce any immediate, abnormal inflammatory response, that is strongly adherent to the body and can resist the usual stress produced by the movement of the animals.
Also, it is possible to develop injectable PAAm-based creams for the endoscopic treatment of fistulas. The use of a special formulation containing the PAAm pre-gel solution, non -toxic thickeners, vegetable oils and food-grade surfactants allows to obtain a product that can be injected using a standard endoscopic sheath, can sustain is own weight and allows the closure of the fistula. Future experiments will be required to confirm that the material can solidify *in-vivo,* adhere to the tissues and allows cicatrization of the wound.

4.5 Experimental part

All the commercial materials employed for hydrogel synthesis were purchased from Sigma-Aldrich and used as received.
alamarBlue®, Alexa Fluor™ 647 Phalloidin and DAPI (4',6-Diamidino-2-Phenylindole, Dihydrochloride) were purchased from Thermofischer.
HeLa cells were purchased from ATCC.
High glucose DMEM was purchased from Thermofischer and 10% FBS, 1% glutamine and 1% penicillin were added.

4.5.1 Synthesis of the hybrid PAAm/alginate hydrogel

1,000 g (6,49 mmol) of N,N'-methylenebisacryalmide and 250 mg (2.42 mmol) of 4-aminobutyric acid were weighted in a glass vial. In a second vial, 6 mL of a 2% Sodium Alginate solution were mixed together with the proper amount of crosslinker, as reported in the discussion.
20 minutes before the expected injection time, the content of the two vials were mixed together and heated in a water bath at 70°C under vigorous stirring. After exactly 22 minutes, the material is quickly cooled down to a tissue-compatible temperature and injected.

4.5.2 Cell seeding

The hydrogels are synthetized as reported before and cut in small slices of about 10 mm x 0,5 mm. Each slice is placed in 95% ethanol for 24 hours, then washed five times with PBS and three times with phenol red-free DMEM media.
HeLa cells in the log phase were washed with PBS, detached from their flask with trypsin, centrifuged and resuspended is DMEM.
DMEM excess is removed from the samples and about 20.000 cells were seeded on top of each hydrogel.

Then, the samples were placed in the incubator (37°C, 5% CO2) for about 3h, to give time to cells to start adhering to the surface of the samples, then fresh phenol-red free DMEM was cautiously added.
Every 24h the samples are carefully washed with PBS and new fresh media is added.

4.5.3 Cell viability

20h after cell seeding, each sample is washed with PBS and placed in a new 24-well plate, to avoid measuring the metabolic activity of cells not attached to the hydrogel. 500 µL of fresh DMEM are added to each sample, then 50 µL of alamarBlue® are added after 24h from cell seeding to the first set of samples. The well-plate is incubated in the dark for 4h. After this time, 150 µL of solution are transferred to a 96-well plate and absorbance is measured in triplicate at 570 and 600 nm using a PerkinElmer Victor X5 2030 Multilabel Reader. The same procedure is repeated at each time point on different set of samples.
For each hydrogel and each time point, the measure is conducted on 4 to 6 samples with cells and on 2 samples without cells as negative control. The results are expressed ad percentage of reduced form.

4.5.4 Cell staining

After seven days from cell seeding, hydrogel slices were washed 5 times with PBS and fixed with 4% PFA for 15 minutes. Samples were then washed three times with PBS and kept in Triton X-100 (0.1 % in PBS) for 10 minutes and then in 1% bovine serum albumin (BSA) in PBS for 20 min. Cells were stained with Phalloidin Alexa Fluor® 647 for F-actin/membrane staining, for 20 min in the dark at room temperature following the manufacturer protocol, then washed three times with PBS. The nuclear region was stained with DAPI (300nM) for 5 minutes and then the material was washed again with PBS three times. DAPI was excited at 405 nm, while with Phalloidin Alexa Fluor® 647 was excited at 650 nm. Confocal imaging was performed with a Zeiss LSM 710 confocal microscope system equipped with a 10x magnification, numerical aperture 0.3 of Zeiss LCI Plan-NEOFLUAR objective lens (Zeiss GmbH, Germany).

4.5.5 Rheological Characterization

Rheological data were obtained with a Malvern Kinexus Lab+ equipped with a 40mm plate/plate geometry. Hydrogel cylinders were synthesized in a glass vial. After 24 hours from gelation time, the glass vial was broken, paying attention not to damage the hydrogel cylinder. Sample diameter and height was recorded with a digital micrometer. Normal force vs gap is recorded, at a 0.6 mm/minute speed. Lubrification with silicon oil was used and the data were analyzed with Origin and the curve interpolated using the equation $F(t) = GS_0(\frac{h_t}{h_0} - \frac{h_0^2}{h_t^2})$, were F(t) is force at time *t*, G is the shear modulus, S_0 is the surface of the base of the cylinder, h_0 is the initial height and h_t is height at time *t*.

4.5.6 PAAm-based cream preparation

In a 50 mL round-bottom flask, the oil phase is prepared by mixing together at 70 °C 60.00g sunflower oil, 28 g of coconut oil, 4 g of Tween-80, 8 g Span-40 and 12 g 1-hexadecanol. In the meantime, a pre-gel solution was prepared with 12 g of MBA (78 mmol), 3 g of GABA (29 mmol), 4.5 g (19 mmol) of PEHA and 90 mL of a solution of 2% m/v Sodium Alginate and 20% v/v glycerol were mixed together at 70°C. After five minutes, 90 mL of water phase and 10 mL of the oil phase were gently mixed together at 70 °C, then blended together with and hand-blender for 10 minutes until the cream reached room temperature.

References

(1) Miller, H. J. Inguinal Hernia, Mastering the Anatomy. *Surg. Clin. NA* **2018**, *98* (3), 607–621.

(2) Jenkins, J. T.; O'Dwyer, P. J. Inguinal Hernias. *Br. Med. J.* **2008**, *336* (February), 269–272.

(3) Kulacoglu, H. Current Options in Inguinal Hernia Repair in Adult Patients. *Hippokratia* **2011**, *15* (3), 223–231.

(4) *The SAGES Manual of Hernia Repair*; Jacob, B. P., Ramshaw, B., Eds.; Springer, 2013.

(5) Köckerling, F. Biological Meshes for Inguinal Hernia Repair – Review of the Literature. **2015**, *2* (September), 1–5.

(6) Montgomery, R. B. M. A.; Bansal, E. A. V. *Update of Guidelines on Laparoscopic (TAPP) and Endoscopic (TEP) Treatment of Inguinal Hernia (International Endohernia Society)*; 2015.

(7) Song, K. D.; Lee, M. W.; Rhim, H.; Kang, T. W.; Cha, D. I.; Sinn, D. H.; Lim, H. K. Percutaneous US/MRI Fusion–guided Radiofrequency Ablation for Recurrent Subcentimeter Hepatocellular Carcinoma: Technical Feasibility and Therapeutic Outcomes. *Radiology* **2018**, *288* (3), 878–886.

(8) Minami, Y.; Kudo, M. Ultrasound Fusion Imaging of Hepatocellular Carcinoma: A Review of Current Evidence. *Dig. Dis.* **2014**, *32* (6), 690–695.

(9) Toshikuni, N.; Tsutsumi, M.; Takuma, Y.; Arisawa, T. Real-Time Image Fusion for Successful Percutaneous Radiofrequency Ablation of Hepatocellular Carcinoma. *J. Ultrasound Med.* **2014**, *33* (11), 2005–2010.

(10) Ahn, S. J.; Lee, J. M.; Lee, D. H.; Lee, S. M.; Yoon, J. H.; Kim, Y. J.; Lee, J. H.; Yu, S. J.; Han, J. K. *Real-Time US-CT/MR Fusion Imaging for Percutaneous Radiofrequency Ablation of Hepatocellular Carcinoma*; 2017; Vol. 66.

(11) Botezatu, I.; Marinescu, R.; Laptoiu, D. Minimally Invasive – Percutaneous Surgery – Recent Developments of the Foot Surgery Techniques. **2015**, *8*, 87–93.

(12) Bauer, T. Percutaneous Forefoot Surgery. *Orthop. Traumatol. Surg. Res.* **2014**, *100* (1 S), S191–S204.

(13) Gimenez, M. E.; Davrieux, C. F.; Serra, E.; Palermo, M.; Houghton, E. J.; Acquafresca, P. A.; Dallemagne, B.; Kwak, J.; Gonzalez, C. A. Percutaneous Image-Guided Surgery Training : Model IHU-DAICIM. **2017**, *00* (00), 1–6.

(14) Giménez, M. E.; Houghton, E. J.; Davrieux, C. F.; Serra, E.; Pessaux, P.; Palermo, M.; Acquafresca, P. A.; Finger, C.; Dallemagne, B.; Marescaux, J. Percutaneous Radiofrequency Assisted Liver Partition with Portal Vein Embolization for Staged Hepatectomy (PRALPPS). *ABCD Arq Bras Cir Dig* **2018**, *31* (1), 4–7.

(15) Wood, B. J.; Ramkaransingh, J. R.; Fojo, T.; Walther, M. M.; Libutti, S. K. Percutaneous Tumor Ablation with Radiofrequency. *Cancer* **2002**, *94* (2), 443–451.

(16) Shiina, S.; Sato, K.; Tateishi, R.; Shimizu, M.; Ohama, H.; Hatanaka, T.; Takawa, M.; Nagamatsu, H.; Imai, Y. Percutaneous Ablation for Hepatocellular Carcinoma: Comparison of Various Ablation Techniques and Surgery. *Can. J. Gastroenterol. Hepatol.* **2018**, *2018*.

(17) Wichterle, O.; Lím, D. Hydrophilic Gels for Biological Use. *Nature* **1960**, *185* (4706), 117–118.

(18) Ahmed, E. M. Hydrogel: Preparation, Characterization, and Applications: A Review. *J. Adv. Res.* **2015**, *6* (2), 105–121.
(19) K. Y. Lee, D. J. M. Alginate : Properties and Biomedical Applications. *Prog. Polym. Sci.* **2012**, *37* (1), 106–126.
(20) Scognamiglio, F.; Travan, A.; Rustighi, I.; Tarchi, P.; Palmisano, S.; Marsich, E.; Borgogna, M.; Donati, I.; De Manzini, N.; Paoletti, S. Adhesive and Sealant Interfaces for General Surgery Applications. *J. Biomed. Mater. Res. - Part B Appl. Biomater.* **2016**, *104* (3), 626–639.
(21) Fiorini, F.; Prasetyanto, E. A.; Taraballi, F.; Pandolfi, L.; Monroy, F.; López-Montero, I.; Tasciotti, E.; De Cola, L. Nanocomposite Hydrogels as Platform for Cells Growth, Proliferation, and Chemotaxis. *Small* **2016**, *12* (35), 4881–4893.
(22) Ferruti, P. Poly(Amidoamine)s: Past, Present, and Perspectives. *J. Polym. Sci. Part A Polym. Chem.* **2013**, *51* (11), 2319–2353.
(23) Peng, B.; Lai, X.; Chen, L.; Lin, X.; Sun, C.; Liu, L.; Qi, S.; Chen, Y.; Leong, K. W. Scarless Wound Closure by a Mussel-Inspired Poly(Amidoamine) Tissue Adhesive with Tunable Degradability. *ACS Omega* **2017**, *2* (9), 6053–6062.
(24) Maturavongsadit, P.; Bi, X.; Metavarayuth, K.; Luckanagul, J. A.; Wang, Q. Influence of Cross-Linkers on the in Vitro Chondrogenesis of Mesenchymal Stem Cells in Hyaluronic Acid Hydrogels. *ACS Appl. Mater. Interfaces* **2017**, *9* (4), 3318–3329.
(25) Holloway, J. L.; Ma, H.; Rai, R.; Burdick, J. A. Modulating Hydrogel Crosslink Density and Degradation to Control Bone Morphogenetic Protein Delivery and in Vivo Bone Formation. *J. Control. Release* **2014**, *191*, 63–70.
(26) Lou, J.; Stowers, R.; Nam, S.; Xia, Y.; Chaudhuri, O. Stress Relaxing Hyaluronic Acid-Collagen Hydrogels Promote Cell Spreading, Fiber Remodeling, and Focal Adhesion Formation in 3D Cell Culture. *Biomaterials* **2018**, *154*, 213–222.
(27) Kot, B. C. W.; Zhang, Z. J.; Lee, A. W. C.; Leung, V. Y. F.; Fu, S. N. Elastic Modulus of Muscle and Tendon with Shear Wave Ultrasound Elastography: Variations with Different Technical Settings. *PLoS One* **2012**, *7* (8), 2–7.
(28) Falconi, M.; Pederzoli, P. The Relevance of Gastrointestinal Fistulae in Clinical Practice: A Review. *Gut* **2001**, *49 Suppl 4*, iv2-10.
(29) Turégano, F.; García-Marín, A. Anatomy-Based Surgical Strategy of Gastrointestinal Fistula Treatment. *Eur. J. Trauma Emerg. Surg.* **2011**, *37* (3), 233–239.
(30) Stringel, G.; McBride, W.; Sweny, A. Extraperitoneal Closure of Persistent Gastrocutaneous Fistula in Children. *JSLS J. Soc. Laparoendosc. Surg.* **2013**, *17* (1), 1–4.
(31) Simpson, J. A.; Banerjea, A.; Scholefield, J. H. Management of Anal Fistula. *BMJ* **2012**, *345* (7879), 1–9.
(32) Evenson, A. R.; Fischer, J. E. Current Management of Enterocutaneous Fistula. *J. Gastrointest. Surg.* **2006**, *10* (3), 455–464.
(33) Bubbers, E. J.; Cologne, K. G. Management of Complex Anal Fistulas. *Clin. Colon Rectal Surg.* **2016**, *29* (1), 43–49.
(34) Bhat, Y. M.; Banerjee, S.; Barth, B. A.; Chauhan, S. S.; Gottlieb, K. T.; Konda, V.; Maple, J. T.; Murad, F. M.; Pfau, P. R.; Pleskow, D. K.; et al. Tissue Adhesives: Cyanoacrylate Glue and Fibrin Sealant. *Gastrointest. Endosc.* **2013**, *78* (2), 209–215.
(35) Mueller Storrer, C. L.; Cardoso, G.; Zielak, J. C.; Miranda Deliberador, T.; Rychuv Santos, F.; Ricardo Lopes, T. Cyanoacrylate Surgical Glue as an Alternative to

Suture Threads for Connective Tissue Graft in Gingival Recession: A Case Report. *Chir.* **2014**, *27* (1), 55–59.
(36) Deolekar, S.; Thakur, B. A.; Bairolia, K.; Deolekar, S.; Jan, S. J. Comparison of Conventional Suturing and Tissue Adhesive (2-Octyl Cyanoacrylate) for Port Site Skin Closure in Laparoscopic Surgeries. **2017**, *4* (1), 204–208.
(37) Leggat, P. A.; Smith, D. R.; Kedjarune, U. Surgical Applications of Cyanoacrylate Adhesives: A Review of Toxicity. *ANZ J. Surg.* **2007**, *77* (4), 209–213.
(38) Leggat, P. A.; Kedjarune, U.; Smith, D. R. Toxicity of Cyanoacrylate Adhesives and Their Occupational Impacts for Dental Staff. *Ind Heal.* **2004**, *42* (2), 207–211.
(39) Lapointe, S. P.; N-Fékété, C.; Lortat-Jacob, S. Early Closure of Fistula after Hypospadias Surgery Using N-Butyl Cyanoacrylate: Preliminary Results. *J. Urol.* **2002**, *168* (4 Pt 2), 1751–1753.
(40) Spotnitz, W. D. Fibrin Sealant: The Only Approved Hemostat, Sealant, and Adhesive—a Laboratory and Clinical Perspective. *ISRN Surg.* **2014**, *2014*, 1–28.
(41) Abel, M. E.; Chiu, Y. S. Y.; Russell, T. R.; Volpe, P. A. Autologous Fibrin Glue in the Treatment of Rectovaginal and Complex Fistulas. *Dis. Colon Rectum* **1993**, *36* (5), 447–449.
(42) Loungnarath, R.; Dietz, D. W.; Mutch, M. G.; Birnbaum, E. H.; Kodner, I. J.; Fleshman, J. W. Fibrin Glue Treatment of Complex Anal Fistulas Has Low Success Rate. *Dis. Colon Rectum* **2004**, *47* (4), 432–436.
(43) Rabbani, S.; Rabbani, A.; Mohagheghi, M. A.; Mirzadeh, H.; Amanpour, S.; Alibakhshi, A.; Anvari, M. S.; Ghazizadeh, Y. A Novel Approach for Repairing of Intestinal Fistula Using Chitosan Hydrogel. *J. Biomater. Appl.* **2010**, *24* (6), 545–553.
(44) Mehta, H. J.; Malhotra, P.; Begnaud, A.; Penley, A. M.; Jantz, M. A. Treatment of Alveolar-Pleural Fistula with Endobronchial Application of Synthetic Hydrogel. *Chest* **2015**, *147* (3), 695–699.
(45) Kim, H. J.; Hwang, B. H.; Lim, S.; Choi, B. H.; Kang, S. H.; Cha, H. J. Mussel Adhesion-Employed Water-Immiscible Fluid Bioadhesive for Urinary Fistula Sealing. *Biomaterials* **2015**, *72*, 104–111.
(46) *Cosmetic Formulation of Skin Care Products*; Draelos, Z. D., Thaman, L. A., Eds.; Taylor & Francis, 2006.
(47) Che, A. M. M. Æ. Y. B.; Nazimah, M. Æ. S. A. H.; Amin, I. Chemical Properties of Virgin Coconut Oil. **2009**, 301–307.
(48) Butler, H. *Poucher's Perfumes, Cosmetics and Soaps*, 10th ed.; Butler, H., Ed.; Kluwer Academic Publishers, 2000.
(49) Hargreaves, T. *Chemical Formulations*; The Royal Society of Chemistry, 2003.
(50) Pagels, R. F.; Prud'Homme, R. K. Polymeric Nanoparticles and Microparticles for the Delivery of Peptides, Biologics, and Soluble Therapeutics. *J. Control. Release* **2015**, *219*, 519–535.
(51) Siqueira, J. F.; Rôças, I. N.; Provenzano, J. C.; Guilherme, B. P. S. Emulsions and the HLB System. *Alcohol* **2011**, *55391* (952), 1345–1348.
(52) McClements, D. J.; Jafari, S. M. Improving Emulsion Formation, Stability and Performance Using Mixed Emulsifiers: A Review. *Adv. Colloid Interface Sci.* **2018**, *251*, 55–79.
(53) Barkat Ali Khan,. Basics of Pharmaceutical Emulsions: A Review. *African J. Pharm. Pharmacol.* **2011**, *5* (25).

5. Hyaluronic acid crosslinking with L-lysine

One of the most requested cosmetic procedure is the use of a dermal filler, such as hyaluronic acid, to give a younger appearance by replacing volume loss during the normal ageing.[1] Hyaluronic acid is a polysaccharide naturally present in the human body and involved in different physiological process, such as wound healing or scar formation. It was first discovered by Karl Meyer and John Palmer[2] in 1934 and today it is recognized as one of the major component of human skin and has been linked to wrinkle formation and skin elasticity.[3] For this reason, hyaluronan-based formulations are widely used in cosmetics and skin care and it is employed as an injectable dermal filler to reduce the amount and severity of wrinkles in ageing persons.[4] Pure hyaluronic acid is, however, quickly metabolized and degraded in the skin and thus frequent injections are required. Indeed, modern commercial formulation contains crosslinked hyaluronic acid - with the most common employed crosslinker being 1,4-butanediol diglycidyl ether (BDDE) – to ensure a long-lasting effect.

Herein, we present a different lysine-based crosslinking strategy, in order to avoid the use of highly-reactive and possibly dangerous chemicals such as BDDE. The rationale behind our idea is to use activation of hyaluronan to promote the coupling with L-lysine, following different strategies based on chemical modification of hyaluronic acid or activation of the -COOH groups.

We would like to acknowledge the financial support of Qventis GmbH and its Managing Director, Dr. Lidia Nachbaur, for the support and the fruitful discussions.

We would like to thank Dr. Martina Torelli, visiting PhD student in our laboratory during the early phases of this project, for the useful advices and support.

5.1 Introduction

5.1.1 Hyaluronic acid chemistry and physiology

Hyaluronic acid is a linear polysaccharide naturally present in the human body, where it is involved in a number of different functions: it is a major component of the skin, the extracellular matrix, the cartilages[5], the vitreous and of the synovial fluid. Recent findings suggest that it may play a role also in cancer[6–10] and metastasis diffusion[11,12] and the oligomers produced by its degradation are involved in cell signaling.[13]

Today, hyaluronic acid is under intensive investigation for several different applications, such as in cosmetics and plastic surgery[1], orthopedics, 3D scaffold for cell growth[14], tissue engineering or drugs and nucleic acid delivery.[15,16]

From a chemical point of view (***Figure 5.1***), hyaluronic acid is an anionic, non-sulfated glycosaminoglycan composed by repeating disaccharide unit of D-glucuronic acid and N-acetyl-D-glucosamine connected by alternating β 1–3 and β 1–4 bonds. It can be found either in the protonate or deprotonated form, and for this reason the term *hyaluronan* (HA) is commonly employed to refer both to hyaluronic acid and hyaluronate ion.

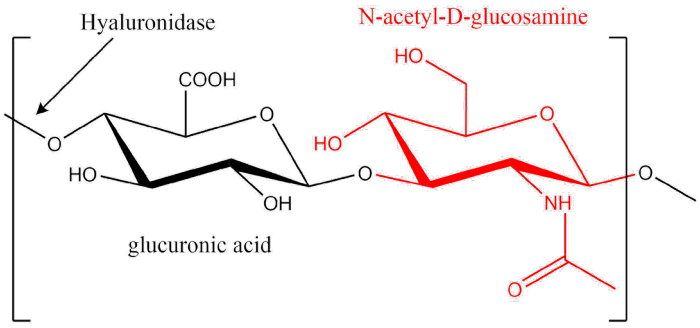

Figure 5.1. Chemical structure of hyaluronic acid

Glycosaminoglycans (GAGs)[17] are a class of linear polysaccharides that acts as shock absorber and lubricants, they are component of the cell membrane, of the extracellular matrix and they are present in all animals. They are composed by a repeating disaccharide unit comprising an amino-functionalized monomer (such as N-acetylglucosamine or N-acetylgalactosamine) and galactose or an hexuronic acid (glucuronic or iduronic acid). Most GAGs are sulfated - with hyaluronic acid being the only exception - and the sulfate

group, together with the carboxylic moiety on the uronic monomer, give to GAGs a distinctive negative charge.

In particular, it is possible to distinguish four main classes of GAGs:

a) heparin/heparan sulfate
b) chondroitin sulfate/dermatan sulfate
c) keratan sulfate
d) hyaluronic acid

The presence of a carboxyl and of different OH groups gives to HA a strong hydrophilic character and a very high viscosity even at low concentration. The molecular weight of HA depends from his origin and it is one of the most important differences between human and bacterial HA. Hyaluronic acid obtained from bacteria forms shorter chains of ≈ 5000 disaccharide units (for a molecular weight of ~2 MDa), while animal-derived HA has a molecular weight that can range from 4 to 6 MDa. The chemical structure shows no significative difference between different species, allowing the use of bacteria-derived HA also in humans without the risk of immunologic response[1].

Interestingly, the molecular weight of HA is different in different locations of the same organism, reflecting different functions: high molecular weight HA is usually present in healthy tissue, while low-molecular weight HA is involved in inflammation and angiogenesis. Hyaluronic acid connects cells with the extracellular matrix by binding with hyaladherins, a class of proteins that can be found on the ECM and on the cell surface. The most important among the HA receptors is the CD44 antigen, that by the formation or cleavage of connections with HA affects ECM remodeling. Hyaluronic acid aggregates are involved also in giving resistance to compression to cartilages.

Hyaluronic acid homeostasis is a dynamic process that involves a competition between synthesis and degradation. HA is synthetized by hyaluronan synthases - integral membrane enzymes localized in the surface of the plasma membrane – and degraded by the enzymes hyaluronidases and by free-radical mechanisms not involving any enzymes. In the bloodstream, the half-life of HA is less than 10 minutes, but can be of several weeks in the cartilages.

However, hyaluronic acid is mainly located in the skin, where it accounts for ~50% of the total HA present in the human body.[18]

5.1.2 Skin ageing and injectable fillers for cosmetic applications

The skin is a complex system regulated by the interactions of different layers of specialized cells with the external environment, and together with the breast, skin annexes, the subcutaneous fat and the deep fascia is one of the main components of the integumentary system. It covers the whole surface of the body and its responsible of about 15% of the total adult weight[18]. It and can be divided in three main layers: the epidermis (outer layer), the dermis and the hypodermis (or subcutis, the deepest layer).

The epidermis is a continuously renewing structure composed primarily of keratinocytes cells, even if a small amount of other cell lines is present. Keratinocytes are responsible for the synthesis of keratin, a fibrous protein with an important protective role. Depending on the activity and morphology of the keratinocytes, the epidermis can be further divided into four layers, including the basal cell layer (stratum germinativum), the squamous cell layer (stratum spinosum), the granular cell layer (stratum granulosum), and the outermost cornified or horny cell layer (stratum corneum, mainly composed of ECM and dead cells).

The dermis is separated from the stratum germinativum through the dermal-epidermal junction and occupies the major volume of the skin, it is responsible for its turgor and for the elastic and mechanical properties, contains most of the skin receptors and help with the physiological homeostasis. In the dermis are located three major cell lines - fibroblasts, macrophages and adipocytes – together with cells of the immune system, a great amount of proteins of the ECM, such as collagen and elastin, and components of the so-called extrafibrillar matrix, such as GAGs, of which hyaluronic acid is one of the most important representatives. More than 75% of the dermis is composed by collagen, secreted by fibroblast, that is also responsible for the mechanical strength of the skin, while elastin is responsible for the elastic behavior.[19]

Skin ageing is a complex natural process that involves drastic changes in the dermal layer with age[20] and is associated with wrinkling and loss of skin tone and elasticity. It is possible to distinguish between two different ageing processes. Innate (or intrinsic) ageing is a physiological process involving all the organs of the body and is influenced, among the other factors, by the reduced production of sexual hormones. Extrinsic ageing is an effect of the influence of the external environment and it is caused by factors such as UV exposure, mechanical stress, pollution, smoking or exposure to chemical agents. From a molecular point of view, both extrinsic and intrinsic ageing lead to oxidative stress,

cellular senescence and increase in the activity of matrix metalloproteases, that in the end results in a degradation of the collagen fibers, reduced collagen synthesis and reduced skin moisture, that lead to a significative decrease in skin volume.[21]

Another important marker for skin ageing is the reduction of hyaluronic acid in the epidermis, despite being still present in the dermis. In the epidermis, HA is normally synthetized in the basal stratum germinativum (where it is present intracellularly), and then it is excreted in the spinosum and granular layer where it is one of the components of the ECM. Here it plays a fundamental role in protecting the skin from dehydration. A study by E. Papakonstantinou and coworkers[22] published in 2009 suggests that extrinsic ageing induced by photodamage may influence the balance between hyaluronan synthase and hyaluronidases and to a lower molecular HA in the epidermis.

Dermal fillers have been widely employed to contrast the loss in skin volume and thus reducing the amount and severity of wrinkles and folds.[23] The first use of a facial filler was reported by Dr. Franz Neuber in 1893, who used autologous upper arm fat to remodel facial defects caused by tuberculosis,[24] an invasive procedure that can cause severe consequences, such as embolism, even if is still occasionally used. In the following years, other researches started to use paraffine or silicon oil, that however were still prone to severe complications and were banned from FDA in 1970.

A big step forward was made in 1981 when FDA approved the use of bovine collagen (Zyderm), that however can sometimes lead to immunologic response.

The first hyaluronic acid-based product – Restylane - was first approved in 2003 and had an immediate success because of the safety and because no immunologic response is prompted from his injection. Today, a broad range of products are available on the market, from synthetic fillers based on calcium hydroxyapatite (Radiesse) to other polymer-based products (Sculptra and Artefill), with different cosmetic applications depending on the characteristic of the gel injected. Some of the most famous products available on the market based on hyaluronic acid are Restylane, Perlane, Juvéderm, Juvéderm Voluma and Belotero, that differs for the percentage of crosslinking of the hyaluronic acid, pendant groups, swelling, molecular weight or presence or absence of hyaluronic acid particles.

In 2016 the market for hyaluronic acid was estimated to be around 7.2 billion USD and it is forecast to grow at 8.8% CAGR to 15.4 billion USD in 2025.[25]

As stated before, pure hyaluronan is not suitable as it is as a dermal filler, because of the fast turnover rate in the skin that would require multiple injections. A variety of

crosslinking strategies are possible and effect deeply the final properties of the cosmetic. In particular:

a) Crosslinking reduces the speed of degradation, allowing each injection to last for several months up to one year;

b) Crosslinking changes the mechanical properties of hyaluronan and lead to a soft and hydrogel instead of a very viscous fluid.

The fillers currently available on the market generally have a range in the elastic modulus that goes from 0,1 to 1 kPa, well below the elastic modulus of the skin of 3 MPa.[26,27] Rheological properties are of great importance both for the physician and for the patient. Harder gel, such as Restylane or Perlane (G'= 600-700 Pa) can better resist the deformation induced by muscle movement but can also more easily induce pain and inflammation or be "felt" by the patient, while softer gel (Hylaform or Juvederm, G'= 100-250 Pa) are smoother to inject and feel more natural for the patient, but are less resistant to deformation.

5.1.3 Hyaluronic acid crosslinking: state of the art

The degree of crosslinking and the molecular structure of the crosslinker employed are the two most important differences between all the products available on the market.[4] Hyaluronic acid crosslinking is generally performed in the cosmetic industry by acting on the hydroxyl groups present in the molecules. The two most used crosslinking agents are divinylsulfone (DVS), employed by Prevelle Silk, Captique and Hylaform families of products, and butanediol diglycidyl ether (BDDE), that is used in Restylane, Perlane and Juvéderm fillers. Other possibilities are the use of biscarbodiimide (BCDI, Elevess) and of 1,2,7,8-diepoxyoctane (DEO, Puragen). However, a great number of other possibilities are under investigation, but they are not in common use in cosmetic industry,[28] including direct modification of hyaluronic acid by acrylation[29,30] and oxidation,[31–33] crosslinking with adipic acid dihydrazide,[33] oximes[34] and coupling of other molecules through the carboxylic group on the glucuronic moietiy.[13,30,35,36]

However, most of these methods are not scalable to the industrial level due to the number of purification steps involved, the very high price of the molecules employed or the toxicity of initiators and other byproducts.

The most common methods used to crosslink hyaluronic acid for dermal filling require the use of BDDE or DVS.

DVS is commonly used because the crosslinking can be performed at room temperature and basic pH. This method is thus interesting because it greatly reduces the amount of degradation observed when hyaluronic acid is warmed at lower pH.[37]

BDDE is the most used crosslinker in the hyaluronic acid industry,[28,38,39] because of the low toxicity and of the stability of the ether bond compared to the ester bond.[40]However, even if BDDE-crosslinked hyaluronic acid is considered to be safe, and this is true also for all the related byproducts of degradation after injection, BDDE by itself is toxic and it is of the utmost importance to remove all the unreacted crosslinker from the final product. This can be a problem also if we consider that a certain amount of BDDE can react only on one of the two extremities of the molecule, thus leaving a free reactive epoxy group.

The purpose of this work is to develop a strategy for the crosslinking of hyaluronic acid with a natural amino acid, L-lysine, to have a final product that is completely natural and biocompatible. We imagined two different possible strategies to reach the intended target:

- Methacrylation of HA and subsequent aza-Michael addition with L-lysine
- Activation of the -COOH group of the glucuronic acid and coupling with L-Lysine to form an amide

In the first case, after methacrylation HA can be recovered and purified and the following reaction with Lysine should proceed without the need of any special initiator or catalyst, as reported for PAAm hydrogels in the previous chapters.

As an alternative, it is possible to activate the -COOH group using reagents with a lower toxicity profile compared to BDDE or DVS.

This would be the first HA-based material in the market crosslinked with a biomolecule.

5.2 Discussion

5.2.1 Aza-Michael addition on methacrylated hyaluronic acid

In the previous chapters we have shown that it is possible to form hydrogel through an aza-Michael addition of nucleophilic amines on conjugated double bonds. Functionalization of hyaluronic acid with acrylic group is well-known and several protocols are reported in literature. After the reaction, modified hyaluronic acid can be purified and directly crosslinked by reaction with L-Lysine.

Methacrylation of HA was performed as already reported in literature (***Figure 5.2a***).[29] Briefly, a 10x molar excess of methacrylic anhydride was added to a 1 wt % solution of HA in water. The pH was adjusted at 8.5 with NaOH and the reaction was carried out at 4 °C for 24 h. The product was precipitated with cold ethanol, purified in water by dialysis for 7 days and freeze-dried. FT-IR (***Figure 5.2b***) showed the presence of a band at 1750 cm^{-1} typical of the methacrylic double bond.

The product obtained was investigated for crosslinking with L-lysine and, for comparison, with pentaethylenhexamine (PEHA). 50 mg of methacrylated hyaluronic acid were dissolved in 1.5 mL of water, a 2-molar excess of crosslinker was added and the mixture was stirred at 40° or 60 °C for up to 24 h.

Unfortunately, in both cases, no significative differences in mechanical properties of the final products were observed after the reaction.

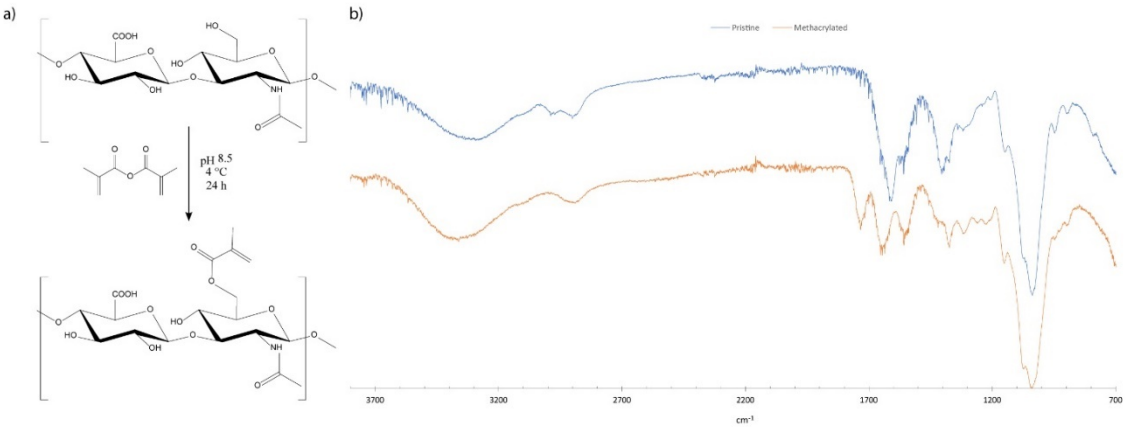

Figure 5.2. Methacrylation of hyaluronic acid (a). FT-IR spectrum of purified methacrylated hyaluronic acid and pure hyaluronic acid (b).

5.2.2 Hyaluronic acid degradation with pH

Hyaluronic acid crosslinking and sterilization requires pH and temperature conditions that may negatively influence its properties. In particular, thermal degradation and hydrolysis are serious problems that needs to be investigated.

Hydrolysis can be promoted by acidic pH - as it is already widely known for polysaccharides - and can lead to a sharp decrease in molecular weight, viscosity and degree of crosslinking. The starting material for the work here presented is hyaluronic acid sodium salt (NaHA), that when dissolved in pure water has a slightly basic pH. However, as will be shown in the following paragraphs, the optimal reaction conditions for EDC/HOBt or EDC/NHS crosslinking are reported to be at pH 4-6.

However, it is difficult to exactly adjust the pH of the NaHA solutions after the dissolution, due to the very high viscosity that can lead to relevant inhomogeneity. The use of buffer solution is also problematic, considering that the widely used MES buffer is not applicable for *in-vivo* applications. To evaluate the degradation kinetic, we have decided to investigate the degradation of pure hyaluronic acid at different theoretical initial HCl concentration, performing a frequency sweep at different time point and analyzing the change in phase angle shift (δ). A 3.3% solution of NaHA was prepared in water, HCl 0.003 M and HCl 0.01 M. 2 hours were required to obtain clear and homogeneous

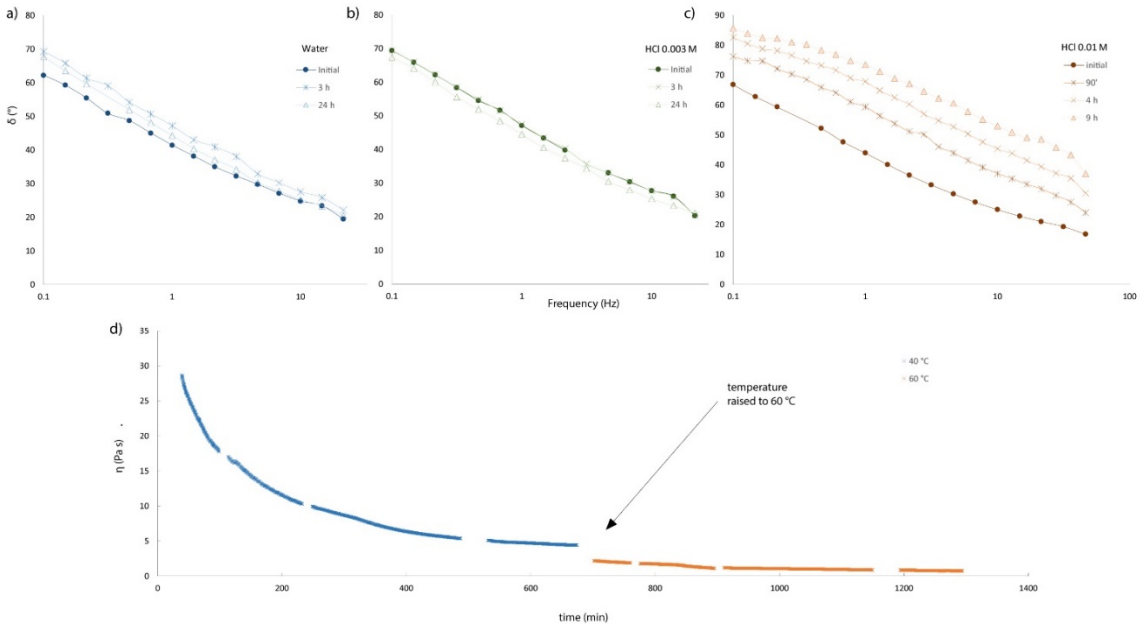

Figure 5.2 Hyaluronic acid degradation at 40 °C with pH. Frequency sweep (at 25 °C) of a 3.3% HA solution in water (a), HCl 0.003 M (b) and HCl 0.01 M (c). Change of shear viscosity (ẏ=10 s-1) over time at 40 °C for HA in HCl 0.01 M. Temperature was raised at 60 °C after 680 minutes to complete the degradation (d).

solutions at room temperature. The solutions were then warmed at 40 °C and frequency sweeps were performed at set time points.

The measures were performed at 25 °C with a plate-plate geometry at 0.5 mm gap and stress= 1% (LVR>50%). As shown in ***Figure 5.3a-c***, no degradation was observed for HA in water or in 0.003 M HCl solution even after 24 hours, with a difference in phase angle shift between each sample of no more than 5° and compatible to the instrumental error. On the opposite, at 0.01 M theoretical initial HCl concentration a clear degradation was observed. To better evaluate the process, we continuously measured the shear viscosity of HA in 0.01 M HCl using a 25 mm coaxial cylindrical geometry, in order to reduce experimental errors and to avoid evaporation (***Figure 5.3d***). The initial shear viscosity was found to be 28 Pa·s ($\dot{\gamma}$=10 s^{-1}, measure started after 2 h 30' at room temperature to ensure complete dissolution and homogeneity of the material), while after 150 minutes it decreased to 14 Pa·s, to finally reach a plateau of ~ 4 Pa·s after 10 h. The temperature was then raised to 60 °C and, after an initial drop to ~ 2 Pa·s that can be attributed to the change in temperature, the shear viscosity dropped to ~ 0.8 Pa·s after other 10 hours.

This confirms that it is indeed extremely important to be cautious during the crosslinking process to avoid degradation, considering that even with a small amount of acid can be significative. This problem seems to be not appropriately taken in consideration in most of the reported literature, where often the pH is kept low for long time.

5.2.3 Coupling of hyaluronic acid with L-lysine *via* sulfo-NHS

A second crosslinking strategy can be the activation of the carboxylic group of the glucuronic acid part of hyaluronic acid to promote a reaction with the amino groups of the lysine crosslinker to form an amide bond.

This reaction is well known in literature, especially for it its use in peptide synthesis and in protein labeling,[41] with different reagents and strategy available depending on the specific need.

One promising approach is the use of 1-ethyl-3-(-3-dimethylaminopropyl) carbodiimide hydrochloride (EDC) as an activating agent for the carboxylic group, together with N-hydroxysulfosuccinimide (sulfo-NHS) or 1-hydroxybenzotriazole (HOBt) to further facilitate the reaction.

The reaction scheme and mechanism are reported in ***Figure 5.4***. The first step of the reaction is the formation of an O-acylisourea ester of EDC with the carboxylic group of hyaluronic acid. The ester obtained is not stable in water, but it can react with sulfo-NHS to form a more stable intermediate. The activated ester can thus react with an amino group from free L-lysine or from a L-lysine already linked to another chain of the polysaccharide. The byproducts of the reaction are water soluble and they have low toxicity, and thus they can be easily removed after the reaction by dialysis against PBS. For these reasons, EDC/sulfo-NHS coupling is widely used in the biomedical field, for example also for in-vivo applications, such as in tendons repair[42,43] or cardiac valve crosslinking.[44]

In a typical synthesis, a 3.3 wt % hyaluronic acid solution were mixed with a slight excess of EDC and sulfo-NHS at 40 °C. Then, a 1.5x excess of L-Lysine was added and the mixture was kept at 40 °C for one hour, before being allowed to return to room temperature. The final product can be dialyzed against PBS for one week using 6000-8000 MWCO dialysis bag.

Rheological examination of the crude product confirms the efficiency of the crosslinking reaction. ***Figure 5.4c*** shows shear viscosity of pure hyaluronic acid (HA) compared with crosslinked hyaluronic acid (NHS-HA). Low-shear viscosity is one order of magnitude higher for NHS-HA (5600 Pa.s at 0.0063 s^{-1}) compared to pristine hyaluronic acid (600 Pa.s at the same shear rate). However, both the samples show a clear shear-thinning behavior, with a marked drop in viscosity to ≈ 45 Pa.s at $\dot{\gamma} = 10\ s^{-1}$ for both HA and NHS-HA.

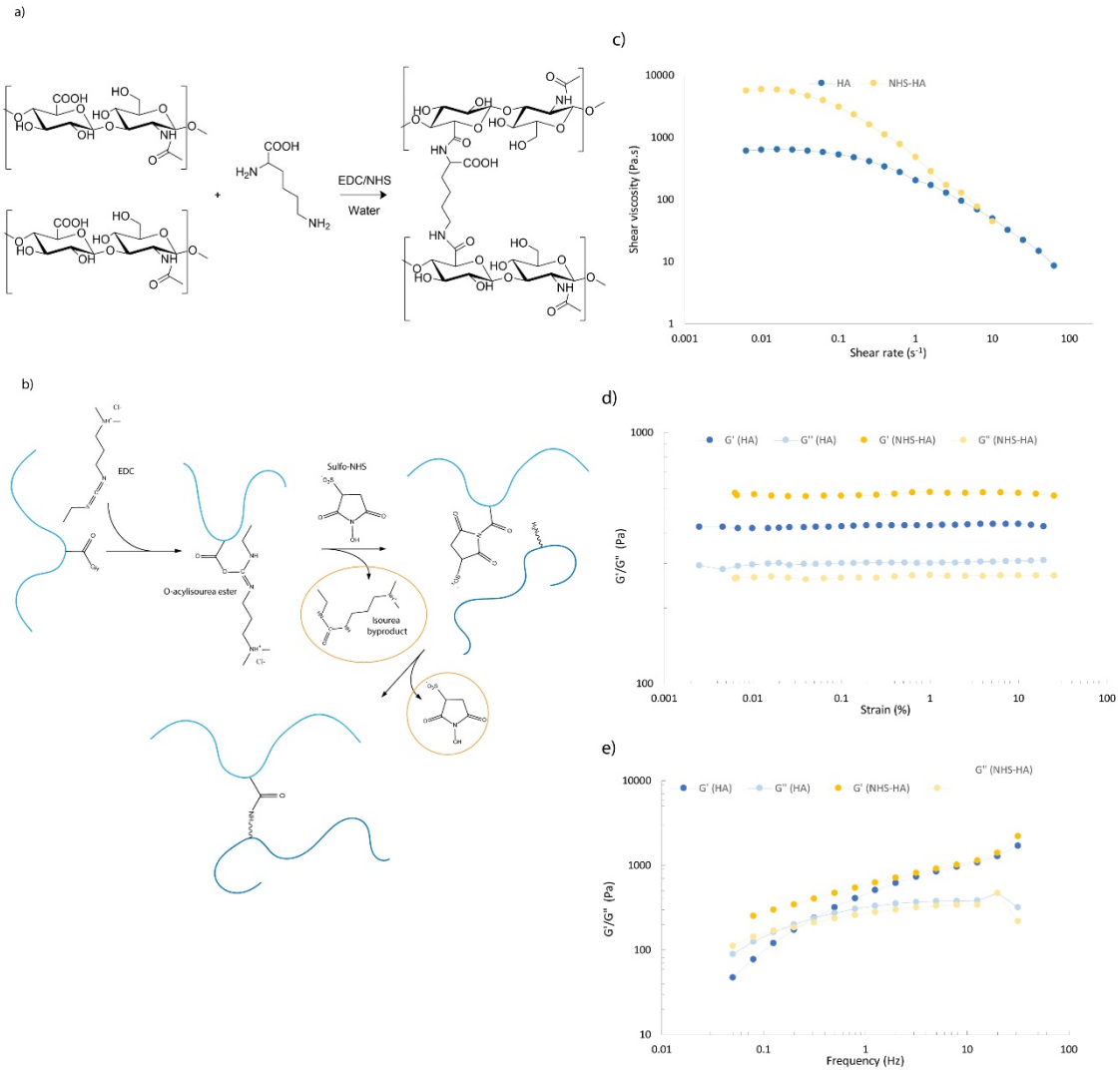

Figure 5.4 Hyaluronic acid crosslinking with L-Lysine and EDC/sulfo-NHS and reaction mechanism (a-b). Shear viscosity of pure hyaluronic acid (blue) and crosslinked hyaluronic acid (yellow) (c). Strain sweep (f= 1 Hz) and frequency sweep (σ=1%) of pure and crosslinked hyaluronic acid (d-e).

Oscillatory analysis further confirms the crosslinking. Amplitude sweeps reveals a broad linear viscoelastic range up to 20% at f= 1 Hz for both samples, with NHS-HA having a greater G' and a lower G" in respect to pure hyaluronic acid, confirming that the material behaves more as an elastic solid in comparison to pure hyaluronic acid. This is confirmed by the analysis of the phase angle, 35° for pure hyaluronic acid and 25° for crosslinked HA.

Frequency sweep at σ= 1% shows that pure hyaluronic acid, as expected, has a crossover point at f≈ 0.3 Hz and G'= G" ≈ 230 Pa - and thus behaves as a viscous fluid at lower frequencies and as an elastic solid at higher frequencies - while crosslinked hyaluronic acid always behave as an elastic solid, with G'>G'' in all the frequency range.

5.2.4 Coupling of hyaluronic acid with L-lysine *via* EDC/HOBt

Hyaluronic acid coupling with EDC/NHS has high efficiency but it is too expensive for realistic commercial applications is the cosmetic field, considering that sulfo-NHS is sold for more than 150$/g. Among the different possible strategies, the crosslinking of hyaluronic acid with L-lysine by using N-(3-Dimethylaminopropyl)-N'-ethylcarbodiimide hydrochloride (EDC) and 1-Hydroxybenzotriazole (HOBt) as coupling reagents seems thus the most promising. The reaction with HOBt follows the same mechanism[45] we have already reported for sulfo-NHS, i.e. the formation of the O-acylisourea ester with EDC, then the activated intermediate with HOBt lead to the formation of an amide bond by reaction with a nucleophilic amino group.[46] A similar strategy was employed by Tae Gwan Park and co-workers[47] to crosslink hyaluronic acid with cystamine in 2007 and for dermal filling application by S. K. Hahn and coworkers to crosslink HA with hexamethylendiamine.[39]

However, some other issues need to be considered. In particular, HOBt is only slightly soluble in water and, despite the fact that EDC/HOBt crosslinked hyaluronic acid protocols have been reported for different applications in biomedicine,[36,48] more safety issues have to be considered in comparison to sulfo-NHS. In particular, it should be noticed that dry HOBt is explosive, but present no danger in the hydrated form, as it is normally sold.

To optimize the crosslinking degree of the final product, several parameters must be tuned, such as temperature, adding order of the reagents and, overall, the pH during the synthesis. This last parameter is of the utmost importance for several reasons:

- EDC/HOBt activation of the -COOH group work better at pH between 5 and 6. Basic pH greatly reduce the yield of the reaction by accelerating the hydrolysis of the intermediate;
- L-lysine coupling work the in best at slightly basic pH, to have unprotonated amino groups;
- Hyaluronic acid can be degraded during the synthesis or the following sterilization process if the pH is not correct.

Five samples were prepared as follow. In five vials, 100 mg of sodium hyaluronate were dissolved in 2 mL of water and left to rest for 3 hours. 400 µL of a 100 mg/mL L-Lysine

solution were added and the mixture was left under shaking for 1 hour. The following acidic or basic solutions were added to the homogeneous viscous solution obtained:

A. 100 µL of water
B. 75 µL of water and 25 µL of HCl 0.01 M
C. 50 µL of water and 50 µL of HCl 0.01 M
D. 75 µL of water and 25 µL of saturated $NaHCO_3$ (~ 1 M)
E. 50 µL of water and 50 µL of saturated $NaHCO_3$

To each sample then were added 500 µL of a water suspension of EDC (100 mg/mL) and HOBt (80 mg/mL). The samples were left shaking for 3 hours and then stored at 4°C overnight.

Rheological examination of the sample was performed using a 35 mm plate-plate geometry at 25 °C, at a working gap of 0.5 mm.

The protocol consisted in a frequency sweep from 0.01 to 50 Hz at 25 °C and γ=1%, followed by an amplitude sweep at 1 Hz from γ=0.1% to 100% and all the results are reported in ***Figure 5.5***.

The amplitude sweep (***Figure 5.5a***) shows a broad elastic range, from 0.1% up to around 30%, with no significative difference between crosslinked and non-crosslinked sample. As expected, the sample C that was prepared at lower pH shows the higher elastic modulus (G' ≈ 0.45 kPa), followed by B (0.42 kPa). Hydrogel D and E, prepared in slightly more basic conditions, have an inferior modulus compared also to hydrogel A prepared in water.

Frequency sweep measurements (***Figure 5.5c***) show that at very low frequency, such as f= 0.01 Hz, pure hyaluronate solution behave like a viscous liquid, as expected, with G''> G' (G''≈ 20.6 Pa and G'≈ 4 Pa). The crossing point G'=G''≈ 190 Pa is reached at a frequency of a 0.3 Hz. This is the typical behavior of an entangled polymer solution, that act as a viscous fluid at low frequency and as a soft solid at higher frequency.

The crosslinked hyaluronate hydrogel B and C show instead a gel-like behavior in all the frequency range, with G' always higher than G''. However, sample A has very similar values of G' and G'' at very low frequency. This confirms that crosslinking is more effective at lower pH. Hydrogel D show an interesting behavior, considering that has an elastic modulus inferior to the one of A, as expected, but has a higher difference between G' and G'' at lower frequency.

This is confirmed also by the analysis of the phase-shift angle (δ, Figure 5.d), that decrease almost linearly from ≈ 80° at 0.01 Hz to ≈ 15° at 40 Hz for the pure hyaluronate, while is always under 45° for the samples A, B, C, D and E, with the phase-shift angle of D lower than A, similar to B and higher then C, while for sample E the phase angle is lower than B but higher than C.

From this data we can conclude that the crosslinking reaction is effective even with a small addition of a base, because all the samples shows an elastic solid-like behavior clearly different from the one of pure hyaluronic acid.

At the same time, hydrogel C prepared in more acidic conditions is the one showing the higher G' and the more solid-like characteristics (lower δ, ***Figure 5.5b***). Sample D and E show generally lower G' but also lower phase angle compared to B and A. This can be justified by that two competitive process may take place. At slightly basic pH, the hydrolysis of EDC is faster, but it is also faster the reaction with Lysine, that is not protonated. At slightly lower pH, EDC hydrolysis is less important, but lysine may be protonated and thus less prone to crosslinking. This may lead a phenomenon of self-crosslinking of hyaluronic acid, in which the activated -COOH groups may react with the -OH groups of another HA molecule.[37]

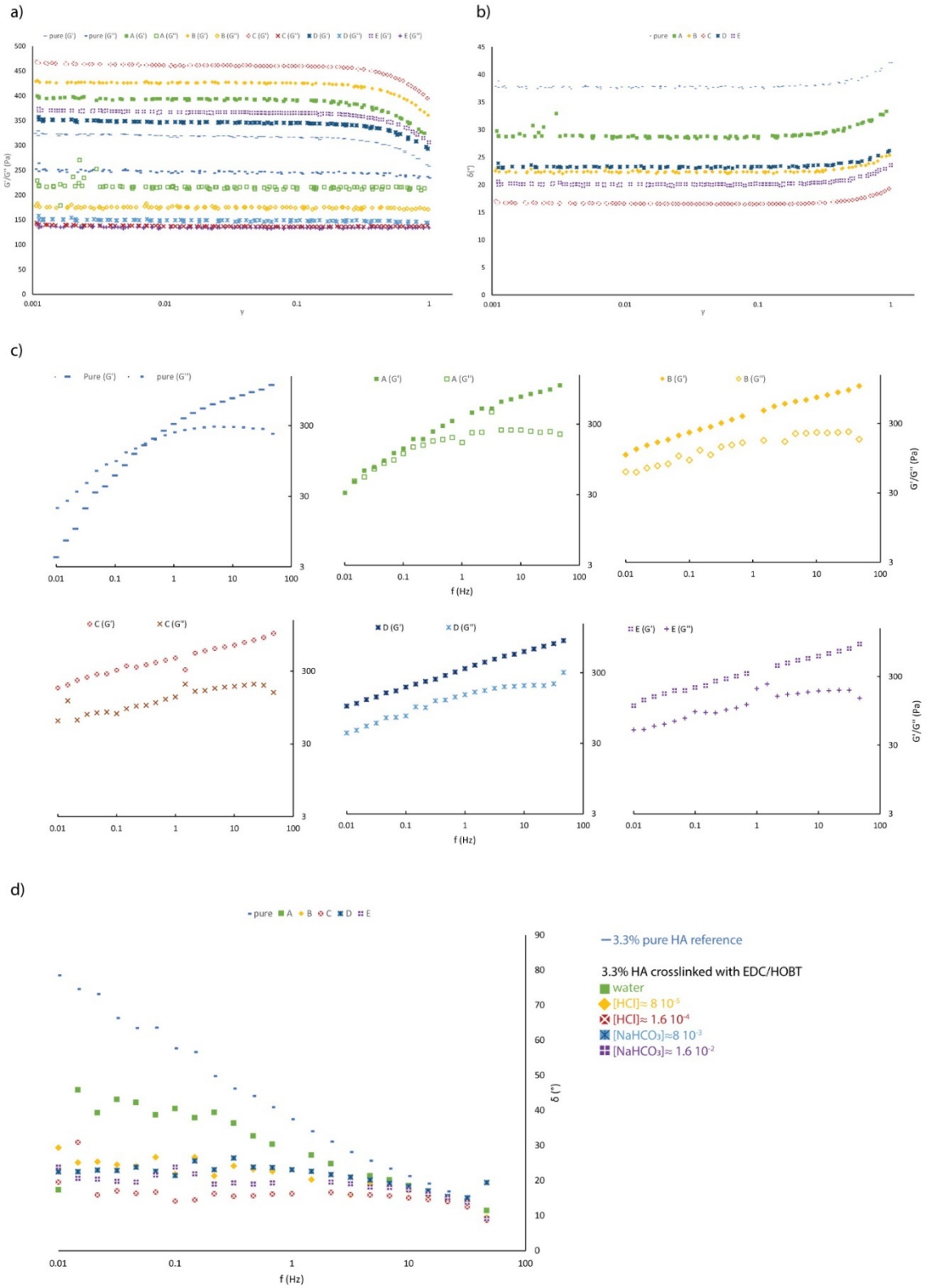

Figure 5.5 *Rheological characterization of Lys-EDC/HOBt crosslinked HA hydrogel. G' and G'' (a) and phase-shift angle δ (b) at variable stress and constant frequency (f= 1 Hz); G' and G'' (c) and phase-shift angle δ (d) at variable frequency and constant stress (σ= 1%). All the measures were performed with a 35 mm plate geometry at a gap of 0.5 mm.*

Preliminary *in-vitro* studies were conducted to evaluate the cytotoxicity of the material after crosslinking and purification and to confirm that any possible not biocompatible byproduct is eliminated.

Lysine-crosslinked hyaluronic acid was dialysed against PBS for seven days. Then, it was transferred in a sterile environment and sterilized with UV light for 30 minutes. The material was then washed again with PBS and then with high-glucose DMEM supplemented with 1% glutamine and 10% FBS and HeLa cells at a concentration of ~50.000 cells/gram were seeded. The nucleus of the cells was previously stained with Hoechst 3334 for better visualization, following the protocol reported by the producer.[49]

After 24 h of incubation at 37 °C, the samples were observed at a confocal microscope and excited at 355 nm. The fluorescence from Hoechst was collected between 420 and 480 nm.

In ***Figure 5.6*** it is shown that the material is completely colonized by normal healthy cells, as confirmed also by z-stack experiments.

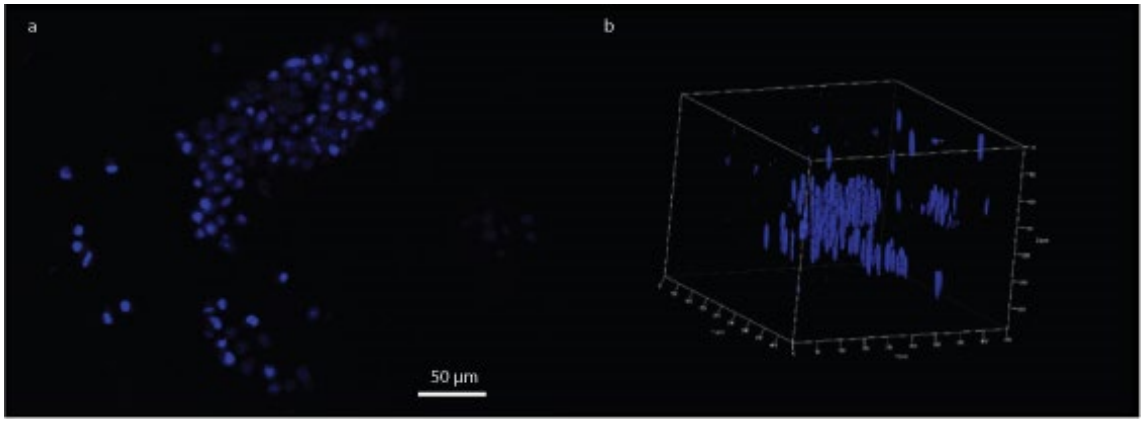

Figure 5.6 Confocal picture of HeLa cells growing on a crosslinked HA scaffold (a). Z-stack image that demonstrate how the material have colonized the hydrogel (b). The nucleus was stained with Hoechst 33342 and the images were taken after 24 hours of incubation at 37°C.

5.3 Conclusions

Hyaluronan is natural material that is widely employed in the biomedical, pharmaceutical and cosmetic industry for many different applications, the most relevant one being as an injectable dermal filler to restore volume loss during skin ageing. Despite being a hot topic in research for several decades, there are still several issues to be solved about is crosslinking and functionalization.

In this chapter, we have shown that it is possible to crosslink hyaluronic acid with a natural amino acid, L-Lysine, and that the final material is promising for applications in aesthetic facial surgery.

Crosslinking was performed using a EDC/HOBt coupling protocol, that required several optimization steps to take into account the effect of pH, parasite reactions and degradations.

Further studies will be conducted in the future to ensure the stability of the material during sterilization process and to assess its biocompatibility both *in-vitro* and *in-vivo*.

5.4 Experimental part

Hyaluronic acid sodium salt (Mw= $1.7 \cdot 10^6$ Da) was purchased from HTL Biotechnology and provided by Qventis Gmbh.
EDC was purchased from ABCR.
All the other commercial materials employed were purchased from Sigma-Aldrich and used as received.
Hoechst 33342 was purchased from Thermofischer.
HeLa cells were purchased from ATCC.
High glucose DMEM was purchased from Thermofischer and 10% FBS, 1% glutamine and 1% penicillin were added.

5.4.1 Hyaluronic acid methacrylation

1 g of sodium hyaluronate (2.64 mmol) is dissolved in 100 mL of water and mechanical stirred to obtain a homogeneous viscous solution. The pH is adjusted to 8.5 with NaOH 5M, then 3.911 mL of methacrylic anhydride (26.4 mmol) are added at 4 °C. The solution is hand-stirred for 10 minutes, then left to rest at 4°C under magnetic stirring for 24 h.
The product is precipitate with cold ethanol (- 20 °C), filtered, washed with cold water, re-dissolved in water and purified by dialysis against distilled water for 1 week using a 6-8000 MWCO membrane.
The purified methacrylated acid is then recovered by freeze-drying.
Yeld: 0.91 g (91%)

5.4.2 Hyaluronic acid coupling with EDC/sulfo-NHS

0.1 g of sodium hyaluronate (0.248 mmol) are dissolved in 2 mL of distilled water. 51 mg of EDC·HCl (0.266 mmol) are dissolved in 150 µL of water and added to the HA solution, immediately followed by a solution of 60 mg of N-hydroxysulfosuccinimide sodium salt (0.276 mmol) in 350 µL of water. After, a solution of 40 mg of L-Lysine (0.274 mmol) in 0.5 mL of water is added and the mixture is kept at 40 °C for one hour. The final product is purified by dialysis against distilled water for 1 week using a 6-8000 MWCO membrane.

Rheological examination was conducted on the crude material with a Thermofischer HAAKE Mars 40 rheometer equipped with a plate/plate 35 mm geometry at 0.5 mm gap and 25 °C.

5.4.3 Hyaluronic acid crosslinking with EDC/HOBt

In a standard procedure, 0.1 g of sodium hyaluronate (0.264 mmol) are dissolved in 2 mL of distilled water. After, 51 mg of EDC·HCl (0.266 mmol) are dissolved in 150 µL of water and added to the HA solution, immediately followed by a solution of 37 mg of 1-Hydroxybenzotriazole hydrate (0.274 mmol) in 350 µL of water. Then, a solution of 40 mg of L-Lysine (0.274 mmol) in 0.5 mL of water is added and the mixture is kept at 40 °C for one hour. The final product is purified by dialysis against distilled water for 1 week using a 6-8000 MWCO membrane.

5.4.4 Rheological analysis

All the rheological analysises were performed on a Thermofischer HAAKE Mars 40 rheometer equipped with a Peltier temperature module TM-PE-C for cylinders. Depending on the experiment, a coaxial cylinder geometry composed of rotor CC25 DIN Ti and cup CCB25 DIN or a plate P35 Ti L rotor and a lower plate TMP35 and an adapter for TMP lower plate insert for TM-PE-C were used.
A solvent trap was used in all the experiment to avoid water evaporation.

5.4.5 Confocal imaging

In a 96 well-plate, 1 gram of Lys-HA were placed after 7 days of dialysis. The material was washed with PBS and then with phenol-red free DMEM. In the meantime, the nuclear region of HeLa cells at P7 in the log phase was stained with Hoechst (1 µg/mL) for 15 minutes. Briefly, the adherent cells were washed with PBS, incubated with Hoechst for 15 minutes, then washed again with PBS, detached from their flask with trypsin, centrifuged and resuspended is DMEM. 50.000 cells/g were seeded on top of each HA-Lys hydrogel and incubated for 24 h (37°C, 5% CO2).

Confocal imaging was performed with a Zeiss LSM 710 confocal microscope system equipped with a 10x magnification, numerical aperture 0.3 of Zeiss LCI Plan-NEOFLUAR objective lens (Zeiss GmbH, Germany).

References

(1) Tezel, A.; Fredrickson, G. H. The Science of Hyaluronic Acid Dermal Fillers. *J. Cosmet. Laser Ther.* **2008**, *10* (1), 35–42.

(2) Palmer, W.; John, K. M. Polysaccharide of Vitreous Humor. *Ophthalmology* **1934**, *107*, 629–634.

(3) Necas, J.; Bartosikova, L.; Brauner, P.; Kolar, J. Hyaluronic Acid (Hyaluronan): A Review. *Vet. Med. (Praha).* **2008**, *53* (8), 397–411.

(4) Beasley, K. L.; Weiss, M. A.; Weiss, R. A. Hyaluronic Acid Fillers: A Comprehensive Review. *Facial Plast. Surg.* **2009**, *25* (2), 86–94.

(5) Bastow, E. R.; Byers, S.; Golub, S. B.; Clarkin, C. E.; Pitsillides, A. A.; Fosang, A. J. Hyaluronan Synthesis and Degradation in Cartilage and Bone. *Cell. Mol. Life Sci.* **2008**, *65* (3), 395–413.

(6) Cadete, A.; Alonso, M. J. Targeting Cancer with Hyaluronic Acid-Based Nanocarriers: Recent Advances and Translational Perspectives. *Nanomedicine* **2016**, *11* (17), 2341–2357.

(7) Delpech, B.; Chevallier, B.; Reinhardt, N.; Julien, J. -P; Duval, C.; Maingonnat, C.; Bastit, P.; Asselain, B. Serum Hyaluronan (Hyaluronic Acid) in Breast Cancer Patients. *Int. J. Cancer* **1990**, *46* (3), 388–390.

(8) Benitez, A.; Yates, T. J.; Lopez, L. E.; Cerwinka, W. H.; Bakkar, A.; Lokeshwar, V. B. Targeting Hyaluronidase for Cancer Therapy: Antitumor Activity of Sulfated Hyaluronic Acid in Prostate Cancer Cells. *Cancer Res.* **2011**, *71* (12), 4085–4095.

(9) Lokeshwar, V. B.; Mirza, S.; Jordan, A. Targeting Hyaluronic Acid Family for Cancer Chemoprevention and Therapy. **2016**, 1–26.

(10) Sato, N.; Kohi, S.; Hirata, K.; Goggins, M. Role of Hyaluronan in Pancreatic Cancer Biology and Therapy: Once Again in the Spotlight. *Cancer Sci.* **2016**, *107* (5), 569–575.

(11) Lan, T.; Pang, J.; Wu, Y.; Zhu, M.; Yao, X.; Wu, M.; Qian, H.; Zhang, Z.; Gao, J.; Chen, Y. Cross-Linked Hyaluronic Acid Gel Inhibits Metastasis and Growth of Gastric and Hepatic Cancer Cells: In Vitro and in Vivo Studies. *Oncotarget* **2016**, *7* (40), 65418–65428.

(12) Hirose, Y.; Saijou, E.; Sugano, Y.; Takeshita, F.; Nishimura, S.; Nonaka, H.; Chen, Y.-R.; Sekine, K.; Kido, T.; Nakamura, T.; et al. Inhibition of Stabilin-2 Elevates Circulating Hyaluronic Acid Levels and Prevents Tumor Metastasis. *Proc. Natl. Acad. Sci.* **2012**, *109* (11), 4263–4268.

(13) Lam, J.; Truong, N. F.; Segura, T. Design of Cell-Matrix Interactions in Hyaluronic Acid Hydrogel Scaffolds. *Acta Biomater.* **2014**, *10* (4), 1571–1580.

(14) Lou, J.; Stowers, R.; Nam, S.; Xia, Y.; Chaudhuri, O. Stress Relaxing Hyaluronic Acid-Collagen Hydrogels Promote Cell Spreading, Fiber Remodeling, and Focal Adhesion Formation in 3D Cell Culture. *Biomaterials* **2018**, *154*, 213–222.

(15) Dosio, F.; Arpicco, S.; Stella, B.; Fattal, E. Hyaluronic Acid for Anticancer Drug and Nucleic Acid Delivery. *Adv. Drug Deliv. Rev.* **2016**, *97*, 204–236.

(16) Puranik, A. S.; Dawson, E. R.; Peppas, N. A. Recent Advances in Drug Eluting Stents. *Int. J. Pharm.* **2013**, *441* (1–2), 665–679.

(17) Zhang, F.; Zhang, Z.; Linhardt, R. J. Glycosaminoglycans. *Handb. Glycomics* **2010**, 59–80.

(18) Kolarsick, P. A. J.; Kolarsick, M. A.; Goodwin, C. Anatomy and Physiology of the

Skin. *J. Dermatol. Nurses. Assoc.* **2011**, *3* (4), 203–213.
(19) Chu, D. Overview of Biology, Development, and Structure of Skin. *Fitzpatrick's Dermatology Gen. Med.* **2012**, 55–73.
(20) Papakonstantinou, E.; Roth, M.; Karakiulakis, G. Hyaluronic Acid, a Key Molecule in Skin Aging. *Dermatoendocrinol.* **2012**, No. December, 253–258.
(21) Jenkins, G. Molecular Mechanisms of Skin Ageing. *Mech. Ageing Dev.* **2002**, *123* (7), 801–810.
(22) Tzellos, T. G.; Klagas, I.; Vahtsevanos, K.; Triaridis, S.; Printza, A.; Kyrgidis, A.; Karakiulakis, G.; Zouboulis, C. C.; Papakonstantinou, E. Extrinsic Ageing in the Human Skin Is Associated with Alterations in the Expression of Hyaluronic Acid and Its Metabolizing Enzymes. *Exp. Dermatol.* **2009**, *18* (12), 1028–1035.
(23) Attenello, N. H.; Maas, C. S. Injectable Fillers: Review of Material and Properties. *Facial Plast. Surg.* **2015**, *31* (1), 29–34.
(24) Neuber, F. Fat Grafting. *Chir Kongr Verhandl Dtsch Ges Chir* **1893**, *20*, 66.
(25) Grand View Research, Hyaluronic Acid Market Size Worth USD 15.4 Billion by 2025e https://www.grandviewresearch.com/press-release/global-hyaluronic-acid-market (accessed Sep 4, **2018**).
(26) Kablik, J.; Monheit, G. D.; Yu, L. P.; Chang, G.; Gershkovich, J. Comparative Physical Properties of Hyaluronic Acid Dermal Fillers. *Dermatologic Surg.* **2009**, *35* (SUPPL. 1), 302–312.
(27) Malvern. Evaluating the Rheological Properties of Hyaluronic Acid Hydrogels for Dermal Filler Applications. **2015**, 10.
(28) Khunmanee, S.; Jeong, Y.; Park, H. Crosslinking Method of Hyaluronic-Based Hydrogel for Biomedical Applications. *J. Tissue Eng.* **2017**, *8*, 204173141772646.
(29) Babo, P. S.; Pires, R. L.; Santos, L.; Franco, A.; Rodrigues, F.; Leonor, I.; Reis, R. L.; Gomes, M. E. Platelet Lysate-Loaded Photocrosslinkable Hyaluronic Acid Hydrogels for Periodontal Endogenous Regenerative Technology. *ACS Biomater. Sci. Eng.* **2017**, *3* (7), 1359–1369.
(30) Lei, Y.; Gojgini, S.; Lam, J.; Segura, T. The Spreading, Migration and Proliferation of Mouse Mesenchymal Stem Cells Cultured inside Hyaluronic Acid Hydrogels. *Biomaterials* **2011**, *32* (1), 39–47.
(31) Montgomery, R.; Nag, S. Periodate Oxidation of Hyaluronic Acid. *BBA - Biochim. Biophys. Acta* **1963**, *74* (C), 300–302.
(32) Tan, H.; Chu, C. R.; Payne, K. A.; Marra, K. G. Injectable in Situ Forming Biodegradable Chitosan-Hyaluronic Acid Based Hydrogels for Cartilage Tissue Engineering. *Biomaterials* **2009**, *30* (13), 2499–2506.
(33) Su, W. Y.; Chen, Y. C.; Lin, F. H. Injectable Oxidized Hyaluronic Acid/Adipic Acid Dihydrazide Hydrogel for Nucleus Pulposus Regeneration. *Acta Biomater.* **2010**, *6* (8), 3044–3055.
(34) Sestak, J.; Mullins, M.; Northrup, L.; Thati, S.; Laird Forrest, M.; Siahaan, T. J.; Berkland, C. Single-Step Grafting of Aminooxy-Peptides to Hyaluronan: A Simple Approach to Multifunctional Therapeutics for Experimental Autoimmune Encephalomyelitis. *J. Control. Release* **2013**, *168* (3), 334–340.
(35) Sato, T.; Aoyagi, T.; Ebara, M.; Auzély-Velty, R. Catechol-Modified Hyaluronic Acid: In Situ-Forming Hydrogels by Auto-Oxidation of Catechol or Photo-Oxidation Using Visible Light. *Polym. Bull.* **2017**, *74* (10), 4069–4085.
(36) Choi, K. Y.; Chung, H.; Min, K. H.; Yoon, H. Y.; Kim, K.; Park, J. H.; Kwon, I. C.; Jeong, S. Y. Self-Assembled Hyaluronic Acid Nanoparticles for Active Tumor Targeting. *Biomaterials* **2010**, *31* (1), 106–114.

(37) Collins, M. N.; Birkinshaw, C. Physical Properties of Crosslinked Hyaluronic Acid Hydrogels. *J. Mater. Sci. Mater. Med.* **2008**, *19* (11), 3335–3343.
(38) Zhang, J. N.; Chen, B. Z.; Ashfaq, M.; Zhang, X. P.; Guo, X. D. Development of a BDDE-Crosslinked Hyaluronic Acid Based Microneedles Patch as a Dermal Filler for Anti-Ageing Treatment. *J. Ind. Eng. Chem.* **2018**, *65*, 363–369.
(39) Yeom, J.; Bhang, S. H.; Kim, B. S.; Seo, M. S.; Hwang, E. J.; Cho, I. H.; Park, J. K.; Hahn, S. K. Effect of Cross-Linking Reagents for Hyaluronic Acid Hydrogel Dermal Fillers on Tissue Augmentation and Regeneration. *Bioconjug. Chem.* **2010**, *21* (2), 240–247.
(40) De Boulle, K.; Glogau, R.; Kono, T.; Nathan, M.; Tezel, A.; Roca-Martinez, J. X.; Paliwal, S.; Stroumpoulis, D. A Review of the Metabolism of 1,4-Butanediol Diglycidyl Ether-Crosslinked Hyaluronic Acid Dermal Fillers. *Dermatologic Surg.* **2013**, *39* (12), 1758–1766.
(41) Luo, Y.; Prestwich, G. D. Hyaluronic Acid- N-Hydroxysuccinimide: A Useful Intermediate for Bioconjugation. *Bioconjug. Chem.* **2001**, *12* (6), 1085–1088.
(42) Ahmad, Z.; Shepherd, J. H.; Shepherd, D. V.; Ghose, S.; Kew, S. J.; Cameron, R. E.; Best, S. M.; Brooks, R. A.; Wardale, J.; Rushton, N. Effect of 1-Ethyl-3-(3-Dimethylaminopropyl) Carbodiimide and N-Hydroxysuccinimide Concentrations on the Mechanical and Biological Characteristics of Cross-Linked Collagen Fibres for Tendon Repair. *Regen. Biomater.* **2015**, *2* (2), 77–85.
(43) Everaerts, F.; Torrianni, M.; Hendriks, M.; Feijen, J. Biomechanical Properties of Carbodiimide Crosslinked Collagen: Influence of the Formation of Ester Crosslinks. *J. Biomed. Mater. Res. - Part A* **2008**, *85* (2), 547–555.
(44) Leong, J.; Munnelly, A.; Liberio, B.; Cochrane, L.; Vyavahare, N. Neomycin and Carbodiimide Crosslinking as an Alternative to Glutaraldehyde for Enhanced Durability of Bioprosthetic Heart Valves. *J. Biomater. Appl.* **2013**, *27* (8), 948–960.
(45) Schanté, C. E.; Zuber, G.; Herlin, C.; Vandamme, T. F. Chemical Modifications of Hyaluronic Acid for the Synthesis of Derivatives for a Broad Range of Biomedical Applications. *Carbohydr. Polym.* **2011**, *85* (3), 469–489.
(46) Valeur, E.; Bradley, M. Amide Bond Formation: Beyond the Myth of Coupling Reagents. *Chem. Soc. Rev.* **2009**, *38* (2), 606–631.
(47) Lee, H.; Mok, H.; Lee, S.; Oh, Y. K.; Park, T. G. Target-Specific Intracellular Delivery of SiRNA Using Degradable Hyaluronic Acid Nanogels. *J. Control. Release* **2007**, *119* (2), 245–252.
(48) Xu, X.; Jha, A. K.; Harrington, D. A.; Farach-Carson, M. C.; Jia, X. Hyaluronic Acid-Based Hydrogels: From a Natural Polysaccharide to Complex Networks. *Soft Matter* **2012**, *8* (12), 3280–3294.
(49) Thermofischer. Hoechst 33342 Protocol for Imaging https://www.thermofisher.com/fr/fr/home/references/protocols/cell-and-tissue-analysis/protocols/hoechst-33342-imaging-protocol.html (accessed Sep 4, **2018**).

6. Instrumental techniques

In this short, final chapter we present a short overview of some of the less common instrumental techniques employed in this thesis,

For each technique, we explain the theoretical background and the general operating principles behind its use. The exact experimental details are reported in the experimental part of each chapter, where that particular technique has been used.

Common characterization methods, such as IR or NMR, are not discussed. Instead, we will focus on rheology and confocal microscopy. All the information presented are commonly available in textbook and manuals.

6.1 Rheology

Rheology studies how materials flow and deform when a force is applied. Rheological analysis is of great importance material science, but also in formulations, cosmetics, food industry and many other areas. For example, in this thesis we have used rheology to investigate the elastic properties of the hydrogels, their hardness, their degradation, we have used it to follow their kinetic of formation but also to investigate the properties of hydrogel-based cream and to investigate the crosslinking and behaviour of hyaluronic acid.

A rheometer is the instrument used to study the rheological properties of materials. Two different types of rheometers exist: rotational rheometers, in which a shear stress is applied to the sample, and extensional rheometers, in which a normal stress is applied instead.

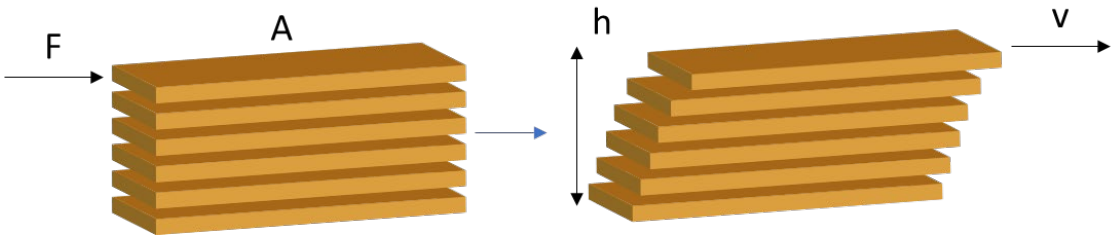

Figure 6.1 Laminar flow of a fluid when a force F is applied tangentially to it.

We define a shear stress as $\sigma = \frac{F}{A}$, where F is the shear force and A is the area of the sample where the force is applied. When we apply a shear stress to a fluid, this start to move at a velocity υ (***Figure 6.1***). In a laminar flow model, we can consider the fluid as flowing between two parallel plates separated from a distance *h,* in which the upper plate moves at velocity υ while the bottom one is steady. We can then define a shear rate as $\dot{\gamma} = \frac{v}{h}$.

The viscosity of a fluid measures its resistance to flowing and can be defined as $\eta = \frac{\sigma}{\dot{\gamma}}$. For an ideal fluid (or Newtonian fluid), viscosity is constant at all shear rate. This means that shear rate linearly increases with shear stress. This is the typical behaviour of water, glycerol, mineral oil and similar fluids, but more complex fluids can behave differently. A shear rheometer can be used to measure the viscosity of a solution at different shear rate.

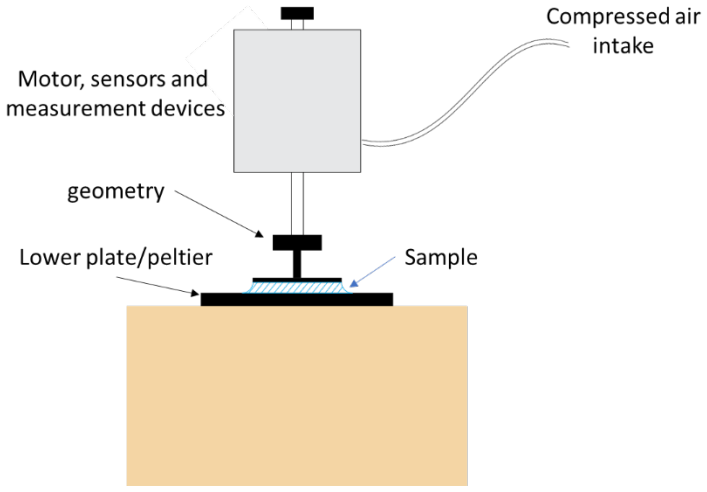

Figure 6.2 Schematic structure of a shear rheometer

A shear rheometer, as the one depicted in ***Figure 6.2***, is formed by a un upper part, containing the motor and all the sensors, connected to a measuring geometry. Each geometry is formed by a rotor, coupled to the upper motor, and by a fixed bottom part that is connected to a Peltier unit for temperature control. As shown in ***Figure 6.3***, different geometries exist for different uses. Plate-plate or cone-plate geometries require only small amount of sample and they are indicated for viscous solutions of soft gel. Coaxial geometries require larger amount of sample, but they are more sensible and allow to measure also solutions of very low viscosity. Also, a small layer of low-viscosity oil may be put on top of the sample in order to prevent evaporation, maxing coaxial geometries ideal for kinetic measures.

A shear rheometer can operate in two modes: continuous flow - where the geometry rotates constantly in one direction at constant or variable speed - and oscillation, where the geometry oscillates near a position of equilibrium.

Continuous flow measures are used to study how material flow in response to a shear stress or a shear rate. When a fluid contains long polymeric chains or concentrated particles, the behaviour changes from the regular Newtonian one because the supramolecular structure changes with shear rate. For example, while in steady state long polymeric chains may be entangled, they may align at higher shear rate. This leads to a decrease in viscosity at higher shear rate, an effect known as shear thinning. Shear thinning is one example of non-Newtonian behaviour, i.e. viscosity is no more constant at all shear rate. Some fluids, as for example concentrated starch solutions, show shear-thickening: their viscosity increases when shear rate increases.

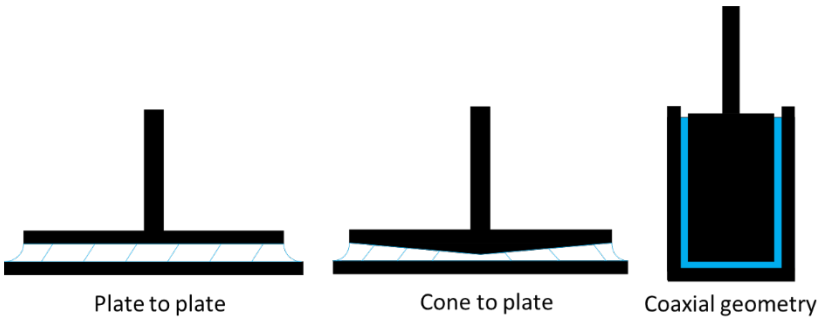

Figure 6.3 Different examples of measuring geometries

Most modern rheometers can operate into controlled shear or controlled rate mode. In controlled rate mode, a shear rate ramp is applied, and the viscosity of the material is recorded.

In controlled stress mode, a shear stress ramp is applied to the sample. If the material behaves as a Newtonian fluid, shear rate will linearly start to rise with shear stress, while viscosity remains constant. Complex sample may show a yield stress: they will start to flow only after a minimum shear stress is applied. Different options exist for measuring yield stress. For example, if the material has a yield stress, then viscosity at the beginning will increase with shear stress (the material deforms but do not flow), then it will start to decrease when the material finally starts to flow.

Continuous flow measures allow the measure of the viscous property of the sample, but however some samples show a viscoelastic behaviour, i.e. they partially behave as an elastic solid.

Oscillation measures are use study the viscoelastic properties of material. In this kind of test, the geometry applies a sinusoidal strain γ on the sample (***Figure 6.4***), and the corresponding shear stress σ is recorded (or, vice versa, a stress is applied and the strain is measured). For an ideal fluid, the stress and strain sinusoidal curves are out of phase, with a phase-shift angle δ of 90°. In ideal elastic solids, the stress and strain curves are perfectly in-phase and δ= 0°. Most of materials have δ oscillating between 0 and 90°, and thus show both a viscous and an elastic behaviour.

In general, we can write that the shear stress is directly proportional to the strain, $\sigma = G\varepsilon$, where G is the elastic modulus of the material. If the strain is oscillating with time, we can write $\sigma = G'\varepsilon_0 \sin(\omega t) + G''\varepsilon_0 \sin(\omega t + \delta)$, where G' is the elastic modulus and G'' is the loss modulus.

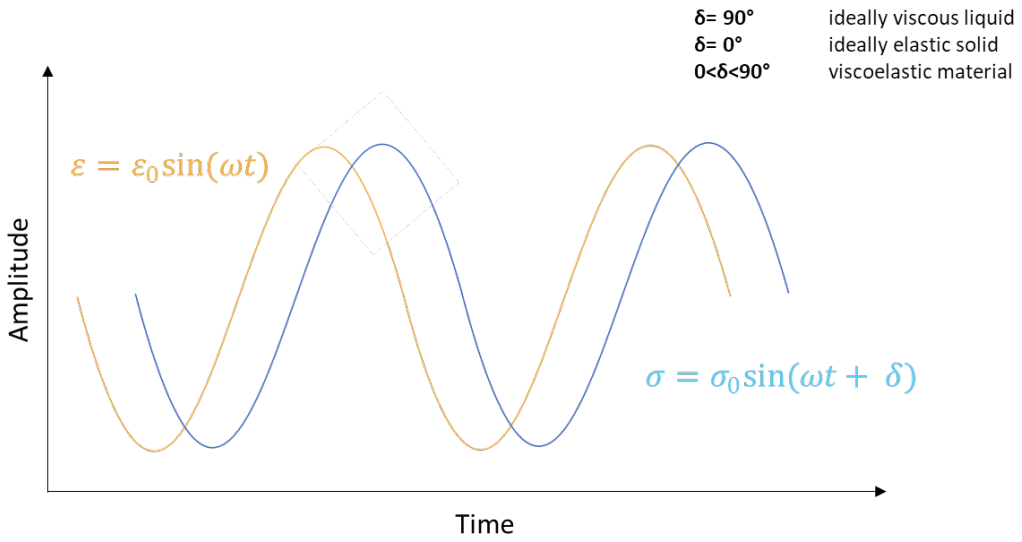

Figure 6.4 Stress and strain sinusoidal curves in a viscoelastic material

G' and G'' are the two components of the complex shear modulus G*. When G'> G'' the material behaves more as an elastic solid than as a viscous fluid, while when G'< G'' the opposite is true. For example, during a process of gelation it is possible to confirm that solidification happened when G' becomes higher than G''.

Different kinds of oscillation measures can be performed.

In an oscillation sweep, the amplitude of the oscillation is changed from point to point at constant frequency. This allow to measure the Linear Viscoelastic Range (LVR) of the material, i.e. the range of deformation in which the material behaves linearly without

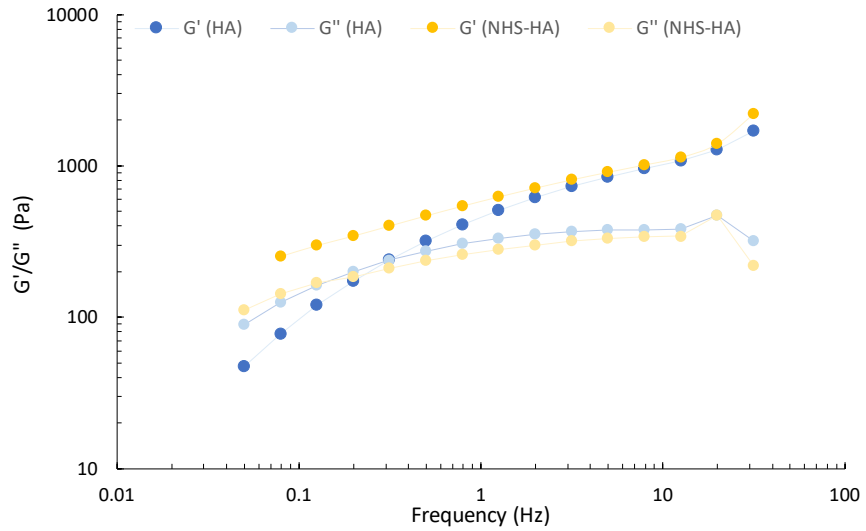

Figure 6.5 Frequency sweep on pure hyaluronic acid (blue) and crosslinked hyaluronic acid (yellow).

destruction of the internal structure. In a frequency sweep, the frequency f of the oscillation is step-wise changed with time. This simulates the behaviour of the material when subjected to a fast motion. For example, un-crosslinked hyaluronic acid behaves as a fluid at low frequencies (slow motion) but start to behave as a solid at high frequencies, while crosslinked HA behaves as a solid in all conditions (***Figure 6.5***).

6.2 Fluorescence and Confocal microscopy

A microscope is a device that allows the operator to observe, through a series of lenses and objectives, a magnified image of a sample, allowing the scientist to identify even the tiniest details of a sample (down to 0.2 μm for a diffraction-limited optical microscope). Fluorescence microscopy is a microscopy technique that employs the lights emitted by a luminescent sample to produce a magnified image. In contrast to traditional microscopy, where all the sample is illuminated and reflects (or transmits) the incoming light, in fluorescence microscopy it is possible to collect the light coming only from selected portions of the sample, which are conjugated to fluorescent probes. The use of specific dyes, such as Hoechst 33342 or DAPI for the cell nucleus, allows the possibility to target only very specific structures in a biological specimen, allowing also co-localization studies and thus increasing the amount of information that it is possible to obtain.

The operating principles behind a fluorescence microscope are relatively simple. A light source emits the exciting radiation, that passes through a monochromator or a filter. The user selects at which wavelength he wants to excite the luminophore, and the monochromator or filter will permit only the light of that specific wavelength to illuminate the sample. The light emitted by the sample arrive to the ocular, after passing through a dichroic mirror and a second monochromator, that allows to reject the parasite and reflected light and to isolate only the light of the appropriate range of wavelength. The light emitted normally has a higher wavelength in comparison to the excitation light and can be easily isolated.

Today, most microscope are epifluorescence microscope, i.e. the light source is located perpendicular to the detector.

However, also the best epifluorescence microscopes are not able to completely remove the light coming from the planes out of focus. Thus, the final image can be blurry, the spatial resolution is poor, and all the three-dimensional information is lost.

Confocal microscopy, born in 1955 thanks to the work of Martin Lee Minsky, allows to select only the light coming from a thin section of the sample, eliminating most of the radiation coming from the planes out of focus, thus increasing the quality of the image and allowing also to reconstruct a 3D picture of the specimen. The biggest difference between confocal and epifluorescence microscopes is in the presence of two pinholes that allows the out-of-focus light to be discarded. The first pinhole is located near the light source, in order to illuminate only a small part of the sample, while the second one is located before the detector in order to eliminate the light coming from the out-of-focus planes.

Illuminating the sample point by point, and not all together as in the regular fluorescence microscopy, is key to avoid light reflection inside the focus plane. However, this leads to a decrease in the intensity of the light emitted. To solve this problem, today most confocal microscopes are Confocal Laser Scanning Microscopes (CLSM). In a CLSM, a laser is used to illuminate the sample pixel by pixel. This allows to have a high photon density and thus a stronger signal. The side-effect is that only a limited number of excitation wavelengths can be used, corresponding to the lasers available. Mirrors are used to move the laser beam and scan the sample, while neutral density filters are used to reduce its intensity. The light emitted by the sample passes through a series of a lenses and through a second pinhole, that allows to remove the light coming from out-of-focus planes. The dimension of the pinhole can be changed, with a lower aperture allowing a higher 3D resolution but reducing the amount of light arriving to the detector while a bigger aperture allows to collect more light but decrease the quality of the image.

Also, the high resolution in the z axis allows to take multiple images at different plane of focus and then reconstruct them to obtain a three-dimensional representation of the specimen.

Summary

Since their introduction in the early 1960[1], hydrogels have attracted considerable interest in the biomedical field due to their biocompatibility, elastic properties, high water content and the porous 3D structure that allows permeation of oxygen and nutrients and thus cell growth and proliferation, mimicking the extra-cellular matrix. [2–4]

Compared to natural hydrogels, such as cellulose or chitosan, synthetic covalent hydrogels offer new opportunities for the incorporation of stimuli-reactive chemical moieties, to reach a better reproducibility, a broader control on their chemical structure and functionalization, and consequently on their rheological properties and stability.

However, synthetic hydrogels can be less biocompatible than their natural counterpart and their synthesis may require toxic radical initiators and several purification steps.

Polyamidoamines (PAAm)[5] are a class of covalent synthetic hydrogels well-known in literature for their biocompatibility, the easy chemical tunability and the mild reaction conditions required for their synthesis. Their preparation is based on an aza-Michael addition of nucleophilic amines to conjugated double bonds and it does not require any radical initiator or purification step. The reaction is conducted in water and gelation time can be precisely controlled by controlling the temperature, that can range from room temperature up to 80 °C. The gelation kinetic of a typical PAAm hydrogel is reported in ***Figure 1***.

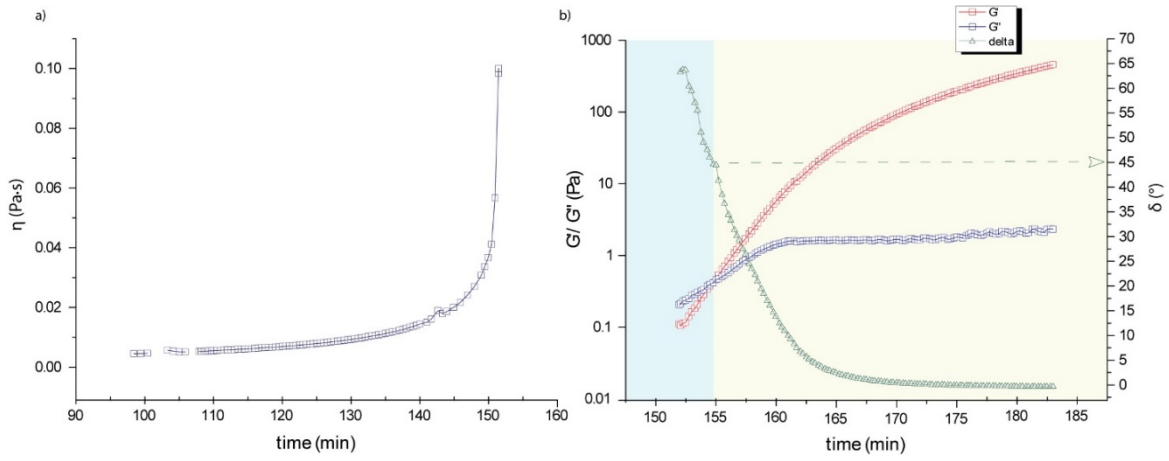

Figure 1 Gelation kinetic at 37 °C of a PAAm hydrogel composed by [MBA]=0.864 M, [GABA]=0.323 M and [PEHA]= 0.215 M. Shear viscosity (γ̇=10 s-1) (a) and oscillation rheology (f= 0.5 Hz, γ=1%) (b) as a function of time from the start of the synthesis.

Our group has already shown the synthesis of a hybrid hydrogel composed by a polyamidoamine network crosslinked with mesoporous silica nanoparticles.[6] We have demonstrated that this system allows mesenchymal stem cells growth and proliferation and that we can control the release of bioactive molecules, such as chemokines, from the nanoparticles.

Following such encouraging results, the aim of this thesis is the synthesis and investigation of a family of poly(amidoamine)s in surgery and biomedicine, with the final goal to use such materials *in vivo*, because they combine the use of mild synthetic conditions and fast gelation.

The thesis is divided in five chapter, with the first one being an introduction that describes the general properties of hydrogels, their use in biomedicine and a general introduction on minimally-invasive procedures.

In Chapter 2, we analyze how different factors, such as temperature or concentration of crosslinking, influence the properties of PAAm-based materials and their rheology. We also show how it is possible to prepare PAAm microgels and to use them for the delivery of antibiotics or for bacteria encapsulation.

Recently, the use of biocompatible soft materials has been investigated to facilitate the resection of early-stage mucosal tumors in minimally-invasive endoscopic procedures. The formation of a submucosal fluid cushion (SFC) is needed to lift the tumor from the underlying muscle layer and during the procedure used for the resection of neoplasia, endoscopic submucosal dissection (ESD). This is of the utmost importance to protect the underlying healthy layers from the risk of perforations, in organs such as the stomach, colon or esophagus.

In Chapter 3, part of which has already been published (DOI: 10.1021/acsabm.8b00189), we present an injectable, biodegradable, nanocomposite hydrogel that is able to be injected endoscopically to form an SFC and to facilitate ESD. The hydrogel - based on poly (amido amine)s - contains breakable silica nanocapsules covalently bound to its network. These particles provide elasticity to the hydrogel and allow the release of molecules upon an external stimulus that destroys the nanocapsules. To promote degradation, the hydrogel is composed of cleavable disulfide moieties that are reduced by the cells through secretion of glutathione. The same stimulus triggers the breaking of the silica nanocapsules; therefore, the entire hybrid material can be completely degraded, and its decomposition depends entirely on the presence of cells.

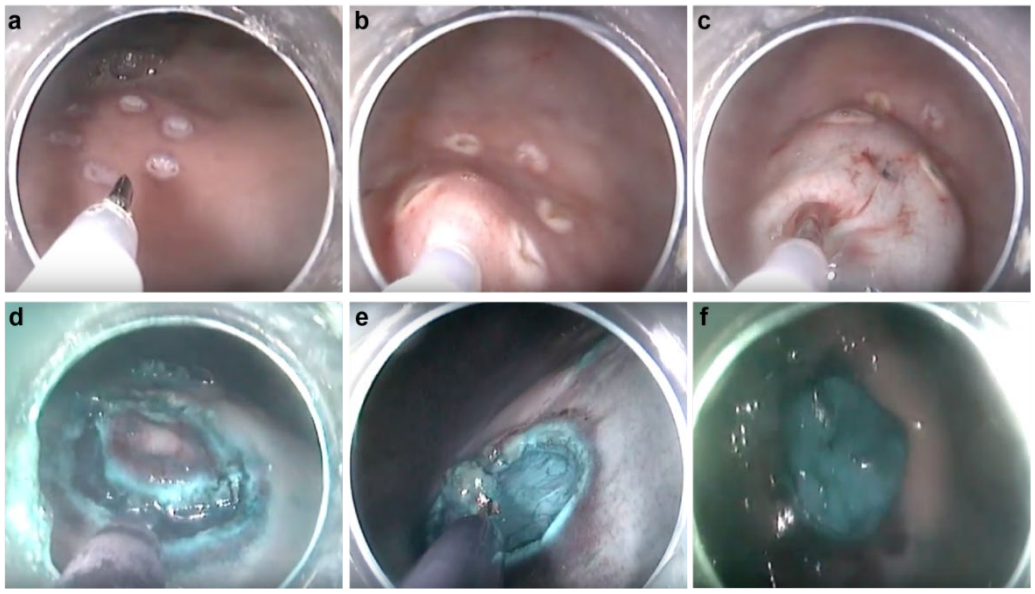

Figure 2 Endoscopic views of the different steps of the ESD procedure performed using the dPAA stained with Methylene Blue. Setting of the lesion, approx. 3 cm in diameter (a); injection of the dPAA solution (b); formation of the SFC after gelation of the dPAA (c); circumferential cutting (d); complete resection with protective layer of dPAA that remained adhered to the muscolaris (e); wound left after ESD with layer of the dPAA (f).

Interestingly, the hydrogel precursor solution showed rapid gelation when injected in vivo and afforded a long-lasting high mucosal elevation, keeping the cushion volume constant during the dissection. The optimal adhesion of the hydrogel to the muscolaris layer provided protection during ESD, decreasing the risk of perforation, and afterwards. This novel material can provide a solution to ESD limitations and promote healing of tissues after surgery (***Figure 2***).

In Chapter 4, we present different formulations of PAAm hydrogels for different applications. First, we discuss a totally new approach for percutaneous hernia repair, in which a non-degradable PAAm hydrogel is injected in the inguinal region, solidifying *in-situ* and thus removing the need for the placement of prosthetic mesh.

Different laparoscopic, endoscopic and even robotic techniques have also been developed for hernia treatment, such as Transabdominal Preperitoneal (TAPP), Extraperitoneal (TEP) or Flexible Endoscopic Preperitoneoscopy (FLEPP). The use of these techniques reduces pain and discomfort for the patients and reduce hospitalization time in comparison to open surgery, but however they require extensive training and have a steep learning curve.[7]

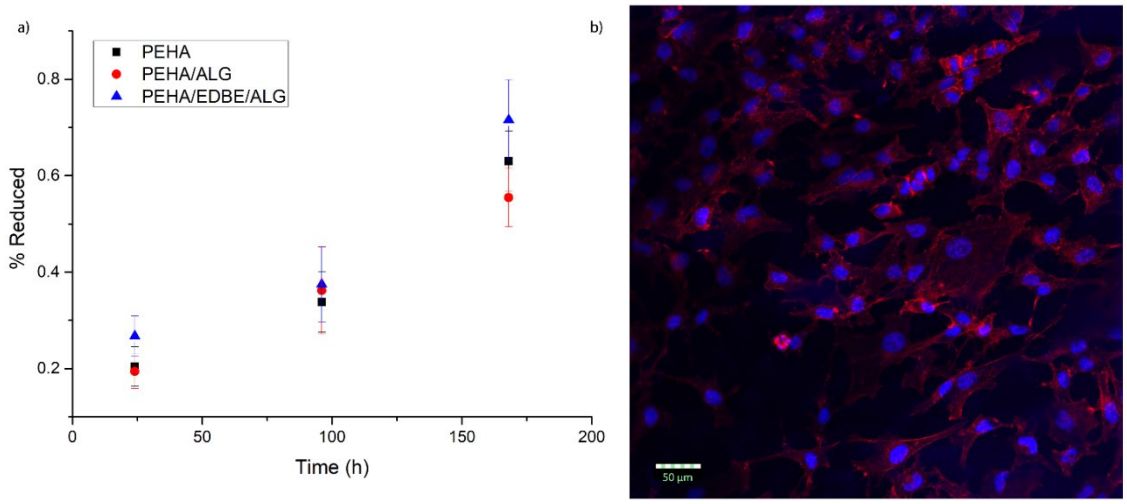

Figure 3 AlamarBlue test on HeLa cells growing on the PEHA/water (black), PEHA/ALG (red) and PEHA/EDBE/ALG (blue) hydrogels after 1, 4 and 7 days (a); Confocal image of HeLa cells growing on top of PEHA/EDBE/ALG hydrogel after seven days. Actin is stained with AlexaFluor Phalloidin 647 and the nuclear region with DAPI (b).

This new technique would allow for a simpler and more patient-friendly treatment of inguinal hernia, without all the side-effects of open or laparoscopic procedures.

In order to be suitable for the desired application, the material should be easy to prepare for immediate application in the operating room, easy to inject but able to gelify before spreading away from the desired area, it should adhere strongly to the surrounding tissue, be non-degradable, elastic and mechanically resistant enough to sustain high stress. It should also be non-cytotoxic and should not promote inflamatory reactions.

We investigated an injectable hydrogel composed of an interpenetrating network of sodium alginate/PAAm for percutaneous hernia treatment, that is able to solidify just after injection forming a stable and elastic hydrogel. *In-vitro* assays (***Figure 3***) show that the material is cytocompatible and preliminary *in-vivo* short-time survival test also confirm that the procedure is feasible, and the material do not show sign of toxicity.

Amongst the possible applications of such materials for wound healing or as fillers we have studied their use for the filling of fistula. Fistulas are abnormal pathological connections between two hollow organs or with the skin, that can result from several reasons, such as complications after surgery or as a side-effect of Chron's Disease. They are very serious pathology that can lead to a poor quality of life, chronic pain, infection and even death.

We envisaged that injectable PAAm hydrogels can be applicable also for this pathology, closing the pathological communication and allowing cell proliferation and cicatrization.

However, standard PAAm hydrogels are not directly applicable in this case, because they would percolate outside the fistula before gelation. To solve this problem, we developed a cream based on a pre-gel PAAm solution in alginate as the water phase, and an organic phase composed by edible vegetable oils, FDA-approved surfactants and other molecules generally recognized as safe in cosmetic formulations. The cream (***Figure 4***) possesses a shear-thinning behavior and a clear yeld-stress, allowing it to be injected and then stay in position until gelation of the PAAm backbone occur. Tests are in progress, at the moment of writing, to demonstrate *in vivo* the applicability of this system.

Figure 4 PAAm-based cream for fistula closure

To have alternatives to the PAAm systems we have also explored the use of hyaluronic acid derivatives in Chapter 5.

Hyaluronic acid has been one of the most used dermal filler for cosmetic applications, since can be extruded by a syringe and applied directly in the skin to give a younger appearance by replacing volume loss during the normal ageing.[8,9] Hyaluronic acid is a polysaccharide naturally present in the human body and involved in different physiological process, such as wound healing or scar formation.

Pure hyaluronic acid is, however, quickly metabolized and degraded in the skin and thus frequent injections are required. Indeed, modern commercial formulation contains crosslinked hyaluronic acid - with the most common employed crosslinker being 1,4-butanediol diglycidyl ether (BDDE) – to ensure a long-lasting effect. [10]

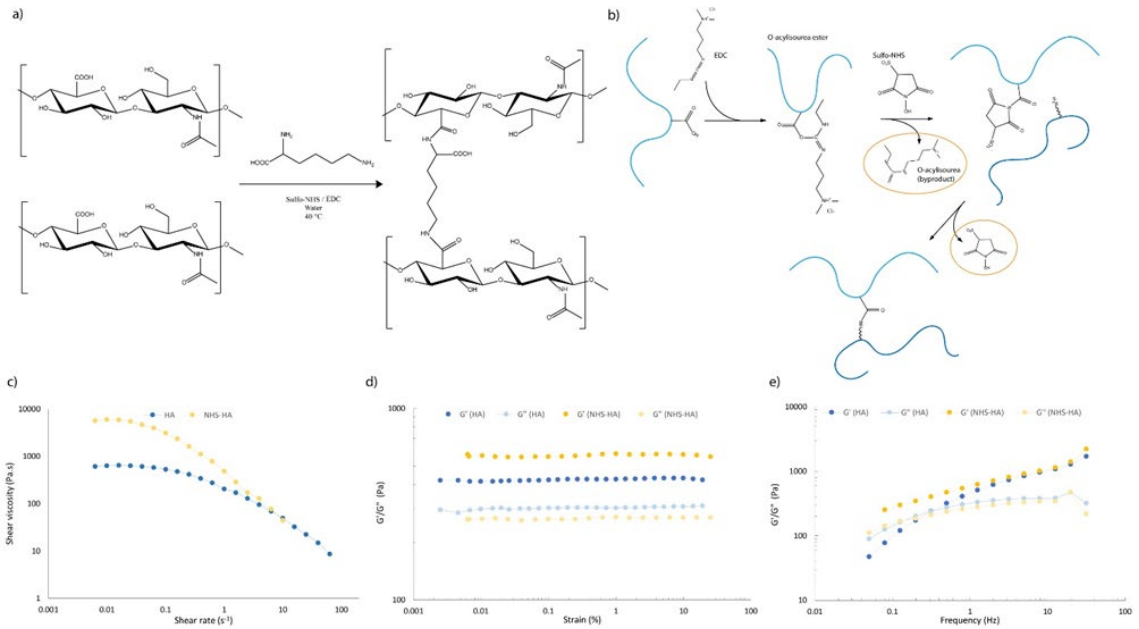

Figure 5 Cross-linked hyaluronic acid with L-lysine et EDC/sulfo-NHS and reaction mechanism (a-b). Shear viscosity of pure hyaluronic acid (bleu) and crosslinked hyaluronic acid (yellow) (c). Frequency sweep (f = 1 Hz) and amplitude sweep (σ = 1%) of pure and crosslinked hyaluronic acid (d-e).

Herein, we present a different crosslinking strategy, based on lysine, in order to avoid the use of highly reactive molecules such as BDDE. The rationale behind our idea is to use activation of hyaluronan to promote the coupling with L-lysine, following different strategies based on chemical modification of hyaluronic acid or activation of the -COOH groups. Different strategies were evaluated, and we found the most promising approach to be the coupling of L-Lysine with the carboxylic groups of the hyaluronic acid through EDC/NHS or EDC/HOBt chemistry. A complete rheological analysis of the final materials was performed (***Figure 5***), showing that this procedure allows to effectively crosslink hyaluronic acid with Lysine.

References

(1) Wichterle, O.; Lím, D. Hydrophilic Gels for Biological Use. *Nature* **1960**, *185* (4706), 117–118.

(2) Caló, E.; Khutoryanskiy, V. V. Biomedical Applications of Hydrogels: A Review of Patents and Commercial Products. *Eur. Polym. J.* **2015**, *65*, 252–267.

(3) Buwalda, S. J.; Boere, K. W. M.; Dijkstra, P. J.; Feijen, J.; Vermonden, T.; Hennink, W. E. Hydrogels in a Historical Perspective: From Simple Networks to Smart Materials. *J. Control. Release* **2014**, *190*, 254–273.

(4) Xu, Q.; Zhang, Z.; Xiao, C.; He, C.; Chen, X. Injectable Polypeptide Hydrogel as Biomimetic Scaffolds with Tunable Bioactivity and Controllable Cell Adhesion. *Biomacromolecules* **2017**, *18* (4), 1411–1418.

(5) Ferruti, P. Poly(Amidoamine)s: Past, Present, and Perspectives. *J. Polym. Sci. Part A Polym. Chem.* **2013**, *51* (11), 2319–2353.

(6) Fiorini, F.; Prasetyanto, E. A.; Taraballi, F.; Pandolfi, L.; Monroy, F.; López-Montero, I.; Tasciotti, E.; De Cola, L. Nanocomposite Hydrogels as Platform for Cells Growth, Proliferation, and Chemotaxis. *Small* **2016**, *12* (35), 4881–4893.

(7) Montgomery, R. B. M. A.; Bansal, E. A. V. *Update of Guidelines on Laparoscopic (TAPP) and Endoscopic (TEP) Treatment of Inguinal Hernia (International Endohernia Society)*; 2015.

(8) Papakonstantinou, E.; Roth, M.; Karakiulakis, G. Hyaluronic Acid, a Key Molecule in Skin Aging. *Dermatoendocrinol.* **2012**, No. December, 253–258.

(9) Attenello, N. H.; Maas, C. S. Injectable Fillers: Review of Material and Properties. *Facial Plast. Surg.* **2015**, *31* (1), 29–34.

(10) Tezel, A.; Fredrickson, G. H. The Science of Hyaluronic Acid Dermal Fillers. *J. Cosmet. Laser Ther.* **2008**, *10* (1), 35–42.

Giuseppe ALONCI

Injectable hydrogels for innovative clinical applications

Résumé

Cette thèse porte sur la conception d'hydrogels injectables pouvant être utilisés en chirurgie mini-invasive, par exemple en dissection endoscopique sous-muqueuse, en réparation de hernie percutanée ou en scellement de fistule.

Les polyamidoamines (PAAm) constituent une classe d'hydrogel particulièrement intéressante à ces fins, en raison de leur biocompatibilité et de leur facilité d'adaptation chimique. Après avoir étudié les différents facteurs qui affectent leurs propriétés, nous montrons qu'il est également possible d'obtenir des microgels à base de PAAm pour la délivrance de médicaments ou l'encapsulation de cellules.

Leur cinétique particulière de formation, associée à la synthèse dans de l'eau à température ambiante, leur permet d'être facilement injectées. Il est possible de synthétiser des hydrogels PAAm dégradables sensibles au rédox qui peuvent être injectés dans la sous-muqueuse de l'estomac, où ils forment un coussin de liquide sous-muqueux qui peut être utilisé pour la dissection endoscopique sous-muqueuse d'un cancer gastrique au stade précoce réduisant les risques de perforation liés l'opération. De plus, ce matériau peut être fonctionnalisé avec des nanocapsules sécables pour libérer des médicaments ou des protéines à la demande.

Nous avons montré que les hydrogels hybrides alginate / PAAm peuvent être utilisés pour le traitement percutané de la hernie inguinale directe et que des crèmes à base d'hydrogel ont été préparées pour être utilisées pour le colmatage des fistules. Le dernier chapitre de la thèse est consacré à la réticulation de l'acide hyaluronique en chirurgie esthétique.

Résumé en anglais

This thesis focuses on the design of injectable hydrogels that can be employed in minimally-invasive surgery, for example in endoscopic submucosal dissection, percutaneous hernia repair or fistula sealing.

Polyamidoamines (PAAm) are a class of hydrogel particularly interesting for these purposes, because of their biocompatibility and easy chemical tunability. After investigating the different factors that affects their properties, we show that it is possible also to obtain PAAm-based microgels for drug delivery or cell encapsulation.

Their peculiar kinetic of formation, together with the synthesis in water at room temperature, allow them to be easily injected. It is possible to synthesize redox-responsive degradable PAAm hydrogels that can be injected in the submucosa of the stomach, where they form a submucosal fluid cushion that can be used to perform endoscopic submucosal dissection of early-stage gastric cancer diminishing the perforation risks related to the surgery. Also, this material can be functionalized with breakable nanocapsules to release on-demand drugs or proteins.

We have shown that hybrid alginate/PAAm hydrogels can be used for the percutaneous treatment of direct inguinal hernia and hydrogel-based creams have been prepared to be used for fistula sealing.

The last chapter of the thesis is devoted to the crosslinking of hyaluronic acid for cosmetic surgery.